University of Milano-Bicocca
Department of Environmental Science (DISAT)

Doctoral School in Environmental Science XXV Cycle
Coordinator: Prof. Marco Vighi

Hydrogeology and hydrogeochemistry of As, Fe, Mn rich groundwater of the multi-layer aquifer in the lower Po Plain, Lombardy region (northern Italy)

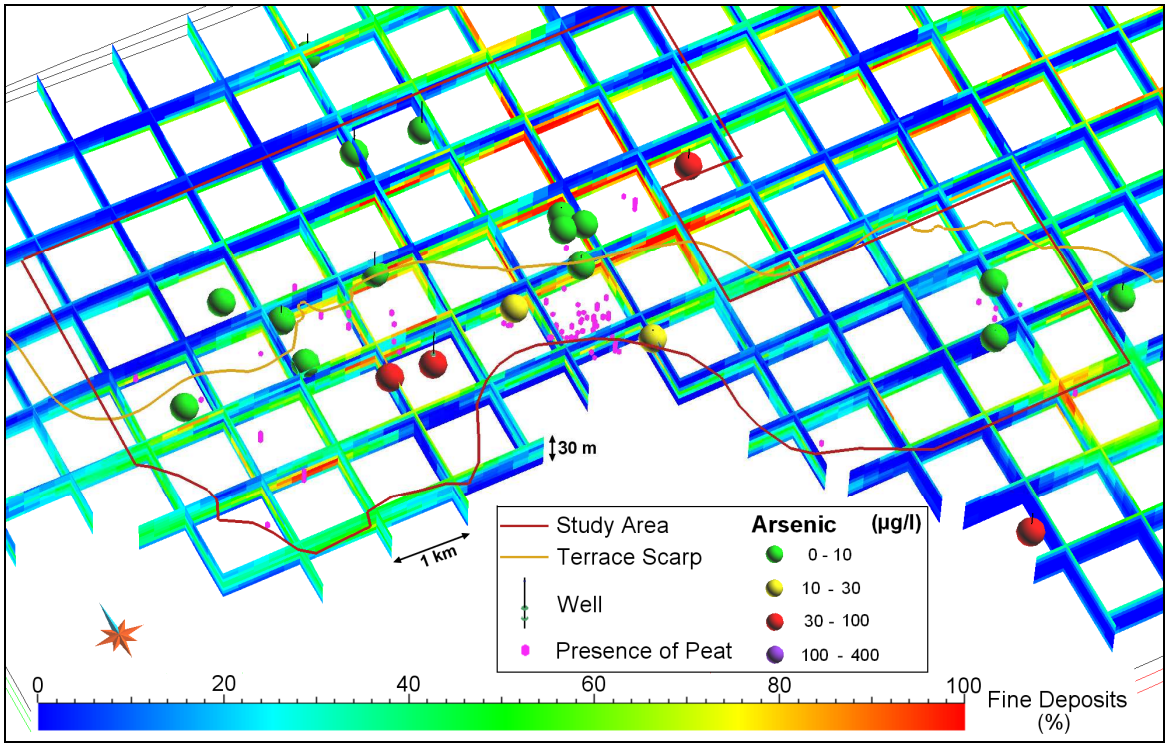

Ph.D. Thesis by **Marco Rotiroti**

Internal Tutor: Prof. Tullia Bonomi
Internal Co-tutor: Dr. Letizia Fumagalli
External Tutor: Prof. Giovanni Pietro Beretta

January 2013

Preface

The present work was funded by the Province of Cremona within the framework of the scientific collaboration with the University of Milano-Bicocca *"Studio della problematica di contaminazione da metalli e sostanze organiche nelle acque sotterranee delle zone industriali di Cremona (Analysis of the groundwater contamination by metals and organic compounds in the industrial areas of Cremona)"* and by the Italian Ministry of Education, University and Research within the PRIN-2008 project *"Salvaguardia e gestione delle risorse idriche strategiche della Pianura Padana s.l. (Water resources management and policy in Po valley)"* which was coordinated by Prof. G. M. Zuppi (Ca' Foscari University of Venice).

The Ph.D. research activities were supervised by Prof. T. Bonomi and Dr. L. Fumagalli (University of Milano-Bicocca) and annually reviewed by Prof. G. P. Beretta (University of Milano). The hydrogeochemical modelling was carried out at Technical University of Denmark for a period of two months under the supervision of Prof. R. Jakobsen (DTU Environment). The interpretation of isotope data was supported by Dr. E. Sacchi (University of Pavia and CNR-IGG).

Citation:
M. Rotiroti (2013) - *Hydrogeology and hydrogeochemistry of As, Fe, Mn rich groundwater of the multi-layer aquifer in the lower Po Plain, Lombardy region (northern Italy).* Ph.D. Thesis, University of Milano-Bicocca, 201 pp.

Index

Short Abstract

The present study concerns the analysis of the hydrogeology and the hydrogeochemistry of the As, Fe, Mn rich groundwater of the alluvial multi-layer aquifer in the lower Po Plain (northern Italy), referring specifically to the territory of Cremona. The main aim is to understand the origins (natural or anthropic) and mechanisms of the high groundwater As, Fe and Mn concentrations.

The specific study area is located near the confluence between Adda and Po rivers. It covers a 50 km^2 wide area around the urban territory of Cremona. The considered aquifer depths are around 200-250 m.

The applied methodology involves the (a) collection of historical data related to water quality, water levels and well logs; (b) storage of collected data in specific databases and geographical information systems; (c) design and execution of two field surveys of water levels and water quality, realized in July 2010 and July 2012; (d) construction of a 3D model of aquifer hydrogeological properties (deposits texture, hydraulic conductivity and effective porosity), built by means of ordinary kriging interpolation of numerical values derived from the coding of well logs; (e) analysis of the hydrodynamic properties of the system; (f) analysis of water quality data (both field and historical data) considering the hydrogeological and hydrodynamic properties of the aquifer system; (g) implementation of a 1D reactive transport model in order to better understand the hydrogeochemical mechanisms in the system; (h) elaboration of a general hydrogeochemical conceptual model concerning possible origins and chemical mechanisms for the high groundwater As, Fe, Mn and NH_4 concentrations, considering also possible anthropogenic influences; (i) development of management tools, as natural background levels derivation, supporting groundwater resources protection by public authorities.

The 3D aquifer modelling underlines the presence of an alternation of sandy layers ($K = 10^{-3}$-10^{-5} m/s) and silty-clayey layers ($K = 10^{-7}$-10^{-8} m/s) with significant peat deposits and leads to the identification of 5 aquifer units. In relation to the hydrodynamic properties analysis, these 5 units are classified as (1) phreatic (F), from 0 to 25 m b.s., (2) semi-confined (S) from 30 to 50 m b.s., (3) confined 1 (C1) from 65 to 85 m b.s., (4) confined 2 (C2) from 100 to 150 m b.s. and (5) confined 3 (C3) from 160 to 250 m b.s.. The aquifer F can locally have semi-confined characteristic due to the presence of superficial silty-clayey deposits, while in the other zones it remains phreatic.

The analysis of field and historical data of water quality underlines the general presence of reduced hydrochemical *facies*, characterized by high concentration of As, Fe, Mn and NH_4, with the exception of the zones with phreatic conditions in aquifer F, where oxidized *facies* are identified. In particular, the survey of July 2010 points out high As concentrations (ranging from 1 to 180 µg/L), especially in the 30-100 m depth range, corresponding to aquifers S and C1. High concentrations of Fe and Mn are also found, they range from 100 to 6000 µg/L and from 10 to 1200 µg/L, respectively. The higher concentrations are found in superficial aquifers: in aquifer F for Mn and in aquifers F and S for Fe. NH_4 is also found with high concentrations (1-5 mg/L, up to 18.9 mg/L) from aquifer S to C3. The measurements of July 2010 can represent the natural background of As, Fe, Mn and NH_4 because no direct sources or indirect anthropogenic influences are found. The survey of July 2012 generally confirms the hydrochemical characterization based on July 2010 data. In the analysis of the hydrochemical historical data, a separation between the data referred to the natural background and to anthropogenic influences is done. Pollutions by hydrocarbons and organic matter in general can be considered as indirect human influences on As, Fe, Mn and NH_4 concentrations, as reported by previous studies. The analysis of historical chemical data referred to the natural background generally confirms the hydrochemical characterization emerged from the data of July 2010 survey. The analysis of historical data also points out a probable anthropogenic influence on As, Fe, Mn and NH_4 concentrations in two sites located in the study area: an oil refinery, affected by hydrocarbons pollution, and a municipal solid waste landfill, with probable organic leachate spills.

In order to understand the origin and the mechanisms of the high As, Fe, Mn and NH_4 concentrations, a hydrogeochemical conceptual model is implemented. The conceptual model considers the process of natural organic matter degradation (i.e. peat) as primary control factor on high As, Fe, Mn and NH_4 concentrations. Degradation of peat is associated with the consecutive reduction of O_2, NO_3^-, Mn(IV), Fe(III), SO_4^{2-}, CO_2. The reductive dissolution of Mn and Fe oxides (contained in the aquifer sediments) leads to high concentrations of dissolved Fe and Mn, but also to high concentrations of dissolved As, which is generally sorbed on Mn and Fe oxides. Dissolved As concentration can be also lowered by different processes (co-precipitation of As in iron sulfides, precipitation of arsenic sulfides, sorption of As on the remaining Fe-oxides and Mn-oxides, etc.). NH_4 is released

from the degradation of organic nitrogen of peat. Therefore, a natural origin of As, Fe, Mn and NH_4 can be assumed.

In order to understand if the hydrogeochemical conceptual model, based on literature, could be reliable on the present case study, a 1D reactive transport model, using PHREEQC code, is implemented. The modelled concentrations result in good agreement with the measured concentrations (July 2010). This result could support the validity of the conceptual model. In addiction, isotope and microbiological analysis, executed in the survey of July 2012, confirms the natural origin of NH_4 and the occurring of Fe-oxide and sulfate reduction in the studied system.

In conclusion, the present work can contribute to understand origins and mechanisms of high groundwater As, Fe, Mn and NH_4 concentrations in the lower Po Plain, supporting the management and protection of groundwater resources by public authorities.

1. Introduction

The present thesis concerns the analysis of the hydrogeology and the hydrogeochemistry of the As, Fe, Mn rich groundwater of the alluvial multi-layer aquifer in the lower Po Plain (northern Italy), referring specifically to the territory of Cremona. The main aim is to understand the origins (natural or anthropic) and mechanisms of the high concentrations of As, Fe and Mn detected in groundwater.

High concentrations of iron and manganese can be considered as a nuisance more than a health risk, giving an unpleasant appearance and taste to drinking groundwater. Otherwise, arsenic in groundwater represents a serious threat to human health involving millions of people all over the world. Arsenic, iron and manganese frequently have a natural origin in groundwater relating to the mineral composition of aquifer sediments. Some of the most countries affected by naturally As rich groundwater are Bangladesh (e.g., McArthur et al, 2001; Neumann et al., 2009; Jung et al., 2011) West Bengal, India (e.g., Dowling et al., 2002; McArthur et al, 2004; Rowland et al., 2006) and Vietnam (e.g., Postma et al., 2007; Jessen et al., 2008; Postma et al., 2012). In Italy, naturally elevated concentrations of As are documented in the volcanic aquifers of central and southern Italy (e.g., Aiuppa et al., 2003; Baiocchi et al., 2011) and in the deep alluvial aquifers of northern Italy (e.g., Zavatti et al., 1995; Bianchi and Pezzera, 1999). The main causes of the high As concentration are probably related to the uprising of geothermal deep fluids (Baiocchi et al., 2011) for the former, and to reducing environments (Zavatti et al., 1995) for the latter.

The whole territory of Cremona was subject to previous hydrogeological and hydrochemical studies (i.e. Beretta et al., 1992; Francani et al., 1994; Zavatti et al., 1995) which underline the presence of high levels of As, Fe, Mn and NH_4 generally in deep aquifers (deeper than 50 m), assuming natural origin. For As in particular, high concentrations are identified in the Oglio river area (up to 200 µg/l), while lower concentrations are found close to the town of Cremona, involving aquifers between 50 and 120 m deep (Zavatti et al., 1995). The analysis of arsenic occurrence in Lombardy region reported by Castelli et al. (2005) underlines the presence of high concentrations of As in the Cremona area, in particular near the Oglio river. The problem of naturally As, Fe, Mn rich groundwater in the Cremona territory is also underlined by Regione Lombardia (2006) which assigned the "particular" environmental status to this area on the basis on the D. Lgs. 152/06.

The present research activity is organised in three steps:

I step - Collection of data

- *Collection of historical data*: a compilation of data and information concerning the geology, hydrogeology, geochemistry and past and present pollution phenomena was done from the archives of public authorities.
- *Creation of databases*: the collected data was organised and stored in specific databases and geographical information systems.
- *Field measurements*: two field surveys of water levels and water quality were designed and executed in July 2010 and July 2012.

II step - Elaboration of data

- *Creation of a model of the multi-aquifer system*: a 3D modelling of deposits texture, hydraulic conductivity and effective porosity distribution was implemented starting from the coding of well logs.
- *Analysis of the hydrodynamic properties of the multi-aquifer system*: the aquifer system was characterized on the basis of the water levels measurements executed in the field surveys.
- *Characterization of groundwater quality*: groundwater chemistry of the aquifer system was analysed on the basis of both field and historical data, considering the hydrogeological properties of the multi-aquifer system.
- *Implementation of numerical hydrogeochemical modelling:* a reactive transport modelling was implemented in order to better understand the hydrogeochemical mechanisms in the system.

III step - Summary of elaborations

- *Implementation of a hydrogeochemical conceptual model*: on the basis of the elaborations, a conceptual model was developed concerning possible origins and chemical mechanisms for the high groundwater As, Fe, Mn and NH_4 concentrations, considering also possible anthropogenic influences.
- *Definition of operational tools supporting the groundwater resources management*: derivation of preliminary natural background levels for As, Fe, Mn and NH_4 in order to support the groundwater resources management and protection by public authorities.

1.1. Study area

In the present work, two specific areas were considered (Figure 1.1). The first one has an extent of around 500 km^2 and represents the hydrogeological characterization area, the second one covers a 50 km^2 wide territory around the town of Cremona and represents the hydrochemical study area. This area includes the industrial zones, located in the western and south-eastern parts of Cremona, in order to verify if the anthropic activities could influence groundwater As, Fe and Mn concentrations.

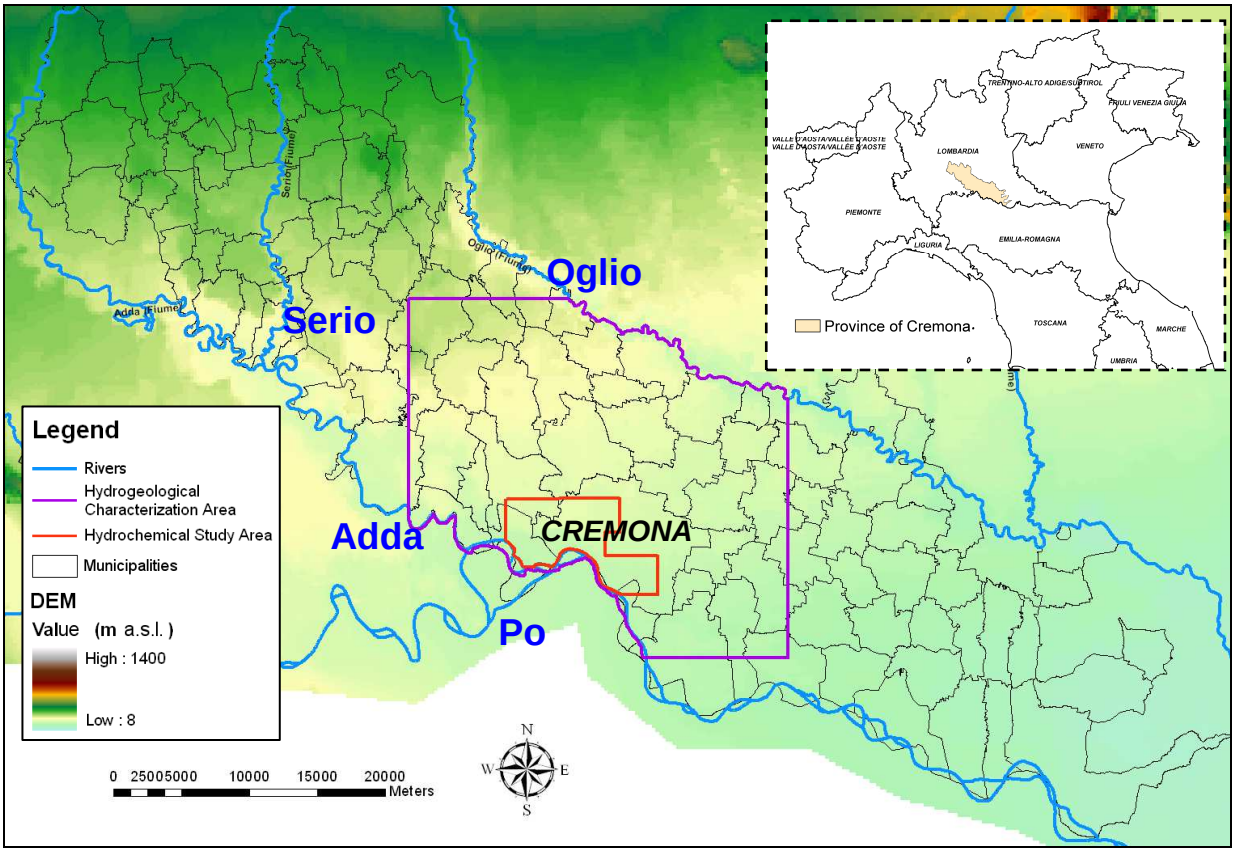

Figure 1.1. Hydrogeological characterization (violet) and hydrochemical study (red) areas.

An aquifer thickness of around 200-250 m was investigated, corresponding to the "Aquifer Group A" (*Gruppo Acquifero A* in Regione Lombardia and Eni Divisione Agip, 2002). The choice of considering the Aquifer Group A instead of the whole "Traditional Aquifer" (*Acquifero Tradizionale* in Martinis and Mazzarella, 1971), which considers both "Aquifer Group A" and "Aquifer Group B", is supported by the

availability of data: only a few wells involve the "Aquifer Group B", and thus, a small number of data and information could be collected for this unit.

1.2. Preliminary schematization of the aquifer system

A subdivision of the multi-layer aquifer of the Cremona area was proposed by the previous studies of Beretta et al. (1992) and Gandolfi et al. (2007). This subdivision defines a superficial phreatic unit, involving approximately the first 50 m of depth, and a deep semi-confined/confined unit, from 50 to around 200 m of depth.

In the present work, the previous subdivision was developed on the basis of the information derived from the analysis of the collected well logs. Five aquifer units were identified: (1) phreatic (F) from 0 to 25 m below surface (b.s.); (2) semi-confined (S) from 30 to 50 m b.s.; (3) confined 1 (C1) from 65 to 85 m b.s.; (4) confined 2 (C3) from 100 to 150 m b.s.; (5) confined 3 (C3) from 160 to 250 m b.s.. The defined depth range for each aquifer is only indicative and could vary from different zones. A schematic representation of the five aquifer units is presented in figure 1.2. This figure shows a N-S hydrogeological section of the hydrochemical study area that was realised by the interpretation of the collected well logs. As shown in Figure 1.2, the different aquifers can be considered as separated units only where sity-clayey deposits are prevalent.

1.3. Preliminary geological and geomorphological characterization

The sediments related to the first 200-250 m of depth are composed by continental fluvio-glacial and alluvial deposits of Pleistocene and Holocene ages. These deposits form the following geological units (Beretta et al., 1992):

- *Holocene Alluvials Auct.:* gravelly-sandy-silty alluvials of watercourses; it crops out in the Adda, Serio and Oglio river valleys.
- *Lower Holocene Alluvials Auct.:* sandy and gravelly alluvials, polygenic, with missing or reduced alteration layer; it covers an extended territory east of the Adda river.

- *Wurm Fluvio-glacial Deposits Auct. (Upper Pleistocene):* sandy and gravelly alluvials, without alteration; it covers the area between the Adda and Po rivers representing the "Main Plain Level" (*Livello Fondamentale della Pianura* in Petrucci and Tagliavini, 1969).
- *Riss-Mindel Fluvio-glacial Deposits Auct. (Middle Pleistocene):* fluvio-glacial and gravelly sediments, with silty-clayey lenses.

In the hydrogeological characterization area, four main geomorphological elements can be detected (Figure 1.3). The first element is the "Main Plain Level" (1, in figure 1.3) which is mainly composed, in this area, by sandy and silty-clayey deposits. The second element is represented by the active valleys of Po, Adda and Oglio rivers (2, in figure 1.3). These valleys were formed from the last (Wurm) glacial maximum by the erosion of the "Main Plain Level" and consecutive deposition/erosion cycles. The sediments forming these valleys are generally composed by sands and gravels. Another geomorphological element is represented by the dead river valleys, which were formed by the erosion activity of ancient watercourses. Two dead river valleys can be identified in the western part of the hydrogeological characterization area (3, in figure 1.3): "Serio Morto" and "Serio di Grumello" (Malerba et al., 1995). The last geomorphological element is the "Navigli" valley (*Valle dei Navigli* in Cremonini Bianchi, 1989) which represents an incision of the "Main Plain Level" extended from North to South (4, in figure 1.3). Burrato et al. (2003) supposed that the "Navigli" valley could represent an abandoned paleo-channel of the Oglio river.

Considering the hydrochemical study area, the surface geology can be described by the following units (Bassi, 2001a):

- *Holocene Alluvials Auct.:* sandy, silty and clayey deposits with peat; it covers the Po and "Navigli" valleys.
- *Wurm Fluvial Deposits Auct. (Pleistocene):* sandy-clayey and silty deposits which form the "Main Plain Level", it is separated by a terrace scarp (5-9 m high) from the Po valley; the area behind the scarp is mainly composed by sands.
- *Riss Fluvial Deposits Auct. (Pleistocene):* sandy-clayey deposits corresponding to ancient terraces.

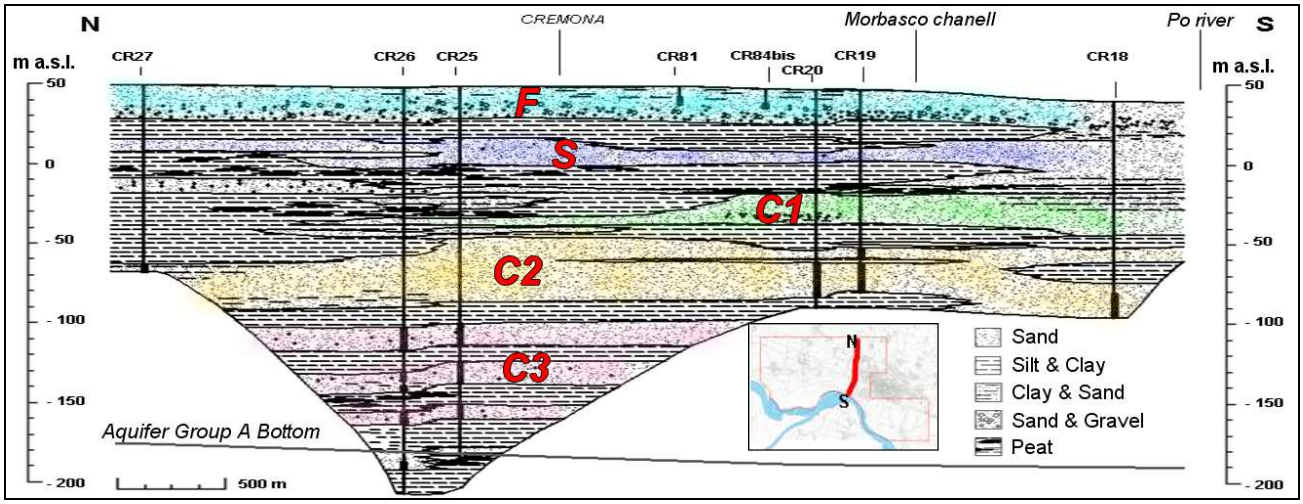

Figure 1.2. Schematic representation of the aquifer system: aquifer F (0-25 m) in light blue, aquifer S (30-50 m) in blue, aquifer C1 (65-85 m) in green, aquifer C2 (100-150 m) in yellow and aquifer C3 (160-250) in pink.

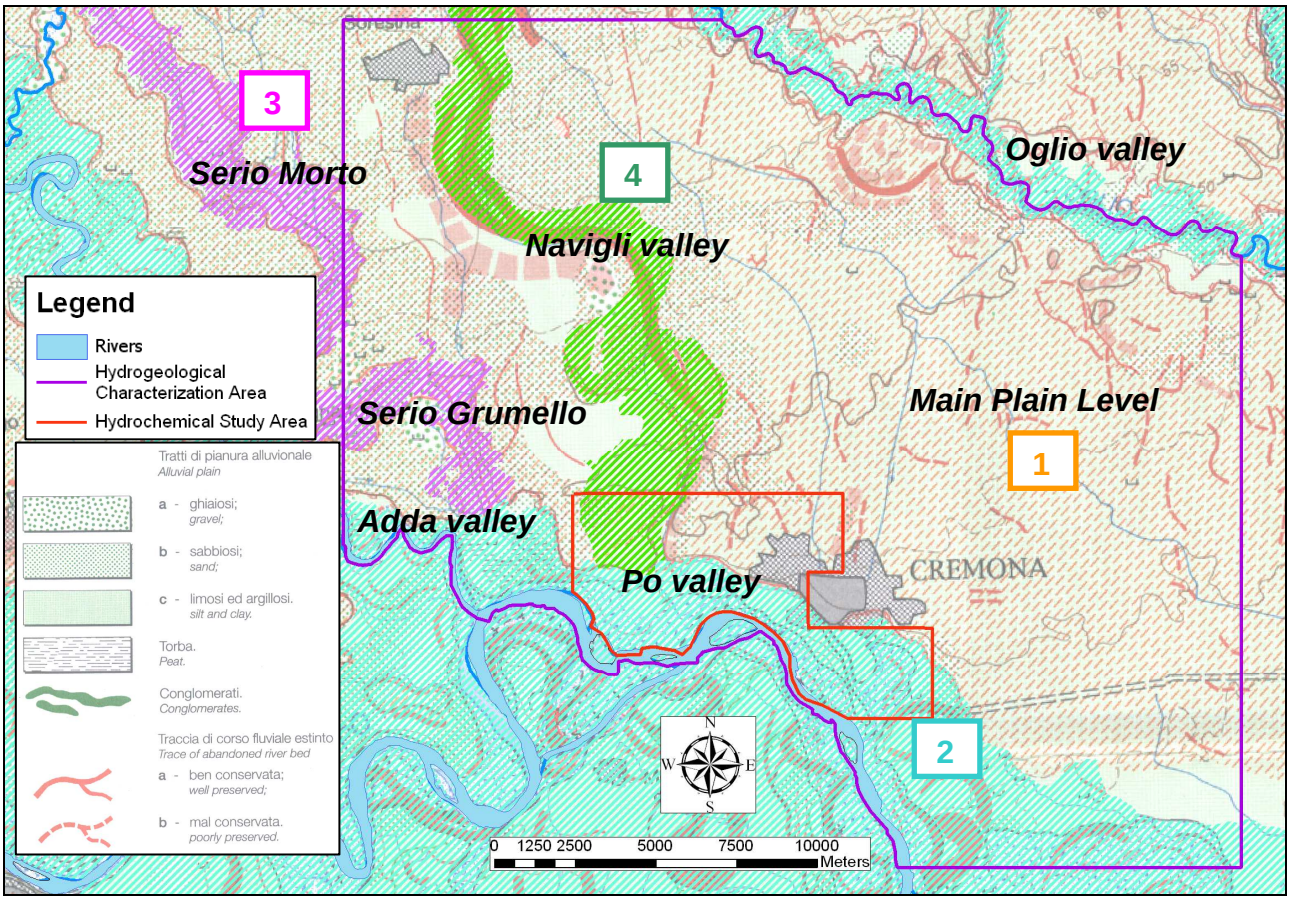

Figura 1.3. Main geomorphological elements in the hydrogeological characterization area: (1) "Main Plain Level"; (2) Active river valleys; (3) Dead river valley; (4) "Navigli" valley. On the background the geomorphological map of the Po Plain (Castiglioni *et alii*, 1997, modified).

The distribution of these units in the study area is showed in figure 1.4 (modified from Bassi, 2001b).

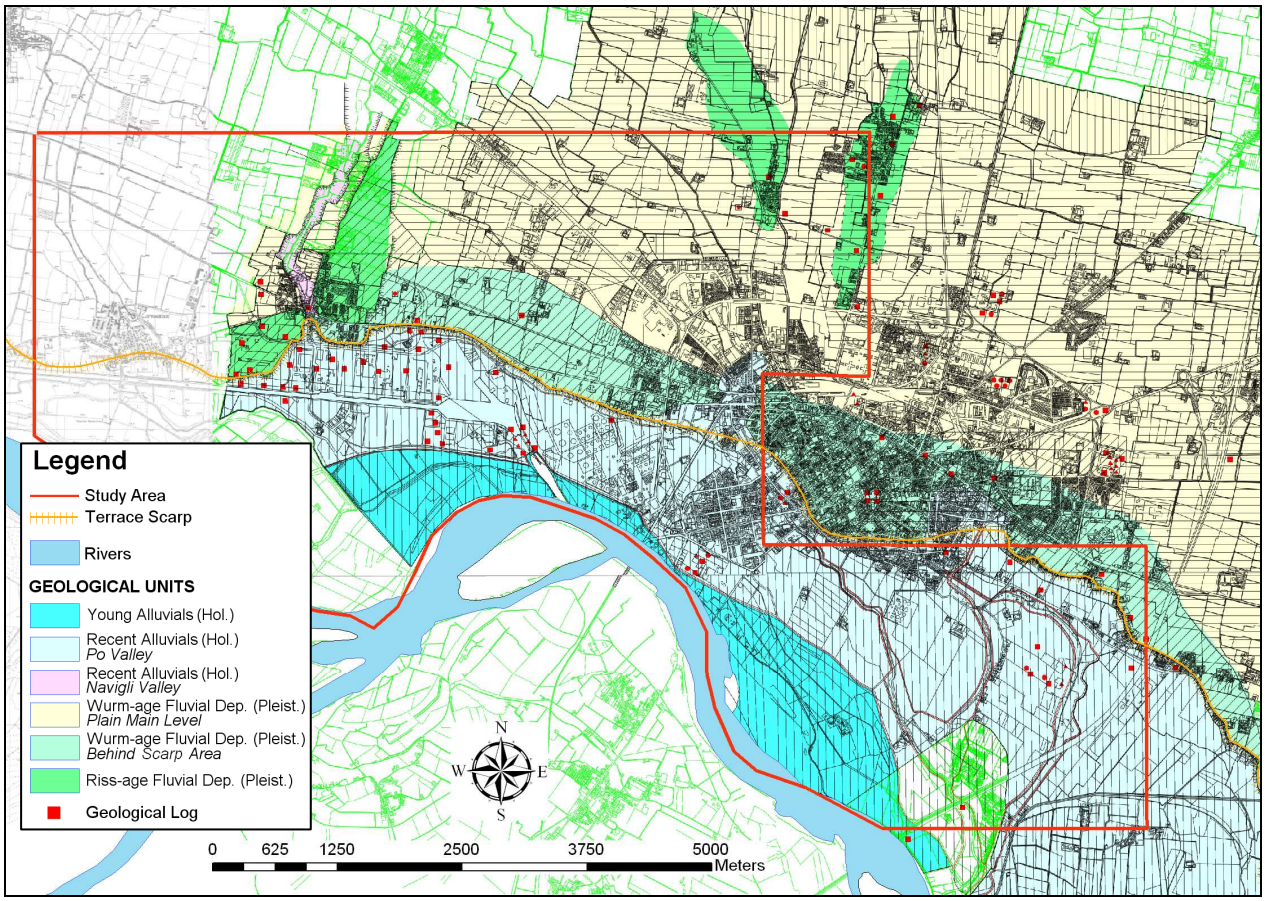

Figura 1.4. First Geotechnical map of the Municipality of Cremona (modified from Bassi, 2001b)

References

Aiuppa A., D'Alessandro W., Federico C., Palumbo B. & Valenza M. (2003) – *The aquatic geochemistry of arsenic in volcanic groundwater from southern Italy*. Applied Geochemistry 18, 1283-1296.

Baiocchi A., Lotti F. & Piscopo V. (2011) – *Influence of hydrogeological setting on the arsenic occurrence in groundwater of the volcanic areas of central and southern Italy*. Aqua Mundi, DOI: 10.4409/Am-035-11-0035.

Bassi G. (2001a) – *Studio Geologico del Territorio Comunale (Geological study of the municipal territory)*. Relazione Tecnico-illustrativa, Comune di Cremona, 36 pp.

Bassi G. (2001b) – *Carta di Prima Caratterizzazione Geotecnica del Comune di Cremona (First Geotechnical map of the Municipality of Cremona).* Scala 1:12˙500. Allegato 3 allo Studio Geologico del Territorio Comunale, Comune di Cremona.

Beretta G. P., Francani V. & Fumagalli L., (1992) – *Studio Idrogeologico della Provincia di Cremona (Hydrogeological study of the Province of Cremona)*. Pitagora Editrice, Bologna, 141 pp.

Bianchi A. & Pezzera G. (1999) – *Il monitoraggio dell'arsenico nelle acque sotterranee della pianura mantovana e bergamasca: aspetti idrogeologici e idrochimici (Arsenic monitoring in groundwater in the Po Plain of Mantova and Bergamo: hydrogeological and hydrochemical aspects)*. Quaderni di geologia Applicata S2, 3.61-3.72.

Burrato P., Ciucci F. & Valensise G. (2003) – *An inventory of river anomalies in the Po Plain, Northern Italy: evidence for active blind thrust faulting*. Annals of Geophysics 46 (5), 865-882.

Castelli A., Chiesa S., Deriu G., Pezzera G., Vescovi E., Zanotti M. & Zonca B. (2005) – *Note sulla presenza di arsenico nel sottosuolo e nelle acque sotterranee della Lombardia (Occurrence of arsenic in aquifer sediments and groundwater in Lombardy region)*. In: Arpa Emilia-Romagna (Eds), Presenza e diffusione dell'arsenico nel sottosuolo e nelle risorse idriche italiane (Occurrence and distribution of arsenic in sediments and water resources of Italy), 39-50. I quaderni di Arpa.

Castiglioni G.B., Ajassa R., Baroni C., Biancotti A., Bondesan A., Bondesan M., Brancucci G., Castaldini D., Castellaccio E., Cavallin A., Cortemiglia F., Cortemiglia G.C., Cremaschi M., Da Rold O., Elmi C., Favero V., Ferri R., Gandini F., Gasperi G., Giorgi G., Marchetti G., Marchetti M., Marocco R., Meneghel M., Motta M., Nesci O., Orombelli G., Paronuzzi P., Pellegrini G.B., Pellegrini L., Rigoni A., Sommaruga M., Sorbini L., Tellini C., Turrini M.C., Vaia F., Vercesi P.L., Zecchi R. and Zorzin R. (1997) – *Carta Geomorfologica della Pianura Padana (Geomorphological map of the Po Plain)*. Scala 1:250˙000. SELCA, Firenze.

Cremonini Bianchi M. (1989) – *Un antico percorso fluviale della pianura cremonese: la "Valle dei Navigli" (An ancient watercourse of the plain of Cremona: the "Navigli" valley)*. Pianura - Scienza e Storia dell'Ambiente Padano 3, 55-68.

Dowling C. B., Poreda R. J., Basu A. R., Peters S. L. & Aggarwal P. K. (2002) – *Geochemical study of arsenic release mechanisms in the Bengal Basin groundwater*. Water Resources Research, DOI:10.1029/2001WR000968.

Francani V., Beretta G. P., Bareggi A., Nobile A., Cremonini Bianchi M. & Cattaneo F. (1994) – *Aspetti idrogeologici del problema della presenza di azoto ammoniacale nelle acque sotterranee della provincia di Cremona. (Hydrogeological aspects of the occurrence of ammonium in groundwater in the province of Cremona).* Pitagora Editrice, Bologna, 101 pp.

Gandolfi C, Ponzini G. & Giudici M. (2007) – *Realizzazione di un modello preliminare del flusso idrico nel sistema acquifero della Provincia di Cremona (Implementation of a preliminary flow model in the aquifer system of the Province of Cremona).* Relazione Tecnica, pp.222. http://www.atlanteambientale.it/atlanteambientale/biblio/Intro.html

Jessen S., Larsen F., Postma D., Viet P. H., Ha T. N., Nhan P. Q., Nhan D. C., Duc M. T., Hue N. T. M., Huy T. D., Luu T. T., Ha D. H. & Jakobsen R. (2008) – *Palaeo-hydrogeochemical control on groundwater As levels in Red River delta, Vietnam*. Applied Geochemistry 23, 3116-3126.

Jung H. B., Bostick C. B. & Zheng Y. (2011) – *Field, experimental and modeling study of arsenic partitioning across a redox transition in a Bangladesh aquifer*. Environmental Science & Technology 46, 1388-1395.

Malerba G., Galli C., Armanini B. & Ferrari V. (1995) – *La geomorfologia della provincia di Cremona (The geomorphology of the Province of Cremona)*. Quaderni del Centro di Documentazione Ambientale, Provincia di Cremona, 23 pp.

Martinis B. & Mazzarella S. (1971) – *Prima ricerca idrica profonda nella pianura lombarda (First deep water research in the plain of Lombardy region).* Memorie dell'Istituto di Geologia e Mineralogia dell'Università di Padova 28, 1-52.

McArthur J. M., Ravenscroft P., Safiulla S. & Thirlwall M. F. (2001) – *Arsenic in groundwater: Testing pollution mechanisms for sedimentary aquifers in Bangladesh.* Water Resources Research 37 (1), 109-117.

McArthur J. M., Banerjee D. M., Hudson-Edwards K. A., Mishra R., Purohit R., Ravenscroft P., Cronin A., Howarth R. J., Chatterjee A., Talukder T., Lowry D., Houghton S. & Chadha D. K. (2004) – *Natural organic matter in sedimentary basins and its relation to arsenic in*

anoxic ground water: the example of West Bengal and its worldwide implications. Applied Geochemistry 19, 1255-1293.

Neumann R. B., Ashfaque K. N., Badruzzaman A. B. M., Ashraf Ali M., Shoemaker J. K. & Harvey C. F. (2009) – *Anthropogenic influences on groundwater arsenic concentrations in Bangladesh*. Nature Geoscience 3, 46-52.

Postma D., Larsen F., Hue N. T. M., Duc M. T., Viet P. H., Nhan P. Q. & Jessen S. (2007) – *Arsenic in groundwater of the Red River floodplain, Vietnam: Controlling geochemical processes and reactive transport modeling*. Geochimica et Cosmochimica Acta 71, 5054-5071.

Postma D., Larsen F., Thai N. T., Trang p. T. K., Jakobsen R., Nhan P. K., Long T. V., Viet P. H. & Murray A. S. (2012) – *Groundwater arsenic concentrations in Vietnam controlled by sediment age*. Nature Geoscience 5, 656-661.

Petrucci F. & Tagliavini S. (1969) – *Note illustrative della Carta Geologica d'Italia (Illustrative notes of the geological map of Italy)*. Foglio 61, Cremona, Servizio Geologico d'Italia, pp.43.

Regione Lombardia & Eni Divisione Agip (2002) – *Geologia degli acquiferi padani della Regione Lombardia (Geology of the aquifers of the Po Plain in Lombardy region).* A cura di Carcano C. & Piccin A. S.E.L.C.A, Firenze, 130 pp.

Regione Lombardia (2006) – *Monitoraggio qualitativo e classificazione delle acque superficiali e sotterranee (Qualitative monitoring and classification of surface water and groundwater).* Allegato 12 alla Relazione Generale, Programma di Tutela e Uso delle Acque.

Rowland H. A. L, Polya D. A., Lloyd J. R. & Pancost R. D. (2006) – *Characterisation of organic matter in a shallow, reducing, arsenic-rich aquifer, West Bengal*. Organic Geochemistry 37, 1101-1114.

Zavatti A., Atramini D., Bonazzi A., Boraldi V., Malagò R., Martinelli G., Naldi S., Patrizi G., Pezzera G., Vandini W., Venturini L. & Zuppi G. M. (1995) – *La presenza di Arsenico nelle acque sotterranee della Pianura Padana: evidenze ambientali e ipotesi geochimiche (Occurrence of arsenic in the groundwater of Po Plain: environmental evidences and geochemical hypothesis).* Quaderni di geologia Applicata S2, 301-325.

2. Historical data collection and organization

The collection and organization of historical data were mainly conducted consulting the archives of the Province of Cremona, in addiction, data from the Regional Environmental Protection Agency (ARPA Lombardia) and the local water supply companies (AEM Cremona and Padania Acque) were acquired. The collected data are referred to public and private wells and to phenomena of organic pollution occurred in the study area, in order to verify possible influences on As, Fe and Mn concentrations.

Concerning the wells, the collected data are referred to: (a) administrative information (property, address); (b) location (longitude, latitude, altitude); (c) structure (depth, diameter, screens, seals, filter packs); (d) stratigraphy; (e) water level; (f) withdrawals; (g) pumping tests; (h) water quality analysis.

Within the hydrogeological characterization area, 514 wells were identified (93 public and 421 private). The stratigraphy was collected for 337 wells. The location of wells, with and without stratigraphy, is represented in figure 2.1. Water quality analysis referred to 193 samples were also acquired, mainly concerning water supply wells. Concerning the pollution phenomena, 24 different sites were identified in the hydrochemical study area (Table 2.1). These sites have an overall number of piezometers equal to 392 (Figure 2.2). For these piezometers, 213 stratigraphies were collected and the water quality analysis referred to 1753 samples were acquired. These chemical analyses consider different chemical parameters and they concern a overall time period of around 11 years (1999-2010).

All the collected data were organised in geographical information systems and specific databases. The hydrogeological well database TANGRAM (Bonomi et al., 1995) and the related hydrochemical database TANGCHIM (Bonomi et al., 1999) were used. The total number of wells and piezometers inserted in TANGRAM is equal to 906, of which 550 are with stratigraphy. The water quality analyses referred to 1946 groundwater samples were inserted in TANGCHIM.

Table 2.1. Lists of identified polluted sites with their main characteristics.

Site ID	N. Piezometer	Time Period of Analysis	Detected Parameters
25	4	April 1997	metals
26	10	from July 2006 to April 2009	metals, hydrocarbons
27	162	from February 2001 to July 2010	metals, hydrocarbons, BTEX, PAH organochlorides
42	4		
43	13	from September 2005 to March 2009	hydrocarbons, BTEX, organochlorides
48	2	from October 2001 to June 2002	metals
53	10	from March 2003 to February 2007	hydrocarbons, BTEX
80	7	from June 2003 to April 2004	metals, hydrocarbons, organochlorides
84	5	from January 2005 to March 2005	metals
87	3	December 2004	metals, hydrocarbons
94	3	from May 2006 to November 2007	metals, BTEX, organochlorides
99	31	from September 2005 to June 2009	metals
100	5	from January 2006 to December 2010	metals, BTEX, organochlorides
101	4	from January 2006 to June 2006	hydrocarbons, BTEX
105	17 + 3 deep logs	from June 1999 to March 2010	metals, hydrocarbons, BTEX, organochlorides
117	3	from October 2008 to January 2010	hydrocarbons, BTEX
124	7	from October 2007 to July 2010	hydrocarbons, BTEX
125	15	from April 2008 to June 2010	metals, hydrocarbons, BTEX, organochlorides
140	5	May 2010	metals, hydrocarbons, BTEX
141	28	from February 2008 to June 2010	metals, hydrocarbons, BTEX, organochlorides
142	4	June 2010	hydrocarbons, BTEX
149	to be carried out	-	-
Disc. P.C.	6	from June 2002 to April 2010	metals, hydrocarbons, BTEX, PAH organochlorides
Dep.	3	from 2006 to 2010	metals

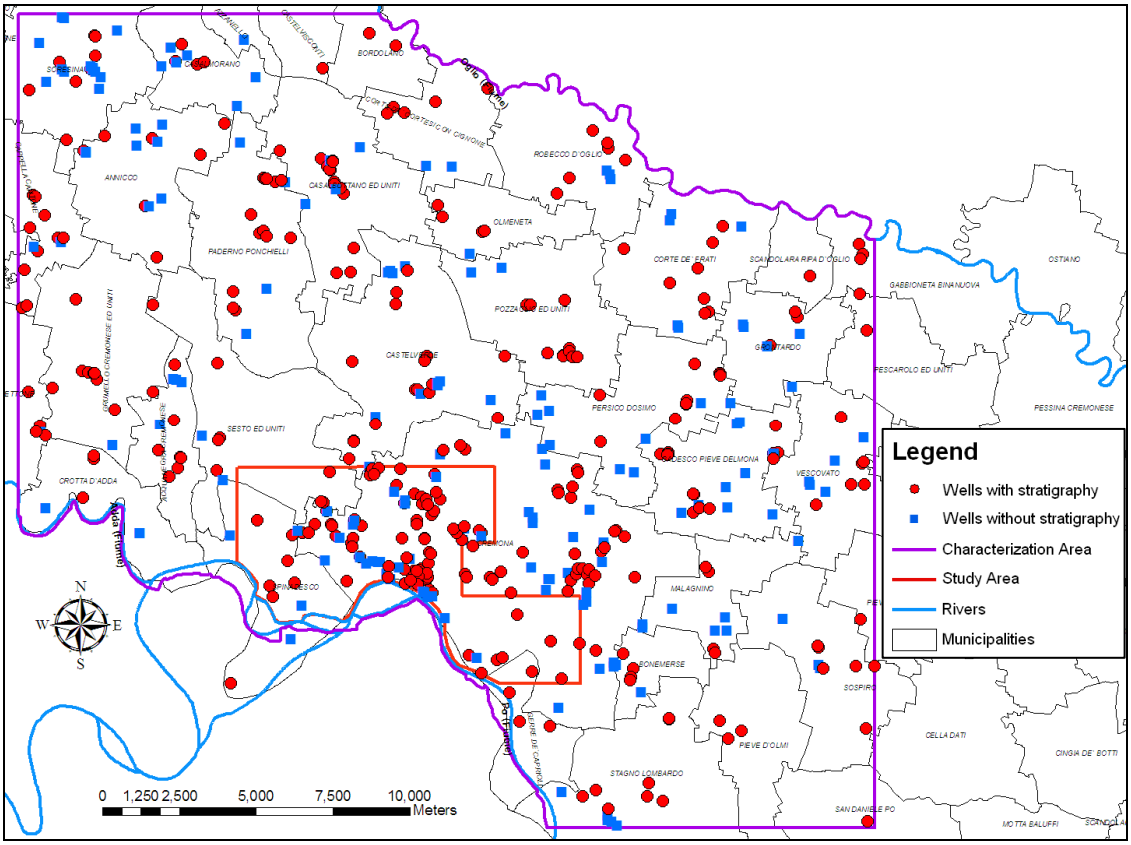

Figure 2.1. Location of identified wells with and without stratigraphy.

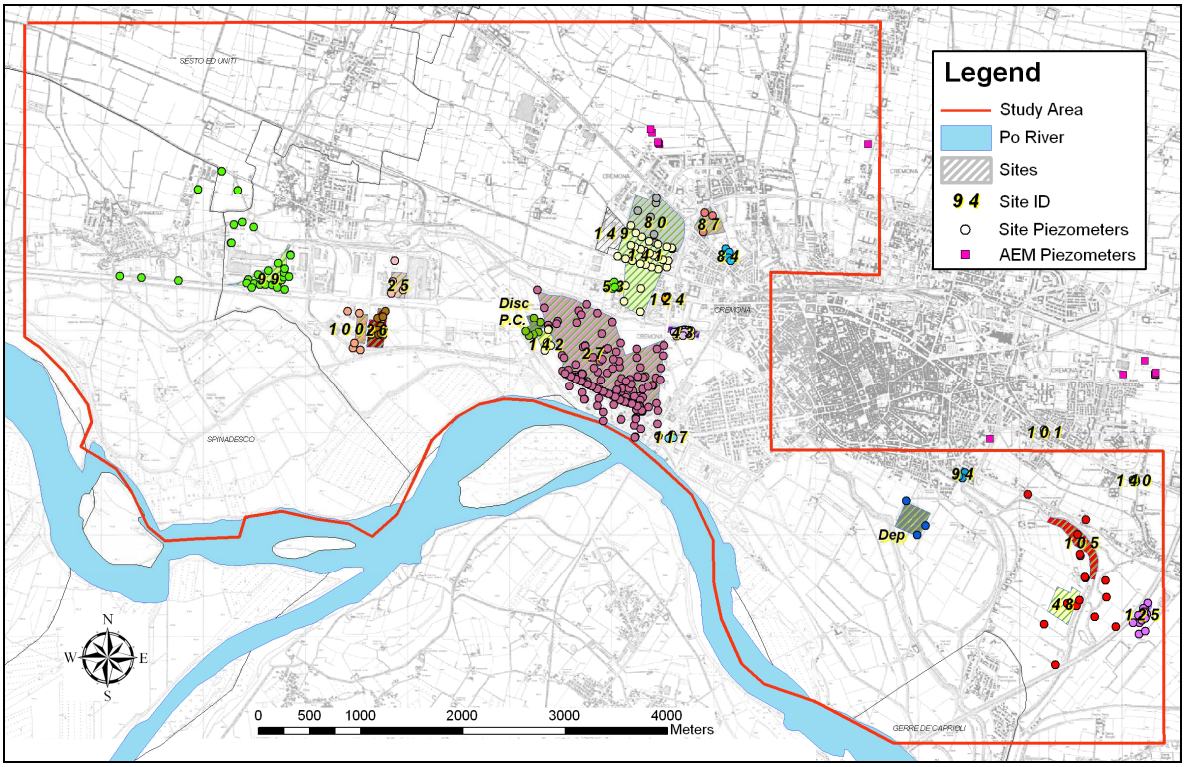

Figure 2.2. Location of polluted sites (Table 2.1) with their piezometers in the study area.

References

Bonomi T., Cavallin A. & De Amicis M. (1995) – *Un database per pozzi: Tangram (A wells database: Tangram)*. Quaderni di Geologia Applicata S3, 3.461-3.465.

Bonomi T., Cavallin A. & De Amicis M. (1999) – *Banca dati idrochimica applicata ai pozzi: protocollo informatico e prototipo di applicazione. (Hydeochemical database applied to wells: computer register and application prototype)*. Quaderni di Geologia Applicata S2, 3.73-3.77

3. Field surveys

In the present work, two field surveys were conducted in July 2010 and July 2012. The surveys concern water level measurements, supported by GPS measurements, and groundwater samplings for chemical analysis. In addiction in the survey of July 2012, groundwater samples were collected for isotope and microbiological analysis. The field surveys involve the following steps: (a) definition of the sampling points, (b) definition of the chemical parameters, (c) definition of the sampling method, (d) execution of the surveys.

3.1. Definition of the sampling points

The sampling points were defined on the basis of existing wells and piezometers due to limited budget which does not allow to drill new boreholes. This aspect limits the creation of a homogeneous sampling grid. Within the identified wells and piezometers (chap. 2), the points with complete information (depth of screens, stratigraphy, etc.) were selected for the surveys.

3.1.1. Survey of July 2010

The survey of July 2010 was realised on 73 points (Table 3.1) located in proximity of the defined hydrochemical study area (Figure 3.1). These points are classified, considering the preliminary schematization of the aquifer system (par. 1.2), on the basis of their depth depths of production intervals and position of seals and filter packs, in order to identify the correct exploited aquifer. This classification leads to the identification of 24 points for aquifer F, 14 for aquifer S, 5 for aquifer C1, 13 for aquifer C2, 8 for aquifer C3 and 9 multi-aquifer points (1 between F and S, 3 between S and C1, 3 between C1 and C2, 2 between C2 and C3).

Table 3.1. Main characteristics of the sampling points in the survey of July 2010.

Code	Depth (m)	Screen (m)	Filter Pack (m)	Bentonite Seal (m)	Concrete Seal (m)	AQU.
CR66	8.2	2-8	**n.a.**	**n.a.**	**n.a.**	F
CR62	10.0	2-10	**n.a.**	**n.a.**	**n.a.**	F
CR88	15.0	2-15	**n.a.**	**n.a.**	**n.a.**	F
SN7bis	10.0	3-10	1-10	0-1	absent	F
CR23b	12.0	3-12	**n.a.**	**n.a.**	**n.a.**	F
CR81	12.0	3-12	**n.a.**	**n.a.**	**n.a.**	F
CR89	15.0	3-15	**n.a.**	**n.a.**	**n.a.**	F
CR82	17.0	3-17	**n.a.**	**n.a.**	**n.a.**	F
CR84bis	12.0	7-12	8-12	absent	0-8	F
CR63	12.0	6-9	5.5-11	2-5.5	0-2	F
SN8	10.0	5-10	8-10	0-8	absent	F
CR86	15.0	6-15	**n.a.**	**n.a.**	**n.a.**	F
CR80	16.0	8-16	7.5-16	6.5-7.5	0-6.5	F
CR50	25.0	10-25	16-25	2-4	absent	F
CR34	30.0	12-27	8-30	0-8	absent	F
CR2	25.0	15-20	15-20	0-15	absent	F
CR11b	30.0	15-25	15-30	14-15	absent	F
CV1	31.5	20-30	**n.a.**	**n.a.**	**n.a.**	F
CR12	40.0	20-33	20-40	0-6	6-20	F
GC1	36.0	21-22	**n.a.**	**n.a.**	**n.a.**	F
GC2	36.0	21-22	**n.a.**	**n.a.**	**n.a.**	F
CV3	32.0	21-27.5	21-27.5	0-21; 27.5-32	absent	F
CR10nw	28.0	23-25	**n.a.**	**n.a.**	**n.a.**	F
CR13	46.0	25-40	25-46	0-6	absent	F
CR7	50.0	25-40; 43-49	**n.a.**	**n.a.**	**n.a.**	F&S
SN2	32.0	25-31	23-30	0-23	absent	S
SN4	34.0	27-33	25-35	0-25	absent	S
SN3	37.0	30-36	28-36	0-28	absent	S
AN3a	88.0	31-40	60-66; 70-88	66-70	absent	S
AN3b	88.0	31-40	60-66; 70-88	66-70	absent	S
CR43	50.0	35-45	20-46	0-8	absent	S
CR24a	45.0	35-45	35-45	0-3; 24-35	absent	S
CR35	60.0	35-40; 43-58	35-40; 43-58	0-35; 40-43	absent	S
CR53	42.0	36-42	**n.a.**	**n.a.**	**n.a.**	S
AN1	47.0	39-45	39-45	0-39	absent	S
CR60	48.0	39-48	39-50	absent	37-39	S
CR21	56.0	40-50	40-56	0-4; 29-40	absent	S
CR49	61.0	41-56	30-61	2-10; 25-30	absent	S
CR36	53.0	47-53	47-53	37-39	0-5	S
CR8a	100.0	29.5-49; 59-65.5; 71.5-78	26-102	15-26	0-15	S&C1
CR8b	104.0	30-45; 60-80	28-104	absent	0-28	S&C1

Code	Depth (m)	Screen (m)	Filter Pack (m)	Bentonite Seal (m)	Concrete Seal (m)	AQU.
CR35nw	80.0	50-56; 65-80	**n.a.**	**n.a.**	**n.a.**	S&C1
CR9	100.0	53-63; 67-81	52-100	absent	45-52	C1
CR10	90.0	69-73; 76-82; 84-87	66-90	absent	17-32; 56-66	C1
CR32	102.0	75-81; 85.5-88.4; 93-95.9	60-102	absent	0-60	C1
CR47	92.0	80-92	**n.a.**	absent	3-20; 30-45; 54-75	C1
CR46	92.0	80-92	**n.a.**	absent	3-20; 30-45; 54-75	C1
CR5	138.0	57-62; 68-79; 102-120; 123-127	**n.a.**	absent	20-50	C1&C2
CR1	122.0	65-120	**n.a.**	**n.a.**	**n.a.**	C1&C2
CR31	135.0	71.8-76; 93.1-96; 106.8-111; 112.5-115.5; 118-124; 125.5-130	60-135	absent	0-60	C1&C2
SN6	102.0	87.5-99.5	83-102	76-83	0-30	C2
CR16	95.0	89-95	**n.a.**	**n.a.**	**n.a.**	C2
SN5	127.0	90.5-100.5	90.5-100.5	2-30	absent	C2
CR54	110.0	99-105	**n.a.**	**n.a.**	**n.a.**	C2
CR27	120.0	100-110	**n.a.**	0-2; 98-100	**n.a.**	C2
CR41	114.0	102-114	**n.a.**	**n.a.**	**n.a.**	C2
CR19	131.0	103.7-108.3; 116.3-128.5	102-108; 114-131	absent	85-102; 103-113	C2
CR33	152.0	109-127; 136-142	90-152	25-35; 80-90	0-10	C2
CR20	141.0	113-133.5	**n.a.**	**n.a.**	**n.a.**	C2
CR38	144.0	123-129	**n.a.**	**n.a.**	**n.a.**	C2
CR48	145.0	125-140	125-140	1-6; 58-65; 100-105; 118-124	86-100	C2
CR18	140.0	125-140	125-140	0-11; 54-59; 86-117	absent	C2
CR14	135.0	129-135	129-135	120-125	0-10	C2
CV2	150.0	122-126; 132-138	122-126; 132-138	25-35; 100-117	absent	C2&C3
CR59	136.0	131-136	**n.a.**	**n.a.**	**n.a.**	C2&C3
AN2	227.5	134-148	134-148	0-28; 88-118	absent	C3
SU2	214.0	135-141; 191-203	135-141; 191-203	0-50; 74-77; 125-128; 145-148; 170-174	absent	C3
PD1bis	202.0	150-159; 164-173	**n.a.**	**n.a.**	**n.a.**	C3
CR25	245.0	154-166; 179.5-191.5; 206-214	144-214.5	20-34; 68-85; 138-144	absent	C3
CR26	260.0	156-169; 184-186; 193-197; 212.5-218.5; 238.5-247.5	146-175; 179-202; 206-260	142-146.5; 175-179; 202-206	0-15	C3

Code	Depth (m)	Screen (m)	Filter Pack (m)	Bentonite Seal (m)	Concrete Seal (m)	AQU.
SU5	175.0	159.3-168.3	159.3-168.3	0-30; 64.5-68; 100-103; 136.5-144	absent	C3
GC3bis	187.0	163-171; 174-180	163-171; 174-180	0-14; 124-128	absent	C3
CR51	251.0	164-174; 188-198; 202-212; 218-224	164-174; 188-198; 202-212; 218-224; 226-251	**n.a.**	**n.a.**	C3

n.a.: not available.

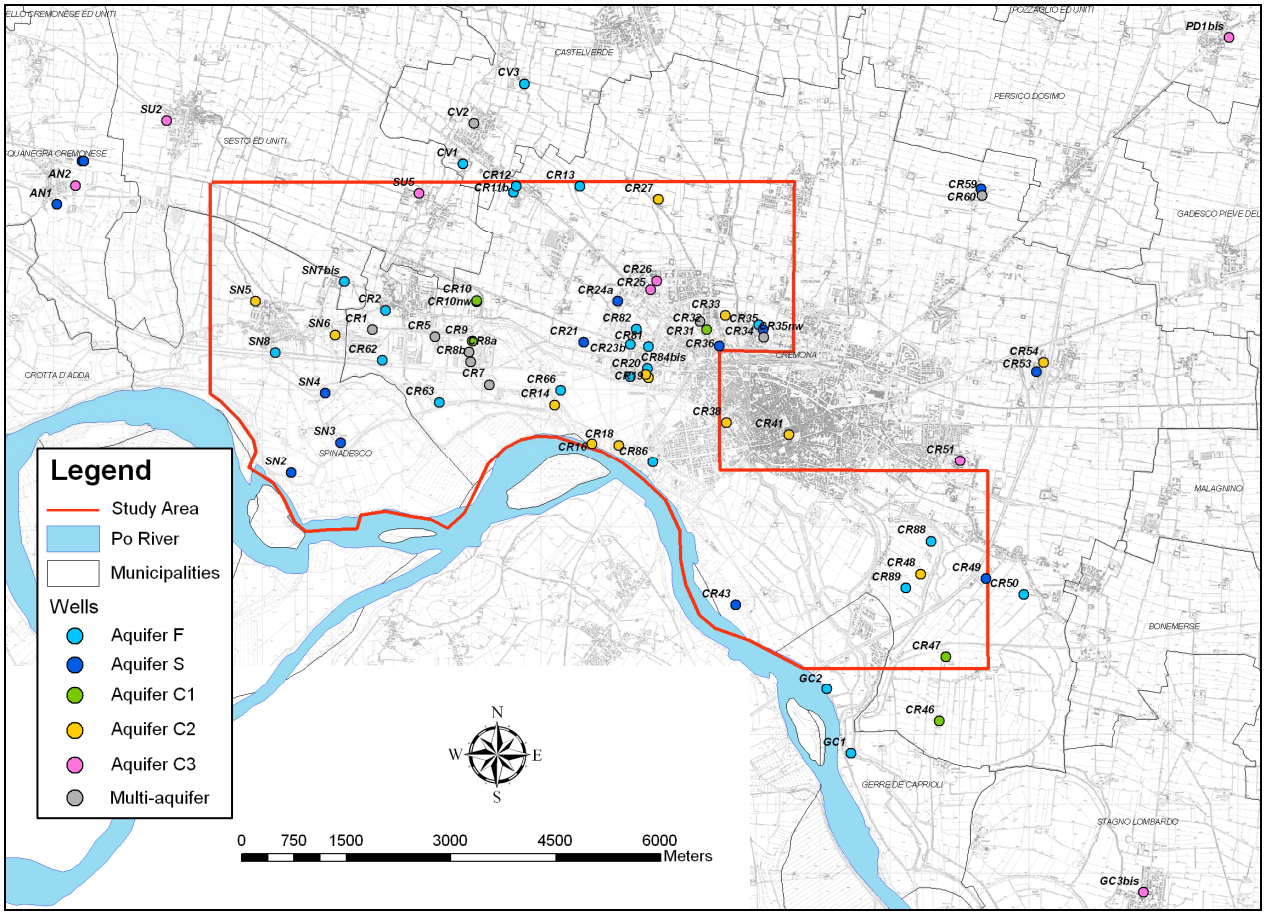

Figure 3.1. Location of sampling points (July 2010) classed for depths of production intervals.

3.1.1. Survey of July 2012

The survey of July 2012 involves a number of 16 sampling points (Table 3.2): 13 points are the same of the survey of July 2010, while 3 points are new (CR91, CR92, CR93). The 16 points, located in figure 3.2, are classified as follow: 4 points for aquifer F, 3 for aquifer S, 3 for aquifer C1, 3 for aquifer C2 and 3 for aquifer C3.

Table 3.2. Main characteristics of the sampling points in the survey of July 2012.

Code	Depth (m)	Screen (m)	Filter Pack (m)	Bentonite Seal (m)	Concrete Seal (m)	AQU.
CR66	8.2	2-8	**n.a.**	**n.a.**	**n.a.**	F
CR82	17	3-17	**n.a.**	**n.a.**	**n.a.**	F
SN8	10	5-10	8-10	0-8	absent	F
CR93	20	4-20	**n.a.**	**n.a.**	**n.a.**	F
SN2	32	25-31	23-30	0-23	absent	S
SN4	34	27-33	25-35	0-25	absent	S
CR24a	45	35-45	35-45	0-3; 24-35	absent	S
CR9	100	53-63; 67-81	52-100	absent	45-52	C1
CR10	90	69-73; 76-82; 84-87	66-90	absent	17-32; 56-66	C1
CR32	102	75-81; 85.5-88.4; 93-95.9	60-102	absent	0-60	C1
CR16	95	89-95	**n.a.**	**n.a.**	**n.a.**	C2
CR27	120	100-110	**n.a.**	0-2; 98-100	**n.a.**	C2
CR20	141	113-133.5	**n.a.**	**n.a.**	**n.a.**	C2
SU2	214	135-141; 191-203	135-141; 191-203	0-50; 74-77; 125-128; 145-148; 170-174	absent	C3
CR91	223	158-184; 195-213	158-184; 195-213	154.5-158; 184.5-188	0-30; 76-88; 140-154.5	C3
CR92	230	153-167; 176-186; 189-197; 206-209; 215-221	152-186.5; 188.5-209.5; 211.5-229	150-152; 186.5-188.5; 209.5-211.5	0-33; 45-67; 101-150	C3

n.a.: not available.

3.2. Definition of chemical parameters

The most important physicochemical parameters and some minor inorganic and organic chemical parameters were selected. Concerning the minor organic parameters, a list of species was defined on the basis of the past pollution phenomena which affected the study area. The detection of organic species is also important to understand the mechanism of mobilisation of As, Fe and Mn. Previous studies pointed out a possible relation between hydrocarbons pollution and Fe, Mn (e.g., Tucillo et al., 1999; Berbenni et al., 2000) and As (e.g., Gosh et al., 2003; Burgess and Pinto, 2005).

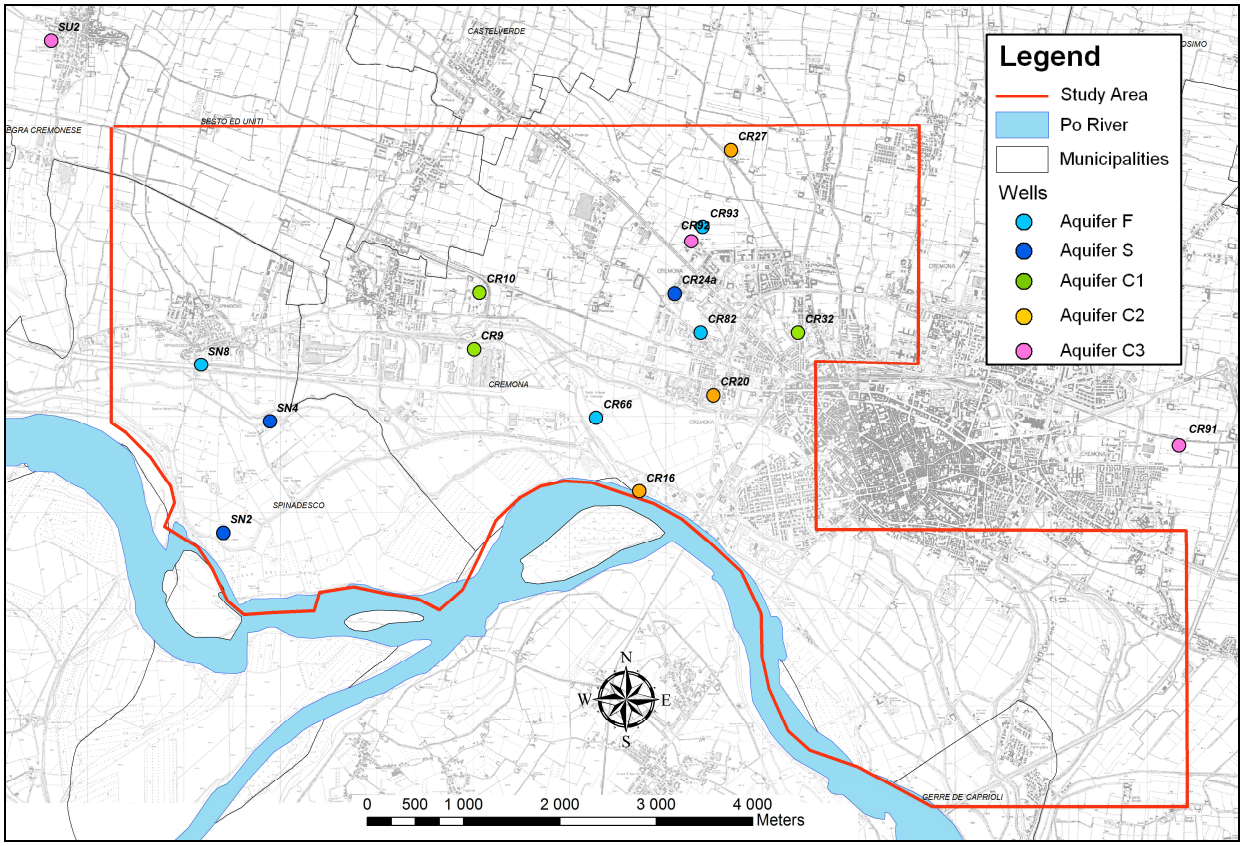

Figure 3.2. Location of sampling points (July 2012) classed for depths of production intervals.

3.2.1. Survey of July 2010

Table 3.3 reports the list of the selected parameters for the survey of July 2010. For the points concerning the superficial aquifers (F and S), the complete set of parameters listed in table 3.3 was detected, while for the deeper points (aquifers C1, C2 and C3) the organic compounds were excluded. This restriction of parameters for the deep aquifers is due to a budget optimization, but it can be also justified by a lower probability of occurrence of organic compounds in deep aquifers due to the anthropic origin (superficial sources) and, in some cases, to the lower density with respect to water (hydrocarbons, BTEX).

3.2.2. Survey of July 2012

The survey of July 2012 also considers stable isotope and microbiological analysis. The complete list of chemical, isotope and microbiological parameters is

reported in table 3.4. Concerning the isotope parameters, the water isotope (δ^2H e $\delta^{18}O$), the $\delta^{13}C$ in total inorganic carbon (TIC) and the $\delta^{15}N$ in ammonium were selected. The most probable number (MPN) of iron-reducing and sulfate-reducing bacteria were selected as microbiological parameters.

Table 3.3. Selected parameters for the survey of July 2010.

Physicochemical		**Minor inorganic**	**Minor organic**		
pH	ammonium	iron	**Aliphatic hydrocarbon**	**Chlorinated aliphatic hydrocarbon**	**Aromatic hydrocarbon**
temperature	nitrate	arsenic	total hydrocarbon	trichloromethane	benzene
RedOx potential	chloride	manganese	light hydrocarbon C<12	vinyl chloride	ethylbenzene
electrical conductivity	sulfate	total chrome	heavy hydrocarbon C>12	1,2-dichloroethane	styrene
	alkalinity	lead	methyl tert-butyl ether	1,1-dichloroethene	toluene
	calcium	zinc		trichloroethene	xylenes
	magnesium			tetrachloroethene	
	potassium			1,1-dichloroethane	
	sodium			1,2-dichloroethene	
				1,2-dichloropropane	
				1,2,3-trichloropropane	
				1,1,1-trichloroethane	

Table 3.3. Selected parameters for the survey of July 2012.

Physicochemical		**Minor inorganic**	**Stable isotope**	**Microbiological**
pH	ammonium	iron	δ^2H	MPN iron-reducing bacteria
temperature	nitrate	arsenic	$\delta^{18}O$	MPN sulfate-reducing bacteria
RedOx potential	chloride	manganese	$\delta^{13}C$	
electrical conductivity	sulfate	sulfide	$\delta^{15}N$	
	alkalinity			
	calcium			
	magnesium			
	potassium			
	sodium			

3.3. Definition of the sampling method

The public and private wells were sampled using the installed submersible pumps, while for the piezometers a portable sampling pump (Grundfos MP1) was used. In both cases, a purging with a number of well volumes between 2 and 4 times (Appelo and Postma, 2005) was done before sampling. The degree of purging was evaluated monitoring the pH and electrical conductivity over time. The sampled groundwater was collected in different sample bottles as reported in table 3.5. The samples for the analysis of metals and arsenic were acidified *in situ* without filtering due to turbidity-free conditions. In 6 samples of the survey of July 2010, a low turbidity was identified, so the samples were filtered and acidified in laboratory.

Table 3.5. Sample bottle for the detected parameters.

Parameters	**Bottle**
ammonium, nitrate, chloride, sulfate, alkalinity	0,5 L polyethylene
sulfide	0,1 L polyethylene acidified
Ca, Mg, K, Na, Fe, As, Mn, Cr, Pb, Zn	0,25 L polyethylene acidified
hydrocarbon C>12	1 L dark glass
hydrocarbon C<12, BTEX, MTBE, organochlorides	1 vial glass
δ2H, δ18O, δ13C	0,5 L polyethylene
δ15N	2 L polyethylene acidified
MPN iron-reducing and sulfate-reducing bacteria	2 L polyethylene

3.4. Execution of the surveys

The measurements and samplings were executed between 5th and 29th July 2010, in the first survey, and between 18th and 26th July 2012, in the second survey. In both cases, the duration of the survey was limited as possible in order to preserve homogeneous hydrogeological and hydrochemical conditions. All the collected information and detected data for each sampling point were organised in monographs.

GPS measurements

The planar coordinates (longitude and latitude) in the Gauss-Boaga system, the altitude of the reference points of the water level measurement and the altitude

of the ground level were measured. The differential GPS method, which allows a nominative error of 1 mm for coordinates and altitude, was used. The differential method is based on the simultaneous application of two receivers, the first one (base receiver) is placed on a reference point, the second one (rover receiver) is placed on the point of interest (wells). The difference between the reference value and the measured value in the reference points is then used to correct the measured value in the point of interest. The points of the downscaling of the IGM95 grid made by Regione Lombardia were used as reference points.

The GPS measurements were executed in the survey of July 2010 on 53 points of the total 73 defined sampling points, on the basis of the possibility of the water level measurement. In addition, GPS measurement was executed in 4 points where the hydrometric levels of the main rivers were measured.

Water level measurements

The water level measurement was only executed in the points where the well structure allows the introduction of the phreatimeter. In the industrial and water supply wells where the withdrawal cannot be stopped, the dynamic level was measured, while the static level was measured in all the other wells.

Concerning the survey of July 2010, the water level measurements were executed in 47 points. In order to relate the water table level to the watercourses level, the hydrometric levels of Po and Adda rivers were measured in 4 different points. In the survey of July 2012, the water level was measured in 9 points.

Hydrochemical analysis

The measurements of pH, electric conductivity, oxidation reduction potential and temperature were executed *in situ* using specific portable probes. The chemical parameters were detected in the laboratory "Servizio Ambiente S.n.c." of Gallarate (VA, Italy) following the analytical methods reported in table 3.6. The conservation of samples was provided by portable refrigerators.

In the survey of July 2010, 68 points were sampled, while, in the survey of July 2012, 14 points were sampled.

Stable isotope analysis

The analysis of stable isotope was conducted by "ISO4 S.n.c." in the laboratory of Torino (Department of Earth Science, University of Torino) and Pavia (CNR-IGG) following the analytical methods listed in table 3.7. Stable isotopes were

detected in 14 groundwater and in 1 surface water (Po river) samples collected in the survey of July 2012.

Microbiological analysis

The microbiological analysis was conducted in the laboratory of the Department of Environmental Science (University of Milano-Bicocca) following the analytical methods reported in table 3.8. These analysis were conducted in only 1 groundwater sample of the survey of July 2012.

Table 3.6. Applied analytical methods for chemical analysis.

Parameters	Method	Method description
ammonium	APAT CNR IRSA 4030 A2 Man 29 2003	spectrophotometry with Nessler's reagent
nitrate, chloride, sulfate	APAT CNR IRSA 4020 Man 29 2003	ion chromatography
alkalinity	APAT CNR IRSA 2010 B Man 29 2003	tritation
Ca, Mg, K, Na, Fe, Mn, Zn	APAT CNR IRSA 3020 Man 29 2003	inductively coupled plasma optical emission spectrometry (ICP-OES)
As	ISS.DAA.003.REV00	electro thermal atomization-atomic absorption spectroscopy (ETA-AAS)
Cr	ISS.DAA.008.REV00	electro thermal atomization-atomic absorption spectroscopy (ETA-AAS)
Pb	ISS.DAA.012.REV00	electro thermal atomization-atomic absorption spectroscopy (ETA-AAS)
hydrocarbon C<12, BTEX, MTBE, organochlorides	EPA 5021 A 2003 + EPA 8260 C 2006	gas chromatography–mass spectrometry (GC-MS)
hydrocarbon C>12	APAT CNR IRSA 5160 B2 Man 29 2003	IR spectrophotometry
sulfide	Standard Methods 4500-D 2001	spectrophotometry with methylene blue

Table 3.7. Applied analytical methods for isotope analysis.

Parameters	Standard	Error	Method
δ2H	V-SMOW2	± 1 δ‰	WS-CRDS
δ18O	V-SMOW2	± 0.2 δ‰	WS-CRDS
δ13C	PDB	± 0.2 δ‰	Kroopnick (1974)
δ15N	AIR	± 0.2 δ‰	Kjeldahl method & IRMS

Table 3.7. Applied analytical methods for microbiological analysis.

Parameters	Method
MPN sulfate-reducing bacteria	MIPAAF (2002)
MPN iron-reducing bacteria	Lovley and Phillips (1986); Braunschweig et al. (2012)

References

Appelo C. A. J. & Postma D. (2005) – *Geochemistry, groundwater and pollution (2nd edition)*. Balkema Publishers, Leiden, 649 pp.

Berbenni P., Pollice A., Canziani R., Stabile L. & Nobili F. (2000) – *Removal of iron and manganese from hydrocarbon-contaminated groundwaters.* Bioresource Technology 74 (2), 109-114.

Braunschweig J., Bosch J., Heister K., Kuebeck C. & Meckenstock R. U. (2012) – *Reevaluation of colorimetric iron determination methods commonly used in geomicrobiology*. Journal of Microbiological Methods 89, 41-48.

Burgess W. G. & Pinto L. (2005) – *Preliminary observations on the release of arsenic to groundwater in the presence of hydrocarbon contaminants in UK aquifers.* Mineralogical Magazine 69 (5), 887-896.

Ghosh R., Deutsch W., Geiger S., McCarthy K. & Beckmann D. (2003) – *Geochemistry, fate and transport of dissolved arsenic in petroleum hydrocarbon-impacted groundwater*. Petroleum hydrocarbons and organic chemicals in groundwater. American Petroleum Institute, National Ground Water Association. Costa Mesa, 266-280.

Kroopnick P. (1974) - *The dissolved O2-CO2-13C system in the eastern equatorial pacific*. Deep Sea Research and Oceanographic Abstracts 21(3), 211-227.

Lovley D. R. & Phillips E.J.P. (1986) – *Organic matter mineralization with reduction of ferric iron in anaerobic sediments*. Applied and Environmental Microbiology 51(4), 683-689.

MIPAAF (2002) – *Approvazione dei metodi ufficiali di analisi microbiologica del suolo (Endorsement of official methods for microbiological analysis)*. D.M. 8 luglio 2002.

Tucillo M. E., Cozzarelli I. M. & Herman J. H. (1999) – *Iron reduction in the sediments of a hydrocarbon-contaminated aquifer.* Applied Geochemistry 14 (5), 655-667.

4. 3D aquifer modelling

A 3D modelling of deposits texture, hydraulic conductivity and effective porosity distribution for the studied multi-layer aquifer was implemented. Special attention was focused on the distribution of peat, which can play a significant role in groundwater chemistry (e.g., Francani et al., 1994; McArthur et al., 2001; Rowland et al., 2006). The modelling was performed using the software GOCAD (Paradigm, 2008).

4.1. Deposits texture and hydrogeological parameters modelling

The modelling consists in ordinary kriging interpolation of deposits texture percentage, hydraulic conductivity and effective porosity values derived from a numerical coding of well logs. The whole hydrogeological characterization area (par. 1.1), where the well stratigraphies were collected (chap. 2), was considered in the modelling.

The implementation of the 3D aquifer modeling involves the following steps: (a) definition of the boundary surfaces of the hydrogeological system; (b) construction of the 3D grid; (c) construction of the input datasets for the interpolation from the well logs coding; (d) analysis of the variograms; (e) execution of ordinary kriging interpolation and (f) description of results.

4.1.1. Definition of the boundary surfaces

The definition of boundary surfaces is necessary to the subsequent 3D grid construction. Two boundary surfaces were defined, representing the top and the bottom of the hydrogeological system. The ground surface was considered as top of the system (Figure 4.2). The digital elevation model (DEM) developed in the RICLIC-WARM project (Cavallin and Maggi, 2006) with a resolution of 250x250 m was used to represent the ground surface. The bottom of the "Aquifer Group A" (Regione Lombardia and Eni Divisione Agip, 2002) was considered as bottom of the system (Figure 4.2). This surface was created by the interpolation of elevation points derived from the isohypse-map of the "Aquifer Group A" bottom, that is available on the webgis "Geoportale della Lombardia" (*www.cartografia.regione.lom*

bardia.it/geoportale). A resolution of 250x250 m was used for the bottom surface elaboration.

4.1.2. Construction of the 3D grid

The construction of the model grid involves the definition of an initial regular grid, which is characterised by a constant cell size and thickness. This regular grid is then vertically deformed due to better reproduce the morphology of the system.

The initial regular grid was set with a cell size of 200x200 m and a thickness of 5 m. The cell size value was chosen on the basis of the average distance between the wells, that is equal to 429 m, in order to obtain one input value every two cells, that can be considered a good ratio for the interpolation. It should be noted that the average distance between the wells was calculated excluding the superficial piezometers in order to obtain a valid information for the deeper parts of the system.

The vertical deformation of the grid was done using the two defined boundary surfaces: the superficial layers were deformed parallel to the DEM, the deeper layers were deformed parallel to the bottom of the Aquifer Group A, while the intermediate layers were deformed proportional to the two surfaces. The final deformed grid (Figure 4.2) results with an average cell thickness of 2.8 m, a minimum thickness of 1.7 m, concerning the north-western part of the study area, and a maximum thickness of 5.3 m, concerning the south-eastern part.

In summary, the resulting 3D grid has 1˙404˙000 cells, arranged in 144 rows, 150 columns and 65 layers. The cell size is constant (200 m), while the cell thickness is variable (average value of 2.8 m) according to the morphology of the system.

4.1.3. Construction of the datasets from the well logs coding

The input datasets for the interpolation were constructed considering the 550 stratigraphies collected and stored in TANGRAM database (chap. 2). TANGRAM elaborates a numerical coding of the stratigraphic logs on the basis of the lithological composition. By means of this coding, TANGRAM can extract numerical values of texture percentage, hydraulic conductivity and effective porosity for each

stratigraphic level, as reported by Bonomi (2009). The texture percentages of each stratigraphic level are calculated from its codified lithological composition using a weighting system, which is derived from the Italian Geotechnical Association (AGI) recommendation. The stratigraphic level can be up to a few centimetres, user-defined. The hydraulic conductivity and effective porosity values are calculated as follow: a default value is assigned for each lithology which composes the stratigraphic level on the basis of the reference values of Freeze and Cherry (1979) and Fetter (1994); these values are then averaged using the same weighting system applied to the lithological composition.

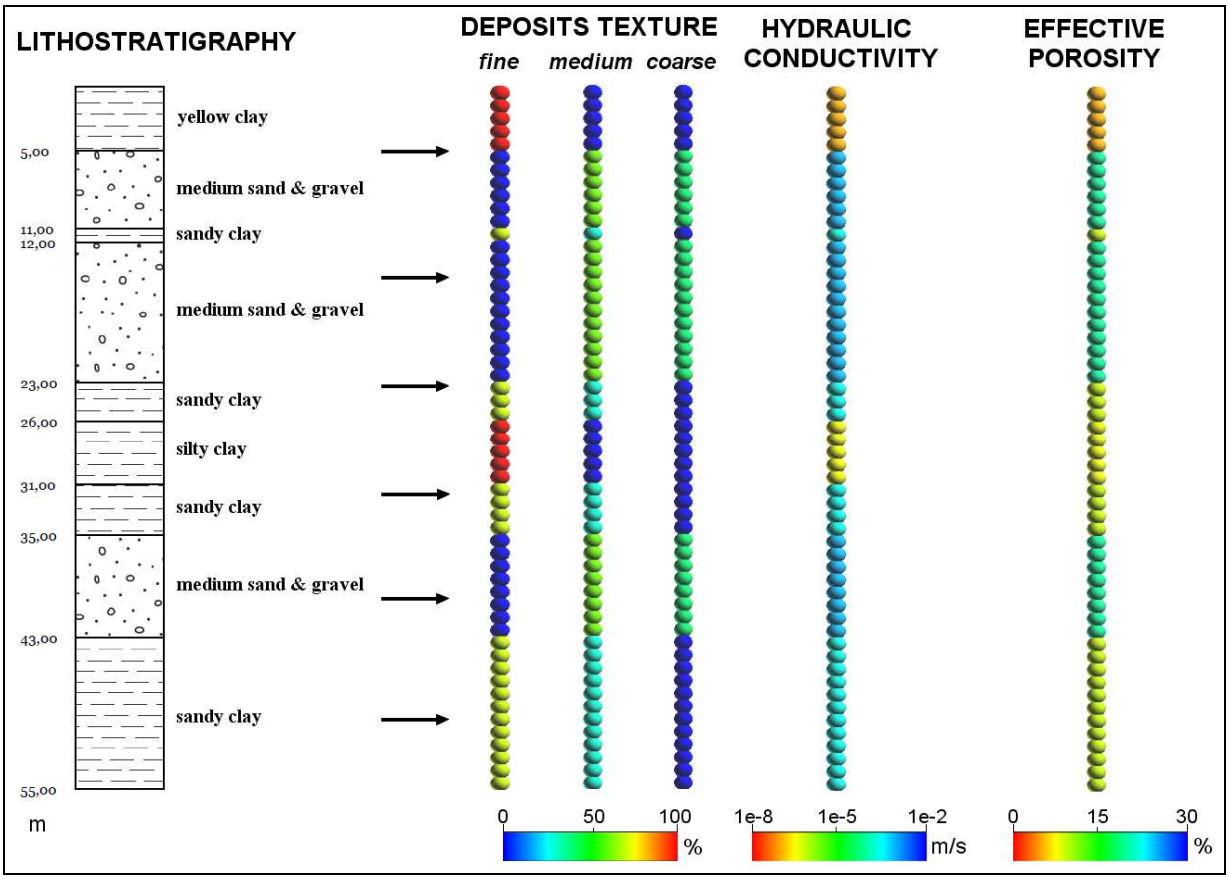

Figure 4.1. Example of numerical coding of well log, in this case the vertical extraction and coding range is equal to 1 m.

In the present work, five datasets were constructed following this well log coding (Figure 4.1) with regard to deposits texture and hydrogeological parameters: (1) percentage values of fine-grained deposits (clays, silts, peats); (2) percentage values of medium-grained deposits (sands); (3) percentage values of coarse-grained deposits (gravels, pebbles); (4) hydraulic conductivity values; (5) effective

porosity values. In the coding process, a vertical extraction range equal to 2 m was imposed. This value represents a compromise between the level of detail and the computational requirements.

4.1.4. Variogram analysis and ordinary kriging interpolation

The five datasets were imported in the 3D grid (Figure 4.2) and they were subsequently subjected to geostatistical analysis.

The experimental variograms were calculated using the *"areal variogram with XYW trasformation using top horizon and bottom horizon"* method (Paradigm, 2008). This method considers the following steps: (a) the data are transformed from the XYZ space, where Z represents the elevation, to the XYW space, where W represents the scaled elevation to the [0,1] interval, considering the two boundary surfaces as upper and lower limits; (b) the 2D variogram function is calculated for different layers, which are created considering the W values (Figure 4.3). By this way, the 3D variogram is composed by the sum of the 2D variograms calculated for each layer - layers that are consistent to the morphology of the system. This method can be applied with good results to stratified system where spatial correlations could be identified along the horizontal direction, while different depositional events are overlapping in the vertical direction.

In order to identify the presence of anisotropies in the datasets, the experimental variograms were calculated along four different azimuths, which are 0° (N-S direction), 45° (NE-SW direction), 90° (W-E direction) and 135° (SE- NW direction). A tolerance of 22.5° was imposed.

The calculated directional experimental variograms have similar profiles for the five analysed parameters, with the exception of coarse-grained deposits percentages. The four directional variograms for this parameter result as follow: the variance quickly increases and then it reaches a constant maximum at short distance. This profile could indicate the absence of significant spatial correlations between the data. A hypothetical cause of this could be the general absence of coarse-grained deposits in the studied system. The analysis of experimental directional variograms calculated for medium-grained and fine-grained deposits percentages, hydraulic conductivity and effective porosity values allows to identify a significant spatial correlation between the data. Figure 4.4 shows the directional variograms for the fine-grained deposits as an example.

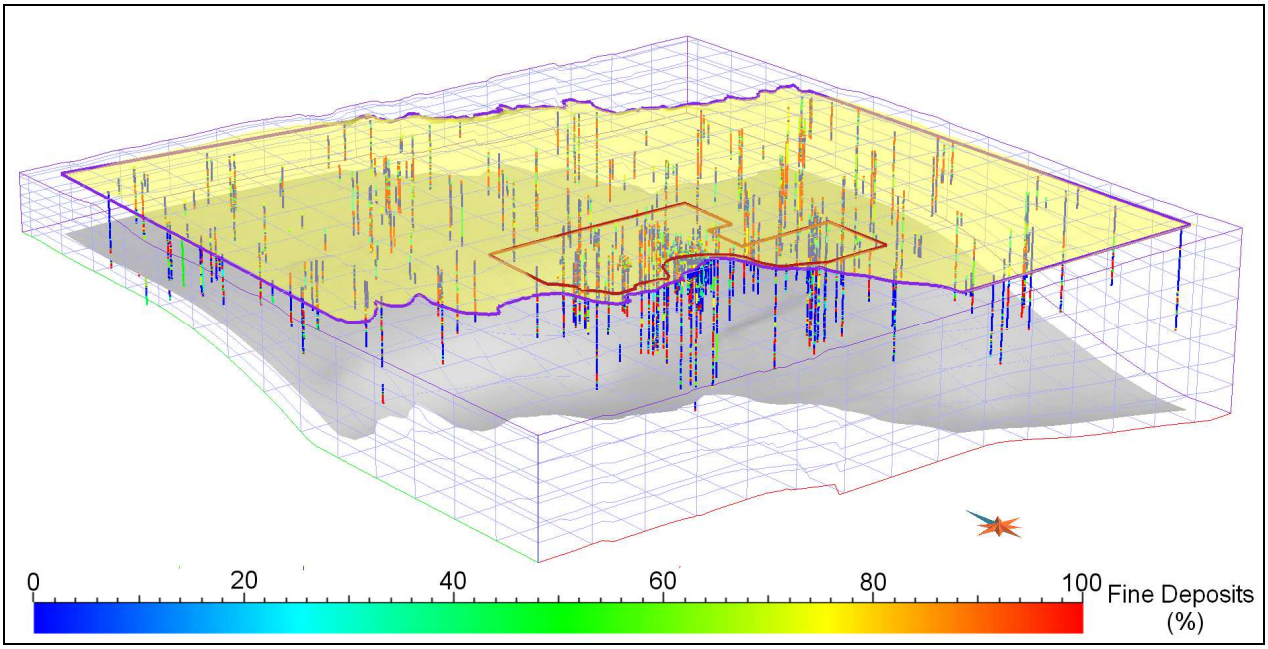

Figure 4.2. Importation of datasets in the 3D grid (example of the fine-grained deposits dataset); the grid is displayed with groups of 1000 cells; violet perimeter: hydrogeological characterization area; red perimeter: study area; yellow surface: top boundary surface (DEM); grey surface: bottom boundary surface ("Aquifer Group A" bottom).

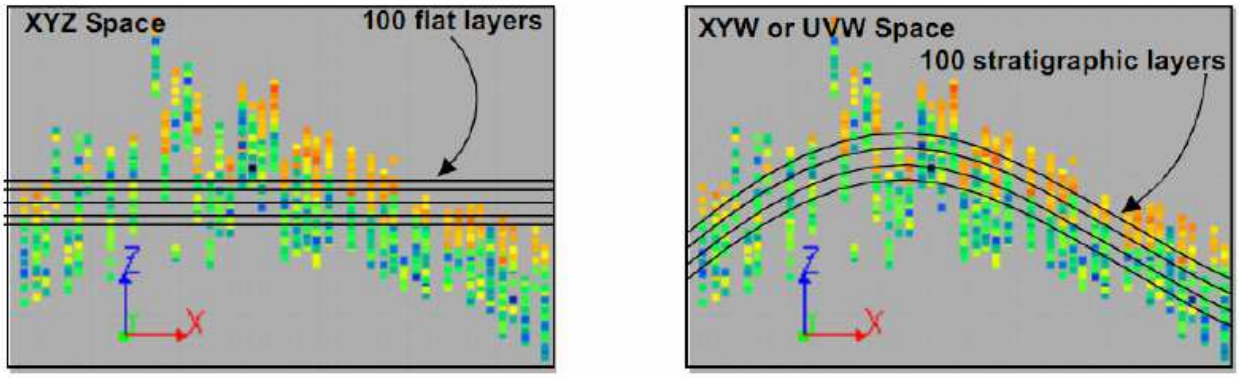

Figure 4.3. Creation of layers for the 2D variogram calculation considering Z (on the left) and W (on the right) values; from Del Rosso (2011).

The four directional variograms generally have a similar profile. A small difference could be seen for the variograms with azimuth 0°, 90° and 45° which have higher range values compared to the variogram with azimuth 135°. This characteristic could be interpreted with the presence of a spatial correlation over longer distance in N-S, NE-SW and W-E directions. A hypothetical geological explanation of this could be related to the presence of different alluvial deposits in the Oglio river zone, which is in the north-eastern part of the study area, with respect to the Adda-Po

rivers zone, which is in the southern and south-western part. The Oglio area is mainly characterized by fine deposits as silt and clay (Beretta et al., 1992), while the Adda-Po area is characterized by medium-coarse deposits as sand and gravel, which could be related to higher energy depositional events. The spatial correlation that can be also observed for the azimuth 135° could be related to the main flow direction of the Oglio, Adda and Po rivers (Ciotoli and Finoia, 2005).

It should be noted that for the hydrogeological conductivity dataset the geostatistical analysis was applied after a $\log_{10}$ transformation. This procedure was used in previous studies (e.g. Martin and Frind, 1998) in order to obtain normally distributed data, which lead to better results with kriging interpolation.

The analysis of experimental directional variograms shows that significant differences were not identified in the four investigated directions for the five analysed parameters. Therefore omnidirectional experimental variograms were considered in the variogram modelling. The main characteristics of the chosen variogram models are listed in Table 4.1. Figure 4.5 shows the variogram model for the fine-grained deposits that fits the omnidirectional experimental variogram, as an example. The exponential model was chosen according to the best data fitting. The ordinary kriging method, which is suitable for the datasets without trends (Armstrong, 1998), was used for the interpolation.

4.1.5. Results description

In the followings, a general description of results of the kriging interpolation in the whole hydrogeological characterization area is given. Afterwards, a focus on the hydrochemical study area is showed: 3D maps of the distribution of the five analysed parameters (percentage of fine-grained, medium-grained and coarse-grained deposits, hydraulic conductivity and effective porosity values) are presented. A detailed description of the hydrogeological characteristics of the hydrochemical study area is finally given.

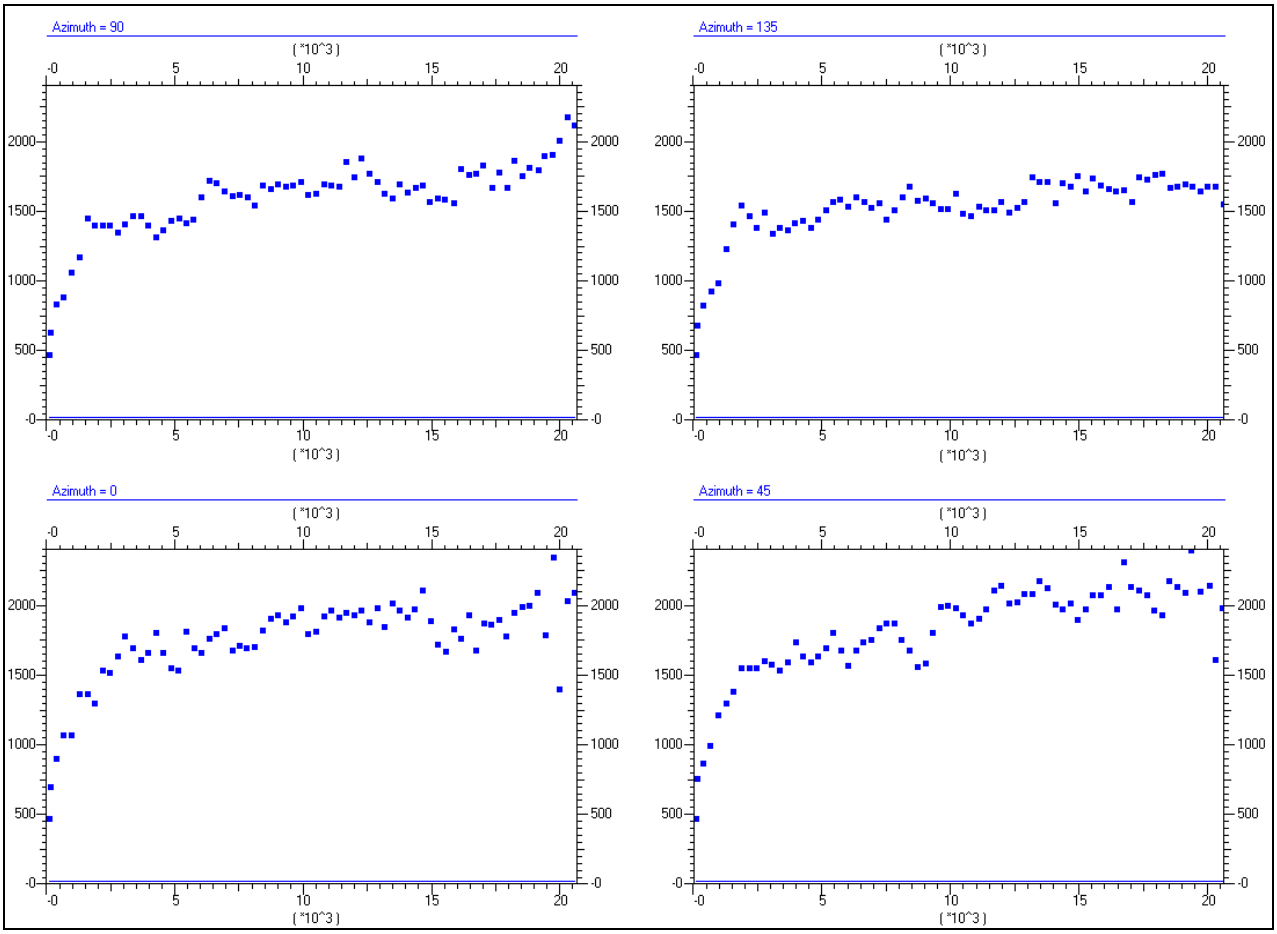

Figure 4.4. Experimental variograms for the fine-grained deposits in the investigated directions (0°, 45°, 90°, 135° azimuths).

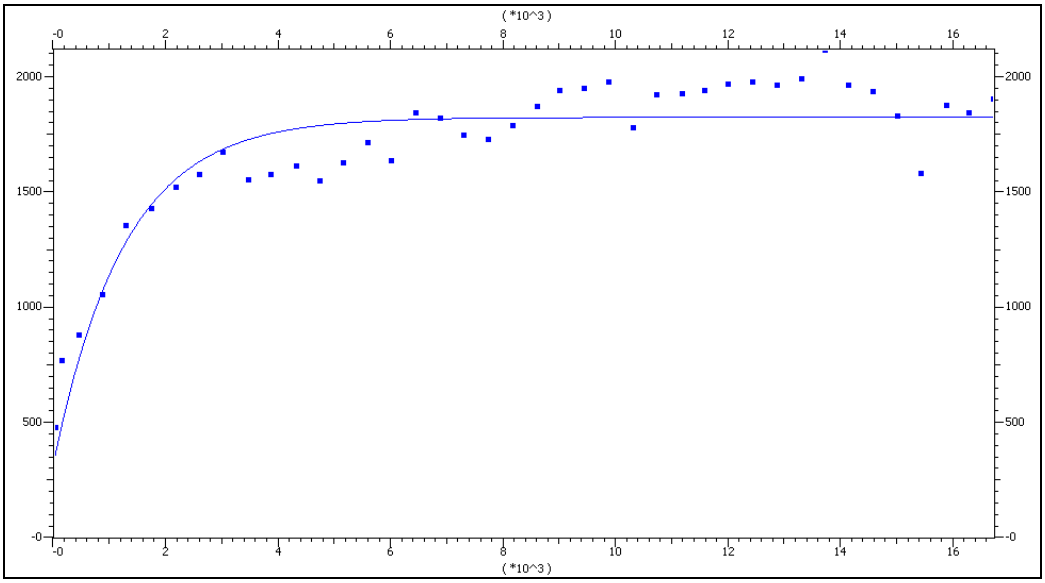

Figure 4.5. Model variogram for the omnidirectional experimental variogram concerning the fine-grained deposits.

Table 4.1. Main characteristics of the imposed variogram models.

Parameter	Model type	Nugget effect	Sill	Range
Fine deposits	exponential	300	1750	4000
Medium deposits	exponential	250	1589	4100
Coarse deposits	exponential	50	263	2081
Log_{10}(conductivity)	exponential	0.4	2.6	4000
Effective porosity	exponential	6	33	3800

Hydrogeological characterization area

Coarse-grained deposits

The mean and median values of coarse-grained deposits percentage result of 0.6% and 4.9%. These values indicate a small presence of coarse-grained deposits (gravels and pebbles) in the area. Higher values can be found in the southern part of the area, in proximity of the Po river. This characteristic could be related to the past Po river activity which was characterized by higher energy depositional events.

Medium-grained deposits

The medium-grained deposits (sands) have higher percentages. The mean and median values result of 50.9% and 50.8%. In the vertical direction, an alternation of layers with high and low percentages of medium-grained deposits can be identified. This is related to the multi-aquifer characteristic of the system. In general, a higher content of medium-grained deposits can be identified in the southern part of the area, near the Po river, while a lower content characterizes the north-eastern part of the area, in proximity of the Oglio river.

Fine-grained deposits

The fine-grained deposits (silts, clays, peats) have also high percentages. The mean and median values result of 43.8% and 44.2%. Considering the substantial absence of coarse-grained deposits, the fine-grained deposits distribution could be considered as complementary to the medium-grained deposits distribution.

Hydraulic conductivity

The mean and median values of hydraulic conductivity result of $2.4 \cdot 10^{-4}$ and $6.8 \cdot 10^{-5}$ m/s. These values can be related to sand and silty sand (Freeze and Cherry, 1976). The whole analysed system can be described as vertical alternation of higher (10^{-3}-10^{-5} m/s) and lower (10^{-7}-10^{-8} m/s) conductivity layers.

Effective porosity

The mean and median values of effective porosity result of 14.4% and 14.8%. As individuated for the hydraulic conductivity, the whole system is characterized by a vertical alternation of higher (15-17%) and lower (5-10%) values.

Hydrochemical study area

The 3D maps of the resulted distribution of fine-grained, medium-grained and coarse-grained deposits percentages, hydraulic conductivity and effective porosity values are showed in figure 4.6, 4.8, 4.9, 4.10 and 4.11. Figure 4.7 reports the kriging variance of fine-grained deposits percentages, as an example. The variance increases in the deeper parts of the system due to a less number of wells which reach these depths. The kriging variance for the other investigated parameters results similar to the variance of fine-grained deposits.

From the analysis of the distribution of deposits textures and hydrogeological parameters, the typical characteristics of the alluvial multi-aquifer system result. The system could be described as alternation of silty-clayey layers with lower conductivity (10^{-7}-10^{-8} m/s) and sandy layers with higher conductivity (10^{-3}-10^{-5} m/s).

The hydrogeological characteristics modelling of the aquifer system leads to the identification of different aquifer and aquitard units. These units are described in the following.

Ground level

In the study area, superficial fine-grained deposits are located in the central-northern part of the area and they generally characterize the Po river valley (Figure 4.12). The presence of superficial silty-clayey deposits can decrease the aquifer recharge rate and it can also influence the groundwater chemistry, favouring the occurrence of reducing conditions. In the central part of the area, behind the Po

river valley, the superficial deposits are mainly formed by sands. This characteristic favours higher recharge rates.

Aquifer F

Aquifer F concerns the first 20-25 m of depth and it is generally characterized by sandy deposits (K ~ 10^{-4} m/s). The conductivity increases up to around 10^{-3} m/s in proximity of the Po river (southern part) and in the "Navigli" valley (western part). A higher content of silty-clayey deposits characterizes the central-northern zone and the Po valley, in continuity with the superficial fine deposits. In these parts, the conductivity is around 10^{-6} m/s. In the north-eastern zone the aquifer has more fine deposits, which can be referred to the "Main Plain Level" unit.

Aquitard F/S

The aquitard between aquifers F and S has a thickness of 5-10 m, from around 25 to 35 m b.s.. Aquitard F/S extends in the central part of the area and it is formed by silty-clayey deposits (K up to 10^{-8} m/s). Therefore, aquifers F and S result locally separated in the central part of the area, while in the remaining zones they result in connection, with possible exchange of water.

Aquifer S

Aquifer S has a thickness of 20-25 m, from around 35 to 60 m b.s.. In the southern part of the area, near the Po river, the aquifer is mainly composed by sandy deposits (K ~ 10^{-4} m/s), while, in the northern part of the area, silty sand deposits are dominant, with a hydraulic conductivity value of around 10^{-5} m/s.

Aquitard S/C1

The aquitard between aquifers S and C1 has a thickness of 15-20 m, from around 60 to 80 m b.s.. The aquitard extends in the central part of the area which with silty-clayey deposits (K between 10^{-7} and 10^{-8} m/s), and in the western part with silty sand deposits (K ~ 10^{-6} m/s). In the eastern part of the area the sediments are mainly composed by sand, and thus, a continuity with the overlaying aquifer S and, in a few zones, with the underlying aquifer C1 can be assumed.

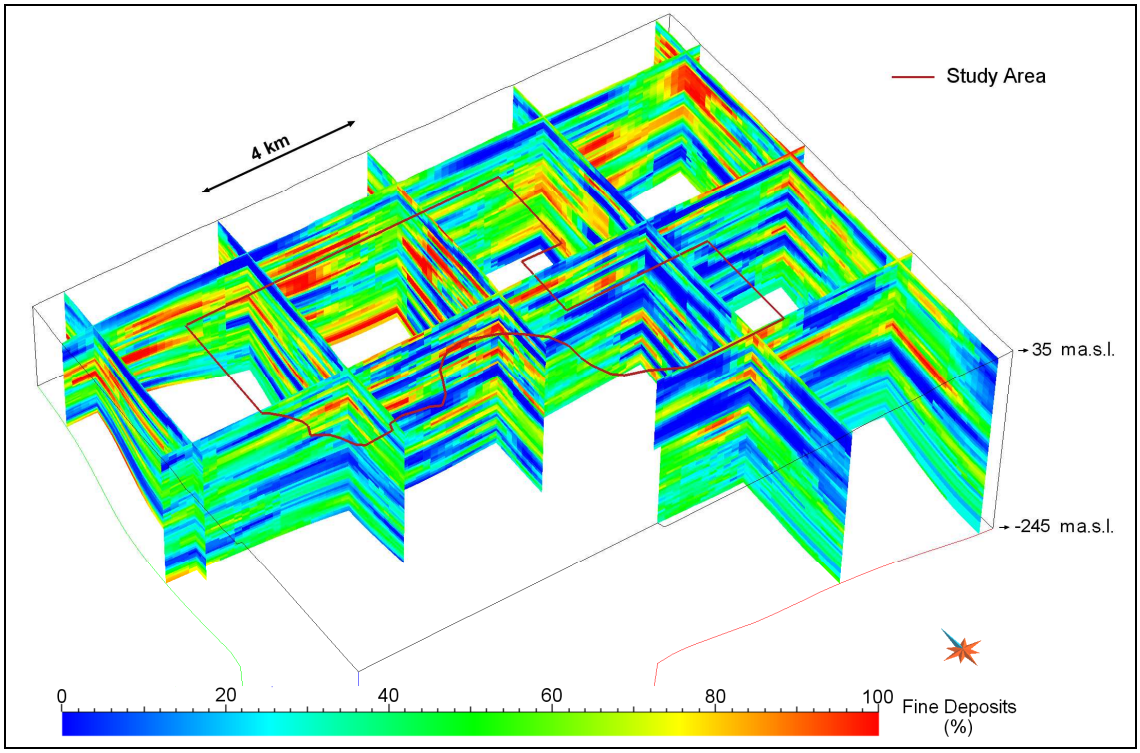

Figure 4.6. 3D distribution of fine-grained deposits in the hydrochemical study area with N-S and E-W cross sections.

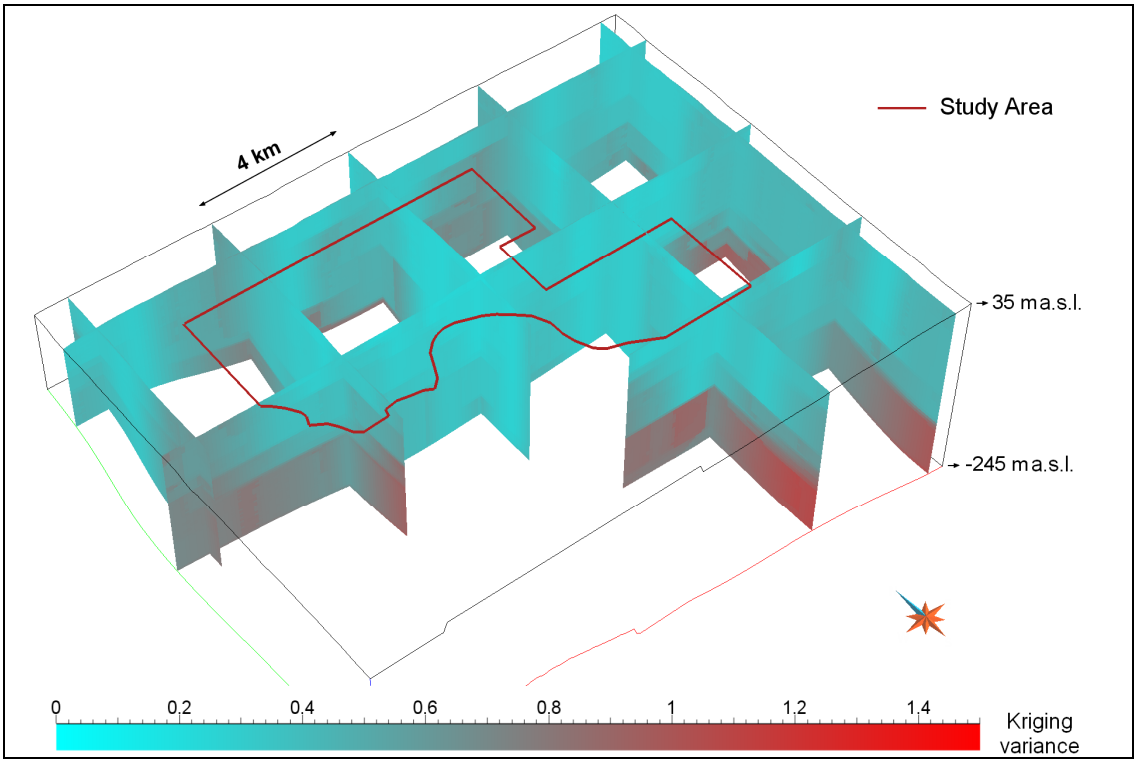

Figure 4.7. 3D distribution of kriging variance for fine-grained deposits interpolation with N-S and E-W cross sections.

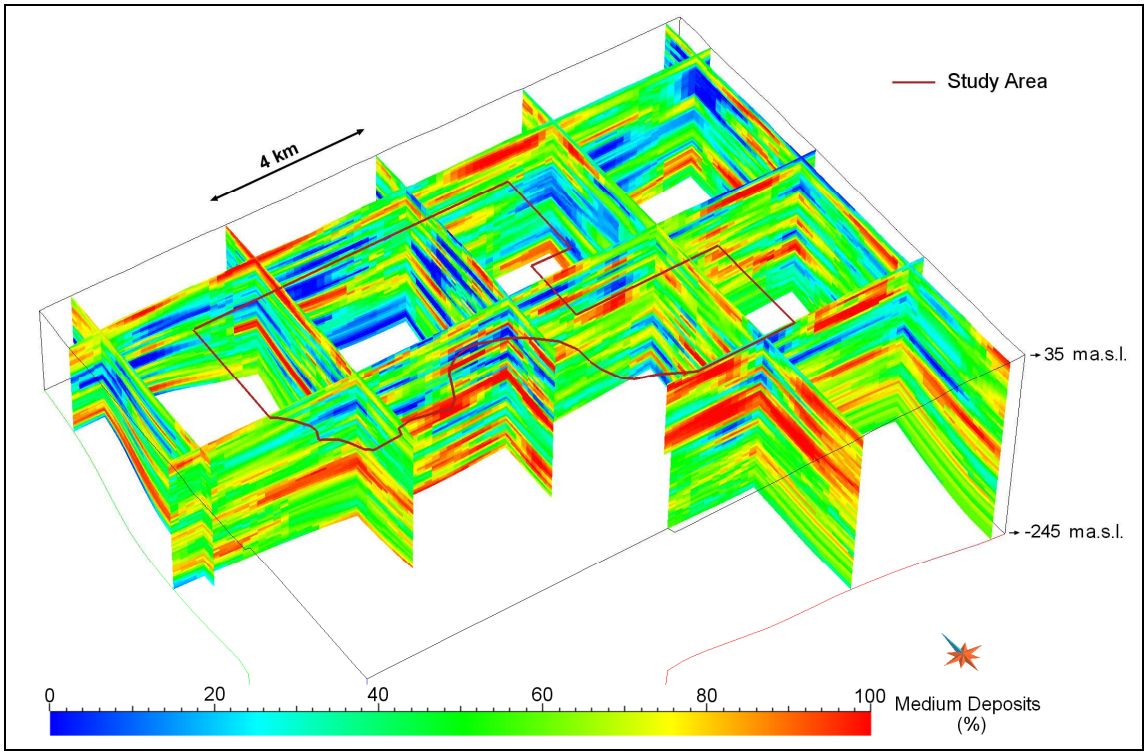

Figure 4.8. 3D distribution of medium-grained deposits in the hydrochemical study area with N-S and E-W cross sections.

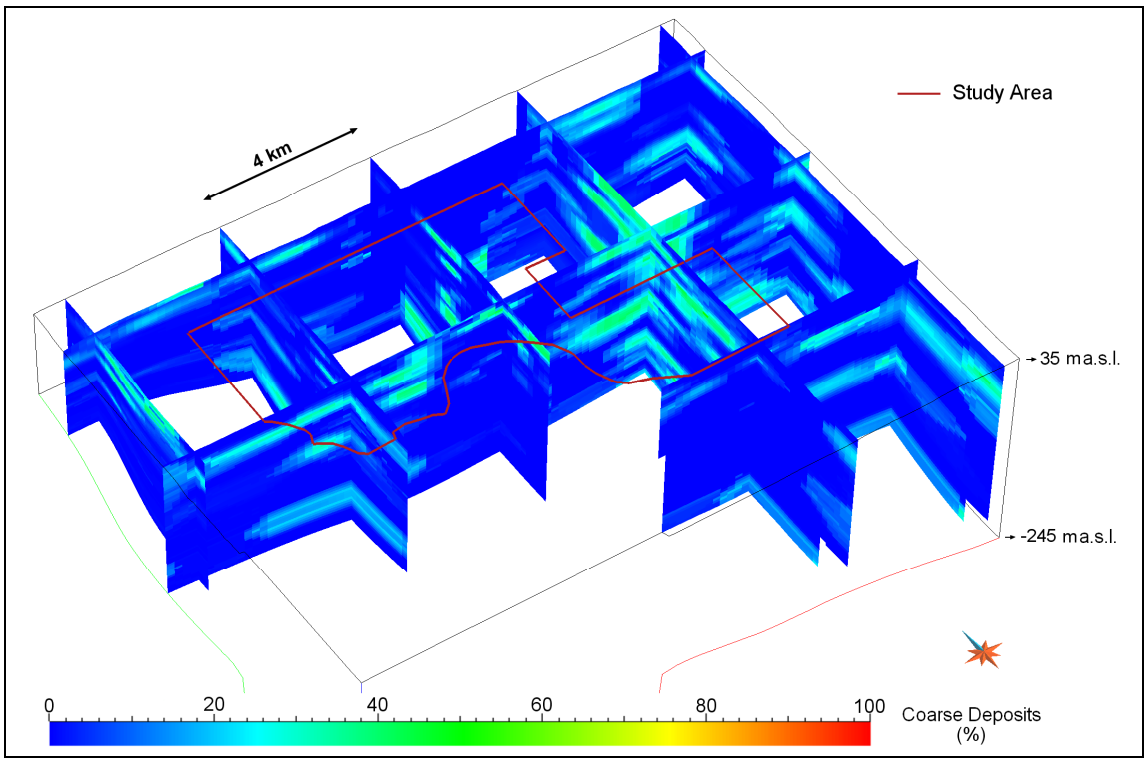

Figure 4.9. 3D distribution of coarse-grained deposits in the hydrochemical study area with N-S and E-W cross sections.

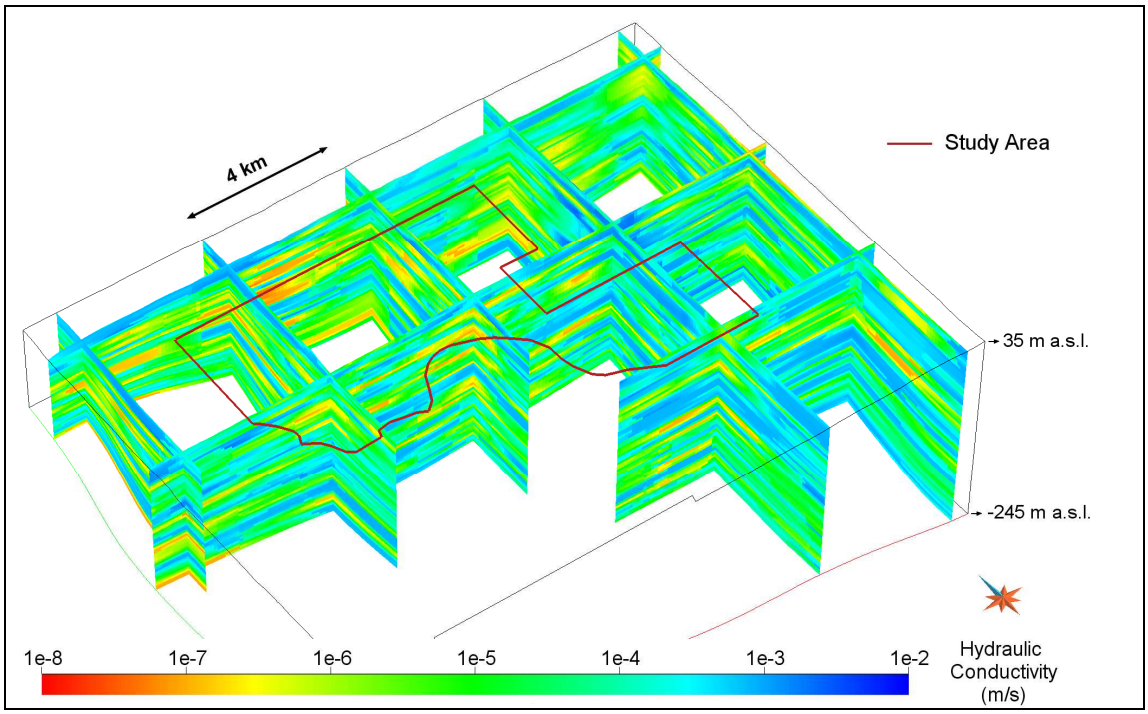

Figure 4.10. 3D distribution of hydraulic conductivity in the hydrochemical study area with N-S and E-W cross sections.

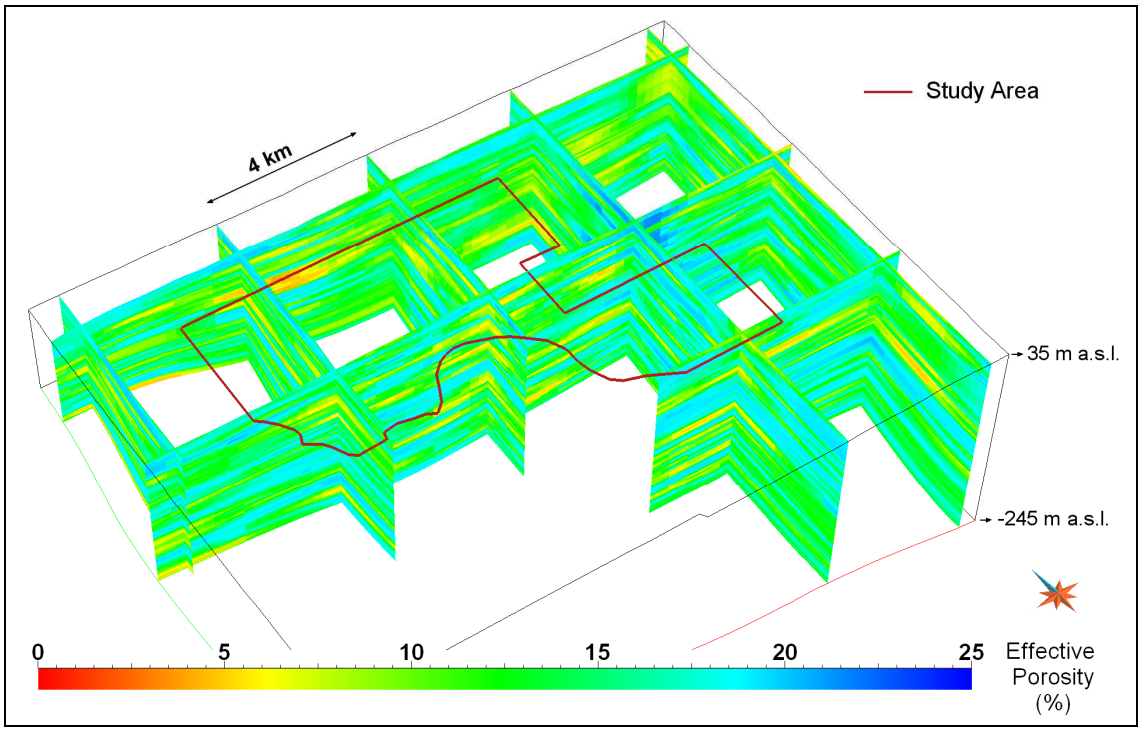

Figure 4.11. 3D distribution of effective porosity in the hydrochemical study area with N-S and E-W cross sections.

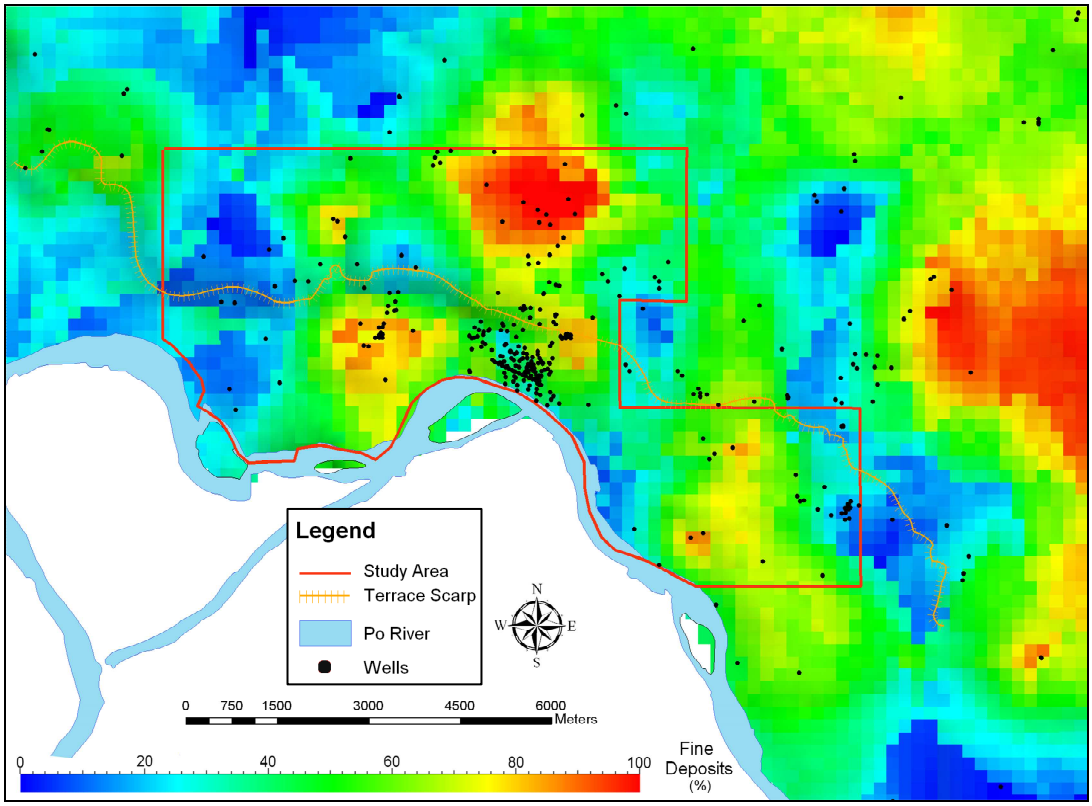

Figure 4.12. Distribution of superficial fine-grained deposits.

Aquifer C1

Aquifer C1 has a thickness of 15-20 m, from around 80 to 90 m b.s.. Aquifer C1 has heterogeneous characteristics: in some zones of the central and eastern part of the area the aquifer is mainly composed by sands (K ~ 10^{-4} m/s), while in the remaining parts silty sand deposits are dominant (K around 10^{-5}-10^{-6} m/s).

Aquitard C1/C2

The aquitard between aquifers C1 and C2 has a thickness of 15-20 m, from around 90 to 110 m b.s.. This aquitard has a heterogeneous distribution of silty-sandy and silty-clayey deposits with an average hydraulic conductivity of 10^{-6} m/s. In the south-eastern part of the area, sandy deposits are dominant (K around 10^{-4}-10^{-5} m/s).

Aquifer C2

Aquifer C2 can be locally separated in an upper part (aquifer C2A) and a lower part (aquifer C2B).

Aquifer C2A

Aquifer C2A has a thickness of 20-25 m, from around 110 to 135 m b.s.. In the central and western parts of the area the aquifer is mainly composed by silty sand deposits (K around 10^{-4}-10^{-5} m/s), while in the eastern part there are mainly sandy deposits (K ~ 10^{-4} m/s). A separation between aquifers C2A and C2B can be identified in the western and central parts of the area due to silty-clayey deposits, while aquifer C2 can be considered as a unique body in the eastern part.

Aquifer C2B

Aquifer C2B has a thickness of 30-35 m, from around 135 to 165 m b.s.. This aquifer has a more homogeneous distribution of sandy deposits. The hydraulic conductivity ranges from 10^{-5} to 10^{-3} m/s. Aquifer C2A can be considered as an important water resource due to its higher thickness and hydraulic conductivity values.

Aquitard C2/C3

The aquitard between aquifers C2 and C3 has a thickness of 15-20 m, from around 165 to 185 m b.s.. This aquitard mainly extends in the central part of the area with silty-clayey deposits (K around 10^{-4}-10^{-5} m/s).

Aquifer C3

Aquifer C3 has a thickness of 70-80 m, from around 185 to 260 m b.s. Considering that only a few wells (35) reach these depths, a general description can be done for this aquifer. Aquifer C3 is considered as a unit even if some separations can be detected. Three aquifer subunits, in the central part of the area, and two aquifer subunits, in the eastern part, can be identified.

Hydrochemical study area summary

The analysis of the resulted distributions of deposits texture and hydrogeological parameters leads to a detailed description of the studied multi-aquifer system. The preliminary classification of the aquifer system (par. 1.2), that concerns the identification of 5 main aquifer units (F, S, C1, C2 and C3), is generally confirmed. The heterogeneity in the vertical and horizontal extent of the aquitards generates a different level of separation between aquifers, which can be

connected in some parts, with possible water exchanges, and separated in other parts. The aquifers result more separated in the central part of the study area, which refers to the western urban territory of Cremona town, and less separated in the eastern part of the study area, which refers to the eastern urban territory of Cremona town.

A qualitative validation of the aquifer modelling was done comparing the results of the kriging interpolation with a classical hydrogeological cross section (Figure 4.13). The figure shows a general good agreement between the fine-grained deposits distribution and the hydrogeological section. Where the input data (well stratigraphies) are absent, the validity of the interpolation results is lower, as shown in the southern deep part of the section.

In addiction, a quantitative validation of the hydraulic conductivity modelling was done, comparing the values that result from the applied methodology (numerical coding of the well stratigraphies executed by TANGRAM) with field pumping test values. A collection of transmissivity values from field tests, executed in the study area, was done from literature and from administrative procedures for groundwater withdrawals (unpublished data). The hydraulic conductivity values were derived from the collected transmissivity values considering the thickness of the involved aquifer. The conductivity value from field test was compared with the mean value of the resulting values from the stratigraphy coding (extraction range of 1 m) for the same wells. This comparison was done for the 9 wells listed in table 4.2. The comparison shows good results (Figure 4.14), the differences between the two hydraulic conductivity values for each considered well are contained into a half order of magnitude.

Table 4.2. Comparison between pumping tests (K test) and codified (K TANGRAM) hydraulic conductivity values considering the same aquifer thickness (b).

Well	Acq.	Reference	T test (m2/s)	b (m)	K test (m/s)	K TANGRAM (m/s)	Log (K t.) - Log (K TAN.)
PA	C2	Cambi et al, 2005	2.75E-02	32.6	8.44E-04	7.17E-04	0.07
PB	C3	Cambi et al, 2005	2.93E-02	45.0	6.51E-04	8.21E-04	-0.10
SN6	C2	A.P. (Daguati, 2001)*	1.30E-02	17.0	7.64E-04	8.80E-04	-0.06
CR49	S	A.P. (Daguati, 2000)*	2.35E-02	15.0	1.56E-03	1.46E-03	0.03
CR24a	S	A.P. (Daguati, 2004)*	3.42E-03	10.0	3.42E-04	1.00E-04	0.53
CR13	F	A.P. (Daguati, 2005)*	9.55E-03	24.0	3.98E-04	8.00E-04	-0.30
CR12	F	A.P. (Daguati, 2005)*	6.41E-03	35.0	1.83E-04	5.41E-04	-0.47
CR2	F	A.P. (Baracca, 2007)*	7.50E-03	15.2	5.00E-04	6.70E-04	-0.13
CR33	C2	A.P. (Daguati, 2005)*	1.21E-02	35.0	3.47E-04	7.94E-04	-0.36

(*) Unpublished data from administrative procedures for groundwater withdrawals.

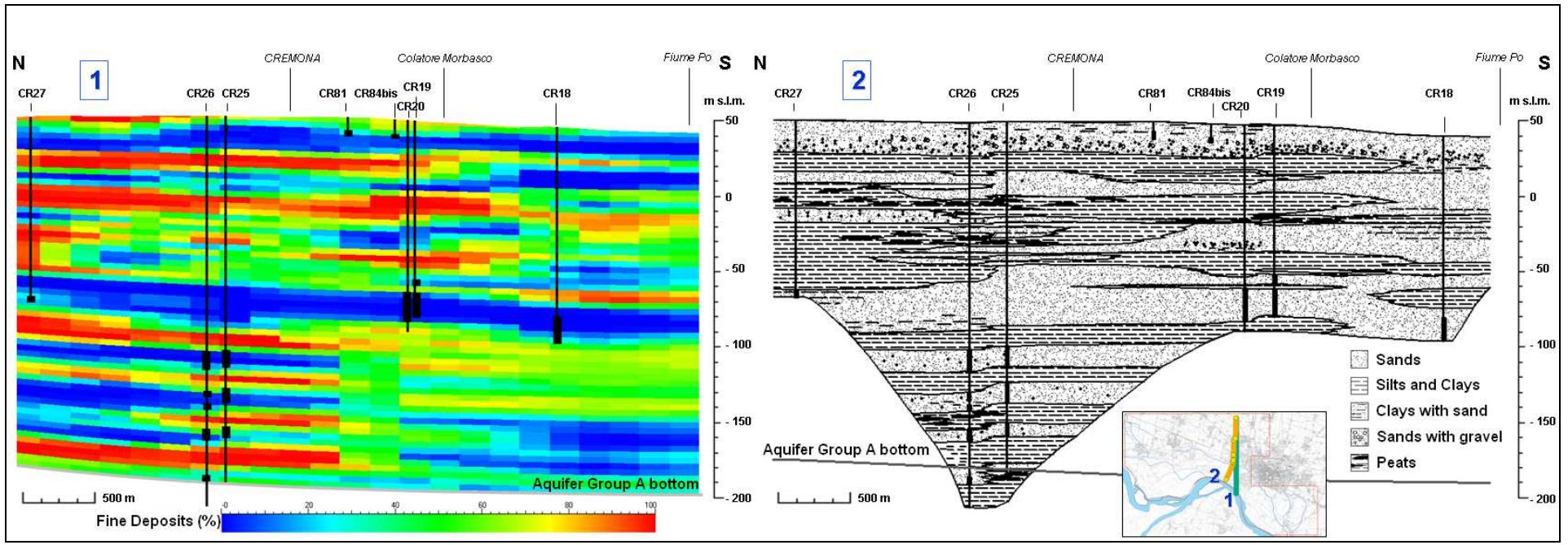

Figure 4.13. Example of comparison between the results of the kriging interpolation (1) and a classical hydrogeological cross section (2).

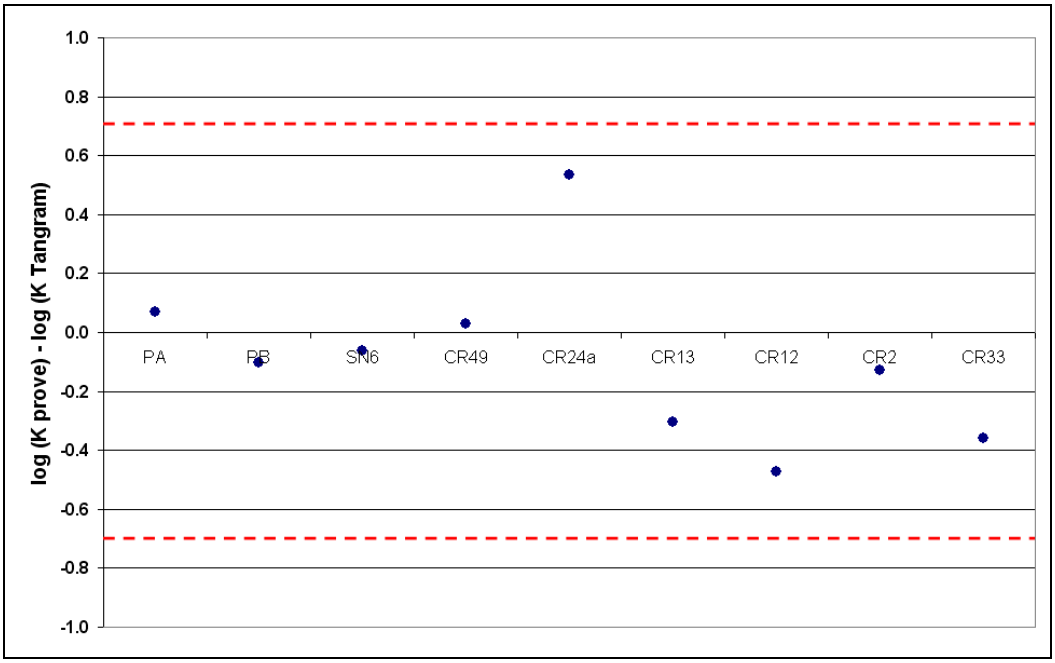

Figure 4.14. Results of the comparison between pumping tests (K test) and codified (K TANGRAM) hydraulic conductivity values; the dotted red lines identify a difference of a half order of magnitude.

4.2. Analysis of the distribution of peats in the study area

Peat deposits are formed by partially decayed vegetation, which accumulated in wet environments with a low presence of oxygen. An example of depositional environment of peats can be the wetlands formed in proximity of rivers.

Previous studies (e.g. McArthur et al., 2001, 2004; Rowland et al., 2006), also referred to Cremona area (Francani et al., 1994; Zavatti et al., 1995), underlined the central role of peat degradation in the chemical mechanisms that favour the mobilization of arsenic, iron, manganese and ammonium in groundwater. Therefore, the definition of peat distribution in the study area can be considered as an important aspect. Peats were previously considered as part of the fine-grained deposits in the reconstruction of the texture percentages. In this paragraph, a detailed representation of the presence of peat in the studied system is presented. Figure 4.15 shows the presence of peat and its content (percentage of peat over all the other reported lithologies) in the collected well stratigraphies. The percentage content of peat is classified in four range values, which are defined on the basis of the 25°, 50° (median) and 75° percentiles of the da ta. Figure 4.15 shows a widespread presence of peat in the studied aquifer system.

It should be noted that the presence and content of peat are probably underestimated due to the following aspects:

- distribution of collected stratigraphies - in the zones where stratigraphies were not collected or do not exist, the identification of the presence of peat is not possible, therefore this zones remain unknown;
- accuracy of the lithological description in the stratigraphies - the collected stratigraphies were made by different authors in different years and with a different precision. In some logs, peat could be detected but not recorded in the stratigraphy.

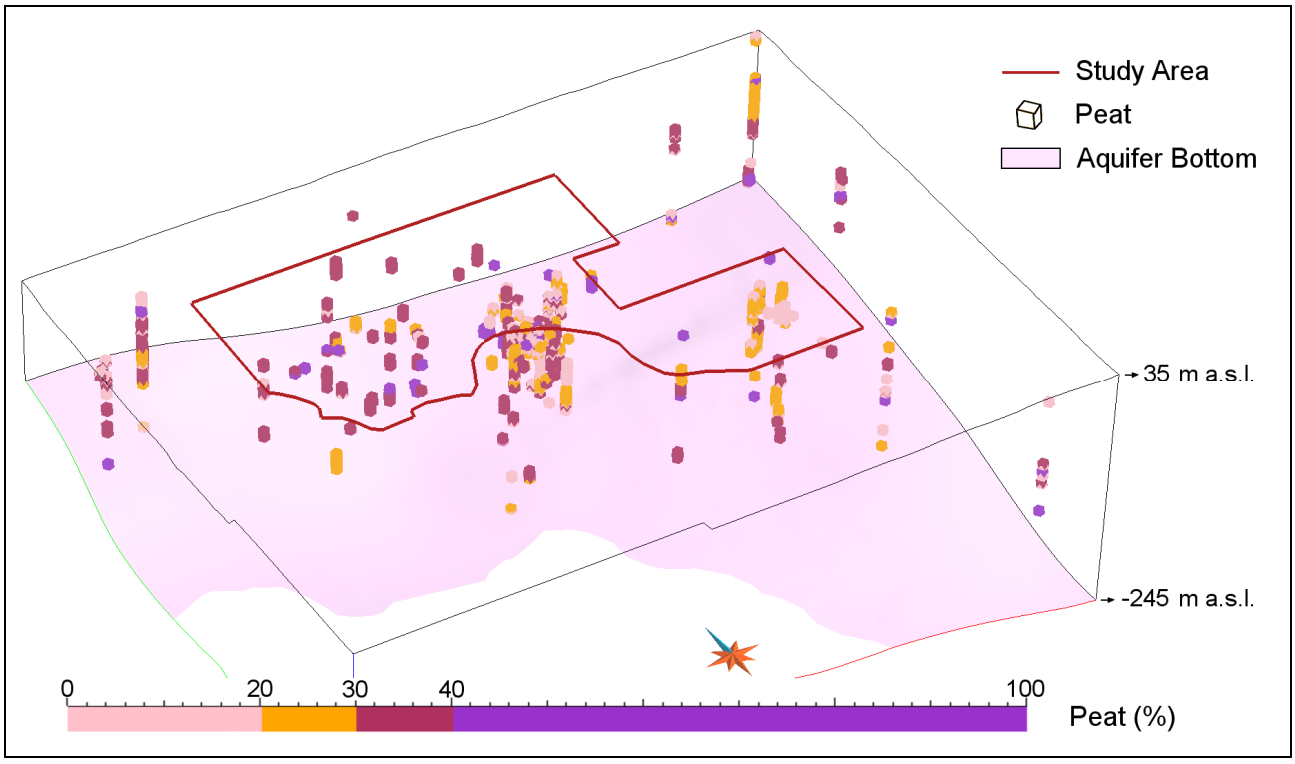

Figure 4.15. Presence and content of peat in the collected well stratigraphies.

A detailed investigation of the individuated presence of peats for each aquifer and aquitard leads to the following outcomes:

- in the aquifer F peat deposits are only located in the Po river valley; these deposits, which are the product of recent depositions, could be generated in the wetland (pond and/or bogs) formed by the Po river activity;

- between aquifers F and S peats are related to the silty-clayey deposits that form the aquitard;
- concerning the other deeper units, peats have a diffuse presence in the study area, they generally concern the fine-grained sediments that form the aquitards, even if peats were also detected, in a few cases, in sandy deposits; this larger diffusion of peat in the deeper part of the aquifer system could be probably related to the past meandering activities of the rivers.

4.3. Conclusions

The 3D aquifer modelling underlines the presence of a multi-layer aquifer system which is characterized by the alternation of silty-clayey layers with lower conductivity (10^{-7}-10^{-8} m/s) and sandy layers with higher conductivity (10^{-3}-10^{-5} m/s). The modelling leads to the identification of five aquifer units (F, S, C1, C2 and C3) which are separated by low-permeable or semi-permeable aquitards. In the zones where the aquitars are absent, overlapped aquifers can interact generating water exchanges. The aquifer system is also characterized by a significant presence of peat deposits, which can influence the groundwater chemistry.

References

Armstrong M. (1998) – *Basic Linear Geostatistics*. Springer Verlag, Berlin, 153 pp.

Beretta G. P., Francani V. & Fumagalli L., (1992) – *Studio Idrogeologico della Provincia di Cremona (Hydrogeological study of the Province of Cremona)*. Pitagora Editrice, Bologna, 141 pp.

Bonomi T. (2009) – *Database development and 3D modeling of textural variations in heterogeneous, unconsolidated aquifer media: Application to the Milan Plain*. Computer and Geosciences 35, 134-145.

Cambi C., Dragoni W., Passeri F. & Valigi D. (2005) – *Contribution to the hydrogeological knowledge of the Cremona aquifer system and the exploitation of new water resources*. Italian Journal of Engineering Geology and Environment 1, 71-89.

Cavallin A. & Maggi V. (2006) – *Regional Impact of Climatic Change in Lombardy Water Resources: Modelling and applications (RICLIC-WARM).* Technical Report of the first year activities*. http://www.riclic.unimib.it/Report_tecnico-Ianno.pdf*

Ciotoli G. & Finoia M. G. (2005) – *Dalla statistica alla Geostatistica: introduzione all'analisi dei dati geologici e ambientali (From statistics to Geostatistics: introduction to geological and environmental data analysis).* Aracne editrice S.r.l., Roma, 418 pp.

Del Rosso F. (2011) – *Ricostruzione tridimensionale delle caratteristiche idrogeologiche della pianura lombarda, finalizzata all'applicazione di modelli di flusso e trasporto (3D reconstruction of the hydrogeological characteristics of the Po Plain (Lombardy Region) for flow and transport model implementation)*. Ph.D. thesis. *http://boa.unimib.it/bitstream/10281/20033/1/phd_unimib_027168.pdf*

Fetter C. W. (1994) – *Applied Hydrogeology*. Prentice Hall, Englewood Cliffs, 691 pp.

Francani V., Beretta G. P., Bareggi A., Nobile A., Cremonini Bianchi M. & Cattaneo F. (1994) – *Aspetti idrogeologici del problema della presenza di azoto ammoniacale nelle acque sotterranee della provincia di Cremona. (Hydrogeological aspects of the occurrence of ammonium in groundwater in the province of Cremona).* Pitagora Editrice, Bologna, 101 pp.

Freeze R. A. & Cherry J. A. (1979) – *Groundwater*. Prentice Hall, Englewood Cliffs, 604 pp.

Martin P. J. and Frind E. O. (1998) – *Modeling a Complex Multi-Aquifer System: The Waterloo Moraine*. Ground water 36 (4), 679-690.

McArthur J. M., Ravenscroft P., Safiulla S. & Thirlwall M. F. (2001) – *Arsenic in groundwater: Testing pollution mechanisms for sedimentary aquifers in Bangladesh.* Water Resources Research 37 (1), 109-117.

McArthur J. M., Banerjee D. M., Hudson-Edwards K. A., Mishra R., Purohit R., Ravenscroft P., Cronin A., Howarth R. J., Chatterjee A., Talukder T., Lowry D., Houghton S. & Chadha D. K. (2004) – *Natural organic matter in sedimentary basins and its relation to arsenic in anoxic ground water: the example of West Bengal and its worldwide implications.* Applied Geochemistry 19, 1255-1293.

Paradigm (2008) – *Paradigm GOCAD 2008, User Guide*. Paradigm Geophisical Corp.

Regione Lombardia & Eni Divisione Agip (2002) – *Geologia degli acquiferi padani della Regione Lombardia (Geology of the aquifers of the Po Plain in Lombardy region).* A cura di Carcano C. & Piccin A. S.E.L.C.A, Firenze, 130 pp.

Rowland H. A. L, Polya D. A., Lloyd J. R. & Pancost R. D. (2006) – *Characterisation of organic matter in a shallow, reducing, arsenic-rich aquifer, West Bengal*. Organic Geochemistry 37, 1101-1114.

Zavatti A., Atramini D., Bonazzi A., Boraldi V., Malagò R., Martinelli G., Naldi S., Patrizi G., Pezzera G., Vandini W., Venturini L. & Zuppi G. M. (1995) – *La presenza di Arsenico nelle acque sotterranee della Pianura Padana: evidenze ambientali e ipotesi geochimiche (Occurrence of arsenic in the groundwater of Po Plain: environmental evidences and geochemical hypothesis).* Quaderni di geologia Applicata S2, 301-325.

5. Hydrodynamic properties analysis

The hydrodynamic properties analysis mainly refers to the water level measurements of the survey of July 2010. These measurements, related to each identified aquifer unit, allow to characterize the hydrodynamic conditions of groundwater in the five aquifers and their relationship to each other and to the rivers. In this chapter, the analysis of the spatial distribution of hydraulic heads for each aquifer and their vertical relations is presented. Afterwards, the analysis of temporal variations of hydraulic head is given. In conclusion, a description of the relations between groundwater and Po river water is presented.

5.1. Spatial distribution of hydraulic head

5.1.1. Aquifer F

The number of water level measurements executed in July 2010 for the aquifer F is equal to 20 (Table 5.1). Even if this number is lower than the minimum value of 50 considered for a significant geostatistical analysis (Webster and Oliver, 2007), a kriging interpolation of the measured heads was done. In the interpolation, the 4 hydrometric level measurements executed in July 2010 (Table 5.2.) were inserted in order to consider the groundwater/surface water relations. The points where the hydrometric levels were measured are located in figure 5.1. Within the 20 hydraulic heads of July 2010, the value of the point CV1 (45.01 m a.s.l.) was excluded from the interpolation due to its inconsistency with respect to the near located points CR12 (45.93 m a.s.l.), CR13 (46.42 m a.s.l.) and CV3 (47.33 m a.s.l.). This inconsistency can have a hydrogeological explanation. These three points are located in central-northern part of the study area characterized by superficial silty-clayey deposits. These deposits can locally produce confined condition generating a higher hydraulic head. In proximity of the point CV1, the aquifer sediments are mainly composed by sands and the hydraulic head is lower. The local confined condition due to silty-clayey lenses can be also identified in the Po river valley for three points (SN8, CR63, CR66). Comparing their water level measurements with the stratigraphies, the hydraulic heads result higher than the level of superficial silty-clayey deposits.

The elaborated piezometric map for aquifer F is showed in figure 5.2. The general groundwater flow direction is N/S, influenced by the drainage effect of Po river. The head ranges from 53 m a.s.l. in the north-eastern zone to 28 m a.s.l. in the south-eastern zone. The resulted flow direction is in agreement with the previous studies of Beretta et al. (1992) and Gandolfi et al. (2007).

Table 5.1. Measured hydraulic heads in aquifer F (July 2010).

Code	Depth (m)	Screen (m)	Aquifer	Measurement Date	Head (m a.s.l.)	Note
CR12	40.0	20 - 33	F	16/07/2010	45.93	
CR13	46.0	25 - 40	F	29/07/2010	46.42	
CR23b	12.0	3 - 12	F	27/07/2010	40.12	
CR50	25.0	10 - 25	F	08/07/2010	35.09	
CR62	10.0	2 - 10	F	13/07/2010	35.39	
CR63	12.0	6 - 9	F	23/07/2010	34.09	
CR66	8.2	2 - 8	F	23/07/2010	35.28	
CR80	16.0	8 - 16	F	27/07/2010	37.31	
CR81	12.0	3 - 12	F	27/07/2010	39.98	
CR82	17.0	3 - 17	F	27/07/2010	41.15	
CR84 bis	12.0	7 - 12	F	06/07/2010	38.53	
CR86	15.0	6 - 15	F	06/07/2010	32.26	
CR88	15.0	2 - 15	F	23/07/2010	34.78	
CR89	15.0	3 -15	F	23/07/2010	33.86	
CV1	31.5	20 - 30	F	21/07/2010	45.01	outlier
CV3	32.0	21 - 27.5	F	21/07/2010	47.33	
GC1	36.0	21 - 22	F	14/07/2010	28.60	
GC2	36.0	21 - 22	F	14/07/2010	27.72	
SN7 bis	10.0	3 - 10	F	13/07/2010	42.15	
SN8	10.0	5 - 10	F	13/07/2010	36.05	

Table 5.1. Measured hydrometric levels in Po and Adda rivers (July 2010).

Point	Measurement Date	LAT. (m)	LONG. (m)	Hydrometric level (m a.s.l.)
Po upstream	08/07/2010	4992395.469	1570823.256	40.65
Po intermediate	08/07/2010	4997764.824	1578291.384	28.56
Po downstream	08/07/2010	4988354.076	1593092.103	24.43
Adda	08/07/2010	5000548.162	1567106.755	32.83

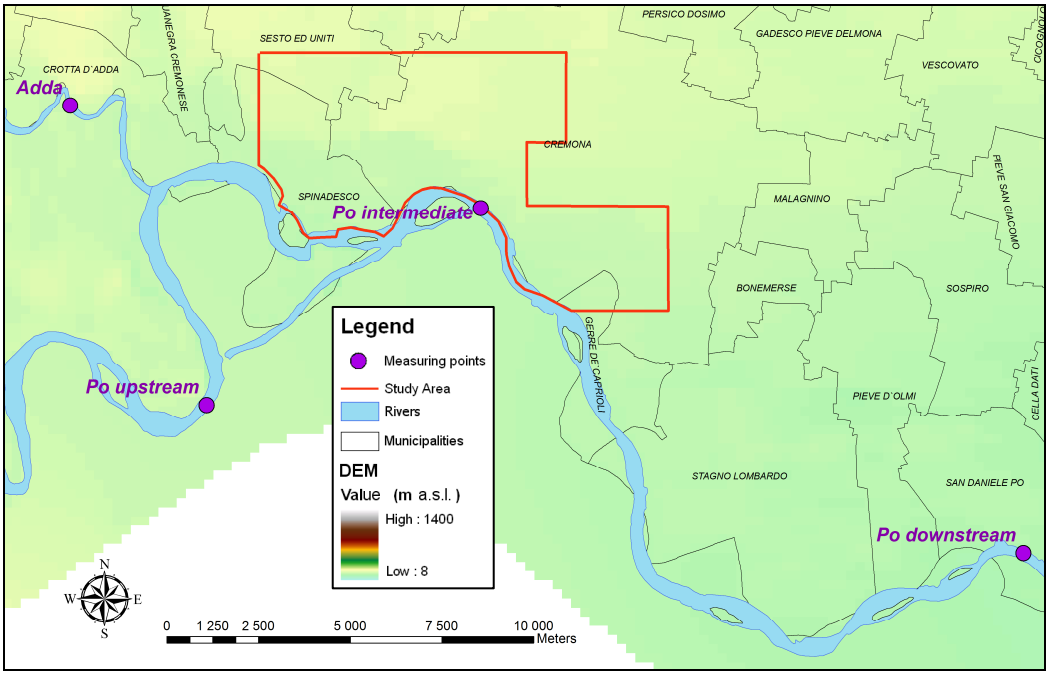

Figure 5.1. Location of measuring points for the hydrometric levels of Po and Adda rivers.

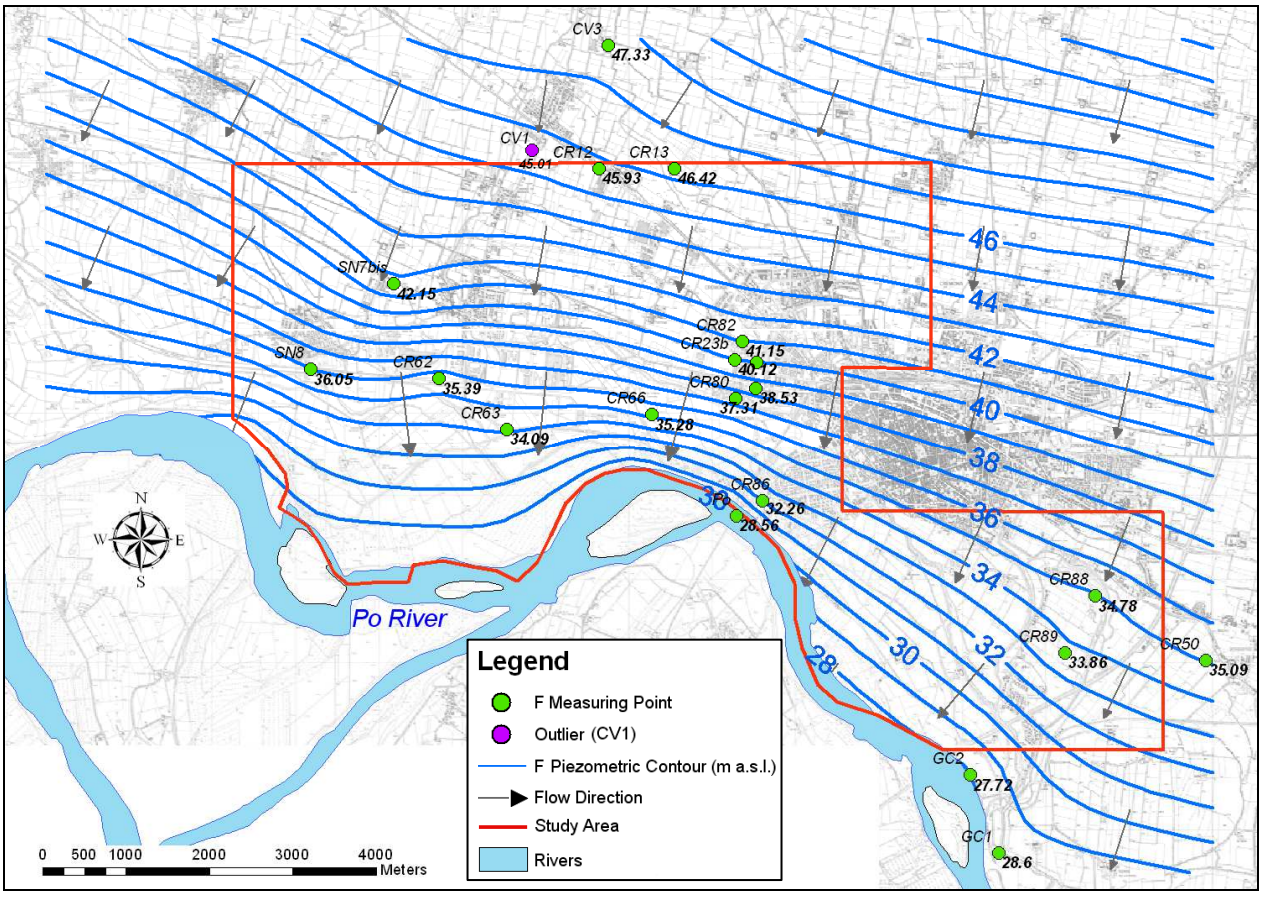

Figure 5.2. Piezometric map of aquifer F (July 2010).

5.1.2. Aquifer S

The number of measurements for the aquifer S is equal to 6 (Table 5.3), including also a multi-aquifer well between aquifers S and C1 (Cr35new). This small number of data does not allow a geostatistical analysis but it can give a useful information on the flow direction. Within these hydraulic heads, the value of the point CR36 (40.25 m a.s.l.) results inconsistent with the other aquifer S measurements, but it results consistent with the aquifer F values. This aspect points out a probable direct connection with aquifer F for the point CR36, probably due to an incorrect placing of bentonite seals. From the analysis of the remaining 5 hydraulic heads, a hypothetical groundwater flow direction from North to South can be identified (Figure 5.3).

Table 5.3. Measured hydraulic heads in aquifer S (July 2010).

Code	Depth (m)	Screen (m)	Aquifer	Measurement Date	Head (m a.s.l.)	Note
AN1	47.0	39 - 45	S	16/07/2010	37.97	
AN3b	88.0	31 - 40	S	14/07/2010	38.36	
CR21	56.0	40 - 50	S	21/07/2010	34.20	
CR24a	45.0	35 - 45	S	21/07/2010	35.95	
CR35 new	80.0	50 - 56; 65 - 80	S&C1	26/07/2010	34.55	multi-aquifer
CR36	53.0	47 - 53	S	05/07/2010	40.25	outlier

5.1.3. Aquifers C1, C2 and C3

Considering the small number of measurements for each aquifer and the presence of multi-aquifer wells, the hydraulic heads referred to aquifers C1, C2 and C3 are represented in a single map (Figure 5.4). A detailed description of each aquifer is presented in the following.

Aquifer C1

The total number of measurements referred to aquifer C1 is equal to 3 (Table 5.4 and Figure 5.4), including 2 multi-aquifer wells: Cr35new between aquifers S and C1 (already cited) and CR31 between aquifers C1 and C2. This small number of measurements does not allow to identify any groundwater flow direction.

Table 5.4. Measured hydraulic heads in aquifer C1 (July 2010).

Code	Depth (m)	Screen (m)	Aquifer	Measurement Date	Head (m a.s.l.)	Note
CR31	135.0	71.8-76; 93.1-96; 106.8-111; 112.5-115.5; 118-124; 125.5-130	C1&C2	05/07/2010	32.56	multi-aquifer
CR9	100.0	53-63; 67-81	C1	13/07/2010	32.27	
CR35new	80.0	50-56; 65-80	S&C1	26/07/2010	34.55	multi-aquifer

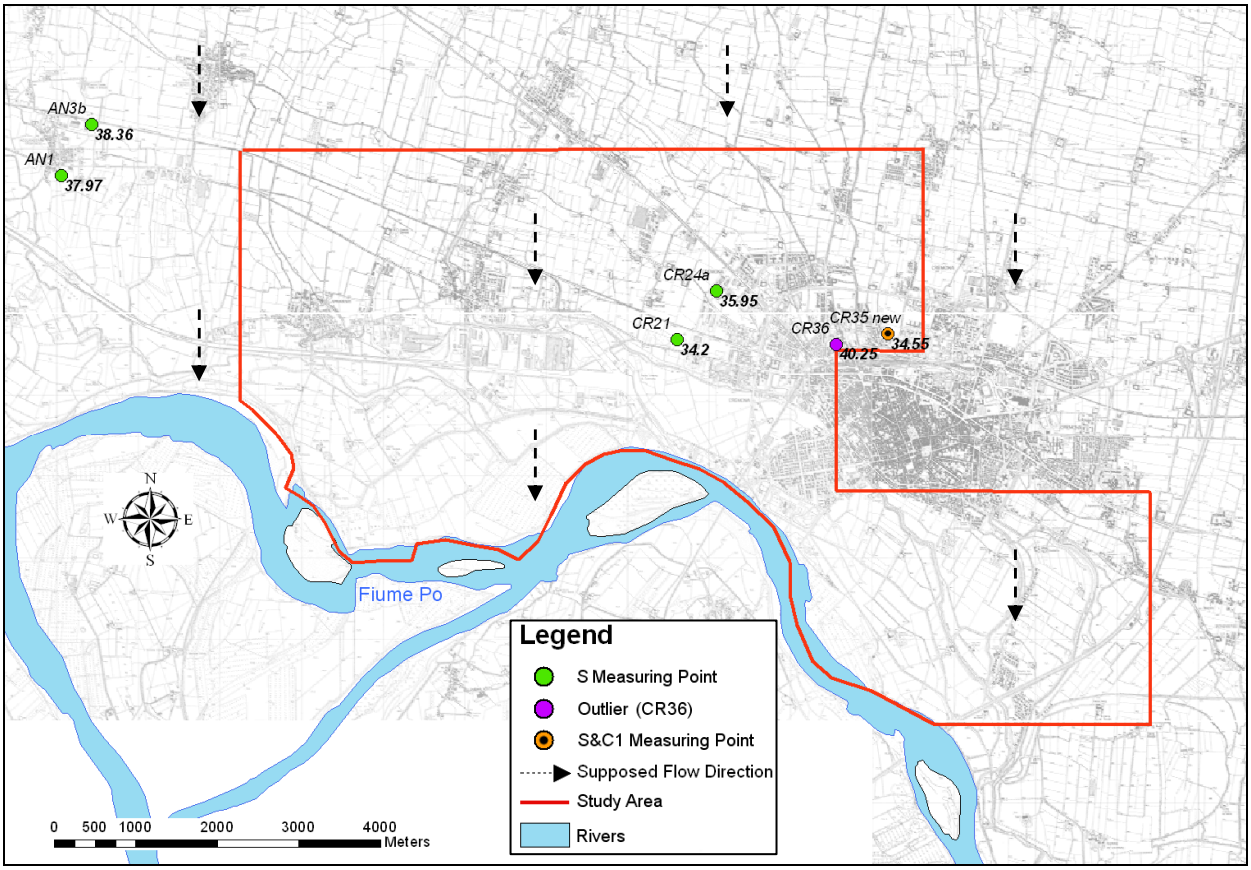

Figure 5.3. Location of the measured hydraulic heads in aquifer S (July 2010).

Aquifer C2

The number of measurements for the aquifer C2 is equal to 8 (Table 5.5 and Figure 5.4), including 3 multi-aquifer wells: CR31 between aquifers C1 and C2 (already cited), CR59 and CV2 between aquifers C2 and C3. As shown in chapter 4, the aquifer C2 has a complex structure: two subunits (C2A and C2B) can be identified in the western and central parts of the study area due to silty-clayey deposits, while an undifferentiated aquifer C2 can be considered in the eastern part. Considering this aspect, the measurements for the aquifer C2 can be classified as follow: CR54 is located in the eastern part of the area, and thus, its

hydraulic head can be referred to the undifferentiated aquifer C2; CR20 and CR48 involve the aquifer C2B; SN5 involves the aquifer C2A; CR19 has the screen in both aquifers C2A and C2B.

Even if there is a small number of hydraulic heads for aquifer C2, an interpolation with kriging method was done (Figure 5.4). In this interpolation the points CR19 and CR31 were excluded. The former, which involves both aquifers C2A and C2B, has a hydraulic head that is lower with respect to the near located point CR20, which only involves the aquifer C2B (CR20 has a higher head due to more confined condition). The latter is between aquifers C1 and C2 and has a lower hydraulic head that is inconsistent with the other points.

The resulted piezometric map allows to identify a general groundwater flow direction from N-W to S-E. This direction reflects the regional flow direction identified by the previous studies of Beretta et al. (1992) and Gandolfi et al. (2007). For the deep aquifers, as opposed to the superficial ones, the flow direction is less or not influenced by the Po river. A detailed description of the relation between groundwater and Po river is given below. The irregular profile of the resulted piezometric contours reflects the complex structure of aquifer C2 as described before.

Table 5.5. Measured hydraulic heads in aquifer C2 (July 2010).

Code	Depth (m)	Screen (m)	Aquifer	Measurement Date	Head (m a.s.l.)	Note
CR19	131.0	103.7-108.3; 116.3-128.5	C2A&B	16/07/2010	31.66	outlier
CR20	141.0	113-133.5	C2B	16/07/2010	33.60	
CR48	145.0	125-140	C2B	23/07/2010	32.72	
CR54	110.0	99-105	C2	08/07/2010	33.00	undiff.
CR59	136.0	131-136	C2&C3	26/07/2010	34.60	multi-aquifer
CV2	150.0	122-126; 132-138	C2&C3	19/07/2010	36.24	multi-aquifer
SN5	127.0	90.5-100.5	C2A	19/07/2010	35.78	
CR31	135.0	71.8-76; 93.1-96; 106.8-111; 112.5-115.5; 118-124; 125.5-130	C1&C2	05/07/2010	32.56	multi-aquifer

Aquifer C3

The total number of measurements referred to aquifer C3 is equal to 6 (Table 5.6 and Figure 5.4), including 2 multi-aquifer wells (CR59 and CV2, already cited). This small number of data does not allow a geostatistical analysis but it can give a useful information on the flow direction. Analysing the hydraulic heads, the ground

water flow direction for aquifer C3 seems to be from N-W to S-E, according to aquifer C2.

Table 5.6. Measured hydraulic heads in aquifer C3 (July 2010).

Code	Depth (m)	Screen (m)	Aquifer	Measurement Date	Head (m a.s.l.)	Note
AN2	227.5	134 - 148	C3	19/07/2010	36.53	
PD1 bis	202.0	150 - 159; 164 - 173	C3	19/07/2010	35.06	
SU5	175.0	159.3 - 168.3	C3	19/07/2010	36.26	
GC3 bis	187.0	163 - 171; 174 - 180	C3	19/07/2010	34.53	
CR59	136.0	131 - 136	C2&C3	26/07/2010	34.60	multi-aquifer
CV2	150.0	122 - 126; 132 - 138	C2&C3	19/07/2010	36.24	multi-aquifer

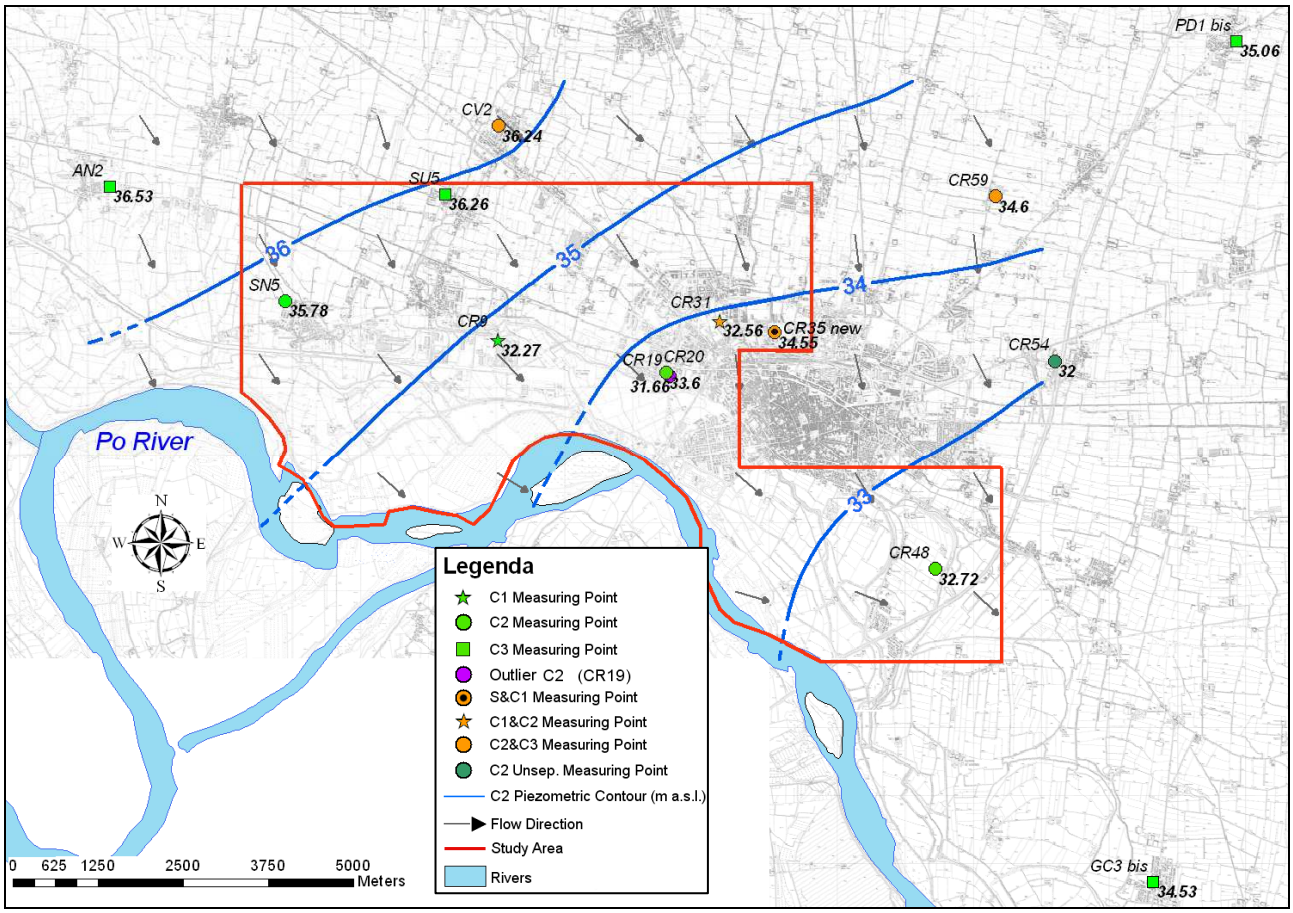

Figure 5.4. Location of the measured hydraulic heads in aquifer C1, C3 and C3 and piezometric map of aquifer C2 (July 2010).

5.2. Vertical hydrodynamic relations between aquifers

The analysis of vertical hydrodynamic relations between aquifers can be done comparing the hydraulic heads between near located wells of different aquifers. Considering the aquifers F and S, the comparison between head values can be implemented for the couple CR82 (41.15 m a.s.l., aquifer F) and CR24a (35.95 m a.s.l., aquifer S) and for the couple CR84bis (38.53 m a.s.l., aquifer F) and CR21 (34.2 m a.s.l., aquifer S). All these wells are located in the central part of the study area. The comparison points out the presence of higher values of around 4-5 m for the aquifer F. This result confirms that aquifers F and S are separated in the central part of the area, where a silty-clayey aquitard is located (par. 4.1.5). In the northern part of the area, where the aquitard is absent, the aquifers F and S can be considered as a single unit with common hydrodynamic properties. This condition is underlined by the point CR13, which has the screen 25-40 m deep and a hydraulic head value (46.42 m a.s.l.) consistent with the aquifer F heads. Concerning the aquifer C1, the analysis is limited by the presence of only one measurement (CR9). The hydraulic head in this point is 32.27 m a.s.l., that is lower with respect to the near located point CR21 (34.2 m a.s.l.) of aquifer S. These data allow to suppose the presence of lower heads for the aquifer C1 compared to aquifer S. The comparison between aquifers C1, C2 and C3 cannot be done considering near located points, but a general indication can be given from the analysis of the map showed in figure 5.4. Aquifer C2 seems to have higher heads compared to aquifer C1, but lower heads compared to aquifer S. Aquifer C3 has similar or higher hydraulic heads with respect to aquifer C2.

The presence of discontinuous silty-clayey aquitards can lead to significant groundwater exchanges between overlapping aquifers. In addiction, vertical exchanges of water could occur due to leakage through semi-permeable aquitards, as verified by pumping tests in the wells of the Cremona water supply system (Geologia Applicata and AEM Cremona, 2002). On the basis of the July 2010 measurements, the vertical exchanges of water could be directed, in the upper part of the system, from aquifer F to S and again to C1 while, in the deeper part of the system, from aquifer C3 to C2 and again to C1. It should be noted that in proximity of the Po river these vertical relations seem to be inverted. The hydraulic connection between superficial aquifers and Po river allows to obtain lower head values for aquifers F and S with respect to aquifers C1, C2 and C3. This condition

can be identified for July 2010, but it can change depending to the seasonal variation of the hydrometric level of Po river (discussed in paragraph 5.4).

5.3. Temporal variations of hydraulic head in the aquifers

The analysis of temporal variation of hydraulic heads was done considering the historical data. Within the collected historical data, only 6 points are characterized by considerable time series of hydraulic head. These points are 5 superficial piezometers (aquifer F) and 1 deep well (aquifer C3). It should be noted that all the water level measurements are static. The 6 points, which are referred to 3 different sites, are showed in figure 5.5. The variation of hydraulic heads over time was compared to the precipitation data of the Cremona station.

The points PZ2 and PZ3 are superficial piezometers referred to the site with ID equal to 100 (Table 2.1). The time series of their hydraulic heads are reported in figure 5.6. These time series are referred to a period that ranges from January 2006 to July 2010, but they are not spaced at uniform time intervals. Figure 5.6 shows a general increase of hydraulic heads over time, in particular from 2007 to 2010, that could be related to the increase of cumulative annual precipitations. The point PZ3, which is located upstream to the groundwater flow, is constantly higher of 1 m with respect to point PZ2. Considering these limited time series, the presence of seasonal variation cannot be identified.

The points PZ1 and PZ6 are superficial piezometers referred to the site with ID equal to "Disc. P.C." (Table 2.1). The time series are referred to the period ranging from January 2001 to April 2010 and they have irregular time intervals and missing data (Figure 5.7). In particular the time series have a short time spacing in the 2002, up to 3 measurements for month, a quite regular spacing from the 2006 (2 measurements for year) and missing data in the 2003 and 2005. Figure 5.7 shows a general decrease of hydraulic heads from 2001 to 2007 and a general increase from 2007, according to the previous site, that can be related to the increase of annual precipitation. The decrease from 2001 to 2007 cannot be related to the precipitation data due to the irregular time spacing and missing data. The point PZ1, which is located upstream to the groundwater flow, preserves a higher head with respect to the point PZ6. The average head difference between the two points is around 0.5-0.6 m, with a maximum of 1.32 m in April 2010 and a minimum of 0.43 m in October 2008. Considering the year 2002, a seasonal variation of

hydraulic heads can be identified (Figure 5.7) with an increase of about 0.5 m from May, that could be explained by the starting of the irrigation. The zones of the medium and lower Po Plain, that are mainly agricultural areas, are characterized by a maximum of the hydraulic heads in superficial aquifers corresponding to the irrigation period (Bonomi et al., 2008).

The points P5E and PZ6E are referred to a water supply pumping station. The point P5E is a water supply well which involves the aquifer C3, while the point PZ6E is a superficial piezometer (aquifer F). The time series are referred to the period ranging from March 2006 to December 2009 (Figure 5.8) and they have a constant time spacing, which is one measurement for month for PZ6E and one measurement for 3 months (not regular) for P5E. Considering the point PZ6E, figure 5.8 shows higher heads raging from 4.5 to 6 m with respect to point P5E. This condition is in agreement with the description of the vertical hydrodynamic relation presented in the previous paragraph. Also in this case, the heads increase over time from the 2007 according to the increase of annual precipitation. Within every year, seasonal variations are not identified, because the heads remain quite constant. Considering the point P5E, the same general increase of heads from the 2007 can be identified. The point P5E has a regular seasonal variation, as opposite to point PZ6E, that is characterized by a maximum in winter/spring and a minimum in summer/fall. This seasonal fluctuation in the deep aquifer could be generated by the variation of infiltration in the recharge area, according to the "piston" effect. The recharge area of the deep aquifer is presumably located between the higher Po Plain and the foothills of the Alps, and it has a pluviometric regime characterized by a first maximum in fall, a second maximum in spring and a minimum in summer. This regime could explain the maximum hydraulic head in winter/spring followed by a minimum in summer/fall for the point P5E.

Another element, that can be evaluated in the analysis of temporal variation of hydraulic heads, is the difference in water level measurements between the surveys of July 2010 and 2012. Six wells were measured in both surveys, the comparison between their hydraulic heads is showed in figure 5.9. The heads of July 2012 result lower in every well, with an average difference with respect to July 2010 of 1.2 m. This difference could be related to different precipitations occurred in the 2012 with respect to the 2010.

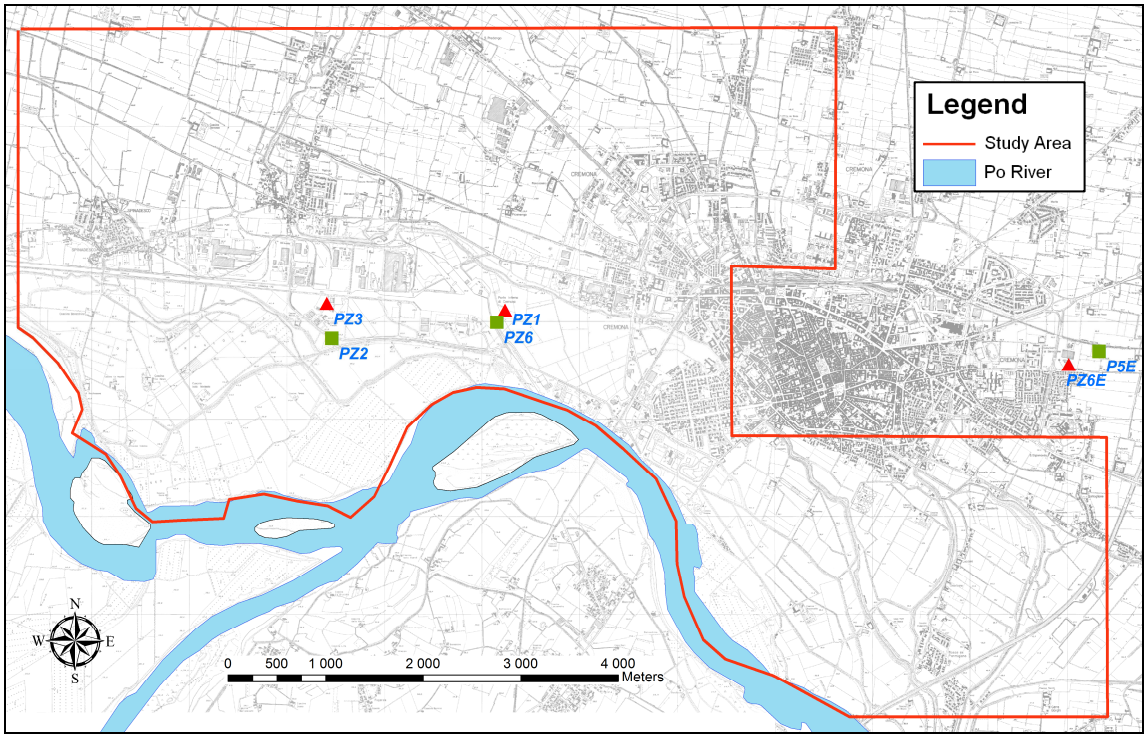

Figure 5.5. Locations of the points where temporal variation of hydraulic heads were analysed, the symbols (red triangle and green square) are the same of figures 5.6, 5.7 and 5.8.

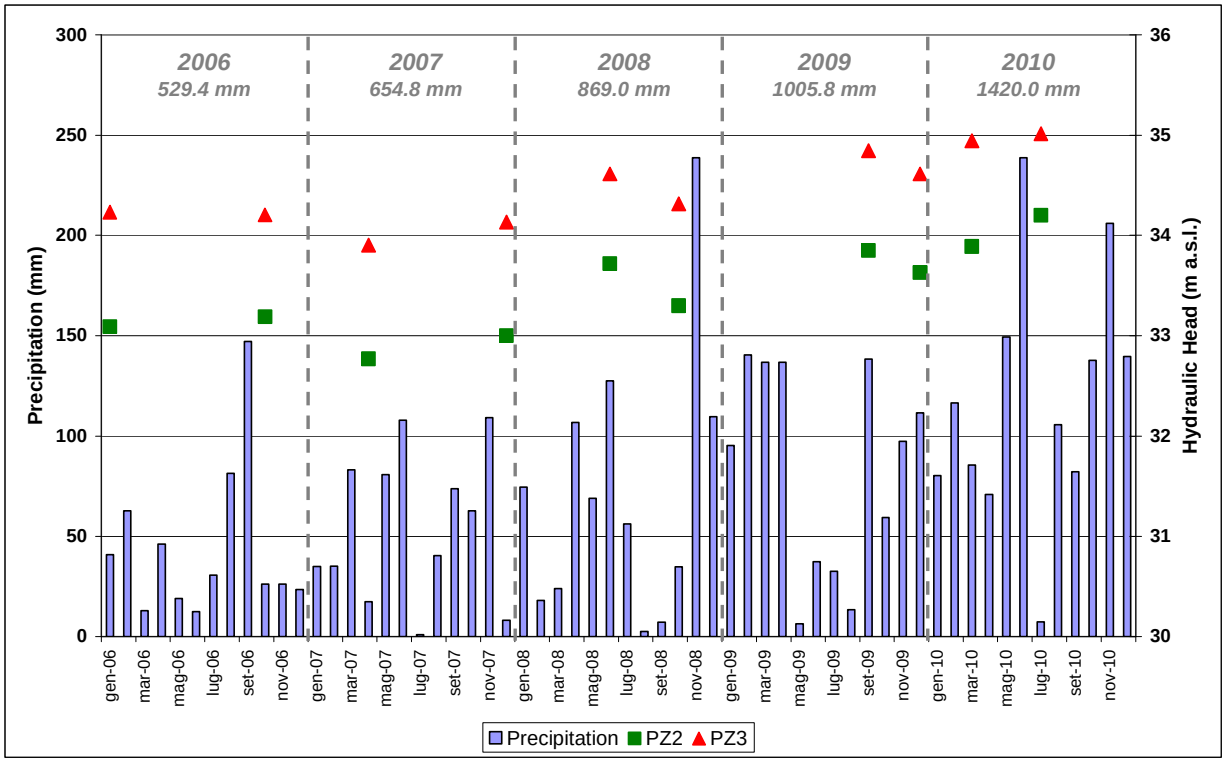

Figure 5.6. Temporal variation of hydraulic heads in the points PZ2 and PZ3 referred to the site "100"; on the top cumulative annual precipitation values.

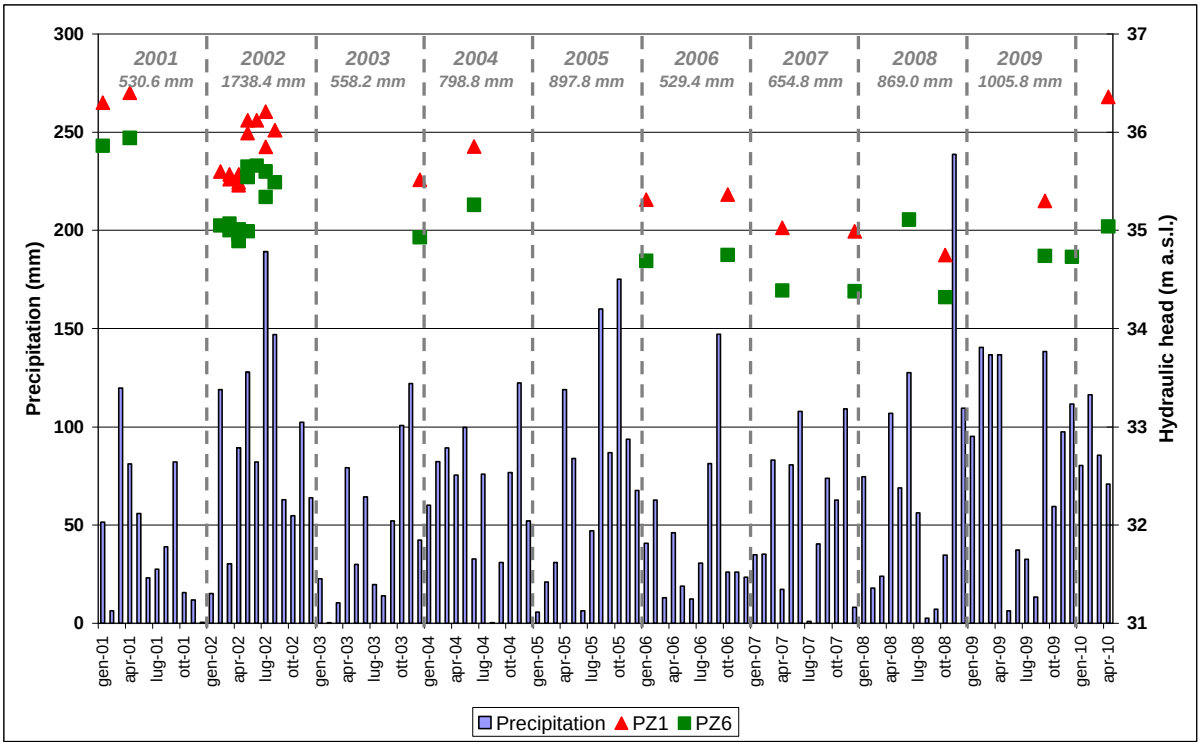

Figure 5.7. Temporal variation of hydraulic heads in the points PZ1 and PZ6 referred to the site "Disc. P.C."; on the top cumulative annual precipitation values.

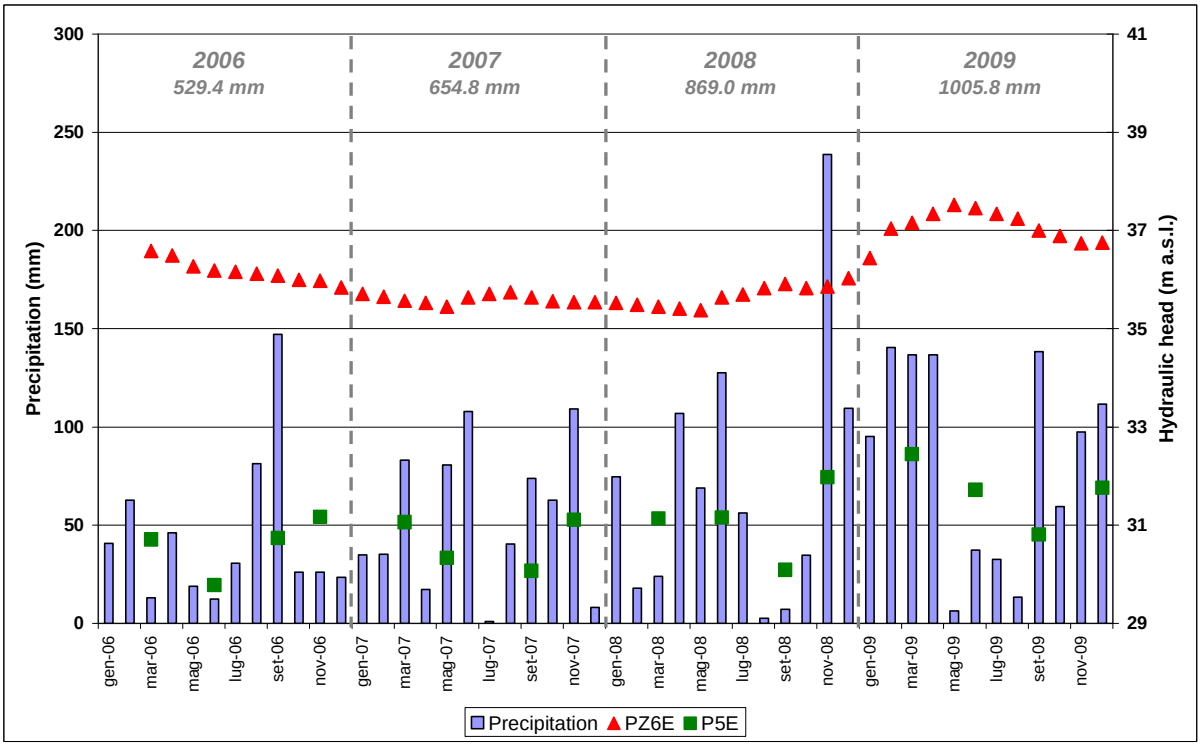

Figure 5.8. Temporal variation of hydraulic heads in the points PZ6E and P5E referred to a water supply pumping station; on the top cumulative annual precipitation values.

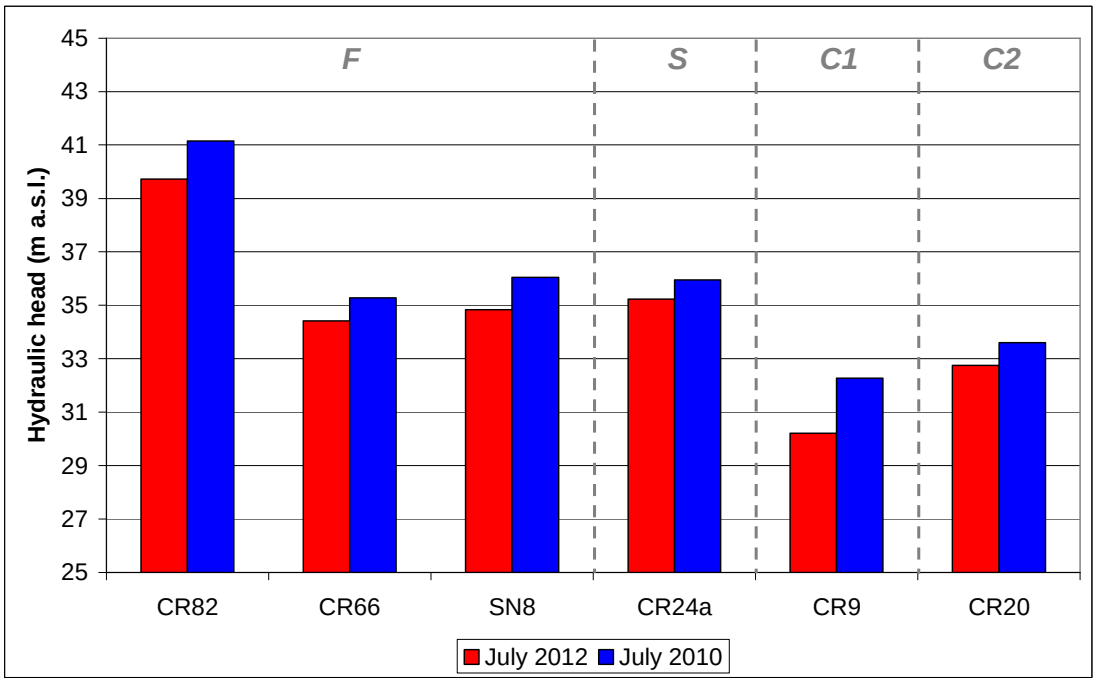

Figure 5.9. Comparison between the hydraulic heads measured in the surveys of July 2010 and 2012.

In fact, analysing the cumulative monthly precipitation values for 6 months before the execution of the surveys (Table 5.9), the precipitations of 2012 (193.4 mm from January to June) result lower than 2010 (741.4 mm from January to June).

Table 5.7. Cumulative monthly precipitation values (mm) for 6 months before the execution of the surveys.

	January	**February**	**March**	**April**	**May**	**June**
2010	80.4	116.4	85.6	71	149.4	238.6
2012	13.4	31.6	5.2	64	72.8	6.4

5.4. Relation between groundwater and Po river

A direct hydraulic contact between the superficial aquifers (F and S) and Po river can be assumed due to the general presence of sandy deposits and the existence of comparable piezometric and hydrometric levels in proximity of the river. The deeper aquifers (C1, C2 and C3) are isolated by silty-clayey aquitards. These aquitards can be discontinuous and/or semi-permeable, therefore a lower degree of water exchange could be assumed between deep groundwater and Po river. This aspect was also underlined by the previous studies of Beretta et al.

(1992) and Francani and Trefiletti (2006). The direction of these water exchanges is governed by the difference between the hydraulic heads of aquifers and the hydrometric level of Po river, which can change over time. With higher hydrometric levels of Po river with respect to hydraulic heads of deep aquifers, the possible water exchange can be directed from the river to the aquifers, as reported by Francani and Trefiletti (2006); while, with lower hydrometric levels of Po river with respect to hydraulic heads of deep aquifers, the possible water exchange can be directed from the aquifers to the river, as underlined by the data of the survey of July 2010.

Considering the relations between superficial aquifers and Po river, the data of July 2010 points out the presence of a drainage effect of the river with respect to groundwater. This condition can change over time depending to the flow rate variation of the river. Daily measurements of precipitation, hydrometric level of Po river and hydraulic heads of 4 superficial piezometers, located in a N/S transect with a distance of 100, 200, 500 and 1000 m from the river, were collected from the historical data, referring from March 2009 to May 2009. Concerning these measurements, which were executed by a private company (unpublished data), only a general description of results is given in the following. The analysis of these measurements points out that the variation of the flow rate of Po river, determined by the precipitation, governs the relations between superficial groundwater and river water. The increment of the flow rate can allow to higher hydrometric levels with respect to groundwater heads, probably generating a pressure transfer rather than a water mass transfer. This pressure transfer causes a perturbation of the superficial groundwater flow which is normally directed from North to South (to the Po river). This phenomenon can involve the area extended up to 0.5-1 km of distance from the river.

5.5. Conclusions

The analysis of the hydrodynamic properties allows to the definition of the following aspects:

- aquifer F generally has phreatic conditions even if it can be subjected to local confined conditions due to the presence of superficial silty-clayey deposits, located in the central-northern part of the study area and in some zones of

the Po valley; the main groundwater flow direction is N/S, with a relevant drainage effect of Po river, that can vary according to the variation of the hydrometric level of the river over time; with high flow rate of the river, the hydrometric levels can be higher with respect to the groundwater heads, generating a perturbation of the groundwater flow that interferes with the normal discharge in the river;

- aquifer S can be defined as semi-confined due to the presence of confined conditions in the central part of the study area, where the silty-clayey aquitard is located, and phreatic conditions in the remaining zones; the supposed flow direction is from N/S; the hydraulic heads seem to be lower than aquifer F but higher than aquifer C1;
- aquifer C1 has confined conditions; a flow direction from NW to SE can be supposed, according to the other confined aquifers; the hydraulic heads seem to be lower than aquifers S and C2;
- aquifer C2 has confined conditions; the general flow direction is NW/ SE; the hydraulic heads seem to be higher than aquifer C1 but lower than aquifer C3;
- aquifer C3 has confined conditions; the supposed flow direction is NW/ SE; the hydraulic heads seem to be similar or higher than aquifer C2 but lower than aquifer S.

References

Beretta G. P., Francani V. & Fumagalli L., (1992) – *Studio Idrogeologico della Provincia di Cremona (Hydrogeological study of the Province of Cremona)*. Pitagora Editrice, Bologna, 141 pp.

Bonomi T., Canepa P., Del Rosso F. & Rossetti A. (2008) – *Relazioni temporali pluridecennali di dati pluviometrici, idrologici e piezometrici nella pianura lombarda tra Ticino e Oglio (Temporal analysis of long-term pluviometric, hydrological and piezometric data in the Po Plain between Ticino and Oglio rivers).* Giornale di geologia applicata 9 (2), 227-248.

Francani V. & Trefiletti (2006) – *Relazioni fra sistema idrico superficiale e contaminazione delle acque sotterranee nella provincia di Cremona (Relations between surface water system and groundwater contamination in the province of Cremona).* Atti del convegno

"Questioni ambientali nella gestione del territorio: strumenti e casi studio nel territorio cremonese", Cremona, 9 giugno 2006.

Gandolfi C, Ponzini G. & Giudici M. (2007) – *Realizzazione di un modello preliminare del flusso idrico nel sistema acquifero della Provincia di Cremona (Implementation of a preliminary flow model in the aquifer system of the Province of Cremona).* Relazione Tecnica, pp. 222. http://www.atlanteambientale.it/atlanteambientale/biblio/Intro.html

Geologia Applicata & AEM Cremona (2002) – *Studio idrogeologico a supporto della realizzazione del campo pozzi Cremona est (Hydrogeological study supporting the realization of the water supply pumping station "Cremona est")*. Relazione Tecnica, pp. 49.

Webster R. & Oliver M. A. (2007) – *Geostatistics for Environmental Scientists*. Wiley & Sons Ltd, pp. 315.

6. Hydrochemical characterization of groundwater

The present hydrochemical characterization of groundwater is mainly based on the data of the survey of July 2010. In the following, a description of the detected concentrations of the chemical parameters considered in the survey of July 2010 and July 2012 is presented. Afterwards, the results of a principal component analysis of the July 2010 data are discussed.

6.1. Results of the survey of July 2010

In this paragraph, a description of the concentration distribution over depth of the considered chemical parameters is initially given. The detected concentrations of each chemical parameter are represented in the figures 6.1, 6.2, 6.3 and 6.4. These figures show the plots of the detected concentration in the sampled wells, which are sorted on the x-axis with respect to the depth of the first screen. The sampled wells are represented in the graph as histograms. The graph area is divided into 5 boxes which include the data of each aquifer (F, S, C1, C2 and C3). Afterwards, a focus on the spatial distribution of As, Fe, Mn and NH_4 concentrations is presented.

6.1.1. Physicochemical parameters

Temperature

The measured temperature value generally ranges from 15 to 16 ℃ (Table 6.1 and Figure 6.1). In the aquifer F, the temperature is generally higher and more variable probably due to the influence of the atmospheric temperature (heterothermic zone). The temperature is generally lower in the aquifer S and gradually increases from aquifer C1 to C3 probably due to the natural temperature gradient.

pH

The measured pH value constantly increases over depth (Table 6.2 and Figure 6.1). In the aquifers F and S, the pH generally ranges from 7.0 to 7.7 according to the common values of natural groundwater environment. From aquifer

C1 to C3, the pH reaches more basic values, that generally ranges between 7.8 and 8.1.

Table 6.1. Statistics of measured temperature values (℃) in July 2010.

	Total	**F**	**S**	**C1**	**C2**	**C3**
Mean	15.8	16.4	15.2	15.6	15.5	16.0
Min	13.9	13.9	14.4	14.7	14.4	14.6
Max	19.1	19.1	16.2	16.9	16.3	17.1
Median	15.6	16.5	15.2	15.6	15.6	15.8
Stand. Dev.	1.0	1.2	0.6	0.7	0.6	0.9

Table 6.2. Statistics of measured pH values in July 2010.

	Total	**F**	**S**	**C1**	**C2**	**C3**
Mean	7.65	7.28	7.54	7.80	7.93	8.25
Min	6.62	6.62	7.30	7.41	7.65	7.84
Max	8.75	7.72	7.99	8.25	8.18	8.75
Median	7.60	7.21	7.52	7.81	7.97	8.10
Stand. Dev.	0.40	0.26	0.16	0.35	0.16	0.28

Electrical conductivity

The measured electrical conductivity (EC) ranges from 336 to 1030 µS/cm (Table 6.3 and Figure 6.1), with the exception of the maximum value (1680 µS/cm) registered in the point CR88, which is located downstream to a landfill. The groundwater can be defined as medium-mineralized with a medium/important degree of mineralization (Celico, 1986). The measured EC generally decreases over depth. In the aquifer F, the EC value is more variable ranging between 500 and 1000 µS/cm, with the exception of CR88. The EC value results more stable in the aquifer S, generally ranging between 400 and 800 µS/cm. The point CR36 (877 µS/cm) seems to be an outlier for aquifer S, assuming a value that is consistent with aquifer F (as also verified for the hydraulic head measurement in paragraph 5.1.2.). In the aquifers C1, C2 and C3, the EC value is quite stable around 430 µS/cm. A significant increase of EC can be seen for the deep points, in particular GC3bis and CR51 (730 and 513 µS/cm, respectively), probably caused by the interaction with the deep brackish waters of Po Plain (Conti et al., 2000). The fresh/salty water interface is located between 400 and 500 m b.s. in the Cremona area (Regione Lombardia and ENI Divisione Agip, 2002), but it could rise due to well abstraction.

Table 6.3. Statistics of measured EC values (µS/cm) in July 2010.

	Total	**F**	**S**	**C1**	**C2**	**C3**
Mean	600	804	587	482	442	462
Min	336	489	411	433	371	336
Max	1680	1680	877	562	556	730
Median	519	736	547	455	430	423
Stand. Dev.	219	247	130	51	49	118

Oxidation reduction potential

The oxidation reduction potential (ORP) was measured in 46 of the 68 collected groundwater samples due to technical problems with the measuring probe. An Ag/AgCl reference electrode was used in the measurements. The measurements reported below are referred to the Ag/AgCl electrode ($E_{Ag/AgCl}$).

The measured ORP has variable values which generally decrease over depth (Table 6.4 and Figure 6.1). In the aquifer F, some points have positive ORP values referring to more oxidised waters, while other points have negative values referring to more reduced waters. The ORP value for the aquifer S is generally negative, with the exception of three points (CR35, CR35new and CR36). In the aquifers C1, C2 and C3, the measure ORP value is negative identifying more reduced groundwater. The most reduced aquifer seems to be the C1, with a median value of -158 mV. In general, the studied aquifer system is characterized by negative ORP values, with the exception of some zones referred to aquifer F.

Table 6.4. Statistics of measured ORP values ($E_{Ag/AgCl}$; mV) in July 2010.

	Total	**F**	**S**	**C1**	**C2**	**C3**
Mean	-32	80	-39	-144	-121	-102
Min	-273	-133	-210	-225	-273	-235
Max	284	284	106	-42	22	-49
Median	-62	73	-67	-158	-119	-70
Stand. Dev.	142	141	108	64	87	77

Bicarbonate (HCO_3^-)

The measured bicarbonate concentration constantly decreases over depth (Table 6.5 and Figure 6.2) ranging between around 200 and 600 mg/L. The higher concentration is referred to the aquifer F (295.5-587.0 mg/L), while the lower is in the aquifer C3 (281.1-371.4 mg/L). The higher concentration could be related to the degradation of organic matter in the aquifer system producing CO_2 which dissolves as carbonates. Celico (1986) reported that concentrations higher than 300 mg/L

could be related to organic matter degradation. The comparison with these measured concentrations with previous studies referred to other near zone of the low Po Plain, that are Lodi (~ 100-400 mg/L; Guffanti et al., 2010), Pavia (~ 100-400 mg/L; Pilla et al., 2010), and Lomellina (~ 50-250 mg/L; Pilla et al. 2006), underlines the presence of higher concentrations of bicarbonates in the Cremona area.

Table 6.5. Statistics of measured bicarbonate concentration (mg/L) in July 2010.

	Total	**F**	**S**	**C1**	**C2**	**C3**
Mean	393.6	461.3	406.2	366.6	330.4	324.4
Min	196.5	295.5	330.5	314.1	196.5	281.1
Max	587.0	587.0	465.5	495.8	411.7	371.4
Median	389.5	454.3	401.5	361.6	341.5	337.0
Stand. Dev.	77.3	73.5	34.6	61.4	47.9	33.3

Calcium (Ca^{2+})

The measured calcium concentration constantly decreases over depth (Table 6.6 and Figure 6.2), similarly to bicarbonates. The calcium concentration ranges between around 50 and 300 mg/L. In the aquifer F, the concentration is more variable ranging from 67 to 270 mg/L. The concentration results less variable with increasing depths. Aquifer C3 has the lower concentration ranging between 55 and 98 mg/L.

Table 6.6. Statistics of measured calcium concentration (mg/L) in July 2010.

	Total	**F**	**S**	**C1**	**C2**	**C3**
Mean	124	168	129	101	93	74
Min	55	67	92	72	72	55
Max	270	270	198	138	152	98
Median	113	170	129	97	90	85
Stand. Dev.	46	44	27	21	18	16

Magnesium (Mg^{2+})

The measured magnesium concentration ranges from 10 to 85 mg/L and generally decreases over depth (Table 6.7 and Figure 6.2). The maximum concentration detected in the point CR88 (85 mg/L) represents an outlier due to the influence of the near located landfill. In the aquifers F and S, the concentration is more variable, while in the confined aquifers (C1, C2 and C3), the concentration is quite stable around 12 mg/L.

Table 6.7. Statistics of measured magnesium concentration (mg/L) in July 2010.

	Total	**F**	**S**	**C1**	**C2**	**C3**
Mean	20	30	20	13	12	14
Min	10	12	12	12	10	11
Max	85	85	38	15	15	22
Median	16	26	19	13	12	12
Stand. Dev.	12	16	6	1	1	3

Chloride (Cl^-)

The measured chloride concentration constantly decreases over depth (Table 6.8 and Figure 6.2), with the exception of the deeper wells which have higher concentration, up to 130 mg/L (GC3bis), due to the interaction with deep brackish waters. Some outliers can be identified in the superficial aquifers (F and S) probably related to anthropogenic influences: CR88 (115 mg/L) located downstream to a landfill, SN4 (80 mg/L) located in a zootechnical/agricultural area, CR80 (63 mg/L) located in a productive area. Without the outliers, the concentration ranges from 3 to 44 mg/L in the aquifer F and from 2 to 29 mg/L in the aquifer S. The concentration is stable around 2 mg/L in the aquifers C1 and C2, and has an average value of 24 mg/L in the aquifer C3.

Table 6.8. Statistics of measured chloride concentration (mg/L) in July 2010.

	Total	**F**	**S**	**C1**	**C2**	**C3**
Mean	17	30	15	2	2	24
Min	1	3	2	1	2	1
Max	130	115	80	3	5	130
Median	5	26	6	2	2	2
Stand. Dev.	24	23	20	1	1	44

Sodium (Na^+)

The measured sodium concentration (Table 6.9 and Figure 6.3) has an evolution over depth that concerns: higher concentration in the aquifer F (5-40 mg/L), lower concentration in aquifer S (4-20 mg/L), and a slight increase from aquifer C1 to C3. Two outliers can be identified, the first one is the superficial point CR88 (83 mg/L) located near a landfill, the second one is the deep point GC3 bis (94 mg/L) influenced by the deep salty waters.

Table 6.9. Statistics of measured sodium concentration (mg/L) in July 2010.

	Total	**F**	**S**	**C1**	**C2**	**C3**
Mean	16	20	9	12	12	31
Min	4	5	4	8	7	10
Max	94	83	20	18	19	94
Median	12	17	9	10	12	12
Stand. Dev.	15	17	4	4	4	28

Potassium (K^+)

The measured potassium concentration (Table 6.10 and Figure 6.3) results under the detection limit of 1 mg/L for the 80% of points. The higher concentration results in the aquifer F ranging from <1 up to 10 (CR88) mg/L. In the underlying aquifers, the concentration is under the detection limit, with the exception of aquifer S ranging from <1 to 3 mg/L.

Table 6.10. Statistics of measured potassium concentration (mg/L) in July 2010.

	Total	**F**	**S**	**C1**	**C2**	**C3**
Mean	1.1	2.0	0.9	0.5	0.5	0.5
Min	<1	<1	<1	<1	<1	<1
Max	10.0	10.0	3.0	<1	<1	<1
Median	0.5	0.8	0.5	0.5	0.5	0.5
Stand. Dev.	1.5	2.3	0.8	0.0	0.0	0.0

Sulfate (SO_4^{2-})

The measured sulfate concentration constantly decreases over depth (Table 6.11 and Figure 6.3) and is generally under the detection limit of 1 mg/L in the aquifers C1, C2 and C3. In the aquifer F, the concentration ranges from 3 to 213 mg/L, excluding the outlier CR88 (523 mg/L). The concentration is lower in the aquifer S ranging between <1 and 86 mg/L.

Table 6.11. Statistics of measured sulfate concentration (mg/L) in July 2010.

	Total	**F**	**S**	**C1**	**C2**	**C3**
Mean	36.9	88.7	33.6	0.5	0.9	0.6
Min	<1	3.0	<1	<1	<1	<1
Max	523.0	523.0	86.0	<1	4.0	1.0
Median	5.5	57.0	22.0	0.5	0.5	0.5
Stand. Dev.	73.3	108.7	29.9	0.0	1.1	0.2

Nitrate (NO_3^-)

The measured nitrate concentration (Table 6.12 and Figure 6.3) results above the detection limit of 1 mg/L in the aquifer F, while it is lower than 1 mg/L in the underlying aquifers, with a few exceptions. In the aquifer F, the concentrations can be classified in three groups: the first group concerns concentrations above the quality standard of 50 mg/L (D. Lgs. 30/2009), the second group concerns concentrations below 5 mg/L, the third group concerns intermediate concentrations between 20 and 30 mg/L. This variability within the aquifer F can be related to different redox condition, in fact the higher nitrate concentrations correspond to the higher measured values of ORP.

Table 6.12. Statistics of measured nitrate concentration (mg/L) in July 2010.

	Total	**F**	**S**	**C1**	**C2**	**C3**
Mean	7.1	20.7	0.9	0.5	0.5	0.5
Min	<1	<1	<1	<1	<1	<1
Max	67.0	67.0	7.0	<1	<1	<1
Median	0.5	3.5	0.5	0.5	0.5	0.5
Stand. Dev.	17.1	25.4	1.6	0.0	0.0	0.0

Ammonium (NH_4^+)

The measured ammonium concentration (Table 6.13 and Figure 6.4) results higher than the limit for the good environmental status of 0.5 mg/L (D. Lgs. 30/2009) for the 75% of points. The evolution of ammonium concentration over depth is characterized by lower values in the aquifer F, generally below the detection limit of 0.1 mg/L, and higher values ranging between around 1.5 and 4.5 mg/L in the aquifers F, C1, C2 and C3. In the aquifer F, in those points where the concentrations are above the detection limit, the values ranging from 0.4 to 3.7 mg/L, with the exception of the outlier SN8 (18.9 mg/L). The concentrations are more variable in the aquifer S ranging from <0.1 to 6.7 mg/L. From aquifer C1 to C3, a slight decreasing of concentration could be identified probably related to the increase of pH. In fact, the chemical equilibrium between ammonium and ammonia can shift to ammonia with an increase of pH, as reported by West (1968).

Table 6.13. Statistics of measured ammonium concentration (mg/L) in July 2010.

	Total	F	S	C1	C2	C3
Mean	2.58	1.52	2.84	3.84	3.09	2.91
Min	<0.1	<0.1	<0.1	2.40	1.60	1.60
Max	18.90	18.90	6.70	4.70	4.40	4.60
Median	2.45	0.05	2.40	4.30	3.10	2.60
Stand. Dev.	2.64	4.04	1.91	1.00	0.92	1.12

6.1.2. Minor inorganic and organic parameters

Iron (Fe)

The measured iron concentration (Table 6.14 and Figure 6.4) results higher than the regulatory limit of 200 µg/L (D. Lgs. 152/2006) for the 75% of points. In the superficial aquifers, the concentration is higher and more variable ranging from <20 to 4756 µg/L in the aquifer F and from <20 to 5975 µg/L in the aquifer S. From aquifer C1 to C3 the concentration decreases, with the exception of the points CR27 (1836 µg/L) and CV2 (2863 µg/L). The concentration is generally below the regulatory limit of 200 µg/L in the aquifer C3.

Table 6.14. Statistics of measured iron concentration (µg/L) in July 2010.

	Total	F	S	C1	C2	C3
Mean	1110	1367	1867	660	596	249
Min	<20	<20	<20	112	108	60
Max	5975	4756	5975	1252	2863	756
Median	601	649	1543	774	332	239
Stand. Dev.	1307	1547	1475	451	755	259

Manganese (Mn)

The measured manganese concentration (Table 6.15 and Figure 6.4) results higher than the regulatory limit of 50 µg/L (D. Lgs. 152/2006) for the 84% of points. The concentration generally decreases over depth. In the aquifer F, the concentration is higher and more variable ranging from <5 to 1255 µg/L. The concentration is generally lower in the aquifer S, ranging between 84 and 543 µg/L. In the aquifers C1, C2 and C3 the concentration is more stable, generally between 50 and 150 µg/L.

Table 6.14. Statistics of measured manganese concentration (µg/L) in July 2010.

	Total	F	S	C1	C2	C3
Mean	186	256	259	106	103	76
Min	<5	<5	84	49	56	34
Max	1255	1255	543	152	208	125
Median	125	159	234	123	86	82
Stand. Dev.	216	335	136	41	41	38

Arsenic (As)

The measured arsenic concentration (Table 6.16 and Figure 6.4) results higher than the regulatory limit of 10 µg/L (D. Lgs. 152/2006) for the 74% of points. The evolution of concentration over depth is characterized by an increase from aquifer F to S and a consequent decrease from aquifer C1 to C3. In the aquifer F, the concentration ranges from <3 to 74 µg/L. The concentration is more variable in the aquifer S, ranging between <3 to 183 µg/L (maximum value). In the aquifer C1 the concentration is generally higher ranging from 22 to 154 µg/L. The concentration is lower in the aquifers C2 and C3, but generally still above the regulatory limit of 10 µg/L.

Table 6.16. Statistics of measured arsenic concentration (µg/L) in July 2010.

	Total	F	S	C1	C2	C3
Mean	37	15	58	76	38	22
Min	<3	<3	<3	22	15	<3
Max	183	74	183	154	95	37
Median	28	2	38	69	33	26
Stand. Dev.	38	21	53	41	20	11

Chrome (Cr)

The measured chrome concentration results lower than the detection limit of 5 µg/L for the 90% of points. The remaining 10% of points is below the regulatory limit of 50 µg/L (D. Lgs. 152/2006).

Lead (Pb)

The measured lead concentration results lower than the detection limit of 3 µg/L, with the exception of the following points: CR12, CR16 and CR41 with a concentration of 3 µg/L; CR84bis with a concentration of 6 µg/L; CR24a with a concentration of 16 µg/L, above the regulatory limit of 10 µg/L (D. Lgs. 152/2006).

The high lead concentration in CR24a can be considered as local phenomenon, probably generating by anthropic activities in proximity of the point.

Zinc (Zn)

The measured zinc concentration results lower than the detection limit of 20 µg/L in all the sampled points.

Chlorinated aliphatic hydrocarbons

In this work, the chlorinated aliphatic hydrocarbons were measured in order to check their general absence or presence and, in the case of relevant presence, to verify a possible correlation with As, Fe and Mn. The measured concentration of chlorinated aliphatic hydrocarbons results low, the sum of all detected organochlorides (Table 3.3) is lower than 0.5 µg/L, with the exception of four points (CR23b, CR80, CR81 and CR86 with 32.7, 42.5, 0.5 and 1.0 µg/L, respectively) which are located in a contamination plume already characterized by public authorities.

Aliphatic and aromatic hydrocarbons

The measured concentration of aliphatic hydrocarbons results lower than the detection limits, which are listed in table 6.17. Concerning the aromatic hydrocarbons, benzene, styrene and toluene result lower than the detection limits. The measured ethylbenzene concentration results higher than the detection limit in three points (CR86, CR43 and CR36), with a maximum value of 5 µg/L, that is below the regulatory limit of 50 µg/L (D.Lgs. 152/06). The measured xylenes concentration results higher than the detection limit in the same three points, with a maximum of 2 µg/L that is below the regulatory limit of 10 µg/L referred to p-xylene (D.Lgs. 152/06).

Table 6.17. Detection limits for the aliphatic and aromatic hydrocarbons.

Aliphatic hydrocarbons	**Detection limit (µg/L)**
total hydrocarbon	30
light hydrocarbon C<12	10
heavy hydrocarbon C>12	20
methyl tert-butyl ether	10

Aromatic hydrocarbons	**Detection limit (µg/L)**
benzene	1
ethylbenzene	1
styrene	1
toluene	1
xylenes	1

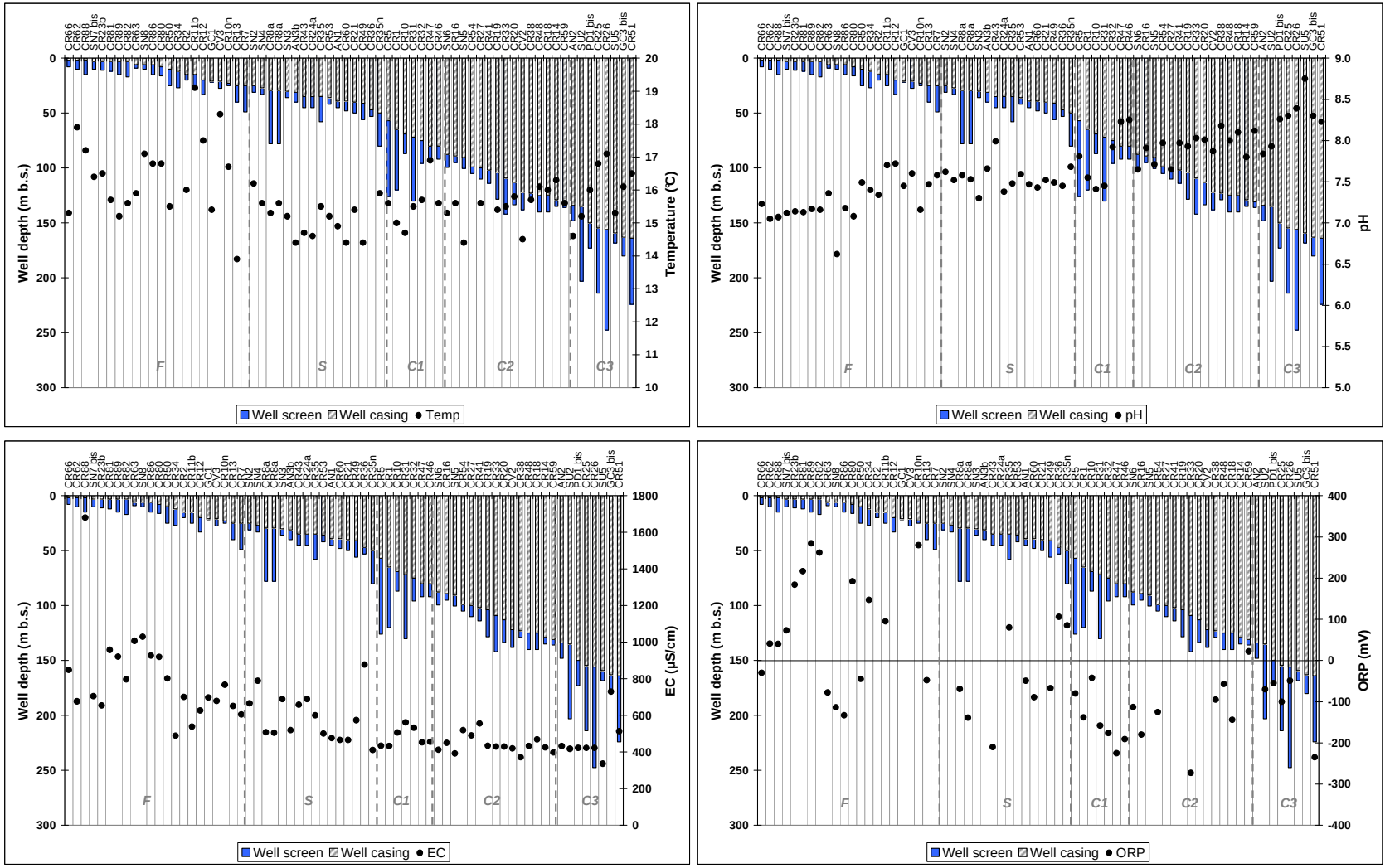

Figure 6.1. Measured values of temperature, pH, EC and ORP ($E_{Ag/AgCl}$) over well depth in July 2010.

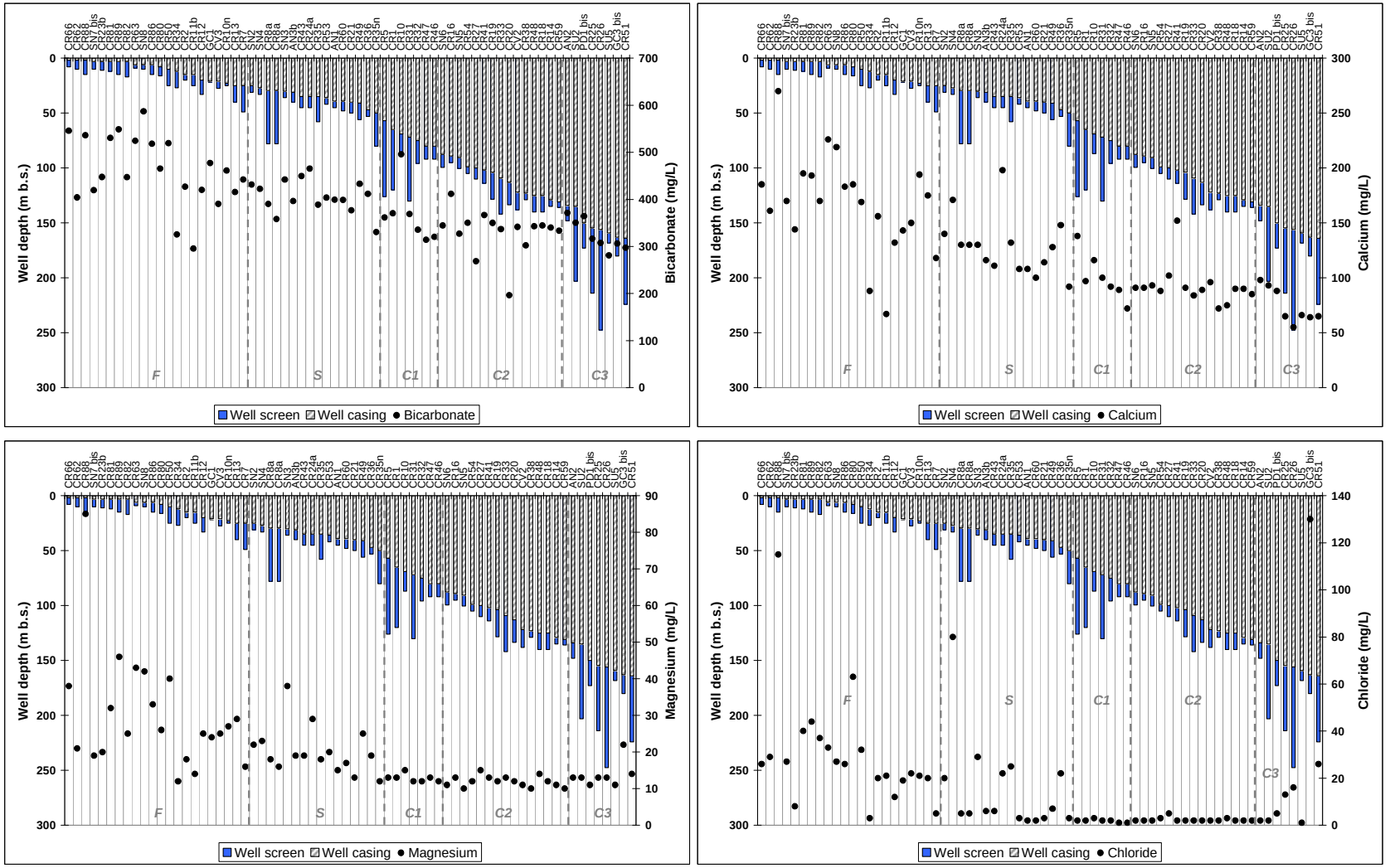

Figure 6.2. Measured concentrations of bicarbonate, calcium, magnesium and chloride over well depth in July 2010.

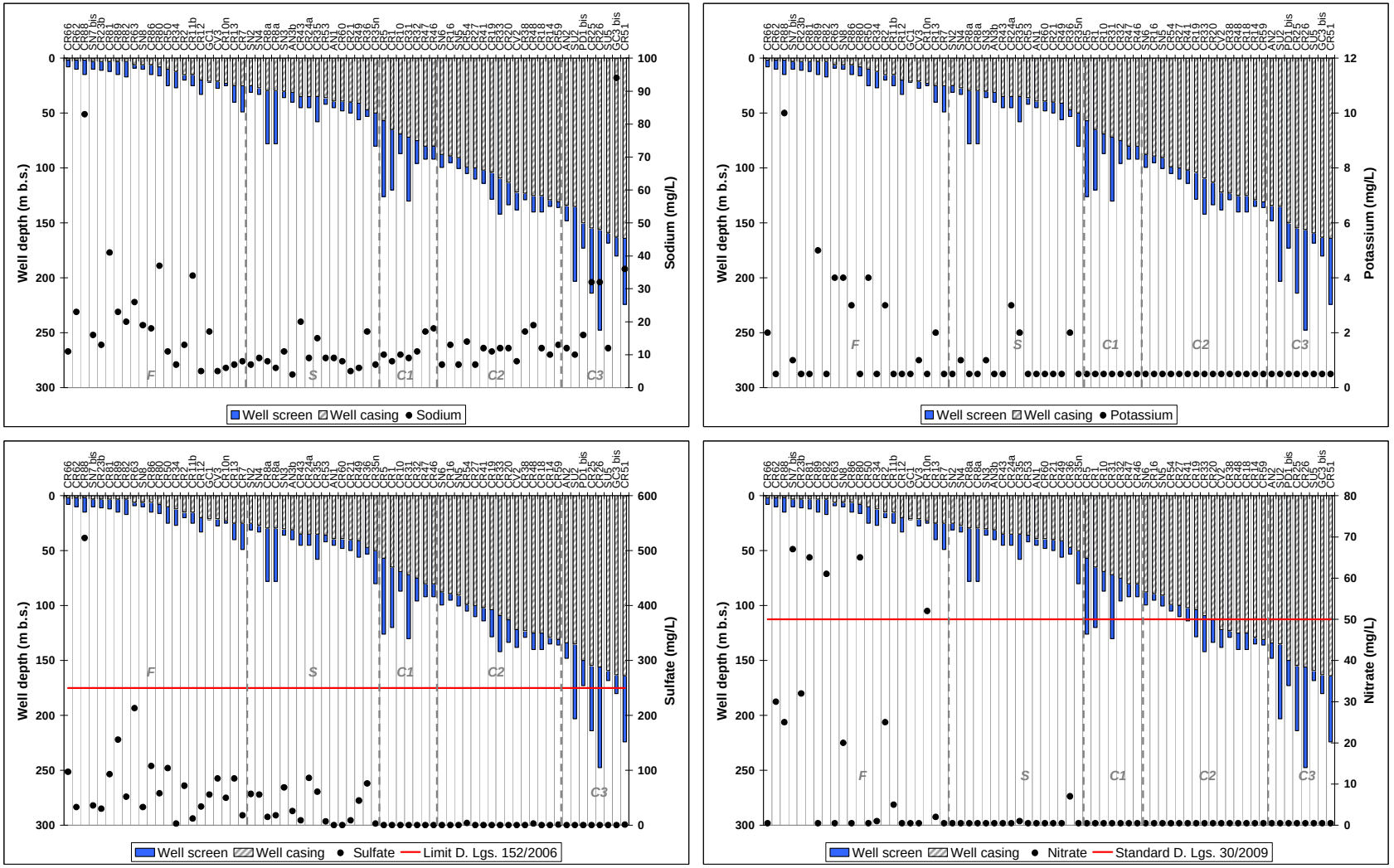

Figure 6.3. Measured concentrations of sodium, potassium, sulfate and nitrate over well depth in July 2010.

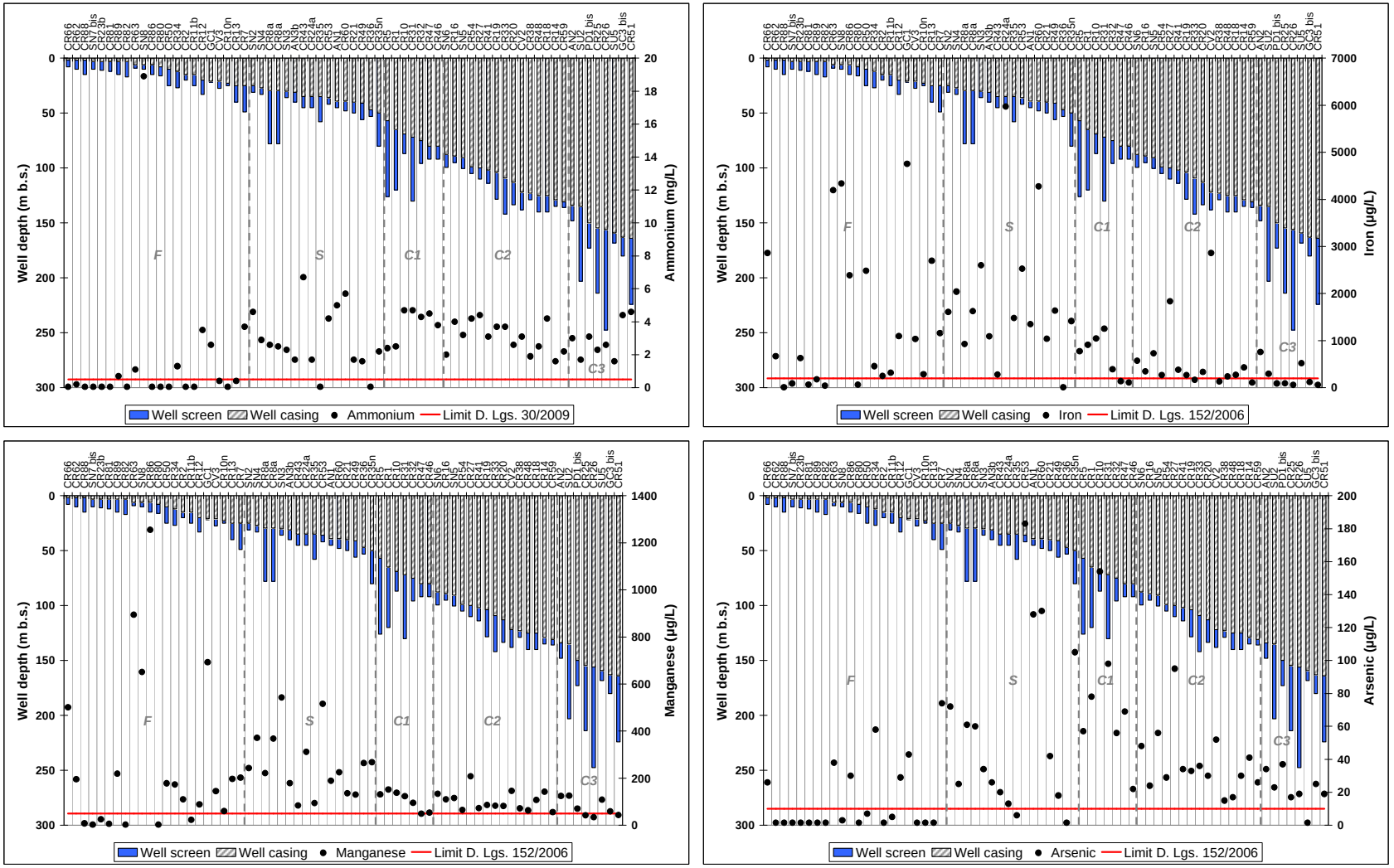

Figure 6.4. Measured concentrations of ammonium, iron, manganese and arsenic over well depth in July 2010.

6.1.3. Spatial distribution of As, Fe, Mn and NH_4 concentrations

In this paragraph, the description of the spatial distribution of As, Fe, Mn and NH_4 concentrations for each aquifer is presented. Special attention is focused on the aquifer F, where zones with different hydrochemical behaviour can be identified. The measured concentrations of As, Fe, Mn and NH_4 in the aquifer F are showed in 3D maps (Figures 6.6, 6.7, 6.8 and 6.9) combining the modelled distribution of fine-grained deposits and the presence of peat. The measured concentrations are represented with spheres located in correspondence of the well screens. These spheres have four different colours corresponding to four classes of concentrations. The maximum and minimum of each class are defined on the basis of multiplier values of the regulatory limits, as reported in table 6.18. For the measurements below the detection limit, a concentration as half the detection limit was considered. The underlying aquifers (S, C1, C2 and C3) generally have more homogeneous hydrochemical behaviour, therefore a general description is given.

Table 6.18. Maximum and minimum values for the 4 classes considered in figures 6.6, 6.7, 6.8, 6.9

Chemical species	Regulatory limit	x 0	x 1	x 3	x 10	x 40
Fe (µg/L)	200 (D. Lgs. 152/06)	0	200	600	2000	8000
Mn (µg/L)	50 (D. Lgs. 152/06)	0	50	150	500	2000
As (µg/L)	10 (D. Lgs. 152/06)	0	10	30	100	400
NH_4 (mg/L)	0.5 (D. Lgs. 30/09)	0	0.5	1.5	5	20

Oxidation reduction potential

In order to relate the As, Fe, Mn and NH_4 concentrations with the redox condition, the distribution of measured ORP ($E_{Ag/AgCl}$) is first showed. As shown in paragraph 6.1.1, the measured ORP values are generally negative, with the exception of aquifer F which has both negative and positive values. The distribution of measured ORP values in aquifer F is represented in figure 6.5. The figure shows that negative values are located in the Po valley, south of the terrace scarp, and in the central-northern part of the study area, while positive values are mainly located in the area behind the scarp. The presence of negative values, and thus more reducing conditions, in the Po valley can be related to: (1) the presence of

superficial silty-clayey deposits which locally produce confined condition limiting the infiltration of recharge water with higher oxygen concentrations; (2) the presence of peat deposits, which can be degraded involving oxygen consumption; (3) the possible presence of a higher dissolved organic carbon (DOC) content generating by the interaction between Po river water and groundwater, that occurs in the case of higher hydrometric level of Po river with respect to groundwater hydraulic head, according to the mechanism reported by previous works (e.g. Beretta, 1992; Petrunic et al., 2005). The more reducing condition in the central-northern part of the study area can be related to the presence of superficial silty-clayey deposits which locally produce confined condition. The presence of positive ORP values, and thus more oxidative condition, in the area behind the scarp can be related to the presence of sandy deposits that allow a higher infiltration rate of recharge water characterized by higher oxygen concentrations.

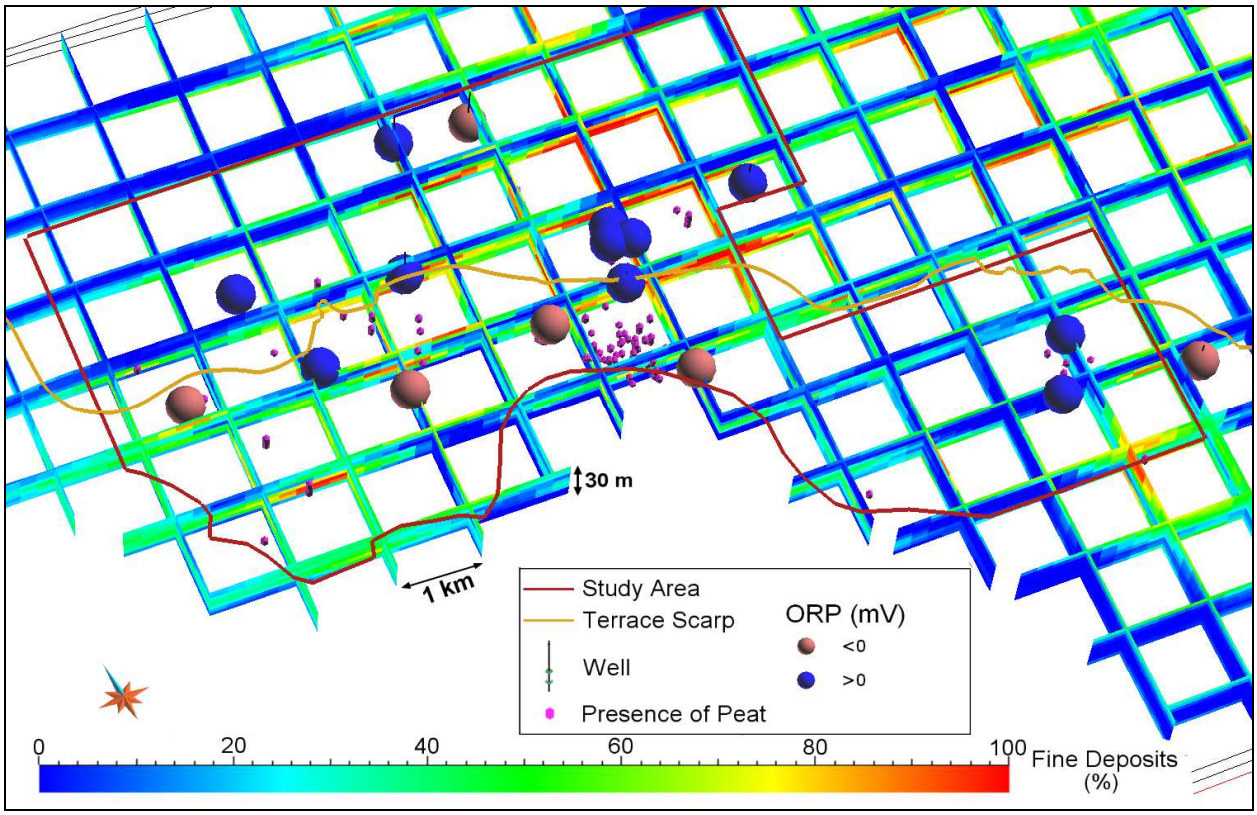

Figure 6.5. 3D location of measured ORP values ($E_{Ag/AgCl}$) in aquifer F (July 2010), combining the modelled distribution of fine-grained deposits and the presence of peat.

Arsenic

Figure 6.6 shows the distribution of measured As concentrations in the aquifer F. The higher concentrations (30–100 µg/L) are located in the Po valley, while in the remaining zones the concentrations are below the regulatory limit of 10 µg/L, with the exception of one point (CR34, 58 µg/L). Aquifers S and C1 have a heterogeneous distribution, with higher values (100-400 µg/L) in the north-eastern part of the study area for the former, and in the central part of the area for the latter. Aquifers C2 and C3 have a more homogeneous distribution with lower concentrations.

Iron

Figure 6.7 shows the distribution of measured Fe concentrations in the aquifer F. The higher values (2000-8000 µg/L) are located in the Po valley and in the central-northern part of the study area, while lower values generally characterize the area behind the scarp. Aquifers S has a heterogeneous distribution, with higher values (2000-8000 µg/L) in the central and eastern parts of the area. Aquifers C1, C2 and C3 have a more homogeneous distribution with lower concentrations.

Manganese

Figure 6.8 shows the distribution of measured Mn concentrations in the aquifer F. The higher concentrations (500-2000 µg/L) are located in the Po valley, while the lower values are generally referred to the area behind the scarp. Aquifer S has a more homogeneous distribution with higher values in the western part of the area. Aquifers C1, C2 and C3 have homogeneous distributions with lower values.

Ammonium

Figure 6.9 shows the distribution of measured NH_4 concentrations in the aquifer F. The higher concentrations (5-20 mg/L) are located in the Po valley, while in the remaining zones the concentrations are generally below 0.5 mg/L. Aquifer S has a heterogeneous distribution with higher values (5-20 mg/L) located in the eastern part of the study area. Aquifers C1, C2 and C3 have a more homogeneous distribution with concentrations ranging between 1.5 and 5 mg/L.

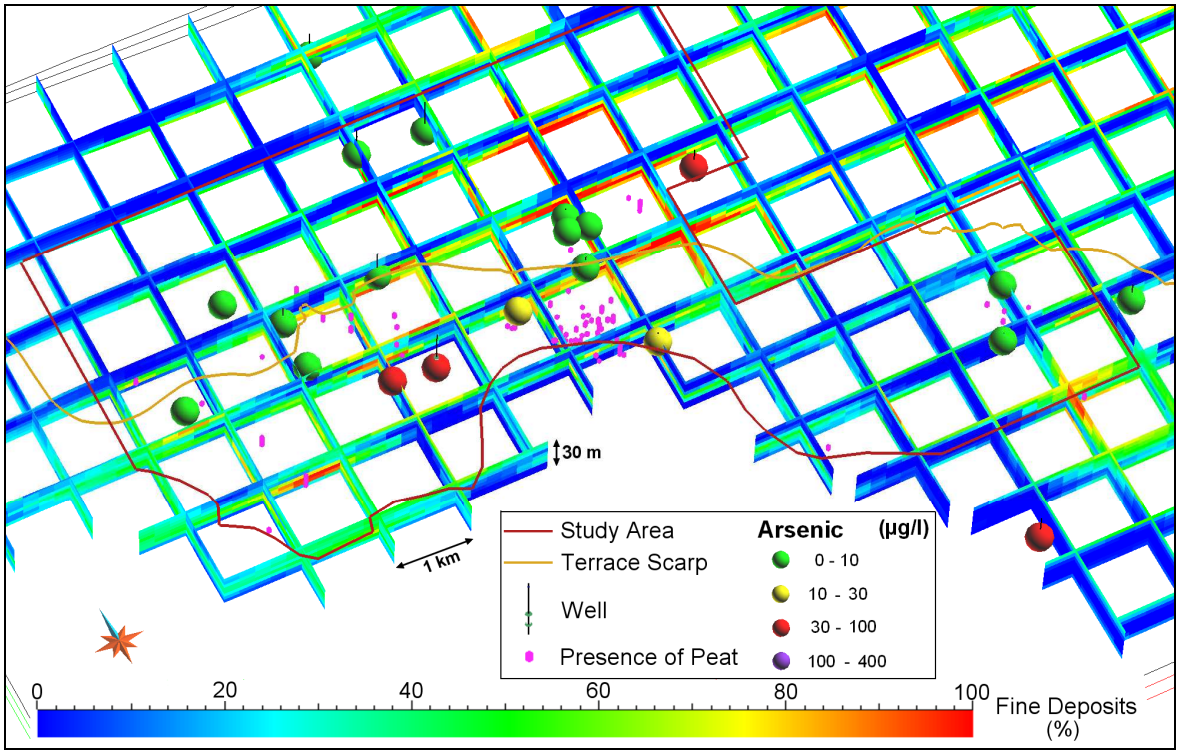

Figure 6.6. 3D location of measured As concentrations in aquifer F (July 2010), combining the modelled distribution of fine-grained deposits and the presence of peat.

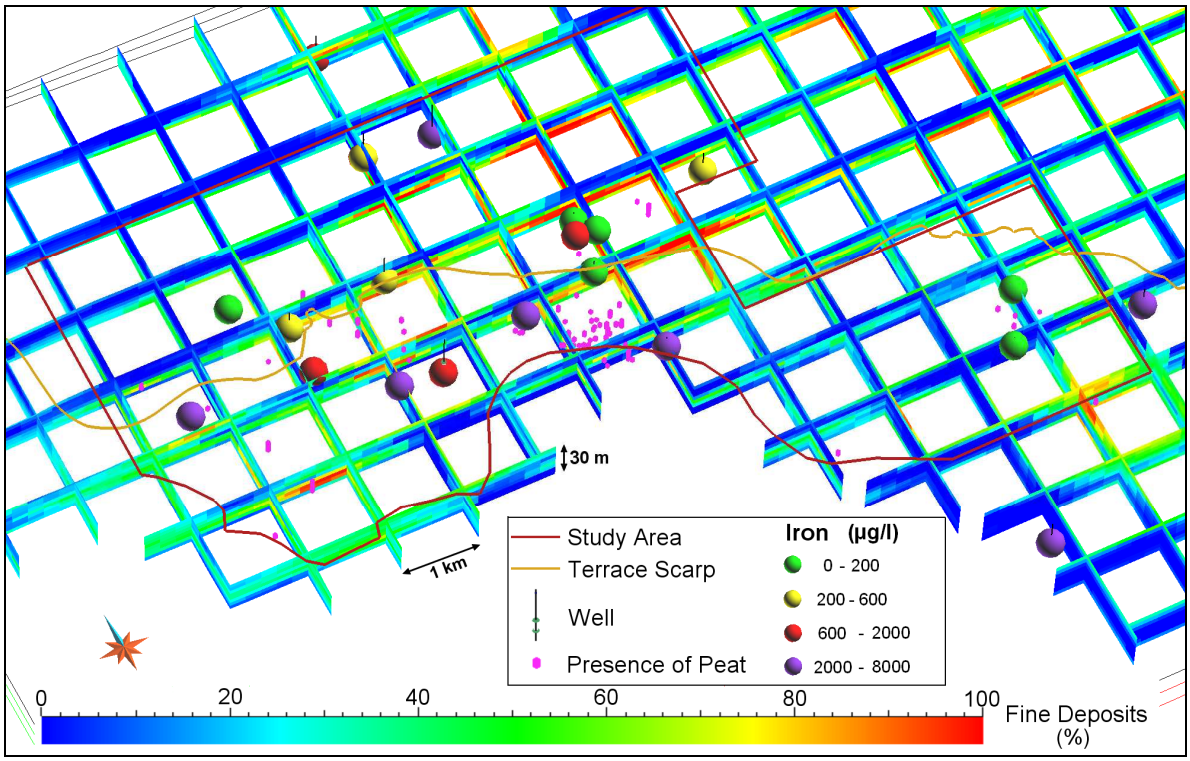

Figure 6.7. 3D location of measured Fe concentrations in aquifer F (July 2010), combining the modelled distribution of fine-grained deposits and the presence of peat.

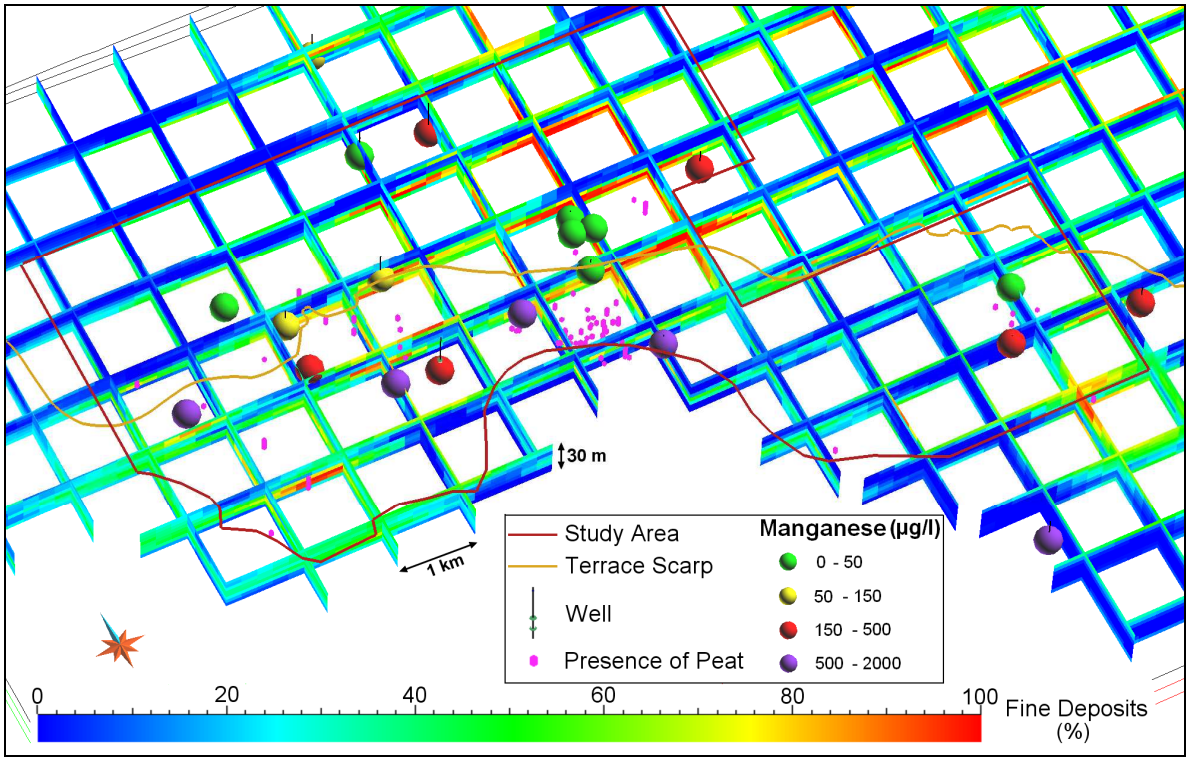

Figure 6.8. 3D location of measured Fe concentrations in aquifer F (July 2010), combining the modelled distribution of fine-grained deposits and the presence of peat.

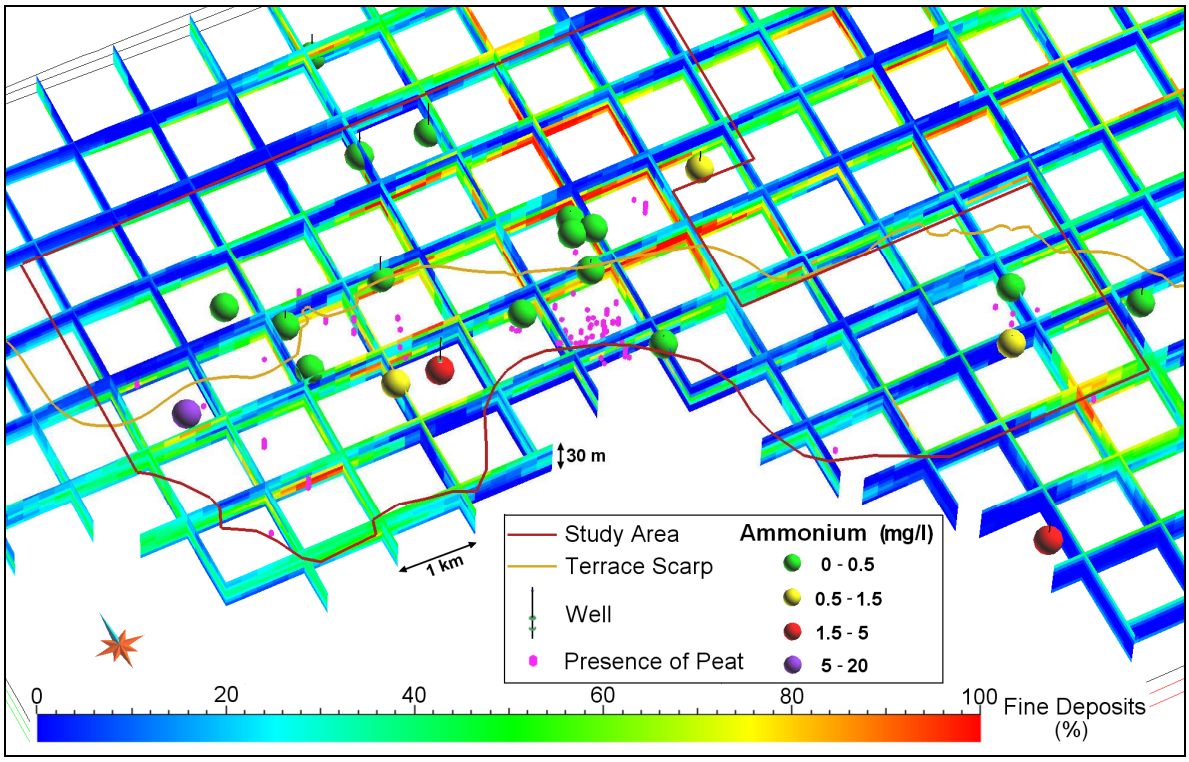

Figure 6.9. 3D location of measured NH_4 concentrations in aquifer F (July 2010), combining the modelled distribution of fine-grained deposits and the presence of peat.

6.1.4. Summary of As, Fe, Mn and NH_4 characterization

The analysis of the water quality measurements of the survey of July 2010 underlines that:

- the measured As, Fe, Mn and NH_4 concentrations can represent the natural background of the study area due to the absence of anthropic activities representing potential direct sources and indirect anthropogenic influences (general absence of hydrocarbons in the measured points);
- each aquifer has a quite homogeneous hydrochemical behaviour, with the exception of aquifer F where reduced *facies* can be identified in the Po valley and in the central-northern part of the study area, while oxidized *facies* can be indentified in the area behind the terrace scarp.

In order to summarize the measured concentrations of As, Fe, Mn and NH_4, four box-plot graph are presented in figures 6.10, 6.11, 6.12 and 6.13. In these graphs, the concentrations referred to aquifer F are separated in three groups: Po valley (F S), central-northern part of the study area (F CN) and area behind the terrace scarp (F RO). Each underlying aquifer is represented by a single group (S, C1, C2 and C3). In the box-plot the data referred to the multi-aquifer wells were excluded in order to represent the distinctive concentrations for each aquifer. The statistical parameters of the four box-plot are listed in tables 6.19, 6.20, 6.21 and 6.22.

The box-plots show that in the aquifer F the concentrations of As, Fe, Mn and NH_4 are higher in the Po river valley (F S), lower in the area behind the terrace scarp (F RO) and with intermediate values in the central-northern part of the study area (F CN). In the underlying aquifers: (1) arsenic concentration increases up to aquifers S and C1 and then decreases in aquifers C2 and C3; (2) iron concentration remains high in aquifer S and then decreases from aquifer C1 to C3; (3) manganese concentration decreases from aquifer S to C3; (4) ammonium concentration increases in aquifer S and then has constant high values in aquifers C1, C2 and C3.

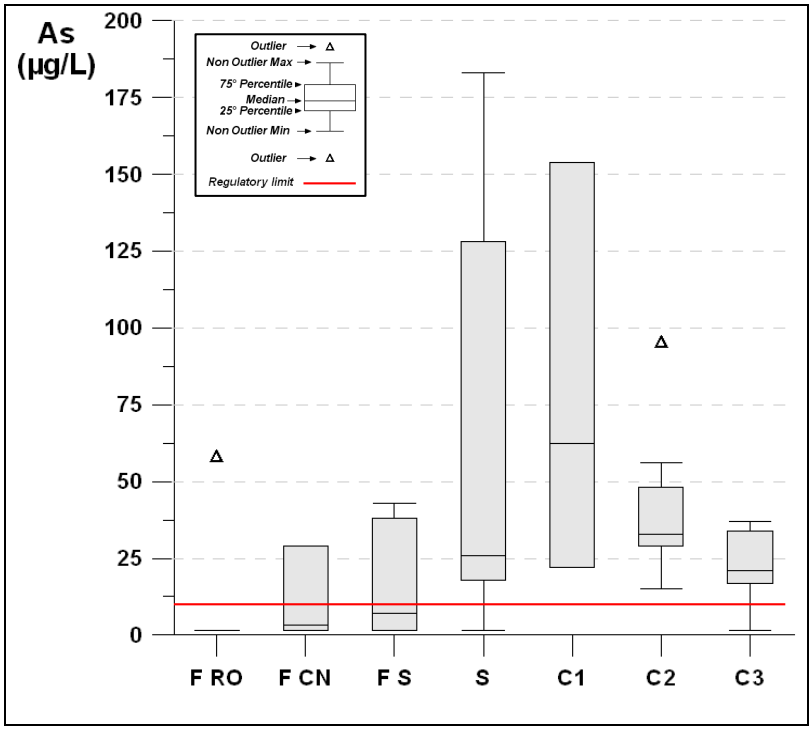

Figure 6.10. Box-plot of measured As concentrations (July 2010) in aquifer F (F RO: area behind the terrace scarp; F CN: central-northern part of the study area; F S: Po river valley) and in the underlying aquifers (S, C1, C2 and C3).

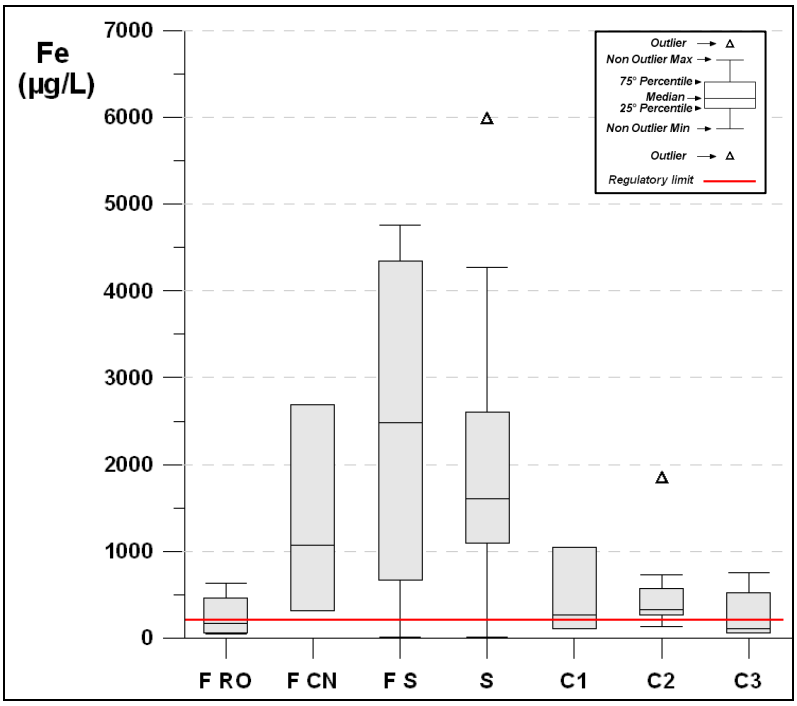

Figure 6.11. Box-plot of measured Fe concentrations (July 2010) in aquifer F (F RO: area behind the terrace scarp; F CN: central-northern part of the study area; F S: Po river valley) and in the underlying aquifers (S, C1, C2 and C3).

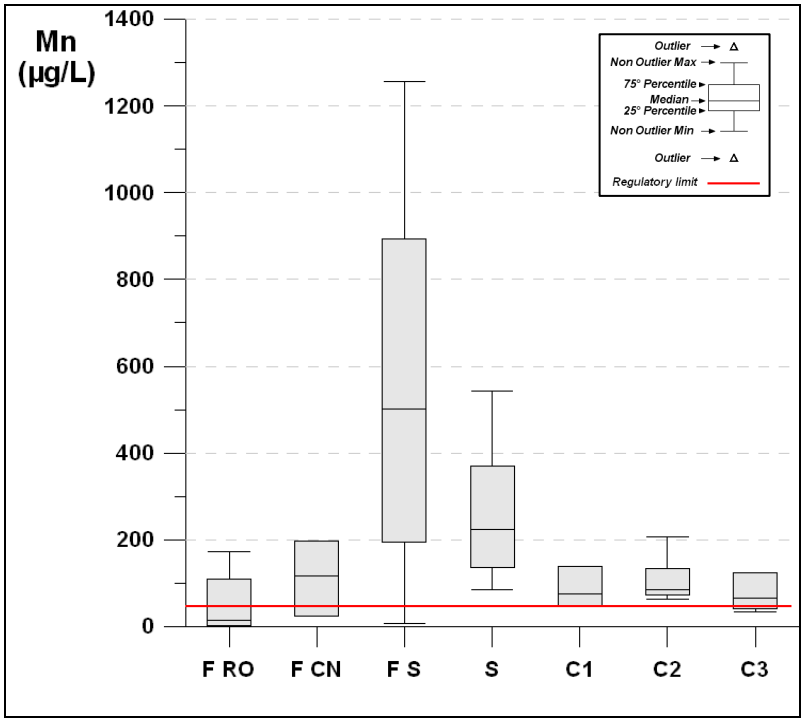

Figure 6.12. Box-plot of measured Mn concentrations (July 2010) in aquifer F (F RO: area behind the terrace scarp; F CN: central-northern part of the study area; F S: Po river valley) and in the underlying aquifers (S, C1, C2 and C3).

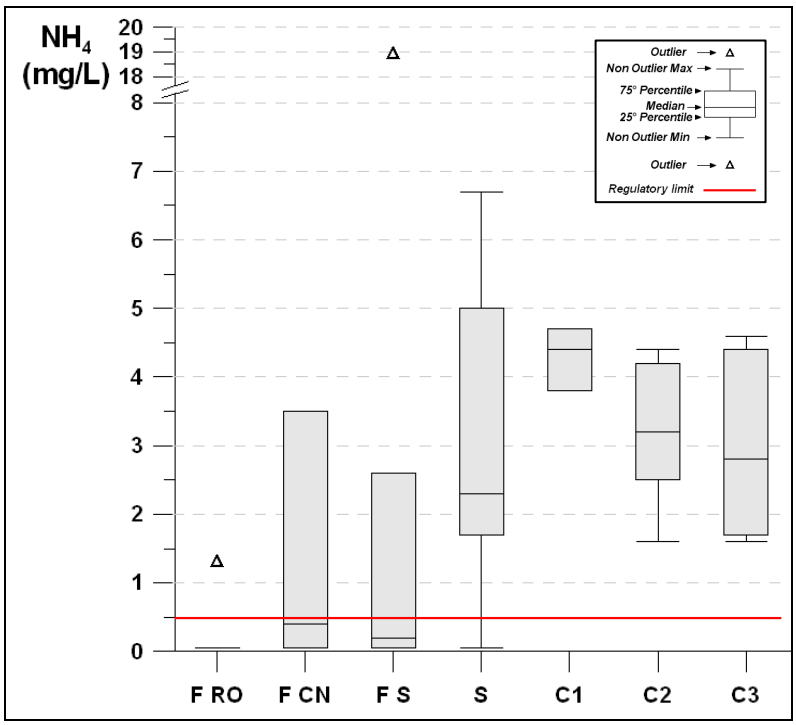

Figure 6.13. Box-plot of measured NH_4 concentrations (July 2010) in aquifer F (F RO: area behind the terrace scarp; F CN: central-northern part of the study area; F S: Po river valley) and in the underlying aquifers (S, C1, C2 and C3).

Table 6.19. Statistical parameters of the As box-plot (Figure 6.10).

As (µg/L)	F RO	F CN	F S	S	C1	C2	C3
N. Measurements	8	4	9	13	4	13	8
Minimum	1.5	1.5	1.5	1.5	22	15	1.5
25° percentile	1.5	1.5	1.5	18	22	29	17
Median	1.5	3	7	26	63	33	21
75° percentile	1.5	29	38	128	154	48	34
Maximum	58	29	43	183	154	95	37

Table 6.20. Statistical parameters of the Fe box-plot (Figure 6.11).

Fe (µg/L)	F RO	F CN	F S	S	C1	C2	C3
N. Measurements	8	4	9	13	4	13	8
Minimum	43	318	10	10	112	132	60
25° percentile	62	318	669	1091	112	267	61
Median	171	1066	2484	1607	263	332	106
75° percentile	457	2694	4340	2601	1045	573	518
Maximum	629	2694	4756	5975	1045	1836	756

Table 6.21. Statistical parameters of the Mn box-plot (Figure 6.12).

Mn (µg/L)	F RO	F CN	F S	S	C1	C2	C3
N. Measurements	8	4	9	13	4	13	8
Minimum	2.5	23	8	84	49	63	34
25° percentile	2.5	23	195	136	49	73	42
Median	16	117	501	225	75	86	65
75° percentile	110	197	894	371	138	134	124
Maximum	173	197	1255	543	138	208	125

Table 6.22. Statistical parameters of the NH_4 box-plot (Figure 6.13).

NH_4 (mg/L)	F RO	F CN	F S	S	C1	C2	C3
N. Measurements	8	4	9	13	4	13	8
Minimum	0.05	0.05	0.05	0.05	3.80	1.60	1.60
25° percentile	0.05	0.05	0.05	1.70	3.80	2.50	1.70
Median	0.05	0.40	0.20	2.30	4.40	3.20	2.80
75° percentile	0.05	3.50	2.60	5.00	4.70	4.20	4.40
Maximum	1.30	3.50	18.90	6.70	4.70	4.40	4.60

6.2. Results of the survey of July 2012

The survey of July 2012 was executed in a smaller number of points (14) compared to the survey of July 2010 (68). In general, the hydrochemical characterization elaborated on the basis of July 2010 data is confirmed by the survey of July 2012. Table 6.23 reports the comparison between the mean values

of concentration of the chemical parameters measured in July 2010 and July 2012. The mean concentrations of the two surveys are generally comparable. In particular, the major anions and cations have quite similar concentrations. Otherwise, a slight difference can be identified for the redox sensitive species: ammonium and sulfate were measured with lower concentrations in July 2012, while arsenic, iron and manganese have higher values in July 2012. These differences could be related to different redox conditions that occurred in the two surveys. A long-term monitoring is probably required to better understand the causes of these temporal variations of concentrations.

The analysis of sulfide, that was not considered in the survey of July 2010, leads to the following result: sulfide was measured below the detection limit of 0.1 mg/L in all the sampled points.

Table 6.23. Mean values of concentration of the chemical parameters measured in July 2010 and 2012.

	July 2010	**July 2012**
ammonium (mg/L)	2.6	1.5
nitrate (mg/L)	7.1	7.5
chloride (mg/L)	16.7	17.6
sulfate (mg/L)	36.9	29.8
bicarbonate (mg/L)	393.6	375.5
calcium (mg/L)	124.1	130.1
magnesium (mg/L)	20.0	18.7
potassium (mg/L)	1.1	1.3
sodium (mg/L)	16.1	15.6
iron (µg/L)	1110.3	1686.1
arsenic (µg/L)	37.2	51.3
manganese (µg/L)	186.2	209.4

6.3. Principal component analysis of July 2010 data

In this paragraph the relation between the measured chemical parameters are analysed by means of a principal component analysis (PCA). The July 2010 data were chosen instead of the July 2012 data for the bigger number of sampled points.

The original variables are the measured chemical parameters in July 2010, with the exclusion of: (1) organic compounds, only measured in the superficial aquifers (F and S); (2) chrome, lead and zinc, generally measured below the

detection limits; (3) ORP, only measured in 46 points. Therefore the total number of original variables is equal to 15. Concerning the observations, the following measured points were excluded: (1) SN8, CR88 and GC3bis, considered as outliers for ammonium, sulfate and chloride, respectively; (2) CR7, CR8a, CR35new, CR5, CR1, CR31, CV2 and CR59, which are multi-aquifer wells; (3) CR13, CR24a, CR47, CR41 and CR20, which have a charge balance error higher than 10%. In summary, the total number of observations considered in the PCA is equal to 51.

The eigenvalues for each principal component (PC) were calculated with the auto-scaling method and are reported in figure 6.14. The Kaiser criterion (Kaiser, 1958) was used to determine the significant principal components. This method concerns the selection of those components for which the eigenvalues are higher or equal to 1. As showed in figure 6.14, only the first four principal components have a eigenvalue higher than 1, and thus, can be considered as significant components. The four significant components explain the 82.4% of the variance in the original dataset (cumulative explained variance). The PC1 and PC2 explain the 47.4% and 19.8% of the variance, respectively, while the PC3 and PC4 explain lower percentages of variance, that are 8.9% and 6.2%, respectively.

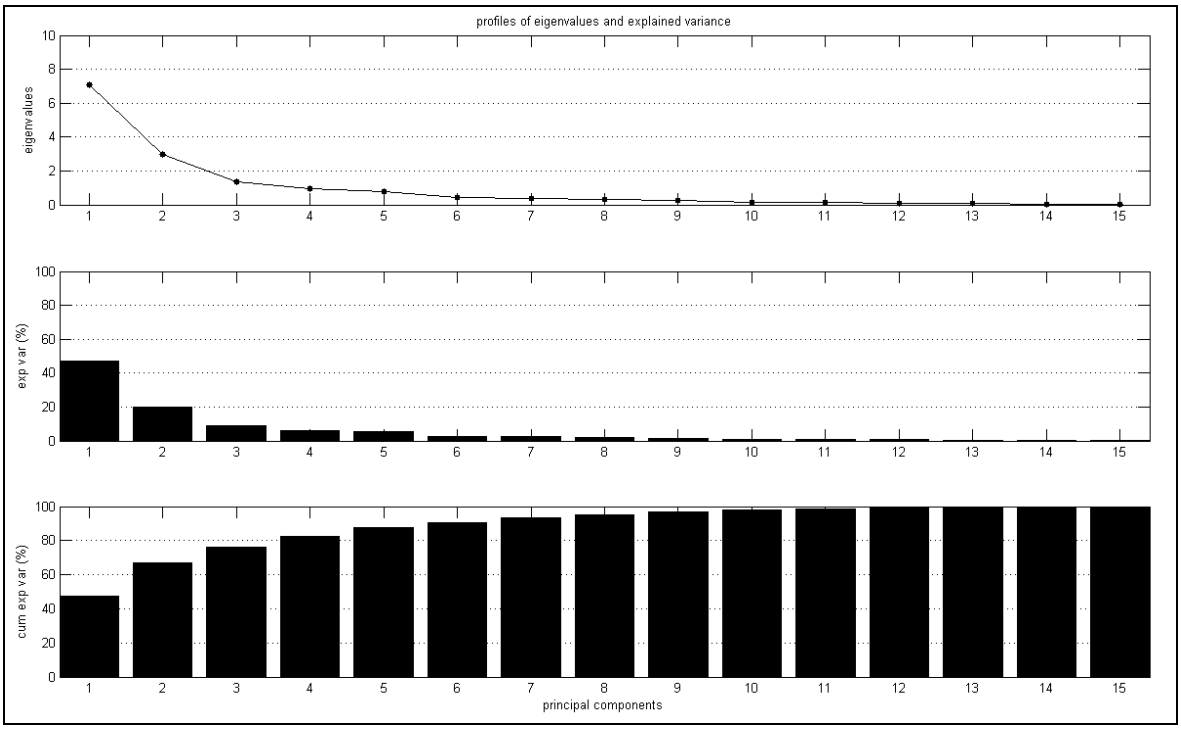

Figure 6.14. Eigenvalue (on the top), explained variance (in the middle) and cumulative explained variance (on the bottom) for each principal component.

Figure 6.15 shows the loading plot and the score plot for the PC1 and PC2. Considering the loadings of PC1, the most important original variables result pH and conductivity, followed by a group of major anions and cations as calcium, sulfate, magnesium, bicarbonate, ammonium and, further apart, chloride and potassium. This result points out that the pH, conductivity and major cations and anions govern the first principal component, which explains around 50% of the variance in the original dataset, and thus, they represent the main parameters which characterize the system. The loading plot also describes the relations between the original variables: (1) pH and conductivity have a strong negative correlation; (2) the major cations and anions are positively correlated, with the exception of ammonium that is negatively correlated; (3) pH and ammonium have a positive correlation. These correlations are probably related to the evolution of these parameters with depth, indeed pH and ammonium increase over depth while the other major cations and anions decrease. Considering the loading of PC2, the most important original variables result nitrate, sodium, temperature, iron, manganese, arsenic and ammonium. The group of nitrate, sodium and temperature is negatively correlated to the group of iron, manganese, arsenic and ammonium. These relations reflect the groundwater redox zoning. In the score plot of figure 6.15, the observations (measured points) are classified for each aquifer, considering the previous three groups for the aquifer F, that are F S (Po valley), F RO (area behind the scarp) and F CN (central-northern part of the study area). The data F RO form a distinct group that is characterized by higher conductivity, nitrate, chloride, sulfate and bicarbonate values, and by lower pH, iron, manganese, arsenic and ammonium values. Also the data F S form a distinct group, which is characterized by higher values of iron, manganese, chloride, sulfate, carbonate and conductivity and by lower values of pH, nitrate, ammonium and arsenic. The data F CN result between the groups F S and F RO, even if an outlier can be identified. The data of aquifer S are characterized by higher values of arsenic, ammonium and pH and by lower values of conductivity, chloride, bicarbonates and sulfate. The data of aquifers C1, C2 and C3 can be considered as a single group which is characterized by higher values of pH and ammonium, lower values of nitrate, conductivity, sulfate and bicarbonate and a slight decreasing of manganese, iron and arsenic. In summary, the score plot for the PC1 and PC2 points out distinctive hydrochemical characteristics for the different zones of aquifer F and for aquifer S,

while the aquifers C1, C2 and C3 result with homogeneous hydrochemical characteristics.

Figure 6.16 shows the loading plot for PC3 and PC4. The most significant original variables result pH and nitrate (negatively correlated) for the PC3 and sodium and potassium (negatively correlated) for the PC4. These two principal components, which explain a lower percentages of the variance (8.9% and 6.2%), do not seem to correspond to easily recognisable hydrochemical characteristics of the studied system.

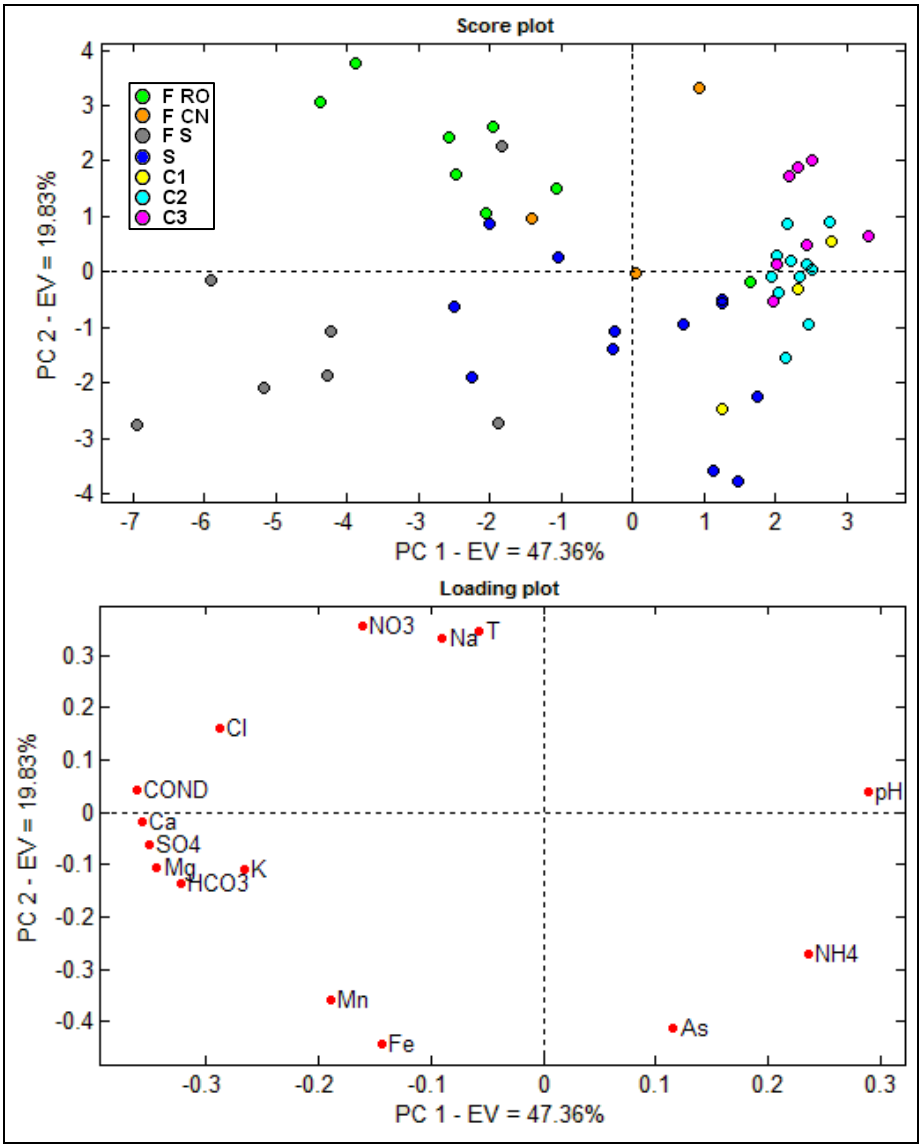

Figure 6.15. Loading plot (on the bottom) and score plot (on the top) for the PC1 and PC2.

Within the results of PCA, the analysis of the relations between As, Fe and Mn can give useful additional information to the understanding of the system. The PC2 points out a positive correlation between As, Fe and Mn. The relations between these species are also described by PC6 and PC9, where As, Fe and Mn are the most important original variables. The PC6, which explains the 2.7% of the variance, underlines a positive correlation between Fe and Mn, which are negatively correlated to As. The PC9, which explains the 1.6% of the variance, points out a negative correlation between Fe and Mn. These two principal components, even if they explain low percentages of variance, point out that different and sometimes conflicting relations between As, Fe and Mn can exist, reflecting complex hydrochemical mechanisms.

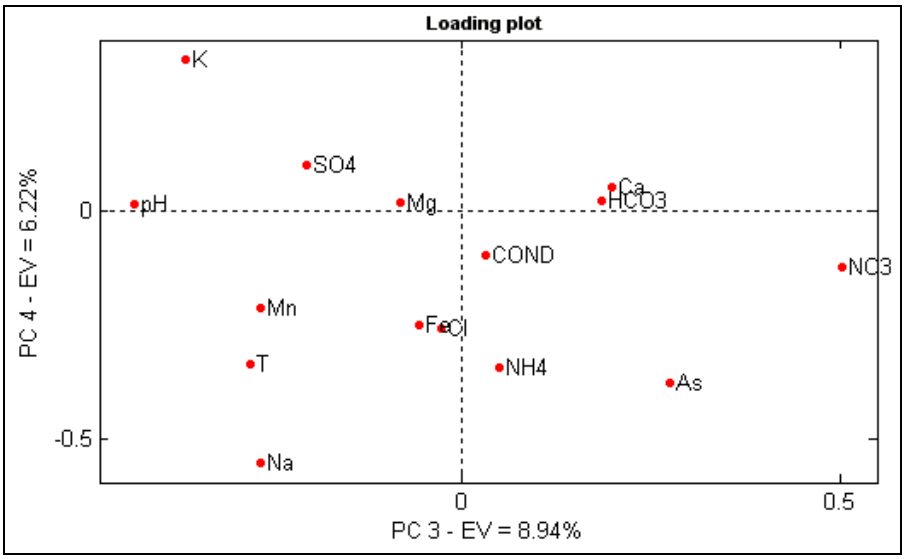

Figure 6.16. Loading plot for the PC3 and PC4.

In order to better understand the relations between the redox sensitive species, the Pearson coefficient (r), which measures the linear correlation between two variables, was calculated (Table 6.24). Considering the ammonium, a moderate positive correlation with arsenic and a moderate negative correlation with nitrate and sulfate can be identified. Nitrate has a week negative correlation with arsenic, iron and manganese. Sulfate is characterized by a moderate positive correlation with iron and manganese and by a week negative correlation with arsenic. Iron has a strong positive correlation with manganese and a moderate positive correlation with arsenic. Concerning the arsenic, a moderate positive correlation with ammonium and iron and a week positive correlation with manganese can be

identified. Manganese has a strong positive correlation with iron and a week positive correlation with arsenic. A hydrogeochemical interpretation of the moderate and strong correlations is discussed in the following chapter 7.

Table 6.24. Pearson correlation coefficients for redox sensitive species.

	NH_4	NO_3	SO_4	Fe	As	Mn
NH_4	1.00	-0.50	-0.55	0.08	0.62	-0.10
NO_3		1.00	0.19	-0.29	-0.35	-0.27
SO_4			1.00	0.42	-0.30	0.55
Fe				1.00	0.41	0.73
As					1.00	0.23
Mn						1.00

6.3. Conclusions

The analysis of the hydrochemical data of July 2010 and 2012, together with the PCA, allows to the definition of the following aspects:

- distinct zones with different hydrochemical characteristics can be identified in the aquifer F: (1) Po river valley, characterized by reduced groundwater with high concentrations of Fe and Mn and medium-high concentrations of As and NH_4; (2) area behind the terrace scarp, characterized by oxidized groundwater with low concentrations of As, Fe, Mn and NH_4; (3) central-northern part of the study area, characterized by reduced groundwater with generally lower concentrations of As, Fe, Mn and NH_4 with respect to the Po valley;
- aquifer S is characterized by reduced groundwater with high concentrations of As, Fe and NH_4 and medium-high concentrations of Mn;
- aquifer C1 is characterized by reduced groundwater with high concentrations of As and NH_4 and medium-low concentrations of Fe and Mn;
- aquifer C2 and C3 are characterized by reduced groundwater with high concentrations of NH_4 and medium-low concentrations of As, Fe and Mn;

References

Beretta G. P. (1992) – Idrogeologia per il *disinquinamento* delle acque sotterranee (Hydrogeology for groundwater remediation). Pitagora Editrice, Bologna, 840 pp.

Celico P. (1986) – *Prospezioni idrogeologiche (Hydrogeological prospection)*. Volume primo. Liguori Ed., Napoli, 735 pp.

Conti A., Sacchi E., Chiarle M., Martinelli G. & Zuppi G.M. (2000) – *Geochemistry of the formation waters of the po plain (Northern Italy): an overview*. Applied Geochemistry 15, 51-65.

Guffanti S., Pilla G., Sacchi E. & Ughini S. (2010) –*Characterization of the quality and origin of groundwater of lodigiano (Northern Italy) with hydrochemical and isotopic instruments*. Italian Journal of Engineering Geology and Environment 1, 65-78.

Kaiser H. F. (1958) – *The varimax criteria for analytical rotation in factor analysis*. Psychometrika 23, 187-200.

Petrunic B. M., MacQuarrie K. T. B. & T. A. Al (2005) – *Reductive dissolution of Mn oxides in river-recharged aquifers: a laboratory column study*. Journal of Hydrology 301, 163-181.

Pilla G., Sacchi E., Zuppi G., Braga G. & Ciancetti G. (2006) – *Hydrochemistry and isotope geochemistry as tools for groundwater hydrodynamic investigation in multilayer aquifers: a case study from Lomellina, Po plain, south-western Lombardy, Italy*. Hydrogeology Journal 14, 795-808.

Pilla G. (2010) – *Gli acquiferi di pianura della provincia di Pavia: origine e qualità della risorsa (The alluvial aquifers in the province of Pavia: origin and quality of water resources).* Provincia di Pavia ed., Pavia, 112 pp.

Regione Lombardia & Eni Divisione Agip (2002) – *Geologia degli acquiferi padani della Regione Lombardia (Geology of the aquifers of the Po Plain in Lombardy region).* A cura di Carcano C. & Piccin A. S.E.L.C.A, Firenze, 130 pp.

Weast R.C. (1968) – *Handbook of chemistry and physics*. The Chemical Rubber Co., Cleveland.

7. Preliminary hydrogeochemical conceptual model

In this chapter, a preliminary hydrogeochemical conceptual model, based on literature, is implemented in order to understand the possible origins and mechanisms of As, Fe and Mn in groundwater in the study area.

Arsenic, iron and manganese in groundwater can have natural or anthropogenic sources. Direct anthropogenic sources for iron and manganese can be represented by industrial effluent. The main anthropogenic sources of arsenic are related to agricultural pesticides and wood preservatives (Nriagu et al., 2007). Arsenic-based pesticides were widespread used until the 1980s. The most common arsenic-based pesticides were organic arsenicals as monomethylarsenic (MMA) and dimethylarsenic (DMA). Still today, widespread contaminations are caused by the use of chromated copper arsenate (CCA) in wood preservation industries (e.g., Townsend et al. 2005).

Human activities can also influence the release of As, Fe and Mn which are naturally contained in aquifer sediments. Two of the most studied anthropogenic phenomena which involve the release of As, Fe and Mn are acid mine drainage and hydrocarbons pollution. Mining processes can lower the groundwater pH favouring the release of arsenic and other metals (Smedley and Kinninburgh, 2002; Cheng et al., 2009). Natural attenuation of hydrocarbons in groundwater involves hydrogeochemical processes that favour the mobilisation of As, Fe and Mn, as reported by U.S. EPA (1999) and by site-specific studies (e.g., Baedecker et al., 1993; Tucillo et al., 1999; Berbenni et al., 2000; Gosh et al., 2003; Burgess and Pinto, 2005).

As discussed in paragraph 6.1.4, the absence of anthropic activities representing potential direct sources and the general absence of hydrocarbons in the sampled points allow to consider the data of July 2010 as representative of the natural background of As, Fe, Mn and NH_4 of the study area. Therefore, a natural origin of As, Fe, Mn and NH_4 can be supposed for the studied system.

Different authors (e.g., McArthur et al., 2001, 2004; Rowland et al., 2006;) underlined that high concentrations of As, Fe and Mn can be found in alluvial aquifers that contain natural organic matter buried in sediments (i.e., peat) keeping reducing conditions. The primary controlling mechanism on the As, Fe and Mn mobilization seems to be the microbial degradation of organic matter of the aquifer sediments. In order to have energetic benefits, microorganisms degrade the organic matter using the following sequence of electron acceptors (McMahon and

Chapelle, 2008): O_2, NO_3^-, Mn(IV), Fe(III), SO_4^{2-} and CO_2. The most energetically favourable electron acceptor is oxygen. When the oxygen is consumed, the next most favourable electron acceptor is nitrate, which is reduced producing gaseous molecular nitrogen (denitrification process). Solid Mn(IV)-oxide is then reduced producing dissolved Mn^{2+} in groundwater. The next favourable electron acceptor is solid Fe(III)-oxide, which is reduced producing dissolved Fe^{2+} in groundwater. Sulfate is then used producing sulfide. Finally, carbon dioxide is reduced involving the production of methane (methanogenesis). However, the sequence of terminal electron accepting processes can be less strict than suggested above. For, example, concomitant reduction of Fe-oxide and methanogenesis was reported by Jakobsen and Postma (1999) and Jakobsen and Cold (2007). In addiction, concurrent reduction of Fe-oxide and sulfate was reported by Canfield (1993), Jakobsen and Postma (1994) and Postma and Jakobsen (1996).

The presence of high concentrations of dissolved Fe^{2+} and Mn^{2+} seems to be related to the electron accepting processes occurring in the aquifer system. High Mn^{2+} and Fe^{2+} concentrations can be referred to the occurring of Mn-oxide and Fe-oxide reduction, respectively. The sulfate reduction can also play a control on the dissolved Fe^{2+} concentration. The produced sulfide can react with the Fe^{2+} producing solid iron sulfides that lower the Fe^{2+} concentration (Chapelle et al., 2009; Root et al., 2009). Arsenic is indirectly involved in the process of organic matter degradation. In fact, the reductive dissolution of Mn-oxide and Fe-oxide also leads to high concentration of dissolved As, which is generally sorbed on the surface of these oxides. In the Mn-oxide reduction, the arsenic is released in groundwater but it can be consecutively sorbed on the surface of iron oxides, which are reduced after the Mn-oxides (McArthur et al., 2004). At the beginning of Fe-oxide reduction, the released arsenic can be resorbed to residual Fe-oxides, which are not yet reduced. Therefore, high concentrations of dissolved arsenic in groundwater can be only reached when Fe-oxides approach to complete reduction (McArthur et al., 2004). The sulfate reduction process also influences the concentration of dissolved arsenic. In fact, the concentration of arsenic can be lowered by the co-precipitation of As in iron sulfides (Thomas et al., 2008) and by the direct precipitation of arsenic sulfides (O'Day et al., 2004). Therefore, the occurring of sulfate reduction can lower the concentration of As in groundwater. The presence of high concentration of ammonium can be also related to organic matter degradation. In fact, the degradation of organic nitrogen produces ammonium, which can persist in groundwater in reducing environment.

The previous hypothesis on the mechanisms of As, Fe and Mn mobilization can be used to interpret the measured concentrations of the survey of July 2010. In the studied multi-aquifer system, longer flow paths, and thus higher residence time, can be assumed for groundwater circulation in the deeper aquifers. The higher residence time of groundwater could imply a higher evolution of the degradation processes of organic matter, particularly peat, which involves the whole studied system (par. 4.2). Therefore, a decrease of redox reactants and an increase of redox products, that are involved in the organic matter degradation, can be expected from superficial to deep aquifers. In addiction, the analysis of hydrodynamic properties (chap. 5) points out a possible vertical leakage, through semi-permeable aquitards, from aquifer F to C1. The interaction with the peats contained in the aquitards could decrease redox reactants and increase redox products in groundwater moving from aquifer F to C1.

Figure 7.1 shows the evolution over depth of redox products and reactants of organic matter degradation, with the addiction of arsenic, that were measured in the survey of July 2010. Nitrate only concerns aquifer F and quickly decreases over depth. This profile could be related to the occurring of denitrification in the superficial part of the aquifer system. Manganese has a peak of concentration in some points of aquifer F (Po river valley) and a consecutive decreasing over depth. This profile could be related to the beginning of Mn-oxide reduction in aquifer F, in particular in the Po valley. Iron has high concentration in some points of the aquifer F (Po river valley) and in aquifer S, and it is characterized by a decrease in the underlying aquifers. This profile could be related to the occurring of Fe-oxide reduction in the Po valley in aquifer F and in the aquifer S. Sulfate concentration constantly decreases from aquifer F to C1. This profile could be related to the increase of sulfate reduction over depth. Arsenic concentration has a peak between aquifers S and C1. Here, the profile of measured iron concentration indicates that, probably, Fe-oxides approach to complete reduction, and thus, As concentration can reach higher values.

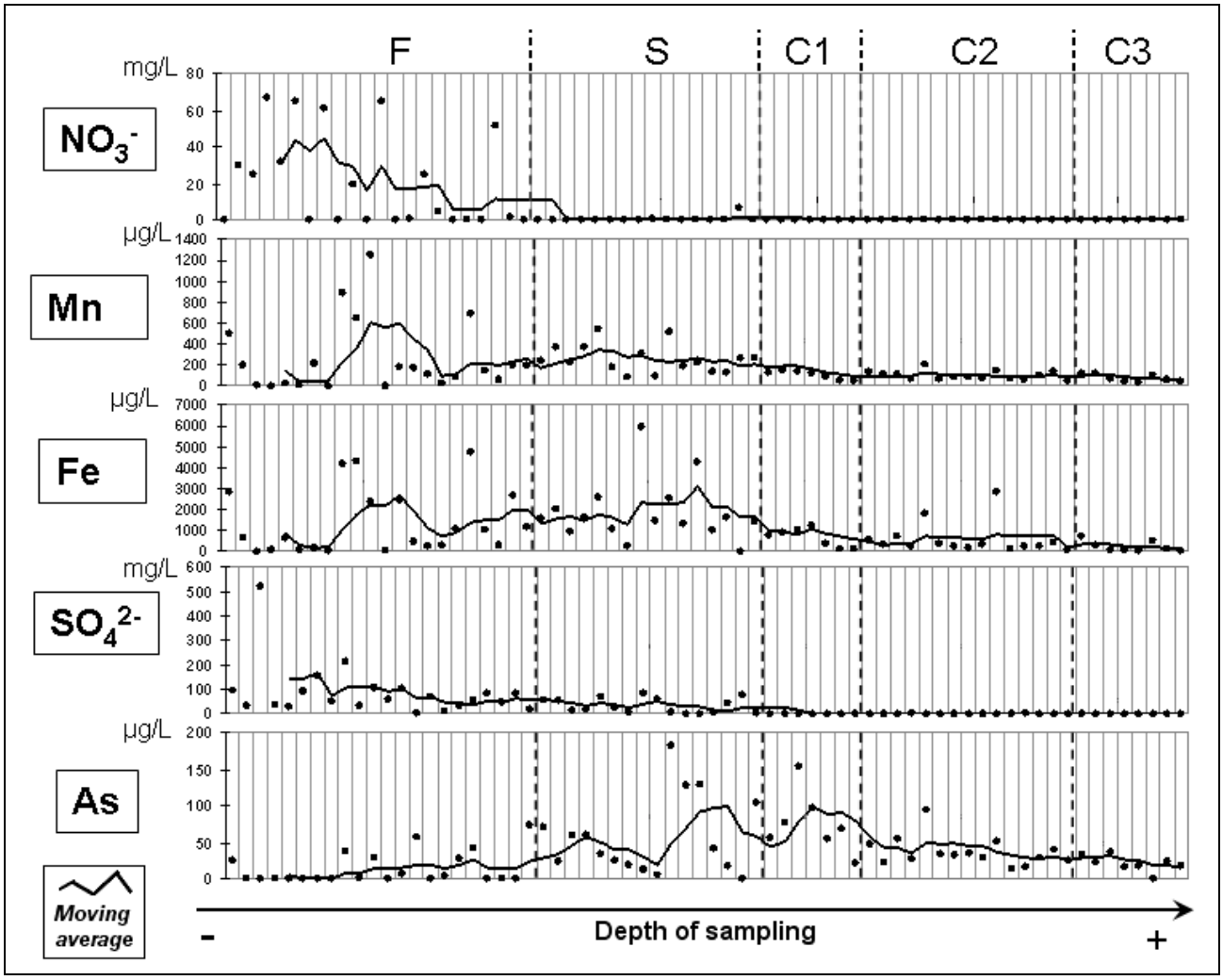

Figure 7.1. Measured concentrations of nitrate, manganese, iron, sulfate and arsenic (July 2010) displayed along the x-axis for increasing depths of sampling; the dotted lines subdivide the graph area into 5 parts corresponding to the 5 identified aquifers (F, S, C1, C2, C3); the solid line represent the moving average calculated using 5 points subsets.

This interpretation can also explain the moderate and strong correlations resulted from the Pearson coefficient calculation (par. 6.3):

- negative correlation between ammonium and sulfate - when the degradation of organic matter evolves, ammonium is produced while sulfate is depleted by sulfate reduction;
- negative correlation between ammonium and nitrate - nitrate is depleted at the beginning of organic matter degradation process, while ammonium increases with the evolving of organic matter degradation;

- positive correlation between manganese and iron - when Fe-oxide reduction begins, high concentration of dissolved manganese involves the system due to the previous Mn-oxide reduction;
- positive correlation between sulfate and manganese, iron - when Mn-oxide and Fe-oxide reduction begins, producing high concentrations of dissolved Mn and Fe, sulfate reduction is probably lower;
- positive correlation between arsenic and ammonium (higher correlation), iron (lower correlation) - the higher correlation between arsenic and ammonium indicates that the release of As is directly coupled to the organic matter degradation, as reported by Postma et al. (2007); the lower correlation of arsenic and iron is probably caused by the resorption of As to residual Fe-oxides, as reported by McArthur et al. (2004).

In conclusion, the primary process controlling the As, Fe, Mn and NH_4 concentrations in the studied system seems to be the degradation of organic matter, in the form of peats deposits. As, Fe and Mn can be released from the aquifer sediments due to redox processes involving peat degradation. The NH_4 can be directly produced from the degradation of the organic nitrogen of peat.

References

Baedecker M.J., Cozzarelli I. M., Eganhouse R. P., Siegel D. I. & Bennett P. C. (1993) – *Crude oil in a shallow sand and gravel aquifer—III. Biogeochemical reactions and mass balance modeling in anoxic groundwater*. Applied Geochemistry 8(6), 569-586.

Berbenni P., Pollice A., Canziani R., Stabile L. & Nobili F. (2000) – *Removal of iron and manganese from hydrocarbon-contaminated groundwaters.* Bioresource Technology 74 (2), 109-114.

Burgess W.G. & Pinto L. (2005) – *Preliminary observations on the release of arsenic to groundwater in the presence of hydrocarbon contaminants in UK aquifers.* Mineralogical Magazine 69 (5), 887-896.

Canfield D. E., Thamdrup B. & Hansen J. W. (1993) – *The anaerobic degradation of organic matter in Danish coastal sediments: Iron reduction, manganese reduction and sulfate reduction*. Geochimica et Cosmochimica Acta 57, 3867-3883.

Chapelle F. H., Bradley P. M., Thomas M. A. & McMahon P. (2009) – Distinguishing Iron-Reducing from Sulfate-Reducing Conditions. Ground Water 47 (2), 300-305.

Cheng H., Hu Y., Luo J. Xu B. & Zhao J. (2009) – *Geochemical processes controlling fate and transport of arsenic in acid mine drainage (AMD) and natural systems*. Journal of Hazardous Materials 165(1-3), 13-26.

Ghosh R., Deutsch W., Geiger S., McCarthy K. & Beckmann D. (2003) – *Geochemistry, fate and transport of dissolved arsenic in petroleum hydrocarbon-impacted groundwater*. Petroleum hydrocarbons and organic chemicals in groundwater. American Petroleum Institute, National Ground Water Association. Costa Mesa, 266-280.

Jakobsen R. & Postma D. (1994) – *In situ rates of sulfate reduction in an aquifer (Rømø, Denmark) and implications for the reactivity of organic matter*. Geology 22, 1103-1106.

Jakobsen R. & Postma D. (1999) – *Redox zoning, rates of sulfate reduction and interactions with Fe-reduction and methanogenesis in a shallow sandy aquifer, Rømø, Denmark*. Geochimica et Cosmochimica Acta 63(1), 137-151.

Jakobsen R. & Cold L. (2007) – *Geochemistry at the sulfate reduction-methanogenesis transition zone in an anoxic aquifer - A partial equilibrium interpretation using 2D reactive transport modeling.* Geochimica et Cosmochimica Acta 71, 1949-1966.

McArthur J. M., Ravenscroft P., Safiulla S. & Thirlwall M. F. (2001) – *Arsenic in groundwater: Testing pollution mechanisms for sedimentary aquifers in Bangladesh.* Water Resources Research 37 (1), 109-117.

McArthur J. M., Banerjee D. M., Hudson-Edwards K. A., Mishra R., Purohit R., Ravenscroft P., Cronin A., Howarth R. J., Chatterjee A., Talukder T., Lowry D., Houghton S. & Chadha D. K. (2004) – *Natural organic matter in sedimentary basins and its relation to arsenic in anoxic ground water: the example of West Bengal and its worldwide implications.* Applied Geochemistry 19, 1255-1293.

McMahon P. B. & Chapelle F. H. (2008) – *Redox processes and water quality of selected principal aquifer systems*. Ground water 46 (2), 259-271.

Nriagu J. O., Bhattacharya P., Mukherjee A. B., Bundschuh J., Zevenhoven R. & Loeppert R. H. (2007) – *Arsenic in Soil and Groundwater: an overview.* In: Loeppert (Eds.), Arsenic in Soil and Groundwater Environment, Chapter 1, 3-60.

O'Day P. A., Vlassopoulos D., Root R. & Rivera N. (2004) – *The influence of sulphur and iron on dissolved arsenic concentrations in the shallow subsurface under changing redox conditions*. Proceedings of the National Academy of Sciences of the U.S.A. 101 (38), 13703-13708.

Postma D. & Jakobsen R. (1996) – *Redox zonation: Equilibrium constraints on the Fe(III)/SO_4-reducing interface*. Geochimica et Cosmochimica Acta 60(17), 3169-3175.

Postma D., Larsen F., Hue N. T. M., Duc M. T., Viet P. H., Nhan P. Q. & Jessen S. (2007) – *Arsenic in groundwater of the Red River floodplain, Vietnam: Controlling geochemical processes and reactive transport modeling*. Geochimica et Cosmochimica Acta 71, 5054-5071.

Root R. A., Vlassopoulos D., Rivera N. A., Rafferty M. T., Andrews C. & O'Day P. A. (2009) – *Speciation and natural attenatuon of arsenic and iron in a tidally influenced shallow aquifer*. Geochimica et Cosmochimica Acta 73, 5528-5553.

Rowland H. A. L, Polya D. A., Lloyd J. R. & Pancost R. D. (2006) – *Characterisation of organic matter in a shallow, reducing, arsenic-rich aquifer, West Bengal*. Organic Geochemistry 37, 1101-1114.

Smedley P.L. & Kinniburgh D.G. (2002) – *A review of the source, behaviour and distribution af arsenic in natural waters*. Applied Geochemistry 17, 517-568.

Thomas M. A., Diehl S. F., Pletsch B. A., Schumann T. L., Pavey R. R. & Swinford E. M. (2008) – *Relation Between Solid-Phase and Dissolved Arsenic in the Griund-Water System Underlying Northern Oreble Country, Ohio*. USGS Scientific Investigations Report 5205, 56 pp.

Towensend T., Dubey B., Tolaymat T. & Solo-Gabrile H. (2005) – *Preservative leaching from weathered CCA-treated wood*. Journal of Environmental Management 75(2), 105-113.

Tucillo M. E., Cozzarelli I. M. & Herman J. H. (1999) – *Iron reduction in the sediments of a hydrocarbon-contaminated aquifer.* Applied Geochemistry 14 (5), 655-667.

U.S. EPA (1999) – *Monitored natural attenuation of petroleum hydrocarbons.* Remedial Technology Fact Sheet, EPA/600/F-98/021, 3 pp.

8. Analysis of possible anthropogenic influence on As, Fe and Mn concentration

One of the main aims of the present work is to verify if possible anthropogenic influences on groundwater As, Fe and Mn concentrations can exist in the study area. The analysis of the anthropic activities in the study area underlines the absence of potential direct sources of As, Fe and Mn in groundwater. Otherwise, indirect influences on As, Fe and Mn concentrations could be generated in the study area by hydrocarbons pollution.

In order to verify if hydrocarbons pollution can influence the As, Fe and Mn concentrations in the study area, a comparison between two water quality surveys was done: (1) the survey of July 2010 executed within the present work (survey UNIMIB), which can be considered as representative of the natural background (par. 6.1.4); (2) a survey executed by the Regional Environmental Protection Agency (ARPA Lombardia) in June 2010 in an oil refinery located in the study area (site ID 27 in Table 2.1 and Figure 2.2), that is affected by hydrocarbons pollution (survey ARPA). The survey ARPA considers a total number of sampled piezometers equal to 64: 38 for aquifers F, 15 for aquifer S and 11 for aquifer C1. The intensity of groundwater pollution in the refinery area can be seen in figure 8.1, which shows the box-plot of measured groundwater concentrations of total hydrocarbons and total BTEX (sum of benzene, ethylbenzene, styrene, toluene and p-xylene). Figure 8.1 shows that the pollution involves the aquifer F, and locally, the aquifer S (one point above the regulatory limits).

Before analysing the measured data, it should be noted that different sampling methods were applied in the two survey. As reported in paragraph 3.3, survey UNIMIB was executed with sampling or installed pumps (dynamic sampling), purging the piezometers/wells before sampling and acidifying the samples *in situ* without filtering (turbidity-free samples). Otherwise, survey ARPA was executed with sampling bailers (static sampling), purging the piezometers one day before sampling and acidifying the samples *in situ* after filtering (45 μm). The application of these two different sampling methods produces some effects in the measured concentrations that must be taken into account in the comparison of the results of the two surveys. In particular, measured concentrations of the survey ARPA could be probably underestimated with respect to the survey UNIMIB due to filtered samples and purging executed one day before sampling. This last aspect may affect the measured iron concentrations, because stagnant well water in

contact with air probably leads to the precipitation of Fe-oxides, as reported by Appelo and Postma (2005). A quantitative estimation of the difference between dynamic sampling and static sampling (purging the piezometer one day before sampling) is given by a previous test executed by ARPA (unpublished data). This test underlined that measured concentrations with static sampling are underestimated of around 260 times for iron, 72 times for manganese and 11 times for arsenic with respect to dynamic sampling.

The comparison of the measured concentrations of the two surveys (UNIMIB and ARPA) is reported in the box-plot graphs in figures 8.2, 8.3 and 8.4. Tables 8.1, 8.2 and 8.3 list the statistical parameters of the box-plots.

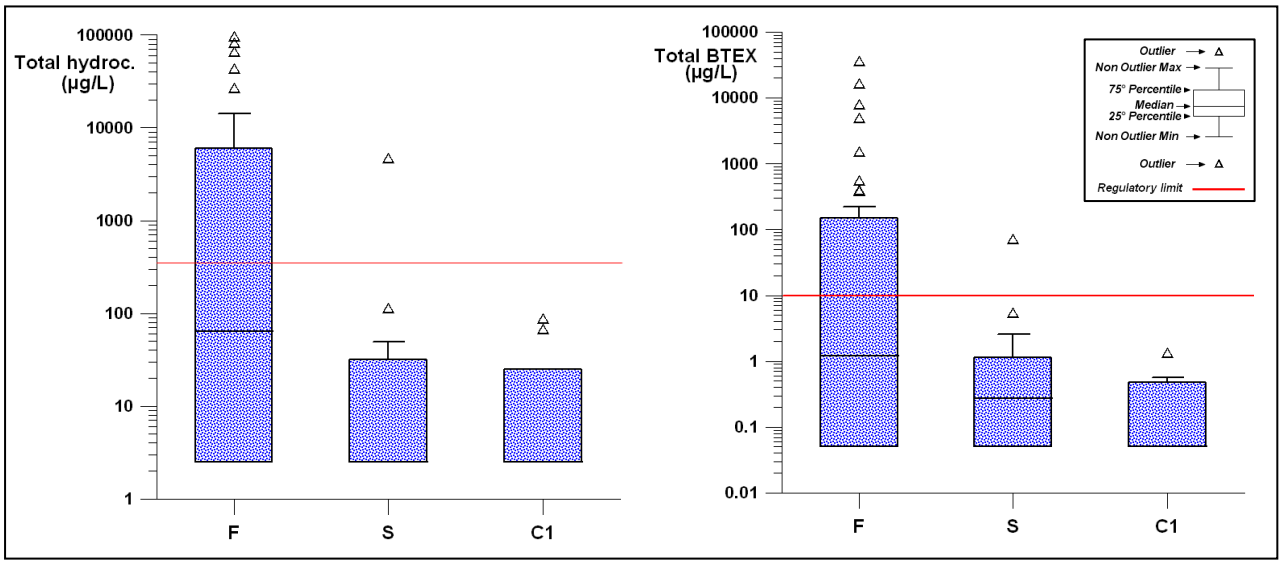

Figure 8.1. Total hydrocarbons (on the left) and total BTEX (on the right) concentrations measured in the survey ARPA in aquifers F, S and C1; red lines: regulatory limit for total hydrocarbons = 350 µg/L (D. Lgs. 152/06) and for p-xylene = 10 µg/L (D. Lgs. 152/06).

Manganese

Figure 8.2 shows higher Mn concentrations in the survey ARPA with respect to the survey UNIMIB for the aquifer F. The median value of Mn concentrations is 854 µg/L for the survey ARPA, while is equal to 145 µg/L for the survey UNIMIB. In the aquifers S and C1 the measured concentrations in the two surveys are comparable. The ratio between the median values of the two surveys (median ARPA/median UNIMIB) is equal to 5.9 for the aquifer F, to 0.7 for the aquifer S and to 0.8 for the aquifer C1. This ratio underlines a probable effect of the hydrocarbons pollution on the Mn concentrations in aquifer F, while the values below 1 for the

aquifers S and C1 are probably due to the effect of underestimation in the survey ARPA.

Iron

Figure 8.3 shows higher Fe concentrations in the survey ARPA with respect to the survey UNIMIB for the aquifer F. The median value of Fe concentrations is 3200 µg/L for the survey ARPA, while is equal to 629 µg/L for the survey UNIMIB. In the aquifers S and C1, the concentrations of the survey ARPA are generally lower than the survey UNIMIB. The median ratio (median ARPA/median UNIMIB) is equal to 5.1 for the aquifer F, to 0.4 for the aquifer S and to 0.7 for the aquifer C1. This ratio underlines a probable effect of the hydrocarbons pollution on the Fe concentrations in aquifer F. In this case the probable effect of underestimation in the survey ARPA is more evident, as shown by the values of the median ratio for aquifer S and C1.

Arsenic

Figure 8.4 shows higher As concentrations in the survey ARPA with respect to the survey UNIMIB for the aquifer F. The median value of As concentrations is 14 µg/L for the survey ARPA, while is equal to 1.5 µg/L for the survey UNIMIB. In the aquifers S and C1, the concentrations of the survey ARPA are generally lower than the survey UNIMIB. The median ratio (median ARPA/median UNIMIB) is equal to 9.3 for the aquifer F, to 1.4 for the aquifer S and to 0.1 for the aquifer C1. Also in this case, a probable effect of the hydrocarbons pollution on the As concentrations in aquifer F can be identified. The values of median ratio for the aquifers S and C1 can be related again to the different sampling methods of the two surveys.

In conclusion, this comparison points out that a probable influence on groundwater As, Fe and Mn concentrations exists in the oil refinery area, which is polluted by hydrocarbons. As reported by previous studies (e.g., Baedecker et al., 1993; Tucillo et al., 1999; Berbenni et al., 2000; Gosh et al., 2003; Burgess and Pinto, 2005), the hypothesis is that the degradation of hydrocarbons involves the processes of Fe-oxides and Mn-oxides reduction that, how discussed in chapter 7, allow high concentration of dissolved As, Fe and Mn. The hydrocarbons are not a direct source of As, Fe and Mn in groundwater, but they intensify the processes of mobilization of As, Fe and Mn, that naturally form the aquifer sediments.

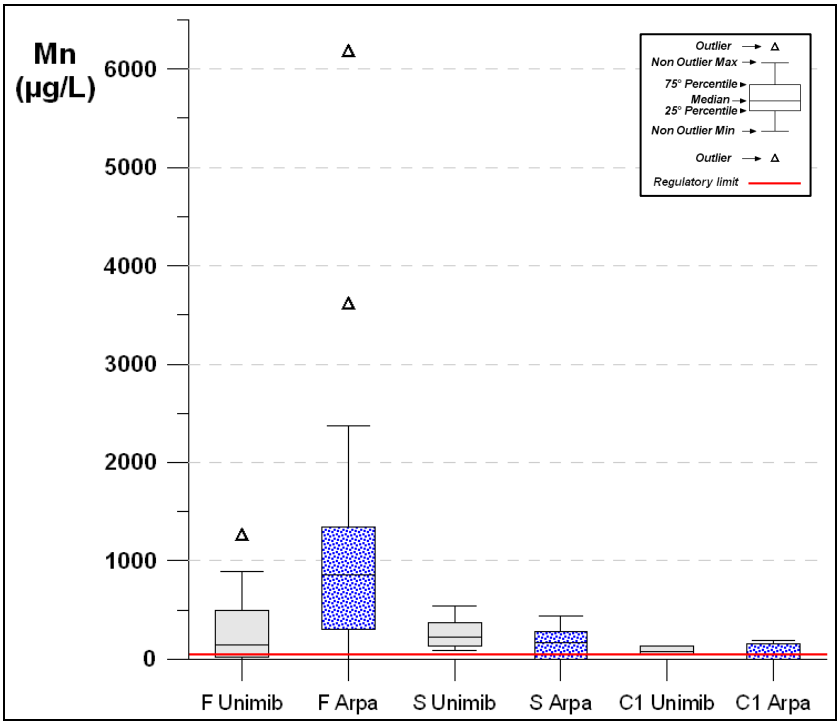

Figure 8.2. Comparison of the measured Mn concentrations of the surveys UNIMIB and ARPA; red line: regulatory limit for Mn = 50 µg/L (D. Lgs. 152/06).

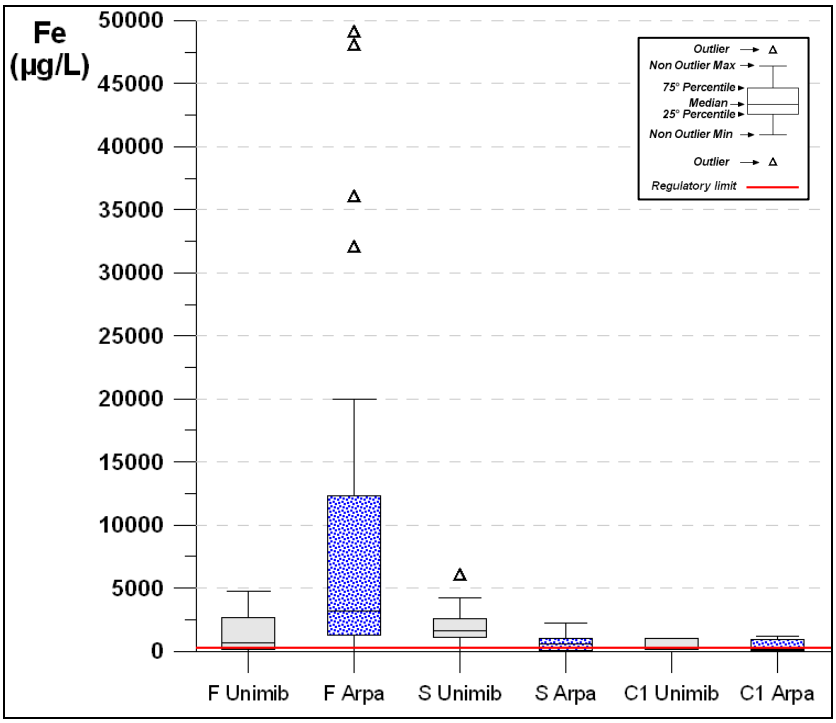

Figure 8.3. Comparison of the measured Fe concentrations of the surveys UNIMIB and ARPA; red line: regulatory limit for Fe = 200 µg/L (D. Lgs. 152/06).

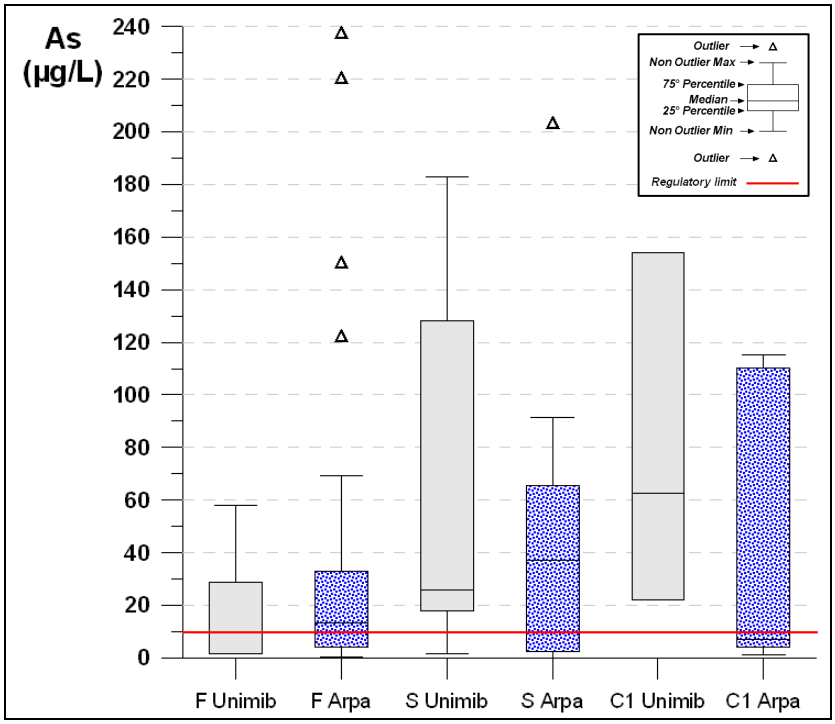

Figure 8.4. Comparison of the measured As concentrations of the surveys UNIMIB and ARPA; red line: regulatory limit for As = 10 µg/L (D. Lgs. 152/06).

Table 8.1. Statistical parameters of the Mn box-plot (Figure 8.2).

Mn (µg/L)	F Unimib	F Arpa	S Unimib	S Arpa	C1 Unimib	C1 Arpa
N. Measurements	21	38	13	16	4	12
25°percentile	23	300	136	4	49	2
Median	145	854	225	166	75	53
75°percentile	501	1346	371	280	138	162
Maximum	1255	6170	543	444	138	188

Table 8.2. Statistical parameters of the Fe box-plot (Figure 8.3).

Fe (µg/L)	F Unimib	F Arpa	S Unimib	S Arpa	C1 Unimib	C1 Arpa
N. Measurements	21	38	13	16	4	12
25°percentile	177	1270	1091	40	112	28
Median	629	3200	1607	575	263	182
75°percentile	2694	12300	2601	1030	1045	960
Maximum	4756	49000	5975	2240	1045	1210

Table 8.3. Statistical parameters of the As box-plot (Figure 8.4).

As (µg/L)	F Unimib	F Arpa	S Unimib	S Arpa	C1 Unimib	C1 Arpa
N. Measurements	21	38	13	16	4	12
25°percentile	1.5	4	18	3	22	4
Median	1.5	14	26	37	63	7
75°percentile	29	33	128	66	154	110
Maximum	58	237	183	203	154	115

References

Appelo C. A. J. & Postma D. (2005) – *Geochemistry, groundwater and pollution (2nd edition)*. Balkema Publishers, Leiden, 649 pp.

Baedecker M.J., Cozzarelli I. M., Eganhouse R. P., Siegel D. I. & Bennett P. C. (1993) – *Crude oil in a shallow sand and gravel aquifer—III. Biogeochemical reactions and mass balance modeling in anoxic groundwater*. Applied Geochemistry 8(6), 569-586.

Berbenni P., Pollice A., Canziani R., Stabile L. & Nobili F. (2000) – *Removal of iron and manganese from hydrocarbon-contaminated groundwaters.* Bioresource Technology 74 (2), 109-114.

Burgess W.G. & Pinto L. (2005) – *Preliminary observations on the release of arsenic to groundwater in the presence of hydrocarbon contaminants in UK aquifers.* Mineralogical Magazine 69 (5), 887-896.

Ghosh R., Deutsch W., Geiger S., McCarthy K. & Beckmann D. (2003) – *Geochemistry, fate and transport of dissolved arsenic in petroleum hydrocarbon-impacted groundwater*. Petroleum hydrocarbons and organic chemicals in groundwater. American Petroleum Institute, National Ground Water Association. Costa Mesa, 266-280.

Tucillo M. E., Cozzarelli I. M. & Herman J. H. (1999) – *Iron reduction in the sediments of a hydrocarbon-contaminated aquifer.* Applied Geochemistry 14 (5), 655-667.

9. Analysis of historical hydrochemical data

The analysis of historical hydrochemical data was done in order to verify the hydrochemical characterization based on the survey of July 2010 (chap. 6) and the presence of possible influences on As, Fe, Mn and NH_4 concentrations generated by past human activities in the study area.

The historical hydrochemical data, collected from the Province of Cremona, concern the chemical analysis of 1946 groundwater samples that were organised in the database TANGCHIM (chap. 2). The data are referred to a temporal period ranging from 1989 to 2010, with most of the data in the range 1999-2010. The analysis of the historical data is focused on As, Fe, Mn and NH_4, which are the objects of the present study.

In this analysis, a separation between the data referred to the natural background (natural component) and to possible anthropogenic influences (anthropic component) was done. Pollutions by hydrocarbons and organic matter in general were considered as possible anthropogenic influences on As, Fe and Mn concentrations, as discussed in chapter 8, and also on NH_4 (concerning vegetable and/or animal organic matter). The identification of the areas affected by hydrocarbons pollution was done analysing the historical maximum concentrations of total hydrocarbons and benzene, considered as parameters indicative of groundwater pollution by hydrocarbons. Figures 9.1 and 9.2 show the maximum detected concentrations of total hydrocarbons and benzene in the study area in the temporal period 2001-2010, considering the aquifer F. With the term "detected", we consider the concentrations measured above the method detection limit (MDL), therefore, figures 9.1 and 9.2 do not represent those points where the concentration was measured below the MDL. The sites where hydrocarbons concentrations were detected and, at the same time, As, Fe and Mn concentrations were measured are underlined in figures 9.1 and 9.2. These sites are an oil refinery (Raff), affected by severe groundwater pollution, and a group of 4 sites (Siti Idr) which were less polluted. The identification of the areas affected by pollution by organic matter in general was done analysing the historical values of chemical oxygen demand (COD). Figure 9.3 shows the maximum measured values of COD in the study area in the temporal period 1999-2010, considering the aquifer F. Only one site, corresponding to a municipal solid waste landfill (Disc), has higher COD values. Within the different sites considered in this analysis, there is also a steel mill (site ID

99 in Table 2.1 and Figure 2.2). The steel mill (Acc) has not productive activities that can influence the groundwater As, Fe, Mn and NH_4 concentrations, therefore its measurements were considered as natural background. Concerning the deeper aquifers (S, C1, C2 and C3), the vulnerability to pollution is lower than aquifer F due to the presence of semi-permeable aquitards. The analysis of historical concentrations of total hydrocarbons, benzene and COD for the deeper aquifers points out that: (1) hydrocarbons were detected in aquifers S and C1 in the oil refinery site; (2) no organic compounds were detected in aquifers C2 and C3.

The possible influence of chlorinated hydrocarbons on As, Fe and Mn concentrations cannot be evaluated due to the general absence of concomitant analysis of chlorinated hydrocarbons, As, Fe and Mn concentrations in the historical data.

In summary, concerning the aquifer F, a possible influence on As, Fe, Mn and NH_4 concentrations can be considered for: (1) the oil refinery, (2) the group of four sites with low hydrocarbons pollution and (3) the municipal solid waste landfill. The remaining historical data are considered as indicative of natural background. These data are subdivided into two groups: data referring to the Po river valley (F S) and to the area behind the terrace scarp (F RO). No historical data are referred to the central-northern part of the study area (F CN). Concerning the aquifers S and C1, a possible influence on As, Fe and Mn concentrations can be only considered for the oil refinery site. For the aquifers C2 and C3, all the data are considered as indicative of natural background.

In order to verify the possible anthropogenic influences on As, Fe, Mn and NH_4 concentrations, a comparison between the data referring to the natural background and to the identified sites with possible influence was done. This comparison is presented with box-plot graphs for each chemical species (As, Fe, Mn and NH_4). In these box-plots, the historical data are subdivided as follow:

- for the aquifer F (Figures 9.4, 9.8, 9.12 and 9.16), five groups are identified, the first two referring to natural background and the other three to possible anthropogenic influences: (1) area behind the terrace scarp (F RO); (2) Po river valley (F S); (3) group of sites with low hydrocarbons pollution (F Siti Idr); (4) municipal solid waste landfill (F Disc); (5) oil refinery (F Raff). The measurements of July 2010 (F Uni) are also included in the box-plots in order to make a comparison with the historical data;

- for the aquifer S (Figures 9.6, 9.10, 9.14 and 9.18), three groups are identified, the first two referring to natural background and the other to possible anthropogenic influences: (1) steel mill (S Acc); (2) municipal solid waste landfill (S Disc); (3) oil refinery (S Raff). Also in this case, the measurements of July 2010 (S Uni) are included;
- for the aquifers C1, C2 and C3 (Figure 9.7, 9.11, 9.15 and 9.19), a single box-plot is presented. For aquifer C1, all the historical data are referred to the oil refinery (C1 Raff), with possible anthropogenic influence. For aquifer C2 and C3, all the historical data are referred to natural background (C2 Area and C3 Area). The measurements of July 2010 are included in these box-plots (C1 Uni, C2 Uni and C3 Uni).

In all box-plots, the data referred to possible anthropogenic influences are presented with red boxes. For the measurements below the detection limit, a concentration as half the detection limit was considered. As reported in chapter 8, differences in the sampling method must be taken into account comparing data from different groups.

Concerning the aquifer F, a detailed representation of the spatial distributions of historical As, Fe, Mn and NH_4 concentrations is presented in figures 9.5, 9.9, 9.13 and 9.17. These figures show the median values of historical concentrations calculated for each point. The median values are represented with 6 classes defined on the basis of multiplier values of the regulatory limits, as reported in table 9.1.

Table 9.1. Definition of the 6 classes representing the median values of concentration in figure 9.5, 9.9, 9.13 and 9.17.

Classes	Multiplier values	Symbols
I	x0 – x1	●
II	x1 – x3	●
III	x3 – x10	●

Classes	Multiplier values	Symbols
IV	x10 – x40	●
V	x40 – x130	●
VI	x130 – x250	★

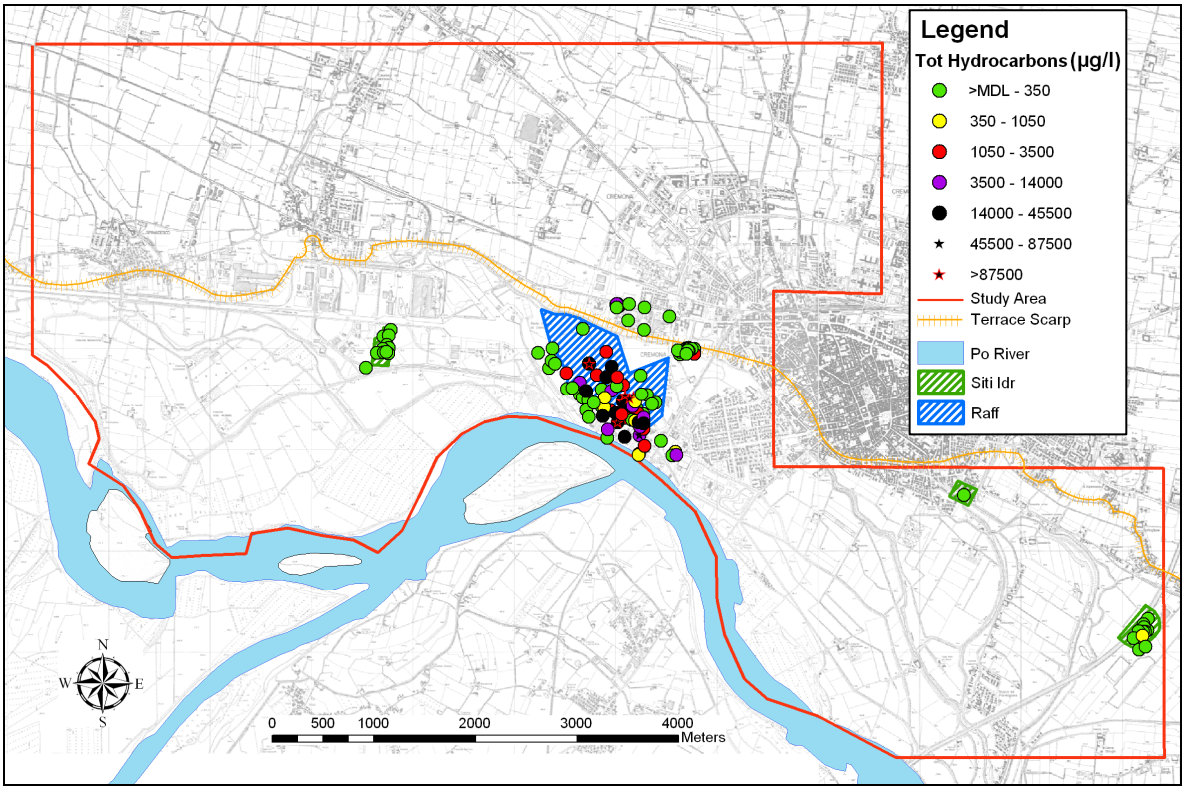

Figure 9.1. Historical maximum detected concentrations of total hydrocarbons in aquifer F.

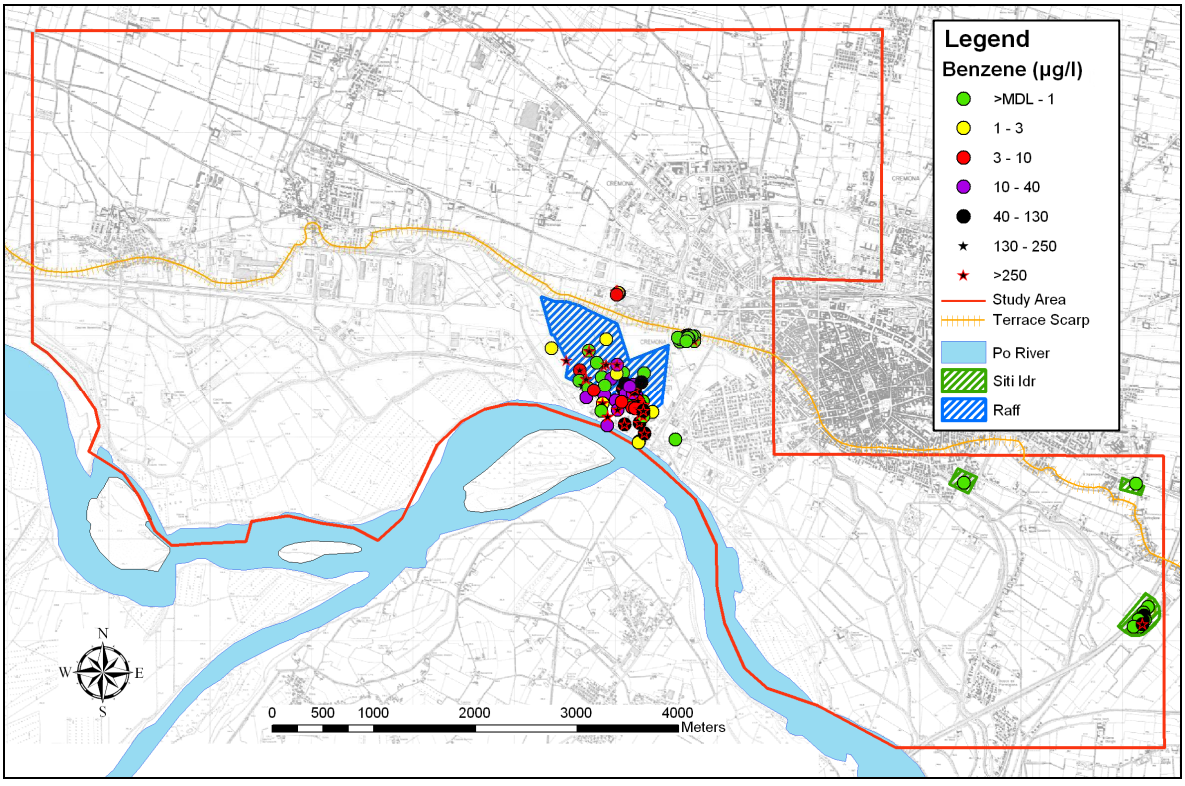

Figure 9.2. Historical maximum detected concentrations of benzene in aquifer F.

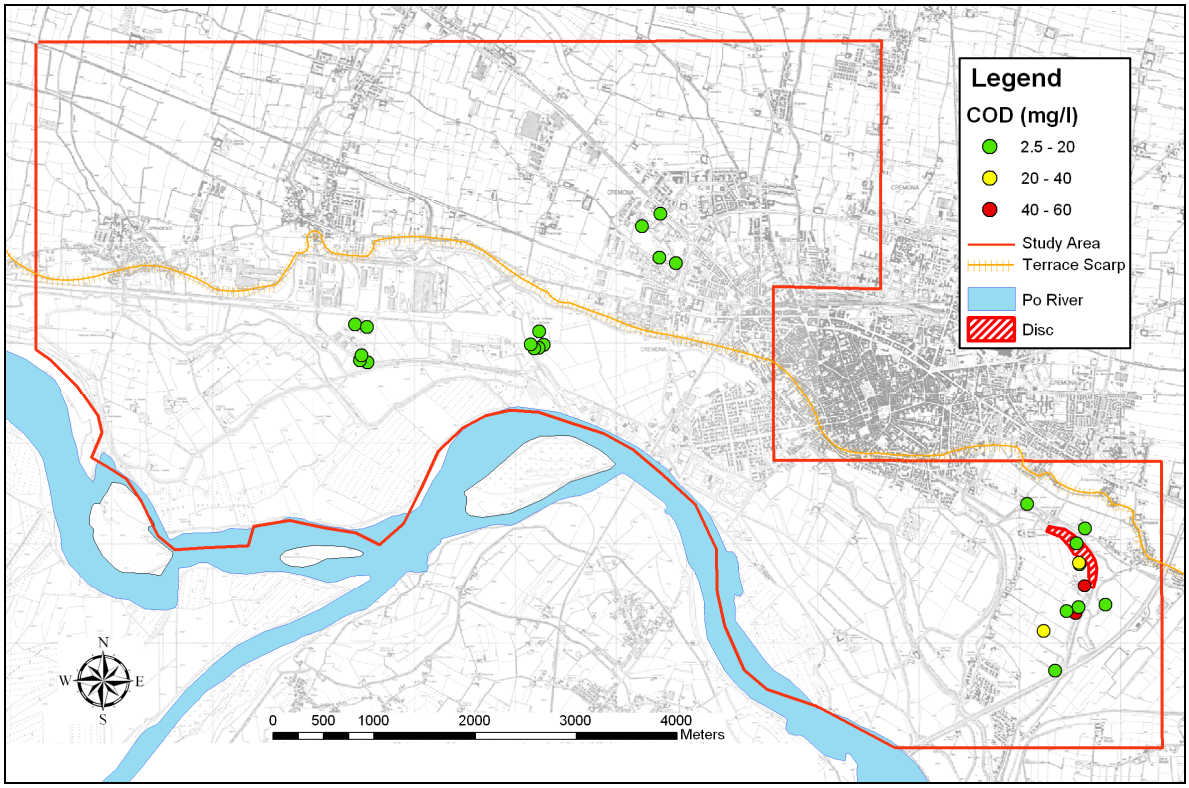

Figure 9.3. Historical maximum values of COD in aquifer F.

9.1. Manganese

Concerning the aquifer F, the box-plot of historical concentrations of Mn is showed in figure 9.4. Table 9.2 lists the statistical parameters of the box-plot. Considering the natural background, Po river valley (F S) has higher concentrations with respect to the area behind the terrace scarp (F RO). The median value is 364 µg/L, for the former, and 5 µg/L, for the latter. Considering the regulatory limit of 50 µg/L (D. Lgs. 152/06), Po valley results 7 times higher while the area behind the scarp is generally below this limit. The concentrations of July 2010 (F Uni) are consistent with the historical data of natural background. Considering the sites with possible anthropogenic influences, the oil refinery (F Raff) is characterized by high concentrations, with a median value of 730 µg/L. The concentrations referred to the landfill (F Disc) and to the group of polluted sites (F Siti Idr) are lower than the refinery, with a median value of 607 µg/L, for the former, and of 520 µg/L, for the latter. In order to quantify the difference between the concentrations of the sites with possible influence and the natural background (F S), the ratio between their

median values is reported. The median ratio is equal to 2.0 for the refinery (median F Raff/median F S), to 1.7 for the landfill (median F Disc/median F S) and to 1.4 for the group of polluted sites (median F Siti Idr/median F S). Figure 9.5 shows the spatial distribution of historical data of Mn in the aquifer F. The map underlines the presence of higher values in the Po valley, south of the terrace scarp, with respect to the area behind (north of) the scarp, with the highest values in the sites with possible influence.

Concerning the aquifer S, the box-plot of historical concentrations of Mn is showed in figure 9.6. Table 9.3 lists the statistical parameters of the box-plot. Comparing the different groups of data, a possible interference caused by different sampling methods can be identified. For the groups S Disc and S Uni a dynamic sampling (with purging immediately before sampling) was executed, while for the groups S Raff and S Acc a static sampling (with purging one day before sampling) was applied. The comparison between the groups S Disc and S Acc, which are both referred to natural background, underlines higher concentrations for the former (median value of 183 µg/L) with respect to the latter (median value of 41 µg/L). The group S Raff, which is referred to possible anthropogenic influence, has generally lower values than group S Disc. The median value of group S Raff is indeed equal to 153 µg/L. The group S Uni results consistent with the group S Disc, with the exception of an outlier.

Concerning the aquifers C1, C2 and C3, the box-plot of historical concentrations of Mn is showed in figure 9.7. Table 9.4 lists the statistical parameters of the box-plot. For the aquifer C1, the data are only referred to the refinery (C1 Raff), and thus, are hardly comparable with the data of July 2010 (C1 Uni). For the aquifer C2, the data of July 2010 (C2 Uni) are consistent with the historical data (C2 Area), while in the aquifer C3 the data of July 2010 (C3 Uni) are slightly higher with respect to the historical data (C3 Area).

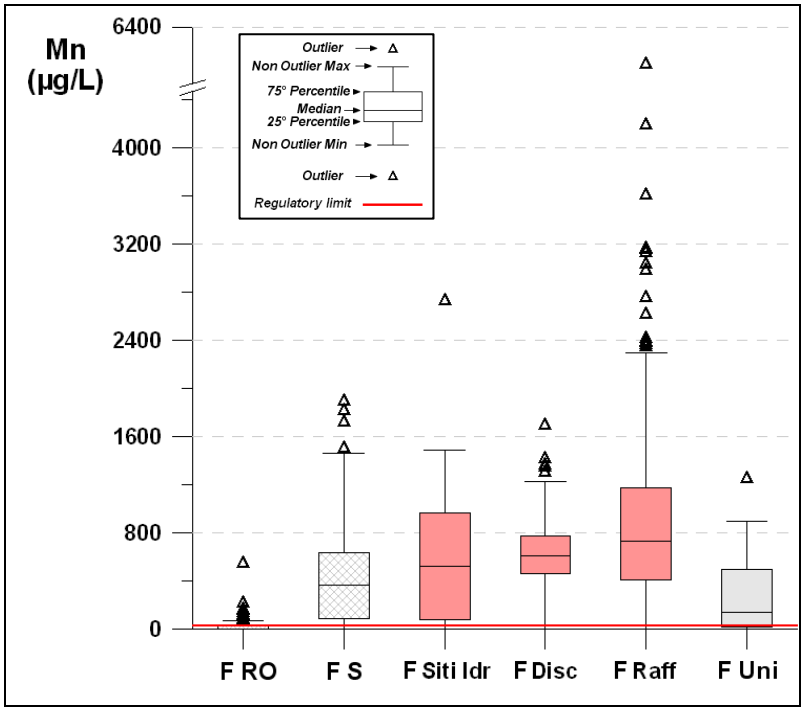

Figure 9.4. Box-plot of historical concentrations of Mn in aquifer F.

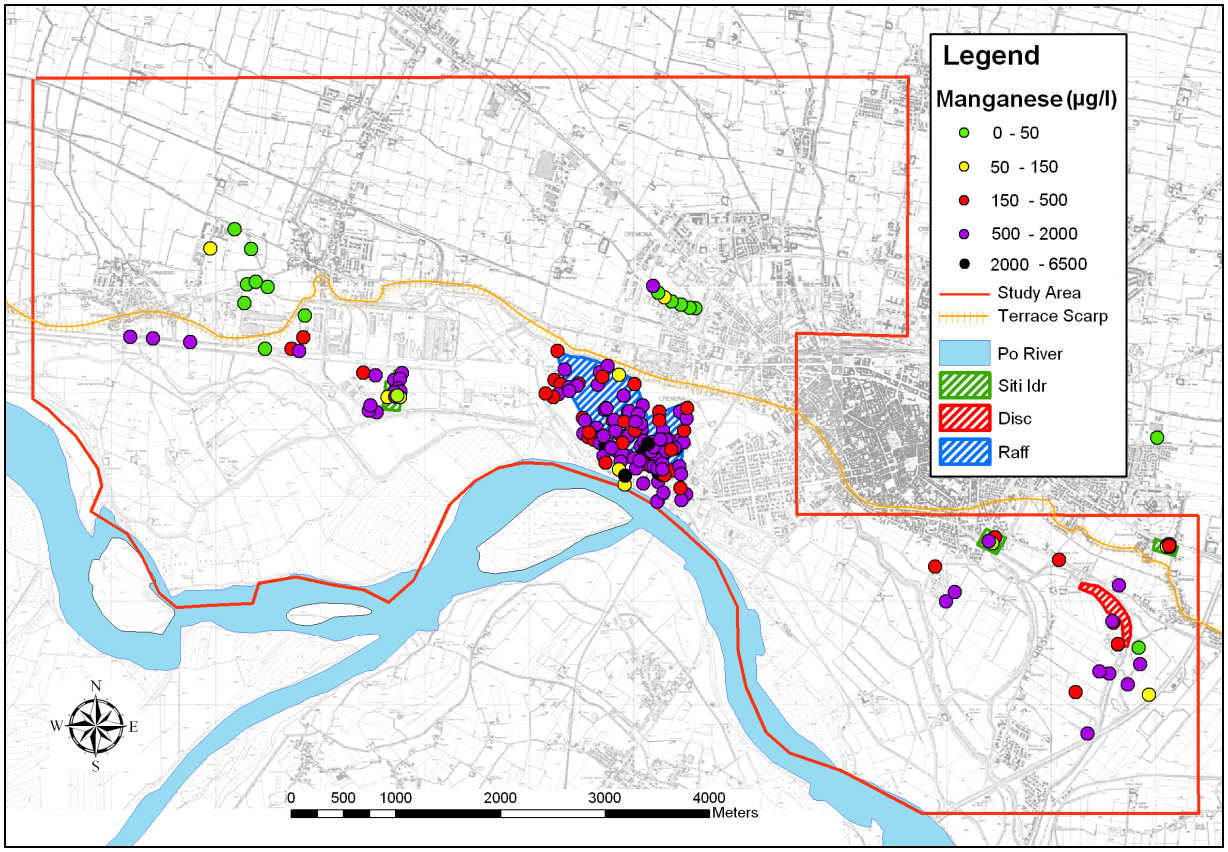

Figure 9.5. Median values of historical Mn concentrations calculated for each point in aquifer F.

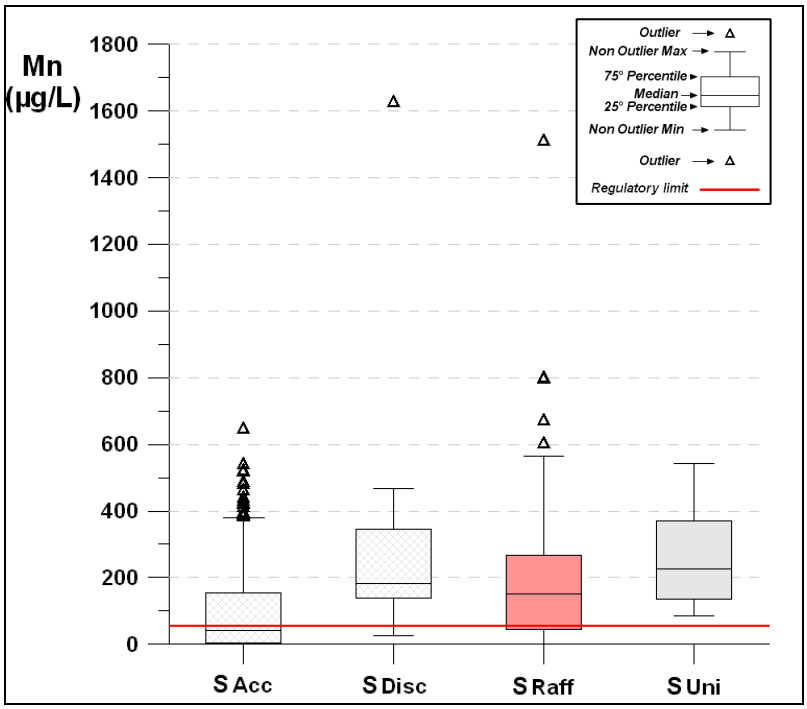

Figure 9.6. Box-plot of historical concentrations of Mn in aquifer S.

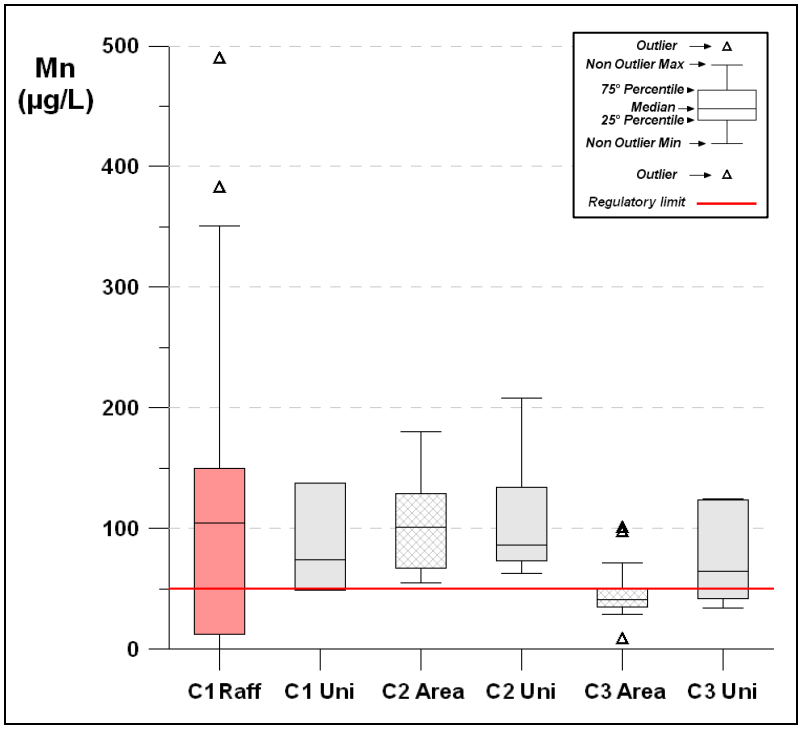

Figure 9.7. Box-plot of historical concentrations of Mn in aquifers C1, C2 and C3.

Table 9.2. Statistical parameters of the box-plot of historical Mn data in aquifer F (Figure 9.4).

Mn (µg/L)	F RO	F S	F Siti Idr	F Disc	F Raff	F Uni
N. Measurements	113	184	43	83	362	21
Period	2005-2009	2005-2010	2006-2010	1999-2010	2001-2010	July 2010
Minimum	1	1	2	4	1	2.5
25°percentile	3	85	80	462	415	23
Median	5	364	520	607	730	145
75°percentile	30	640	970	773	1174	501
Maximum	554	1900	2732	1701	6170	1255

Table 9.3. Statistical parameters of the box-plot of historical Mn data in aquifer S (Figure 9.6).

Mn (µg/L)	S Acc	S Disc	S Raff	S Uni
N. Measurements	349	24	120	13
Period	2005-2009	1999-2010	2001-2010	July 2010
Minimum	1	25	0.3	84
25°percentile	5	145	48	136
Median	41	183	153	225
75°percentile	155	311	264	371
Maximum	646	1626	1510	543

Table 9.4. Statistical parameters of the box-plot of historical Mn data in aquifers C1, C2 and C3 (Figure 9.7).

Mn (µg/L)	C1 Raff	C1 Uni	C2 Area	C2 Uni	C3 Area	C3 Uni
N. Measurements	79	4	21	13	87	8
Period	2001-2010	July 2010	1989-2011	July 2010	1992-2011	July 2010
Minimum	0.5	49	55	63	8	34
25°percentile	13	49	67	73	35	42
Median	105	75	101	86	41	65
75°percentile	150	138	129	134	50	124
Maximum	489	138	180	208	100	125

9.2. Iron

Concerning the aquifer F, the box-plot of historical concentrations of Fe is showed in figure 9.8. Table 9.5 lists the statistical parameters of the box-plot. Considering the natural background, also in this case, Po river valley (F S) has higher concentrations with respect to the area behind the terrace scarp (F RO). The median value is 89 µg/L, for the former, and 21 µg/L, for the latter. The values of F RO are generally below the regulatory limit of 200 µg/L (D. Lgs. 152/06), while the values of F S are often above it. The concentrations of July 2010 (F Uni) are consistent with the historical data of natural background. Considering the sites with

possible anthropogenic influences, the oil refinery (F Raff) is clearly characterized by high concentrations, up to the maximum values of 97900 µg/L. The median value of F Raff is equal to 2548 µg/L. Also the landfill (F Disc) has high concentrations, with a median value of 6326 µg/L. Otherwise, the group of polluted sites (F Siti Idr) has concentrations that are consistent with the values of F S. Comparing the concentrations of the sites with possible influence with the natural background, the median ratio is equal to 28.6 for the refinery (median F Raff/median F S), to 71.1 for the landfill (median F Disc/median F S) and to 0.7 for the group of polluted sites (median F Siti Idr/median F S). Figure 9.9 shows the spatial distribution of historical data of Fe in the aquifer F. The map underlines the presence of higher values in the Po valley, south of the terrace scarp, with respect to the area behind the scarp, with the highest values in the refinery (Raff) and in the landfill (Disc).

Concerning the aquifer S, the box-plot of historical concentrations of Fe is showed in figure 9.10. Table 9.6 lists the statistical parameters of the box-plot. In analogy with the manganese data, a possible interference caused by different sampling methods can be identified. The group S Disc (dynamic sampling) has the highest values, with a median of 2897 µg/L. The groups S Acc and S Raff (static sampling) have lower values, with a median of 30 and 271 µg/L, respectively. However, the concentrations of S Disc can be generally considered consistent with the data of July 2010 (S Uni), representative of the natural background.

Concerning the aquifers C1, C2 and C3, the box-plot of historical concentrations of Fe is showed in figure 9.11. Table 9.7 lists the statistical parameters of the box-plot. For the aquifer C1, the data are only referred to the refinery (C1 Raff), and thus, are hardly comparable with the data of July 2010 (C1 Uni). In analogy with manganese, the data of July 2010 (C2 Uni) are consistent with the historical data (C2 Area) for aquifer C2, while, in the aquifer C3, the data of July 2010 (C3 Uni) are slightly higher with respect to the historical data (C3 Area).

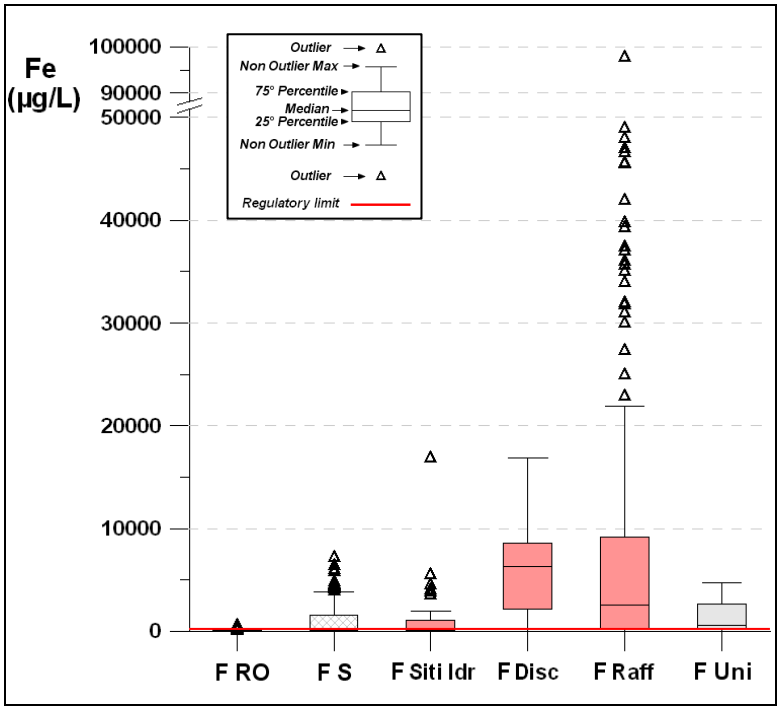

Figure 9.8. Box-plot of historical concentrations of Fe in aquifer F.

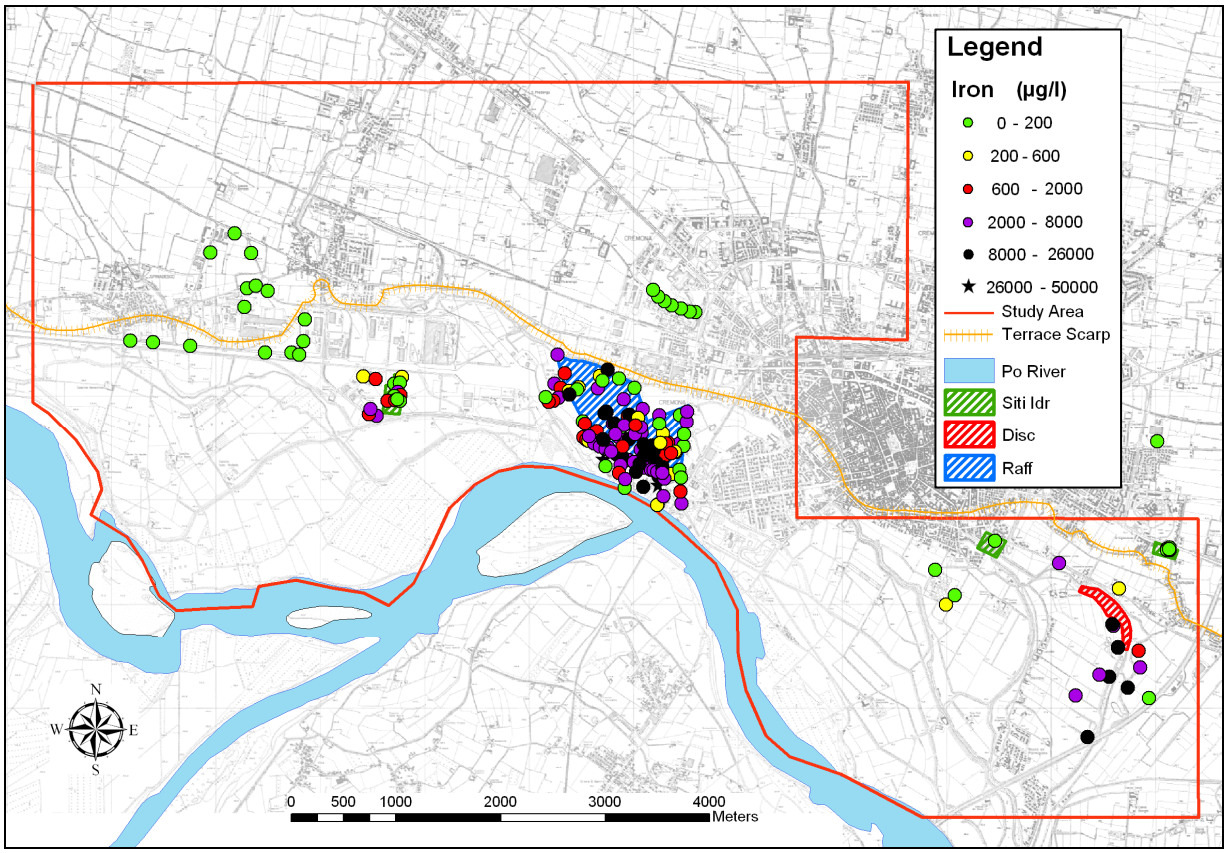

Figure 9.9. Median values of historical Fe concentrations calculated for each point in aquifer F.

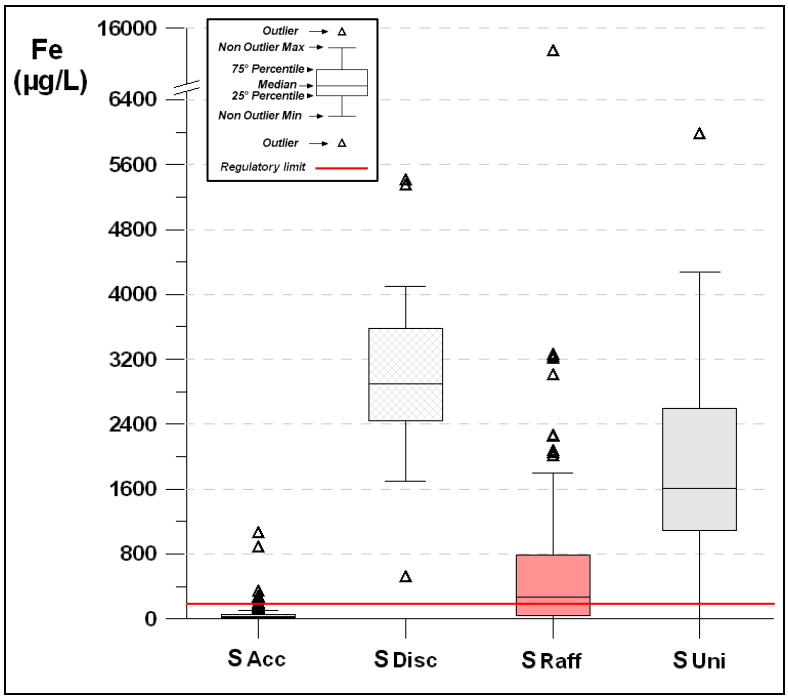

Figure 9.10. Box-plot of historical concentrations of Fe in aquifer S.

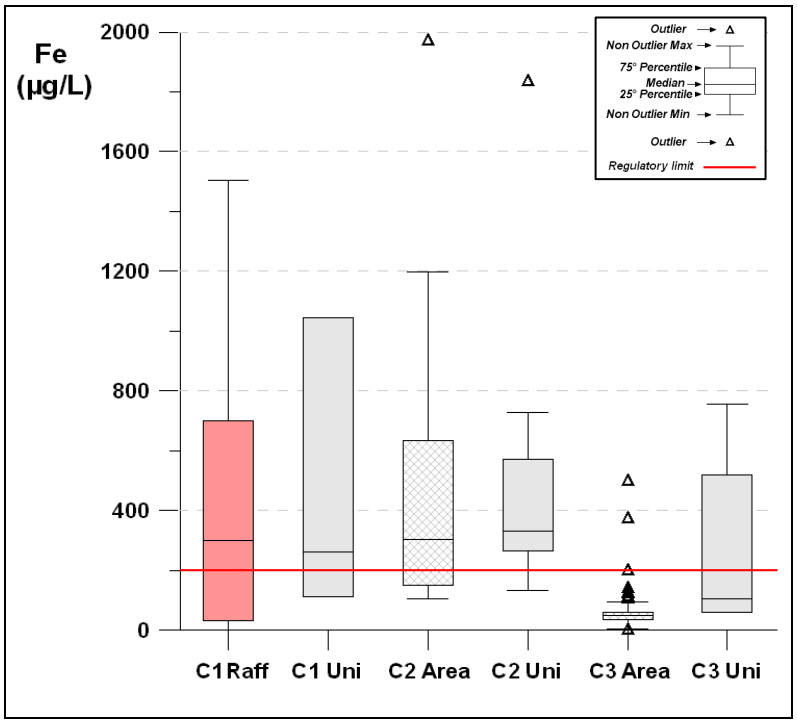

Figure 9.11. Box-plot of historical concentrations of Fe in aquifers C1, C2 and C3.

Table 9.5. Statistical parameters of the box-plot of historical Fe data in aquifer F (Figure 9.8).

Fe (µg/L)	F RO	F S	F Siti Idr	F Disc	F Raff	F Uni
N. Measurements	113	178	41	83	363	21
Period	2005-2009	2005-2010	2006-2010	1999-2010	2001-2010	July 2010
Minimum	1	1	3	26	0.5	10
25°percentile	5	18	12	2198	230	177
Median	21	89	62	6326	2548	629
75°percentile	40	1577	1060	8627	9092	2694
Maximum	630	7199	16911	16850	97900	4756

Table 9.6. Statistical parameters of the box-plot of historical Fe data in aquifer S (Figure 9.10).

Fe (µg/L)	S Acc	S Disc	S Raff	S Uni
N. Measurements	349	24	120	13
Period	2005-2009	1999-2010	2001-2010	July 2010
Minimum	3	504	3	10
25°percentile	15	2446	40	1091
Median	30	2897	271	1607
75°percentile	52	3575	790	2601
Maximum	1050	5400	15900	5975

Table 9.7. Statistical parameters of the box-plot of historical Fe data in aquifers C1, C2 and C3 (Figure 9.11).

Fe (µg/L)	C1 Raff	C1 Uni	C2 Area	C2 Uni	C3 Area	C3 Uni
N. Measurements	80	4	24	13	86	8
Period	2001-2010	July 2010	1989-2011	July 2010	1992-2011	July 2010
Minimum	1	112	104	132	0.5	60
25°percentile	33	112	150	267	37	61
Median	301	263	304	332	49	106
75°percentile	700	1045	634	573	61	518
Maximum	1505	1045	1971	1836	500	756

9.3. Arsenic

Concerning the aquifer F, the box-plot of historical concentrations of As is showed in figure 9.12. Table 9.8 lists the statistical parameters of the box-plot. Considering the natural background, the group F RO has a median value of 5 µg/L, keeping concentrations below the regulatory limit of 10 µg/L (D. Lgs. 152/06), with the exception of a group of measurements which are all referred to one point (piezometer S2 of the steel mill). This point can be considered as a hot spot. The collected information do not allow to understand the causes of the high As concentrations in this point. The group F S has slightly higher concentrations with

respect to F RO, having a median value of 7 µg/L. The concentrations of July 2010 (F Uni) are consistent with the historical data of natural background. Considering the sites with possible anthropogenic influences, the median value results 9 µg/L for F Raff, 10 µg/L for F Disc and 12 µg/L for F Siti Idr. These values are quite consistent with the median value of F S (7 µg/L). For the oil refinery (F Raff), some difference with respect to the natural background can be identified considering the highest measured values. In fact, the group F Raff has a significant number of upper outliers, up to the maximum value of 700 µg/L. The median ratio between the sites with possible influence and the natural background is equal to 1.3 for the refinery (median F Raff/median F S), to 1.4 for the landfill (median F Disc/median F S) and to 1.7 for the group of polluted sites (median F Siti Idr/median F S). Figure 9.13 shows the spatial distribution of historical data of As in the aquifer F. The map underlines the presence of higher values in the Po valley, south of the terrace scarp, with respect to the area behind the scarp, where, however, there is the hot spot. The highest values are located in the area of the refinery (Raff).

Concerning the aquifer S, the box-plot of historical concentrations of As is showed in figure 9.14. Table 9.9 lists the statistical parameters of the box-plot. The groups S Acc and S Disc are characterized by comparable concentrations, with a median value of 7 and 8 µg/L, respectively. The group S Raff has higher concentrations, with a median value of 26 µg/L. However, the concentrations of S Raff are consistent with the data of July 2010 (S Uni), indicative of the natural background.

Concerning the aquifers C1, C2 and C3, the box-plot of historical concentrations of As is showed in figure 9.15. Table 9.10 lists the statistical parameters of the box-plot. For the aquifer C1, the data are only referred to the refinery (C1 Raff), and thus, are hardly comparable with the data of July 2010 (C1 Uni). For the aquifers C2 and C3, the data of July 2010 (C2 Uni, C3 Uni) are slightly higher with respect to the historical data (C2 Area, C3 Area).

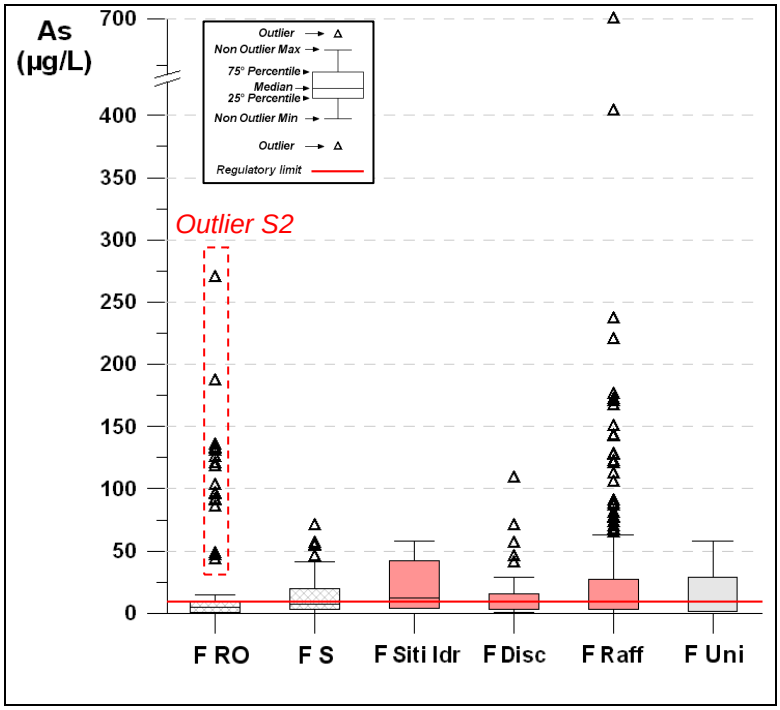

Figure 9.12. Box-plot of historical concentrations of As in aquifer F.

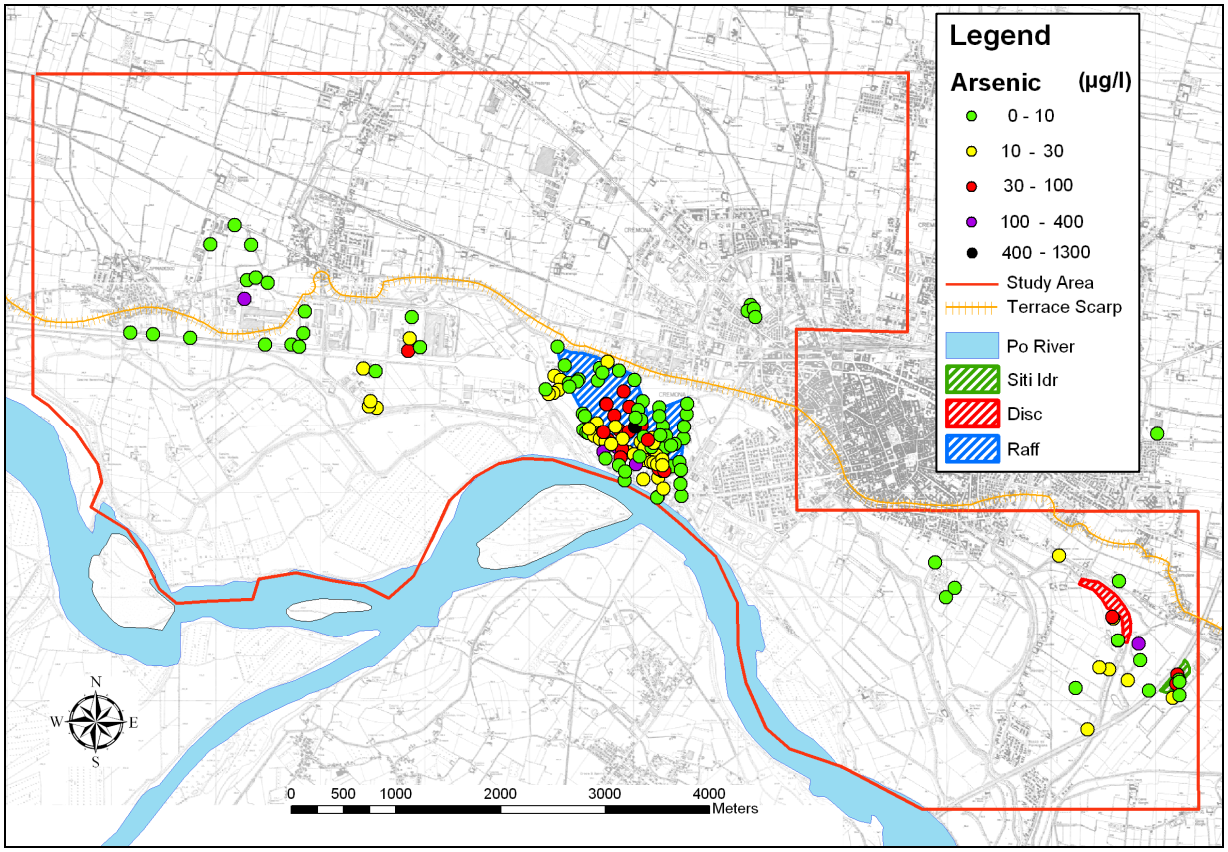

Figure 9.13. Median values of historical As concentrations calculated for each point in aquifer F.

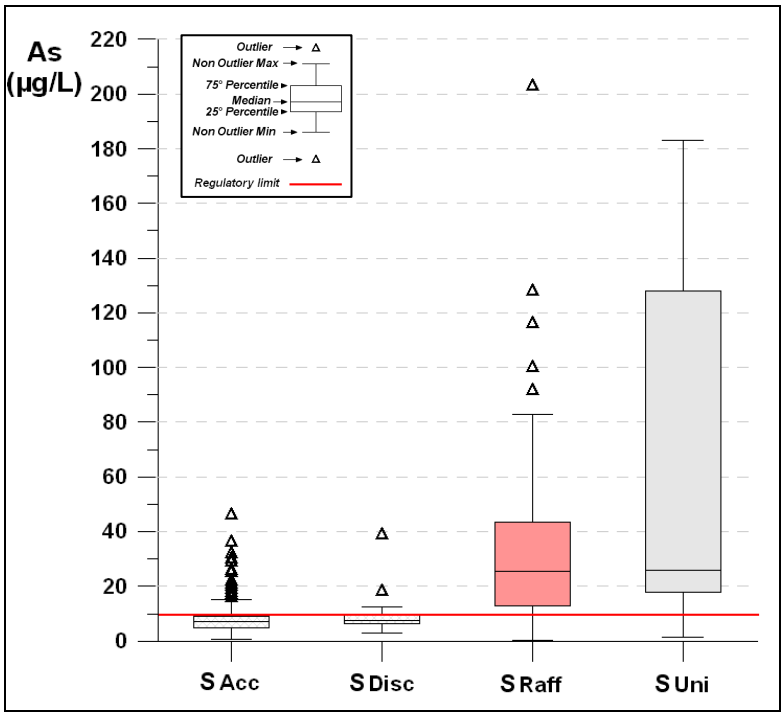

Figure 9.14. Box-plot of historical concentrations of As in aquifer S.

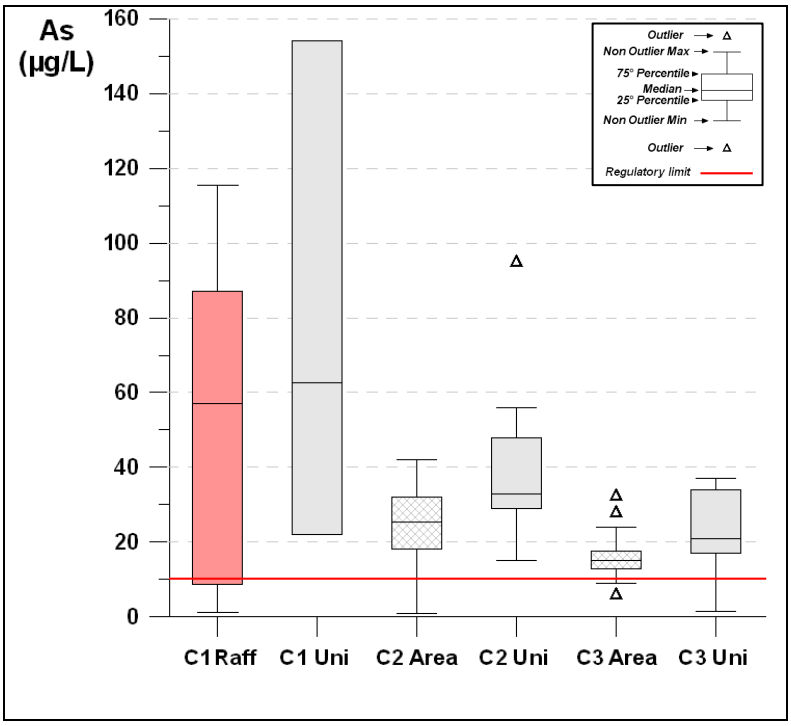

Figure 9.15. Box-plot of historical concentrations of As in aquifers C1, C2 and C3.

Table 9.8. Statistical parameters of the box-plot of historical As data in aquifer F (Figure 9.12).

As (µg/L)	F RO	F S	F Siti Idr	F Disc	F Raff	F Uni
N. Measurements	111	231	6	78	259	21
Period	2005-2009	1997-2010	February 2010	1999-2010	2004-2010	July 2010
Minimum	0.3	0.3	4	1	0.3	1.5
25°percentile	1	3	4	3	3	1.5
Median	5	7	12	10	9	1.5
75°percentile	9	20	42	16	27	29
Maximum	270	71	58	109	700	58

Table 9.9. Statistical parameters of the box-plot of historical As data in aquifer S (Figure 9.14).

As (µg/L)	S Acc	S Disc	S Raff	S Uni
N. Measurements	342	21	109	13
Period	2005-2009	1999-2010	2007-2010	July 2010
Minimum	1	3	0.3	1.5
25°percentile	5	6	13	18
Median	7	8	26	26
75°percentile	9	9	44	128
Maximum	46	39	203	183

Table 9.10. Statistical parameters of the box-plot of historical As data in aquifers C1, C2 ans C3 (Figure 9.15).

As (µg/L)	C1 Raff	C1 Uni	C2 Area	C2 Uni	C3 Area	C3 Uni
N. Measurements	65	4	20	13	74	8
Period	2007-1010	luglio 2010	1994-2011	July 2010	1994-2011	July 2010
Minimum	1	22	1	15	6	1.5
25°percentile	9	22	21	29	13	17
Median	57	63	26	33	15	21
75°percentile	87	154	33	48	18	34
Maximum	115	154	42	95	32	37

9.4. Ammonium

Concerning the aquifer F, the box-plot of historical concentrations of NH_4 is showed in figure 9.16. Table 9.11 lists the statistical parameters of the box-plot. For the ammonium, the degradation of hydrocarbons cannot represent an anthropogenic influence on groundwater NH_4 concentrations. Ammonium, or organic nitrogen, is generally absent in hydrocarbons due to its release in the processes of hydrocarbons formation and maturation, as reported by Williams et al. (1992). On the other hand, pollution by organic matter with vegetable or animal origin can influence the groundwater NH_4 concentration due to the presence of

organic nitrogen. Therefore, for the ammonium, the groups F S, F RO and F Raff can be considered as indicative of the natural background, while the data of the municipal solid waste landfill (F Disc) can be subjected to possible anthropogenic influences. No ammonium measurements were executed in the sites affected by low hydrocarbons pollution (Siti Idr). Considering the historical data of natural background, Po river valley (F S) has higher concentrations with respect to the area behind the terrace scarp (F RO). The median value is 0.19 mg/L, for the former, and 0.05 mg/L, for the latter. The values of F RO are generally below the regulatory limit of 0.5 mg/L (D. Lgs. 30/09). Also the values of F S are generally below the regulatory limit, but there are some points with higher concentrations. The concentrations of the refinery (F Raff), which is located in the Po valley, have a median value of 0.25 mg/L, that is consistent with the value of F S. The concentrations of July 2010 (F Uni) are consistent with the historical data of natural background. Considering the data of the landfill (F Disc), high concentrations are identified. The median value of the group F Disc is 1.97 mg/L, while the maximum concentration is 61.60 mg/L. The median ratio F Disc/F S is equal to 10.4. Figure 9.17 shows the spatial distribution of historical data of NH_4 in the aquifer F. The map underlines the presence of higher values in the Po valley, south of the terrace scarp, with respect to the area behind the scarp, where, however, there is a point with high concentrations. The highest values are located in the area downstream of the municipal solid waste landfill (Disc).

Concerning the aquifer S, the box-plot of historical concentrations of NH_4 is showed in figure 9.18. Table 9.12 lists the statistical parameters of the box-plot. The groups S Acc, S Raff and S Disc have comparable concentration values. The mean values are 1.11, 1.10 and 0.49 mg/L respectively. It should be noted that the group S Disc has an outlier with a concentration of 33.6 mg/L. This concentration could be probably referred to a local infiltration of landfill leachate in the aquifer S. The data of July 2010 (S Uni) are generally higher than the other three groups.

Concerning the aquifers C1, C2 and C3, the box-plot of historical concentrations of NH_4 is showed in figure 9.19. Table 9.13 lists the statistical parameters of the box-plot. For the aquifers C1, C2 and C3, the historical concentrations of the deeper aquifers (C1, C2 and C3) are comparable. The median values are 1.48 mg/L (C1 Area), 1.55 mg/L (C2 Area) and 1.57 mg/L (C3 Area). The concentrations of July 2010 are generally higher, with a median value of 4.40 mg/L (C1 Uni), 3.20 mg/L (C2 Uni) and 2.80 mg/L (C3 Uni).

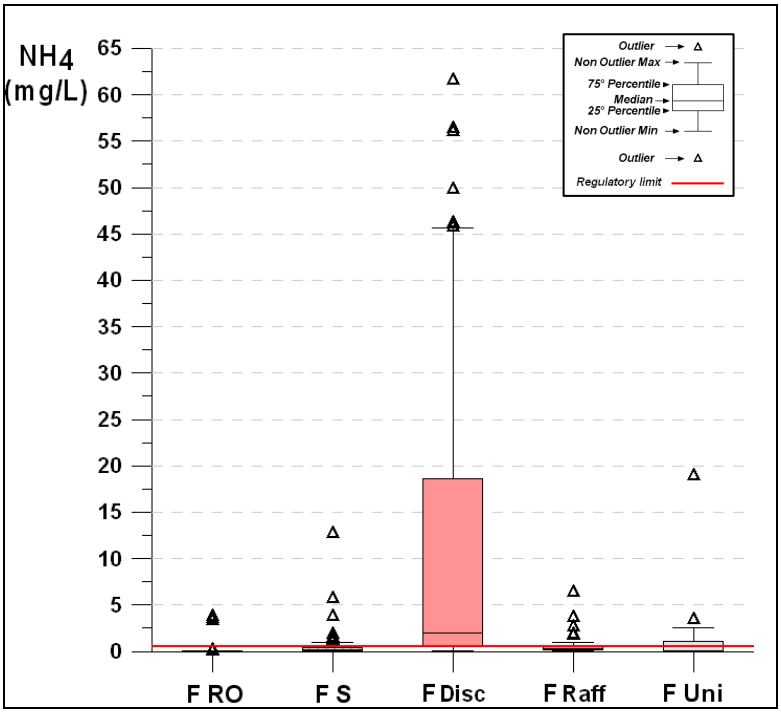

Figure 9.16. Box-plot of historical concentrations of NH_4 in aquifer F.

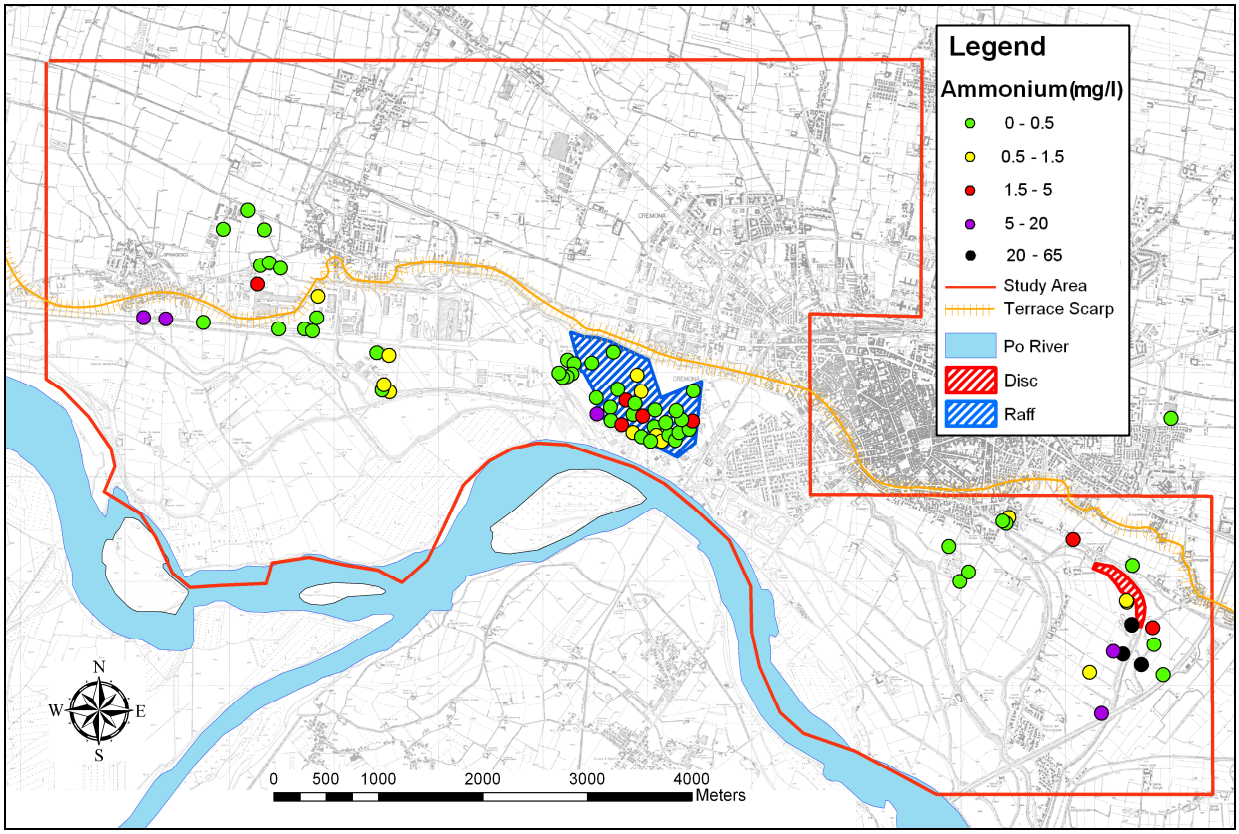

Figure 9.17. Median values of historical NH_4 concentrations calculated for each point in aquifer F.

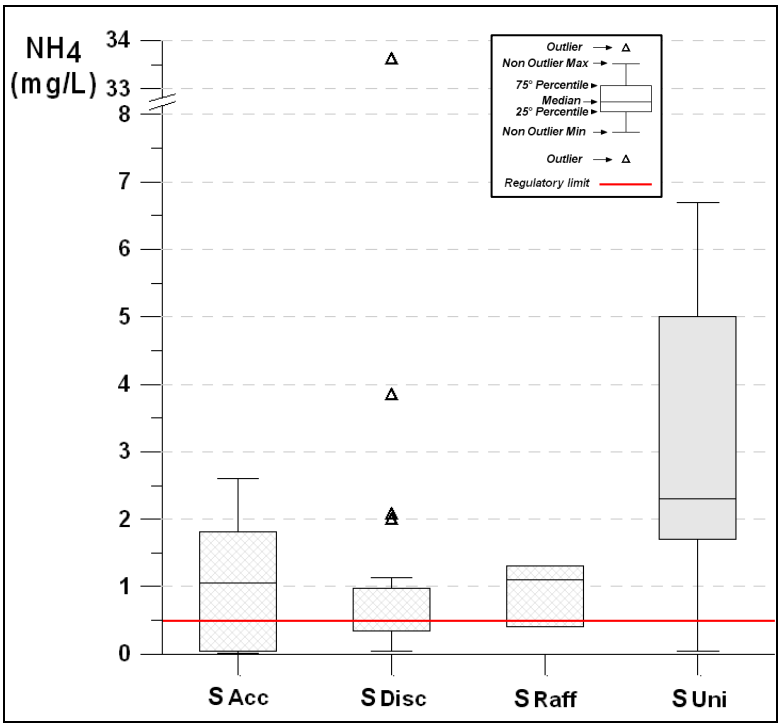

Figure 9.18. Box-plot of historical concentrations of NH_4 in aquifer S.

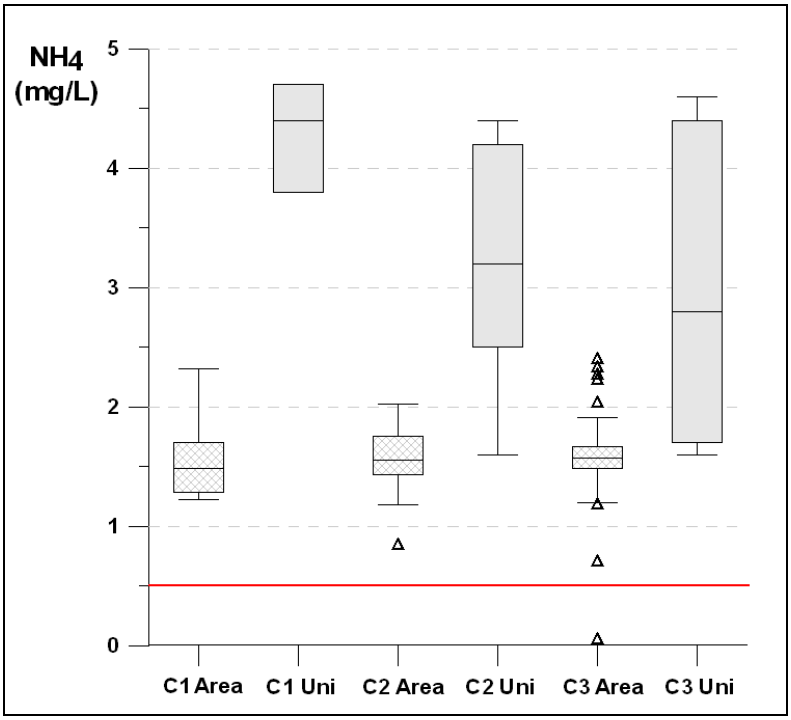

Figure 9.19. Box-plot of historical concentrations of NH_4 in aquifers C1, C2 and C3.

Table 9.11. Statistical parameters of the box-plot of historical NH_4 data in aquifer F (Figure 9.16).

NH_4 (mg/L)	**F RO**	**F S**	**F Disc**	**F Raff**	**F Uni**
N. Measurements	40	111	100	30	21
Period	2005-2009	2006-2010	1999-2010	February 2001	July 2010
Minimum	0.005	0.01	0.05	0.03	0.05
25°percentile	0.02	0.07	0.51	0.14	0.05
Median	0.05	0.19	1.97	0.25	0.05
75°percentile	0.05	0.43	18.60	0.56	1.10
Maximum	3.80	12.70	61.60	6.43	18.90

Table 9.12. Statistical parameters of the box-plot of historical NH_4 data in aquifer S (Figure 9.18).

NH_4 (mg/L)	**S Acc**	**S Disc**	**S Raff**	**S Uni**
N. Measurements	26	27	3	13
Period	2005-2009	1999-2010	February 2001	July 2010
Minimum	0.01	0.05	0.40	0.05
25°percentile	0.05	0.34	0.40	1.70
Median	1.11	0.49	1.10	2.30
75°percentile	1.81	0.98	1.30	5.00
Maximum	4.00	33.60	1.30	6.70

Table 9.13. Statistical parameters of the box-plot of historical NH_4 data in aquifers C1, C2 and C3 (Figure 9.19).

NH_4 (mg/L)	**C1 Area**	**C1 Uni**	**C2 Area**	**C2 Uni**	**C3 Area**	**C3 Uni**
N. Measurements	6	4	25	13	80	8
Period	2001-2010	July 2010	1989-2011	July 2010	1992-2011	July 2010
Minimum	1.22	3.80	0.84	1.60	0.05	1.60
25°percentile	1.28	3.80	1.43	2.50	1.48	1.70
Median	1.48	4.40	1.55	3.20	1.57	2.80
75°percentile	1.70	4.70	1.75	4.20	1.67	4.40
Maximum	2.32	4.70	2.02	4.40	2.40	4.60

9.5. Discussion of results

The comparison of groundwater As, Fe, Mn and NH_4 concentrations between the sites with possible anthropogenic influences and the natural background points out that:

- in the aquifer F, an anthropogenic influence can be identified (1) in the oil refinery, on As, Fe and Mn concentrations; (2) in the municipal solid waste landfill, on NH_4, Fe and Mn concentrations; (3) in the sites with lower hydrocarbons pollution, on Mn concentrations;

- in the aquifer S, any significant anthropogenic influences cannot be identified;
- in the aquifer C1, the presence of data only referred to the refinery does not allow a comparison with the natural background, anyway, the absence of significant influences in the aquifer S leads to suppose the absence of anthropogenic influences in the aquifer C1 too.

Concerning the natural background, a summary of the historical concentrations, with a comparison with the measured concentration of July 2010, is showed in the box-plot graphs of figure 9.20, 9.21, 9.22 and 9.23. It should be noticed that for the As, Fe and Mn historical data, no natural background concentrations are available for the aquifer C1, therefore the group C1 Raff is reported in the graphs. In these box-plots, the natural background concentrations of the historical data involve: (1) the groups F S and F RO for the aquifer F; (2) the sum of the groups S Acc and S Disc for the aquifer S (exclusion of S Raff); (3) the group C1 Raff (the only available data for this aquifer) for As, Fe and Mn, and the group C1 Area for NH_4 concerning aquifer C1; (4) the groups C2 Area and C3 Area for the aquifers C2 and C3. It should be noted that the data referred to the piezometer S2 of the steel mill (hot spot) are excluded from the group F RO in the box-plot of As concentrations (Figure 9.22).

Concerning the manganese (Figure 9.20), the historical concentration has lower values in the area behind the terrace scarp in the aquifer F, highest values in the Po valley in the aquifer F, and decreasing values from aquifer S to C3. The same profile, with consistent values, can be identified in the data of July 2010.

Concerning the iron (Figure 9.21), the historical concentration is characterized by lower values in the area behind the terrace scarp in the aquifer F, highest values in the Po valley in the aquifer F and in the aquifer S, and decreasing values from aquifer C1 to C3. The same profile, with consistent values, can be identified in the data of July 2010.

Concerning the arsenic (Figure 9.22), the historical concentration is characterized by lower values in the area behind the terrace scarp in the aquifer F, higher values in the Po valley in the aquifer F and in the aquifer S, highest values in the aquifer C1, and decreasing values from aquifer C2 to C3. The same profile, with consistent values, can be identified in the data of July 2010, with the exception of the aquifer S, where the historical concentrations are lower.

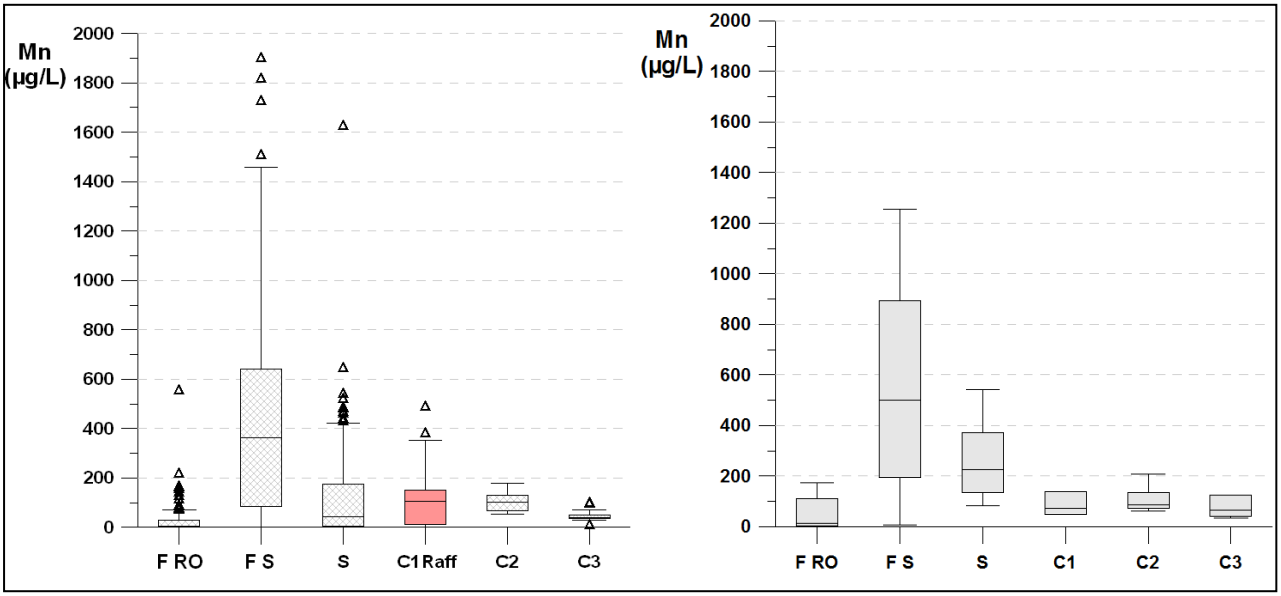

Figure 9.20. Comparison between background Mn concentrations of historical (on the left) and July 2010 data (on the right); in red: C1 Raff, which is not referred to natural background (only available historical data for this aquifer).

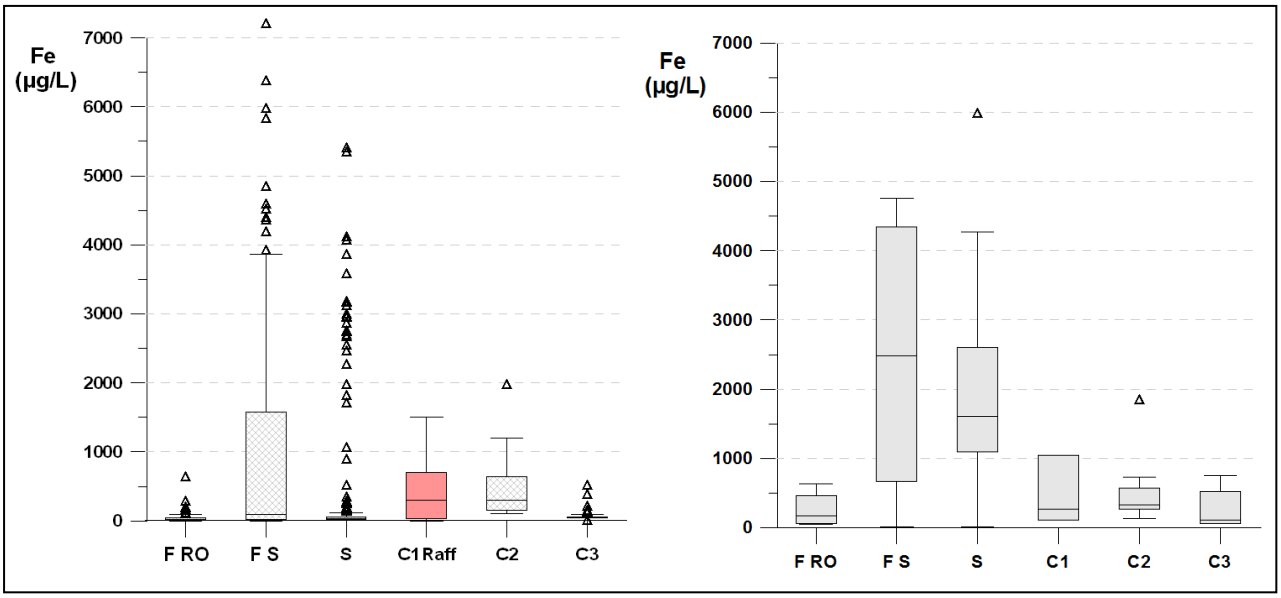

Figure 9.21. Comparison between background Fe concentrations of historical (on the left) and July 2010 data (on the right); in red: C1 Raff, which is not referred to natural background (only available historical data for this aquifer).

Concerning the ammonium (Figure 9.23), the historical concentration has lower values in the area behind the terrace scarp in the aquifer F, higher values in the Po valley in the aquifer F and in the aquifer S, and constant high values in

aquifers C1, C2 and C3. The same profile, but with higher values, can be identified in the data of July 2010. These different values could probably be related to specific conditions, affecting ammonium concentration, occurred in the survey of July 2010. A long-term monitoring is probably required to better understand the causes of these higher concentrations detected in July 2010.

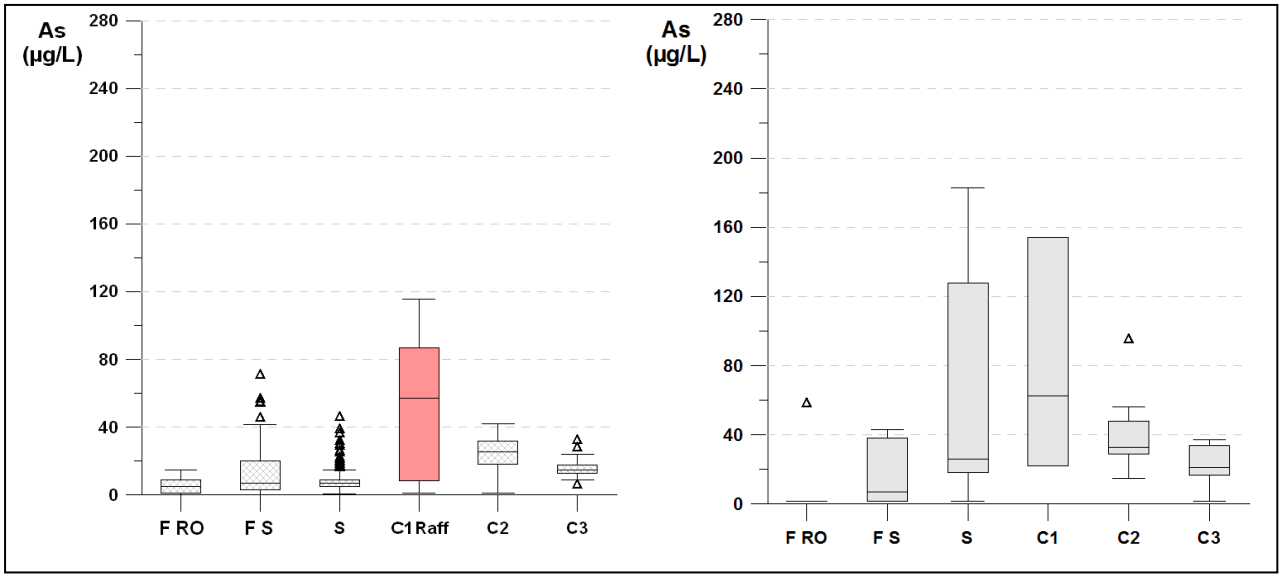

Figure 9.22. Comparison between background As concentrations of historical (on the left) and July 2010 data (on the right); in red: C1 Raff, which is not referred to natural background (only available historical data for this aquifer).

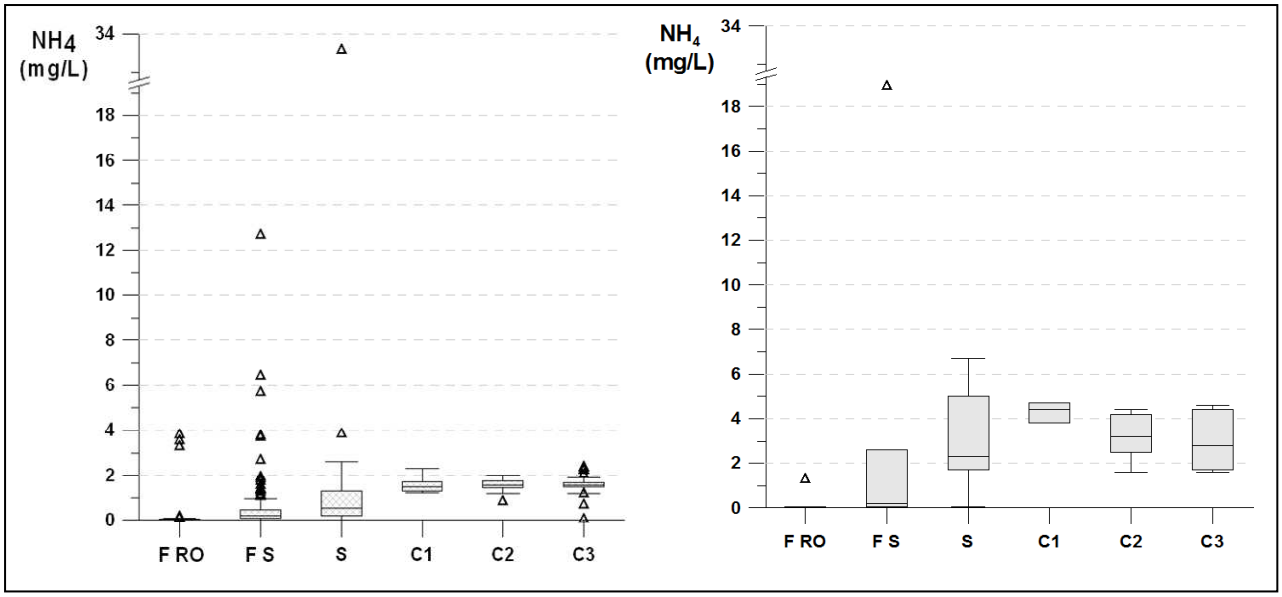

Figure 9.23. Comparison between background NH_4 concentrations of historical (on the left) and July 2010 data (on the right).

9.6. Conclusions

In conclusion, the analysis of historical hydrochemical data underlines that in the study area:

- groundwater pollution by hydrocarbons can influence the As, Fe and Mn concentrations, as verified in the oil refinery, on the basis of the hydrogeochemical mechanisms discussed in chapter 8 and reported by previous studies (e.g., Baedecker et al., 1993; Tucillo et al., 1999; Berbenni et al., 2000; Gosh et al., 2003; Burgess and Pinto, 2005);
- groundwater pollution by organic matter with vegetable or animal origin can influence the As, Fe, Mn and NH_4 concentrations, as verified in the municipal solid waste landfill for NH_4, Fe and Mn probably due to an organic leachate spill. Influences on groundwater As, Fe, Mn and NH_4 concentrations downstream of landfills are reported by previous studies (e.g., Hounslow, 1980; Nicholson et al., 1983; Albrechtsen and Christensen, 1994; Bjerg et al., 1995).

Considering the data referred to the natural background of As, Fe, Mn and NH_4, the hydrochemical characterization based on the July 2010 data (chap. 6) is generally confirmed by the historical data, with the exception of NH_4 for the deeper aquifers. As discussed above, these differences could probably be related to specific conditions occurred in the survey of July 2010. A long-term monitoring is probably required to better understand the causes of this aspect.

References

Albrechtsen H. J. & Christensen T. H. (1994) – *Evidence for microbial iron reduction in a landfill leachate-polluted aquifer (Vejen, Denmark)*. Applied and Environmental Microbiology 60(11), 3920-3925.

Baedecker M.J., Cozzarelli I. M., Eganhouse R. P., Siegel D. I. & Bennett P. C. (1993) – *Crude oil in a shallow sand and gravel aquifer—III. Biogeochemical reactions and mass balance modeling in anoxic groundwater*. Applied Geochemistry 8(6), 569-586.

Berbenni P., Pollice A., Canziani R., Stabile L. & Nobili F. (2000) – *Removal of iron and manganese from hydrocarbon-contaminated groundwaters.* Bioresource Technology 74 (2), 109-114.

Bjerg P. L., Ruegge K., Pedersen J. K. & Christensen T. H. (1995) – *Distribution of redox-sensitive groundwater quality parameters downgradient of a landfill (Grindsted, Denmark)*. Environmental Science and Technology 29(5), 1387-1394.

Burgess W.G. & Pinto L. (2005) – *Preliminary observations on the release of arsenic to groundwater in the presence of hydrocarbon contaminants in UK aquifers.* Mineralogical Magazine 69 (5), 887-896.

Ghosh R., Deutsch W., Geiger S., McCarthy K. & Beckmann D. (2003) – *Geochemistry, fate and transport of dissolved arsenic in petroleum hydrocarbon-impacted groundwater*. Petroleum hydrocarbons and organic chemicals in groundwater. American Petroleum Institute, National Ground Water Association. Costa Mesa, 266-280.

Hounslow A. W. (1980) – *Ground-Water Geochemistry: Arsenic in Landfills*. Ground Water 18(4), 331-333.

Nicholson R. V., Cherry J. A. & Reardon E. J. (1983) *Migration of contaminants in groundwater at a landfill: A case study 6. Hydrogeochemistry*. Journal of Hydrology 63(1-2), 131-176.

Tucillo M. E., Cozzarelli I. M. & Herman J. H. (1999) – *Iron reduction in the sediments of a hydrocarbon-contaminated aquifer.* Applied Geochemistry 14 (5), 655-667.

Williams L.B., Wilcoxon B.R., Ferrell R.E. & Sassen R. (1992) – *Diagenesis of ammonium during hydrocarbon maturation and migration, Wilcox Group, Louisiana, U.S.A*. Applied Geochemistry 7(2), 123-134.

10. Analysis of isotope and microbiological data

In this chapter, the results of the isotope and microbiological analysis on July 2012 groundwater samples are presented.

10.1. Isotope data analysis

The results of the stable isotope measurements of the July 2012 survey are listed in table 10.1. The isotope analysis concerns 14 samples of groundwater and 1 sample of surface water (Po river). The sampled points are showed in figure 10.1.

Table 10.1. Stable isotope measurements of the July 2012 survey.

Code	Depth (m b.s.)	Aquifer	δ18O (‰) *vs* VSMOW2	δ2H (‰) *vs* VSMOW2	δ13C (‰) *vs* PDB	δ15N (‰) *vs* AIR
CR82	17.0	F	-8.18	-54.47	-14.65	n.m.
CR93	20.0	F	-8.72	-56.90	-11.93	n.m.
CR66	8.2	F	-8.70	-56.35	-14.87	n.m.
SN8	10.0	F	-8.00	-53.47	-9.29	5.86
SN2	32.0	S	-9.05	-58.86	-12.46	5.57
SN4	34.0	S	-7.71	-50.13	n.m.	n.m.
CR32	102.0	C1	-8.81	-56.56	-12.76	7.81
CR10	90.0	C1	-8.41	-55.70	-9.82	4.09
CR16	95.0	C2	-8.53	-57.18	n.m.	n.m.
CR27	120.0	C2	-9.01	-58.90	n.m.	n.m.
CR20	141.0	C2	-8.85	-57.47	n.m.	n.m.
CR91	223.0	C3	-8.64	-58.89	n.m.	n.m.
CR92	230.0	C3	-8.67	-60.12	n.m.	n.m.
SU2	214.0	C3	-8.42	-55.59	n.m.	n.m.
Po River	-	-	-9.38	-63.50	n.m.	n.m.

n.m.: not measured.

10.1.1. δ^2H and $\delta^{18}O$ in water

The δ^2H and $\delta^{18}O$ in water was measured in all the collected samples (Table 10.1). Figure 10.2 shows the scatter plot of δ^2H *vs* $\delta^{18}O$ measurements. The measurements are classed in superficial (F and S) and deep (C1, C2 and C3) aquifers. The global meteoric water line (Rosanski et al., 1993) and the linear

regression line of the previous study in the Cremona area (Francani et al., 1994) are plotted. The points fit quite well to the line of Francani et al. (1994), moreover, the general alignment on the global meteoric water line allows to exclude the occurring of evaporation processes in recharge water. The Po river point (blue triangle) is clearly distinct with more depleted values from the groundwater points. The lower value of the Po sample could reflect the alpine origin of the river. The points of superficial and deep aquifers seem to have comparable isotope values, with the exception of 3 superficial points (CR82, SN8, SN4) which have most enriched values. The evolution of $\delta^{18}O$ with depth (Figure 10.3) could give a better understanding.

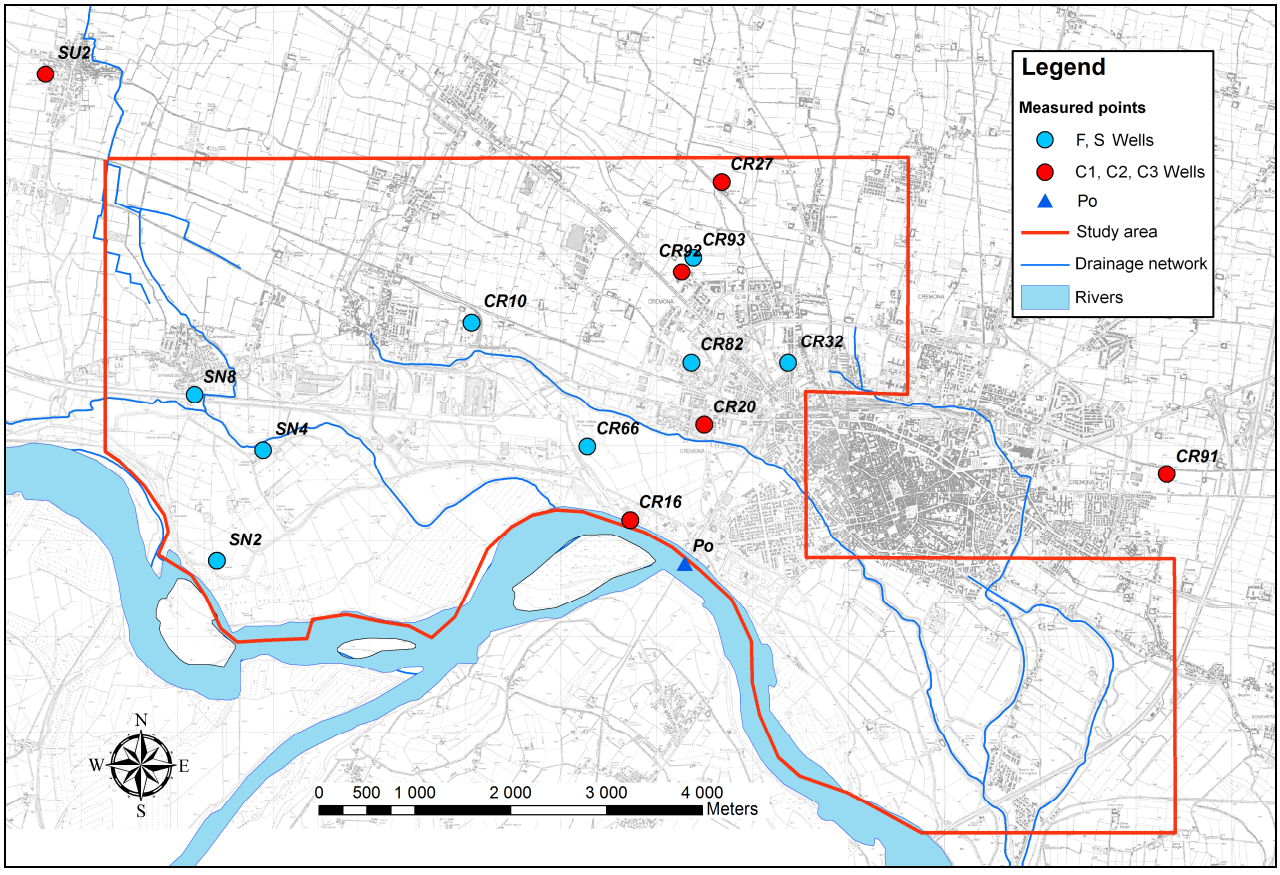

Figure 10.1. Location of the measured points with the surface drainage network.

The $\delta^{18}O$ values of superficial wells are included between the measured Po value (-9.38) and the local precipitation range value (from -5.95 to -7.73). The latter was derived from Longinelli and Selmo (2003) considering the three nearest sampling stations to Cremona (Mantova, Piacenza, Parma).

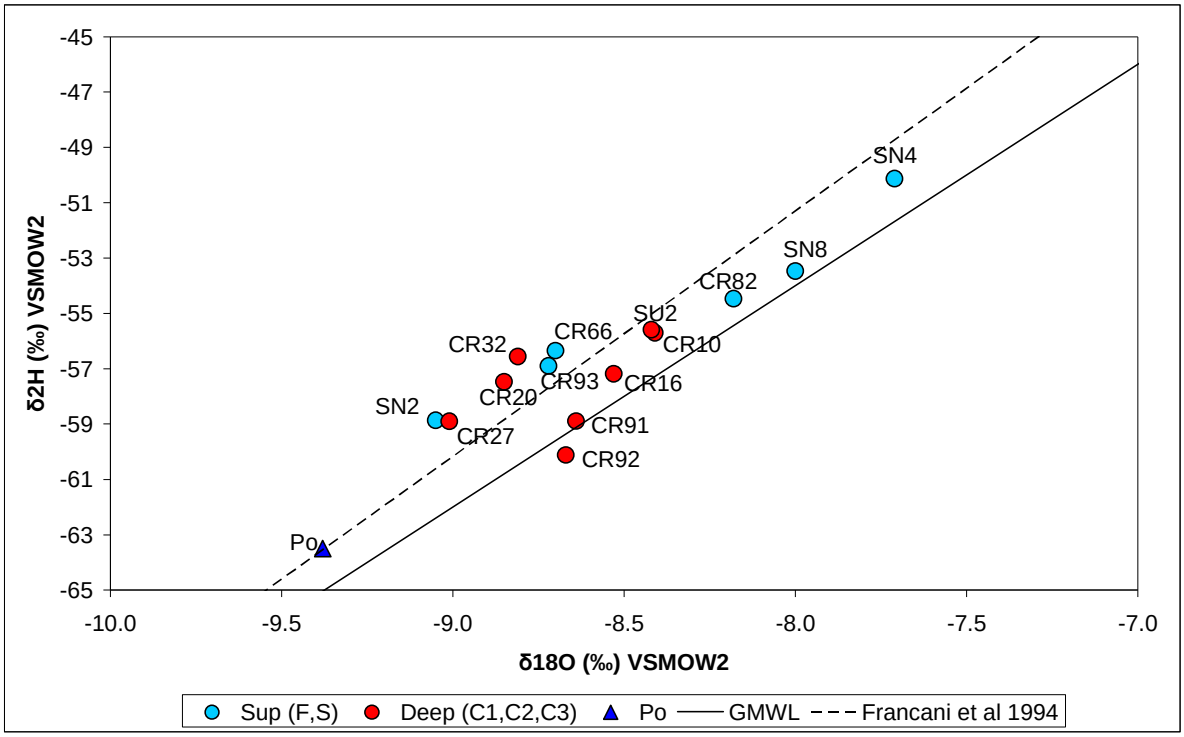

Figure 10.2. Scatter plot of δ^2H *vs* $\delta^{18}O$ measurements; full line: Global Meteoric Water Line (GMWL; Rozanski et al., 1993), dotted line: linear regression of Francani et al. (1994).

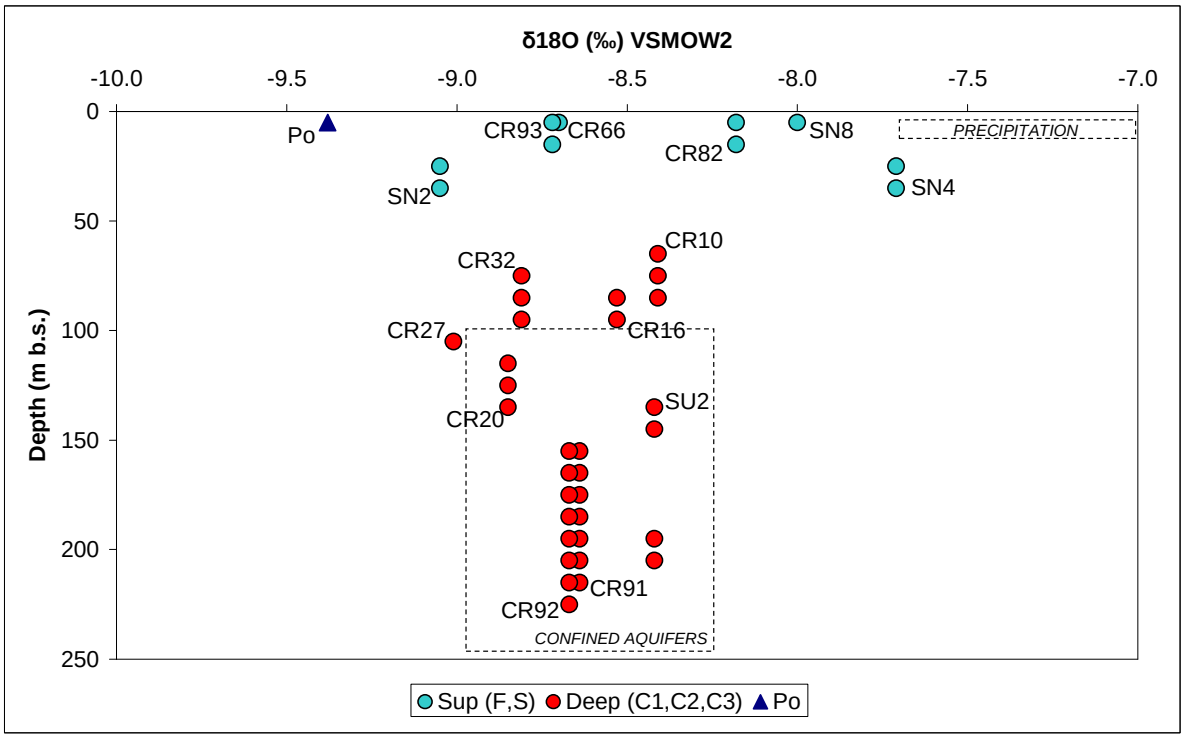

Figure 10.3. Evolution of $\delta^{18}O$ with depth. The number of points for each well represents the screen length.

The 3 points with most enriched values (CR82, SN8, SN4) seem to be influenced by the isotopic ratio of precipitations. In particular, the cause of the enriched value could be related to a higher infiltration rate for CR82, which is located in the area behind the terrace scarp. This area is manly characterized by superficial sandy deposits (par. 4.1.5) and a higher infiltration rate can be expected. For SN8 and SN4, the cause of the enriched values could be related to the interaction with the surface drainage network, which collects the rain water. In fact, the points SN8 and SN4 are located near a channel (Figure 10.1). On the other hand, the point with most depleted value (SN2) seems to be influenced by the isotopic ratio of the Po river. This is probably due to the interaction between groundwater and Po water: SN2 is located near the Po (Figure 10.1) in the zone where groundwater and Po river water can interact in relation to the variation of the Po hydrometric level (par. 5.4).

The $\delta^{18}O$ values of deep wells range from -9.01 to -8.41. These values are consistent with the values of deep confined waters reported in previous studies, concerning the Po Plain in Lombardy region. These studies were referred to Cremona (from -9.97 to -8.30; Francani et al., 1994), Lodi (from -8.93 to -8.33; Guffanti et al., 2010), Pavia (from ~ -8.7 to ~ -8.5; Pilla, 1998), Lomellina (from -9.13 to -8.32; Pilla et al., 2006) and Milano (from ~ -9.8 to ~ -8.3; Avanzini et al., 1994). These similarities in the water isotopic composition of deep groundwater could confirm the hypothesis of a continuous deep aquifer system in the Po Plain, with a common recharge area that is located between the high plain and the foothills of the Alps (Pilla et al., 2006).

The measured $\delta^{18}O$ value of the Po river (-9.38) results higher with respect to the recorded values by Bortolami et al. (1983) of around -10 and by Rapti-Caputo and Martinelli (2009) of -9.9. An explanation of this could be the influence of the Adda river. In fact, the measuring point of Po river is located downstream the confluence with the Adda river. Therefore, the measured isotopic composition of Po river could be influenced by the Adda isotopic ratio, which is probably different from the Po due to different catchment basins. The measurement of the isotopic ratio of both Po and Adda rivers, to be executed in future development, could give a better understanding.

The similarities in measured isotopic composition of superficial and deep groundwater do not exclude a possible exchange of water between superficial and deep aquifers, as supposed in the analysis of vertical hydrodynamic relations (par. 5.2). However, these similarities cannot prove the presence of vertical water

exchanges. In fact, the similar isotopic composition could be only the product of different independent processes. The presence of vertical water exchanges between different aquifers could be investigated with the analysis of chloride concentration over depth (Figure 10.4).

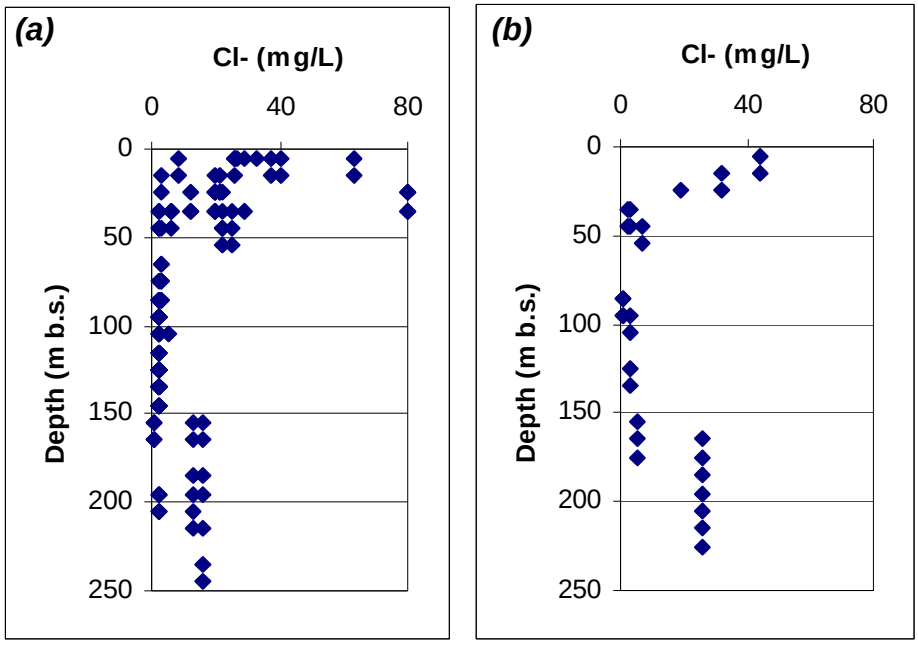

Figure 10.4. Profiles of Cl^- concentration over depth in the western and central parts (a) and in the eastern part (b) of the study area.

Chloride can be considered as conservative in groundwater flow, therefore a slight variation between different aquifers could indicate a possible interaction. Figure 10.4 (a) shows the data from the central and western parts of the study area, where the modelling of the hydrogeological parameters of the aquifer underlines a higher separation between different aquifers. A slight decrease from the top to 50 m b.s. (corresponding to aquifer S) and different values from 60 m b.s. (corresponding to aquitard S/C1) can be identified. Therefore, in these areas the water exchange seems to occur from aquifer F to S. The profile of chloride concentrations over depth for the eastern part of the study area (Figure 10.4 b), where the aquifer modelling underlines a lower separation, shows a slight decrease from the top to 100 m b.s. (corresponding to aquifer C1). This profile could reinforce the hypothesis of a vertical exchange of water from aquifer F to C1 (par. 5.2) in the eastern part of the study area.

10.1.2. $\delta^{13}C$ in DIC

The $\delta^{13}C$ in dissolved inorganic carbon (DIC) was measured in 7 groundwater samples from aquifer F to C1 (Table 10.1). The measured $\delta^{13}C$ values range from -9.29 to -14.87. This range of values is plotted into a graph with distinctive $\delta^{13}C$ values in selected natural compounds (Figure 10.5, modified from Clark and Fritz, 1997). Figure 10.5 shows that the measured $\delta^{13}C$ values are consistent with typical groundwater DIC values. This result could be interpreted as follow: the measured isotopic composition is the product of the $\delta^{13}C$ fractionation during equilibrium exchange of carbon between CO_2, DIC and carbonate minerals, as reported by Clark and Fritz (1997). In this context, the typical depleted values related to organic matter degradation, which probably plays a significant role in the studied system (chap. 7), cannot be registered probably due to carbonates equilibrium. Another process that could influence the $\delta^{13}C$ in DIC is methanogenesis, which leads to more enriched values (Baedecker et al., 1993).

10.1.3. $\delta^{15}N$ in ammonium

The $\delta^{15}N$ in ammonium was measured in 4 groundwater samples from aquifer F to C1 (Table 10.1). The 4 measured values are plotted into a graph with distinctive $\delta^{15}N$ ranges in different materials (Figure 10.6, modified from Clark and Fritz, 1997). The measured values fall within the range of organic nitrogen. They are quite far from the distinctive range of anthropic sources as synthetic fertilizer and manure/septic effluent. These results reinforce the hypothesis of a natural origin of the ammonium, which is probably generated by the degradation of organic nitrogen in peat sediments.

10.2. Microbiological data analysis

The microbiological analysis was conducted in only one groundwater sample, collected in the point SN8. This point is a superficial piezometer (10 m of depth) which has the screens in proximity of a peat deposit (from 5.3 to 7 m b.s.). Therefore, the occurring of organic matter degradation processes can be expected. The microbiological analysis concerns the calculation of the most probable number

(MPN) for iron-reducing and sulfate-reducing bacteria. Table 10.2 reports the results of the analysis. These results confirm the presence of iron-reducing and sulfate-reducing bacteria in the studied aquifer system, and thus, the probable occurring of Fe-oxide and sulfate reduction processes, which are coupled to the degradation of organic matter as peat.

Table 10.2. Results of the microbiological analysis in SN8 point (July 2012).

Parameter	Result	Confidence limit
MPN sulfate-reducing bacteria	90 MPN/100 mL	95% from 10 to 360 MPN/100 mL
MPN iron-reducing bacteria	4300 MPN/100 mL	95% from 700 to 21000 MPN/100 mL

10.3. Conclusions

The isotope and microbiological analysis, executed on the groundwater samples collected in July 2012, represent a first survey that can be enlarged in future developments of the present study. However, these first results point out some important aspects which can confirm the hydrogeochemical conceptual model for the studied system (chap. 7):

- the natural origin of ammonium, which probably derives from the degradation of organic nitrogen of peat;
- the occurring of Fe-oxide and sulfate reduction processes, coupled with the organic matter (peat) degradation; these processes can influence the whole groundwater chemistry, in particular the As, Fe and Mn concentrations.

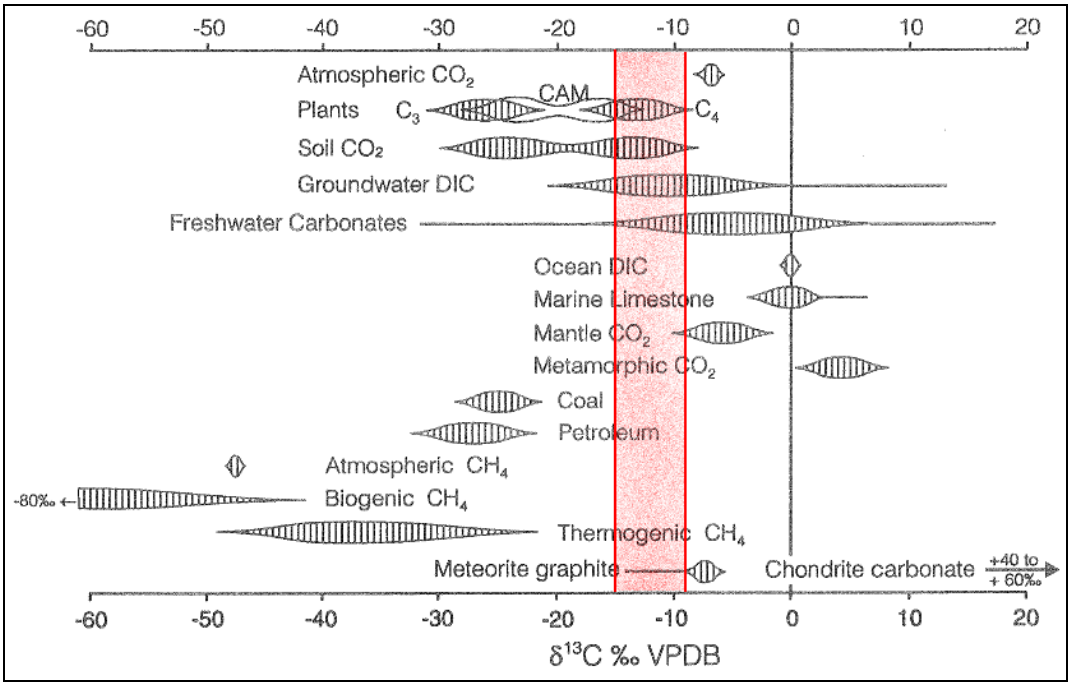

Figure 10.5. Measured $\delta^{13}C$ range value (red stripe) compared to distinctive $\delta^{13}C$ values in selected natural compounds (modified from Clark and Fritz, 1997).

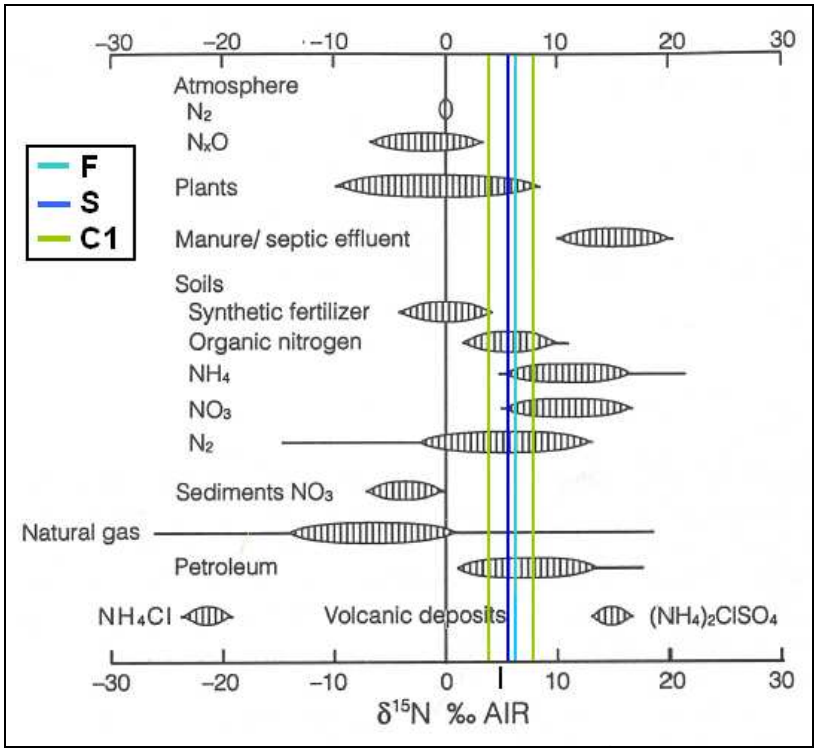

Figure 10.6. Measured $\delta^{15}N$ values in aquifer F (light blue line), S (blue line) and C1 (green lines) compared to distinctive $\delta^{15}N$ ranges in different materials (modified from Clark and Fritz, 1997).

References

Avanzini R., Beretta G. P., Francani V. & Nespoli R. (1994) – *Indagine preliminare sull'uso sostenibile delle falde profonde nella provincia di Milano (Preliminary investigation on the sustainable use of deep groundwater in the Milano province)*. Consorzio Acqua Potabile, Milano.

Bortolami G. C., Olivero G. F., Piovesana F., Ricci B. & Zuppi G. M. (1983) – *Idrogeologia isotopica della pianura vercellese-novarese (Piemonte) (Isotope hydrogeology of the Vercelli-Novara plain (Piemonte))*. Rendiconti Accademia Nazionale dei Lincei classe di scienze fisiche, matematiche e naturali LXXIV-3, 157-166.

Baedecker M.J., Cozzarelli I. M., Eganhouse R. P., Siegel D. I. & Bennett P. C. (1993) – *Crude oil in a shallow sand and gravel aquifer—III. Biogeochemical reactions and mass balance modeling in anoxic groundwater*. Applied Geochemistry 8(6), 569-586.

Clark I. & Fritz P. (1997) – *Environmental Isotopes in Hydrogeology*. Lewis Publishers, New York, 328 pp.

Francani V., Beretta G. P., Bareggi A., Nobile A., Cremonini Bianchi M. & Cattaneo F. (1994) – *Aspetti idrogeologici del problema della presenza di azoto ammoniacale nelle acque sotterranee della provincia di Cremona. (Hydrogeological aspects of the occurrence of ammonium in groundwater in the province of Cremona).* Pitagora Editrice, Bologna, 101 pp.

Guffanti S., Pilla G., Sacchi E. & Ughini S. (2010) –*Characterization of the quality and origin of groundwater of lodigiano (Northern Italy) with hydrochemical and isotopic instruments*. Italian Journal of Engineering Geology and Environment 1, 65-78.

Longinelli A. & Selmo E. (2003) – *Isotopic composition of precipitation in Italy: a first overall map*. Journal of Hydrology 270, 75-88.

Pilla G. (1998) – *Caratterizzazione idrochimica e geochimica isotopica delle falde idriche nel sottosuolo della città di Pavia (Chemical and isotopic characterisation of groundwater from the city of Pavia)*. Atti Ticinensi di Scienze della Terra 40, 185-201.

Pilla G., Sacchi E., Zuppi G., Braga G. & Ciancetti G. (2006) – *Hydrochemistry and isotope geochemistry as tools for groundwater hydrodynamic investigation in multilayer aquifers: a*

case study from Lomellina, Po plain, south-western Lombardy, Italy. Hydrogeology Journal 14, 795-808.

Rapti-Caputo D. & Martinelli G. (2009) – *The geochemical and isotopic composition of aquifer systems in the deltaic region of the Po River plain (northern Italy)*. Hydrogeology Journal 17, 467-480.

Rozanski K., Araguás-Araguás L. & Gonfiantini R. (1993) – *Isotopic patterns in modern global precipitation*. In: Swart et al. (Eds), Climate Change in Continental Isotopic Records, 1-36. Geophysical Monograph 78.

11. Reactive transport modelling

The main aim of the implementation of a reactive transport modelling in this work is to understand if the preliminary hydrogeochemical conceptual model (chap. 7), based on literature, could be reliable on the present case study. In other words, we want to verify if the simulation of the reactions considered in the conceptual model could generate concentration values that are comparable with the field data.

The implementation of the reactive transport modelling involves two main phases: (a) the development of a conceptual model and (b) the reactive transport settings. The development of the conceptual model concerns the definition of the group of chemical reactions that governs the whole system. These reactions are then transferred into the model in the reactive transport settings.

11.1. Conceptual model

The conceptual model identifies the reactions that will be simulated in the numerical model. On the basis of the preliminary hydrogeochemical conceptual model (chap. 7), the studied system seems to be governed by reduction-oxidation processes related to the organic matter (mainly peat) degradation. In addition, mineral precipitation-dissolution processes could play a significant role in the system. In synthesis, the conceptual model considers two types of chemical reactions: (a) precipitation-dissolution processes and (b) reduction-oxidation processes.

11.1.1. Precipitation-dissolution processes

Mineral precipitation-dissolution processes control the groundwater chemistry in many groundwater systems, this is most probably the case for minerals for which the groundwater is close to equilibrium (Bleam, 2011). In order to identify which minerals are near equilibrium in the studied system, we made a speciation of the measured water chemistry (survey of July 2010, 68 samples) and a calculation of the saturation index (SI) of minerals using PHREEQC (Parkhurst and Appelo, 1999) with the *wateq4f* database (Ball and Nordstrom, 1991). The speciation was made considering the pe values calculated from the field ORP measurements. The

conversion from $E_{Ag/AgCl}$ values to E_h values (referred to the standard hydrogen electrode) was made using the potentials of Ag/AgCl reference electrode (E_h) reported by U.S. EPA (2013), depending on temperature. The average pe value for each aquifer was used in the points with missing measurement. The list of minerals that are found to be near equilibrium are reported in table 11.1.

Table 11.1. Average saturation indexes for the near equilibrium minerals;

Minerals	Average SI
Calcite ($CaCO_3$)	0.65
Dolomite ($CaMg(CO_3)_2$)	0.71
Rhodochrosite ($MnCO_3$)	-0.13
Siderite ($FeCO_3$)	-0.12
Vivianite^{+} ($Fe_3(PO_4)_2$:$8H_2O$)	-0.78
Ferrihydrite ($Fe(OH)_3$)	1.73
Lepidocrocite* (FeOOH)	3.35
Goethite (FeOOH)	7.29

($^{+}$) calculated considering the average historical value of PO_4^{2-} concentration (0.5 mg/L);
(*) calculated with the solubility product of Langmuir (1969; logK = -38.7).

Table 11.1 also contains the average value of SI calculated on all samples. For the lepidocrocite, which is not included in the *wateq4f* database, the logK value of -38.7 (25℃) of Langmuir (1969) was used. The calculation of SI for vivianite is only indicative because it was obtained considering the average value of historical data of PO_4^{2-} concentration equal to 0.5 mg/L (PO_4^{2-} was not measured in the survey of July 2010).

The results show that the sampled groundwater is slightly supersaturated with calcite and dolomite, near equilibrium with rhodochrosite, siderite and vivianite, and supersaturated with Fe-oxides. The supersaturation seen for the carbonates is probably linked to the genesis of sediments in the study area, which have an alpine origin and mainly derive from limestone formations (Ori, 1992).

The analysis of the log plots of the activities of the ions which form the minerals (Figure 1 and 2) could give a better understanding. The plots for calcite and dolomite show clearly the supersaturation condition, the different slope between the equilibrium line and the alignment of the points could also indicate that the dissolved carbonates are not controlled by the calcite and dolomite dissolution equilibrium. An hypothetical cause of this supersaturation condition could be the presence of kinetic inhibitors. Appelo and Postma (2005) report the example of calcite and dolomite supersaturation in marine sediments due to the presence of

inhibitors as organic acids (Davis et al., 2000) and phosphates (Walter and Hanor, 1979). A similar mechanism could maybe also take place in the studied system.

On the contrary, the data on the rhodochrosite plot are well aligned along the equilibrium line, with the exception of the F ox points that are subsaturated and some F red and S points that are supersaturated. The F ox points concern the shallow aquifer in the zone where the sediments are mainly composed by sands and there are phreatic and more oxidative conditions. If we assume an origin of the rhodochrosite from the reduction of Mn-oxides and the production of dissolved carbonate from oxidation of organic matter, the subsaturation in the F ox aquifer could be explained by unfavourable condition for Mn-oxide reduction. A different situation is found for the F red points that are in equilibrium and, in many cases, in slight supersaturation with a SI up to 0.3-0.5. These points concern the shallow aquifer but, in this case, the zone where there are superficial clay layers that locally produce confined conditions. This favours reductive condition allowing the Mn-oxide reduction. The presence of higher manganese concentration due to Mn-oxides reduction and a kinetic inhibition of the ongoing rhodochrosite precipitation could explain the supersaturation in these points. The same mechanism could explain the slight supersaturation of some S points. The remaining points concerning deeper aquifers are aligned to the equilibrium line. Therefore, rhodochrosite equilibrium seems to control the dissolved carbonate and manganese concentrations in the deeper part of the system.

The siderite plot looks similar to the rhodochrosite plot but, in this case, the points are not clearly aligned to the equilibrium line. F red and S points result supersaturated with a SI around 0.8, while with the increasing of depth the points seem to approach equilibrium. Even in this case, the supersaturation could be due to higher concentration of Fe^{2+} generated by the Fe-oxides reduction and a kinetic inhibition of the siderite precipitation, with the increasing of depth FeS precipitation could takes place and lower the Fe^{2+} concentration allowing the siderite to approach equilibrium.

The plot for Fe-oxides (Figure 11.2) shows a supersaturation with respect to the considered oxides (ferrihydrite, lepidocrocite and goethite). The points are aligned with the same slope of the equilibrium lines. It should be noted that these plots rely on the measured pe for the speciation of the Fe and thereby the calculation of the Fe^{3+} activity in PHREEQC. Therefore, this graph should be seen considering the limitations characterizing the ORP measurements (Lindberg and Runnells, 1984).

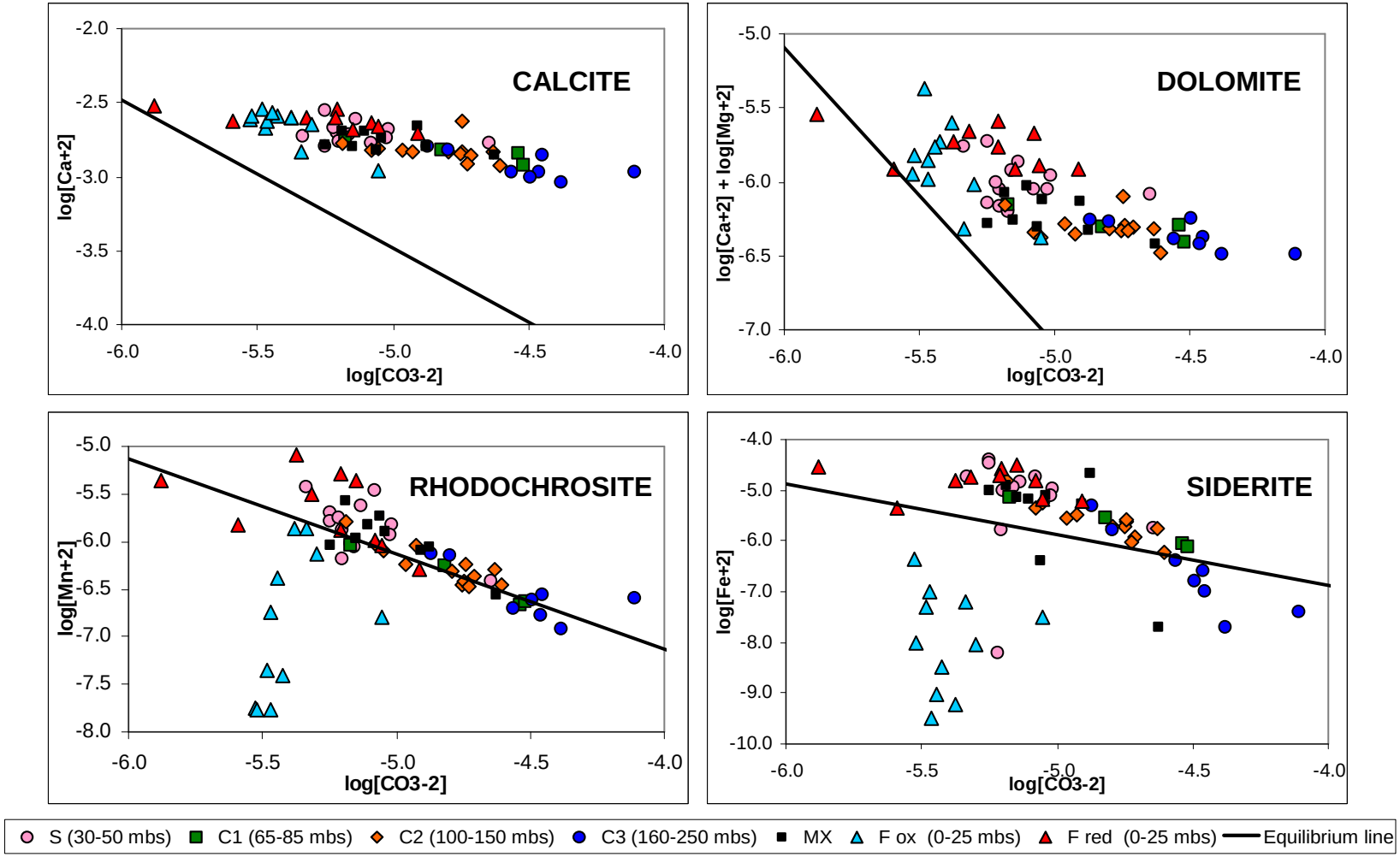

Figure 11.1. Mineral equilibria: log plots of the activities of the ions in calcite, dolomite, rhodochrosite and siderite; points are classed for each aquifer (MX are multiaquifer well points).

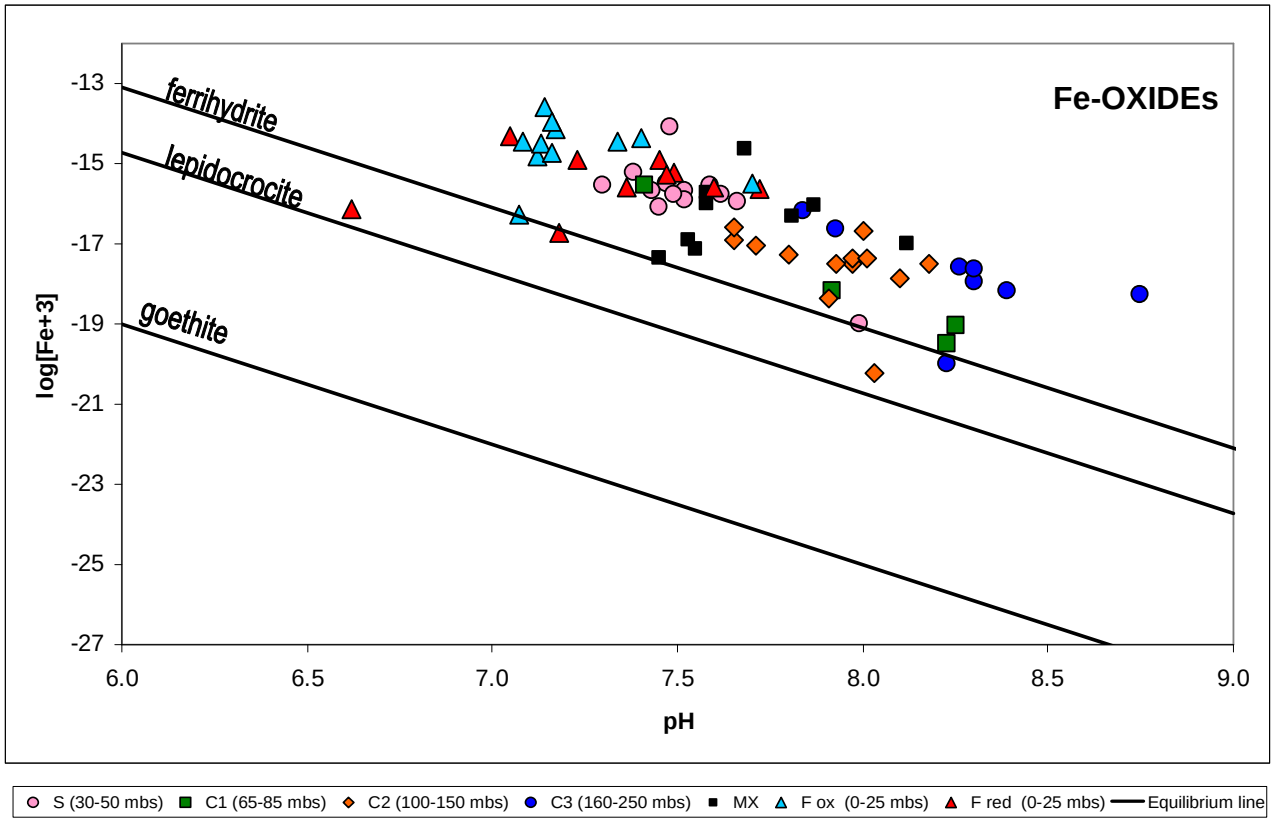

Figure 11.2. Mineral equilibria: log plots of the activities of the ions in Fe-oxides; points are classed for each aquifer (MX are multiaquifer well points).

11.1.2. Reduction-oxidation processes

The conceptual model of redox processes is based on the partial equilibrium approach proposed by Postma and Jakobsen (1996). This approach considers that the degradation of organic matter occurs in two steps: step one is the fermentation of organic matter with the production of molecules as formic acid, acetic acid, H_2 and CO_2; step two is the consumption of the fermentative products by different terminal electron accepting processes (TEAP's). The fermentative step is the only rate controlling process while TEAP'S are assumed to approach equilibrium. This approach is applicable for the microbial reduction of Mn-oxide, Fe-oxide and sulfate and for methanogenesis, while is not applicable for microbial oxygen and nitrate reduction, where the microorganisms may metabolize the organic matter (in the form of alcohols and fatty acids) directly (Postma and Appelo, 2005).

Considering that TEAP'S occur at equilibrium, the order of these processes is based on their energetic favourability and it is governed by the parameters that

could shift the equilibrium. For example, Postma and Jakobsen (1996) report that the occurrence of Fe-oxide reduction instead of sulfate reduction is mainly depending on the stability of the Fe-oxides and the pH. In other words, with the presence of unstable Fe-oxides Fe(III) reduction could be favoured, with stable Fe-oxides sulfate reduction could be favoured, and with the presence of different Fe-oxides the two processes could occur simultaneously.

The comprehension of which redox processes could govern the studied system started analysing the simultaneous equilibrium of Fe-oxide reduction, sulfate reduction and FeS precipitation, on the basis of the scheme proposed by Postma and Jakobsen (1996) for Fe^{2+} containing environments. For the simultaneous equilibrium of Fe-oxides and sulfate reduction and FeS the following reactions were considered:

$$Fe(OH)_3 + 3H^+ + e^- \leftrightarrow Fe^{2+} + 3H_2O \qquad \log K_1 \qquad (1)$$

$$HS^- + 4H_2O \leftrightarrow SO_4^{2-} + 8e^- + 9H^+ \qquad \log K_2 = -33.65 \qquad (2)$$

$$FeS + H^+ \leftrightarrow Fe^{2+} + HS^- \qquad \log K_3 = -3.915 \qquad (3)$$

The total reaction is:

$$8Fe(OH)_3 + FeS + 16H^+ \leftrightarrow 9Fe^{2+} + SO_4^{2-} + 20H_2O \qquad (4)$$

with

$$8\log K_1 + \log K_2 + \log K_3 = 9\log[Fe^{2+}] + \log[SO_4^{2-}] + 16pH \qquad (5)$$

from which the equilibrium line equation is:

$$-\log[Fe^{2+}] = 1.78pH + 0.11\log[SO_4^{2-}] - 0.11(8\log K_1 + \log K_2 + \log K_3) \qquad (6)$$

for $\log K_1$ different values corresponding to different Fe-oxides were considered (Table 11.2). $\log K_3$ is from *wateq4f* database, $\log K_1$ and $\log K_2$ were calculated from *wateq4f* database, with the exception of lepidocrocite which was calculated starting from the solubility product of Langmuir (1969).

Table 11.2. $logK_1$ values for different Fe-oxides.

Fe-oxide	**Reduction reaction**	**$logK_1$**
Ferrihydrite	$Fe(OH)_3 + 3H^+ + e^- \leftrightarrow Fe^{2+} + 3H_2O$	17.911
Lepidocrocite	$FeOOH + 3H^+ + e^- \leftrightarrow Fe^{2+} + 2H_2O$	16.29
Goethite	$FeOOH + 3H^+ + e^- \leftrightarrow Fe^{2+} + 2H_2O$	12.02
Hematite	$0.5Fe_2O_3 + 3H^+ + e^- \leftrightarrow Fe^{2+} + 1.5H_2O$	11.016

The figure 11.3 shows the plot of equilibrium lines (black lines; Eqn. 6) for the considered Fe-oxides in a graph with pH and -log[Fe^{2+}] as coordinates. The equilibrium lines are plotted considering a log[SO_4^{2-}] value of -3 according to Postma and Jakobsen (1996). The authors showed the low sensitivity of these equilibrium lines to changing log[SO_4^{2-}]. Figure 11.3 also contains the plot of the field data, classed for each aquifer and shows that a lot of the field data are closely aligned along a line with a slope similar to the equilibrium lines. This could mean that the concentration of Fe^{2+}, in relation to the pH, is probably mainly governed by the Fe-oxide and sulfate reduction and the FeS precipitation. In particular, the data seem to be aligned to an equilibrium line corresponding to an Fe-oxide with a stability between lepidocrocite and goethite. In figure 11.3 the equilibrium line of a hypothetical Fe-oxide that fits the data is plotted (black dotted line). This line considers a solubility product of Fe-oxide for which logK = 0.78 (41.19 considering the alternative representation of the solubility product; Cornell and Schwertmann, 2003) that is in the range of stability of goethite (Appelo and Postma, 2005) and could probably represent a microcrystalline goethite. This result is comparable with the finding of limonite in the geologic core of San Biagio (RE, Northern Italy; Martinelli et al., 2005), that is representative of the same depositional system of the study area. Limonite is a mixture of Fe-oxides in varying composition where goethite is generally abundant (Degens, 1965).

The points that are not clearly aligned to the microcrystalline goethite line are mainly from the F ox aquifer, where presumably sulfate reduction is not occurring due to the presence of more oxidative condition.

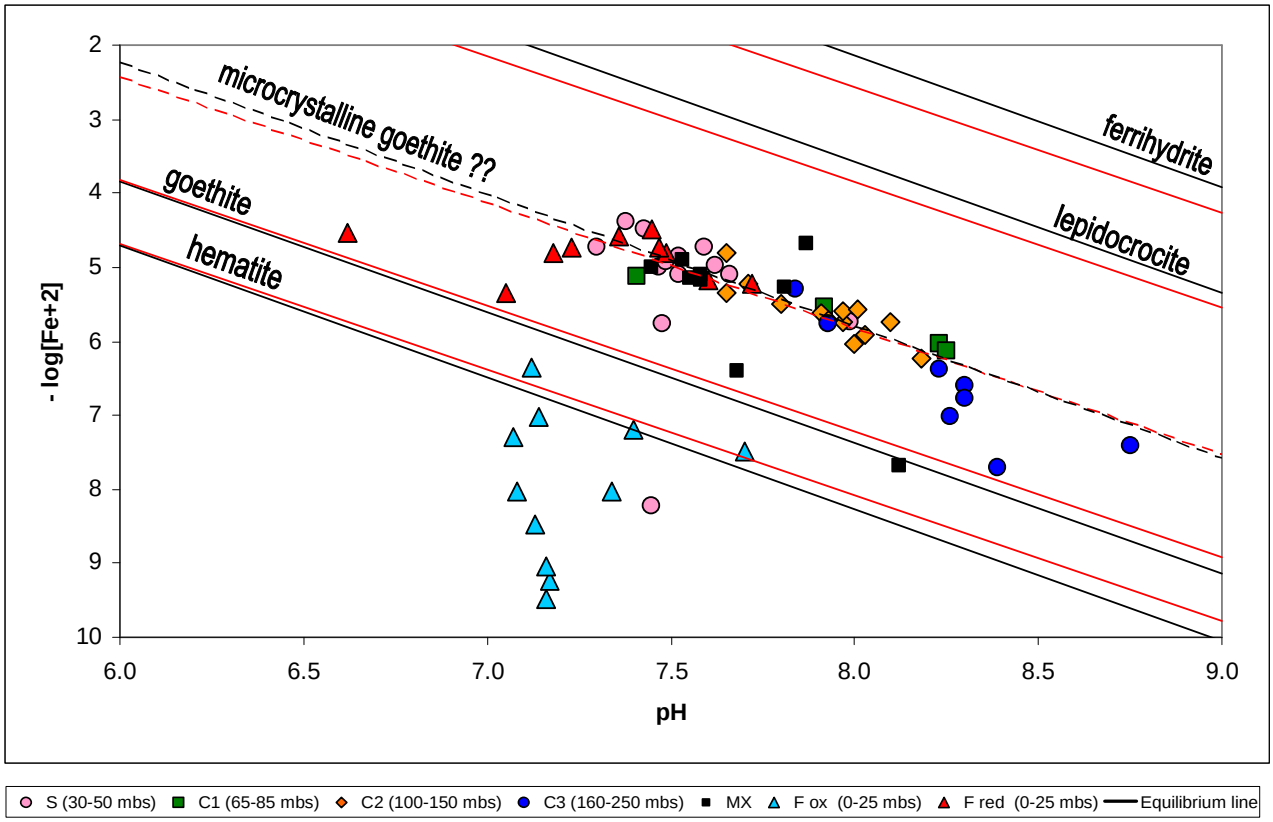

Figure 11.3. Plot of the field data, classed for each aquifer, and of the equilibrium lines for the simultaneous equilibrium of Fe-oxides and sulfate reduction and FeS precipitation (black lines; Eqn. 6) and of Fe-oxides and sulfate reduction and FeS and siderite precipitation (red lines; Eqn. 10) for different Fe-oxides.

In relation to the precipitation-dissolution processes (par. 11.1.2), the studied system results to be near equilibrium with siderite, therefore siderite could probably play a significant role in the reactions involving Fe species. The system of concurrent equilibria described by Eqn. 4 was enlarged to include the siderite equilibrium in the way described below:

$$8Fe(OH)_3 + FeS + 16H^+ \leftrightarrow 9Fe^{2+} + SO_4^{2-} + 20H_2O \quad (4)$$

$$FeCO_3 + H^+ \leftrightarrow Fe^{2+} + HCO_3^- \qquad logK_7 = -0.59 \quad (7)$$

the total reaction is:

$$8Fe(OH)_3 + FeCO_3 + FeS + 17H^+ \leftrightarrow 10Fe^{2+} + SO_4^{2-} + HCO_3^- + 20H_2O \quad (8)$$

with

$$8\log K_1 + \log K_2 + \log K_3 + \log K_7 = 10\log[Fe^{2+}] + \log[SO_4^{2-}] + \log[HCO_3^-] + 17pH \quad (9)$$

from which the equilibrium line equation is:

$$-\log[Fe^{2+}] = 1.7pH + 0.1\log[SO_4^{2-}] + 0.1\log[HCO_3^-] - 0.1(8\log K_1 + \log K_2 + \log K_3 + \log K_7) \quad (10)$$

This equilibrium line, which involves simultaneous equilibrium of Fe-oxide and sulfate reduction FeS and siderite, is plotted in figure 11.3 for the different Fe-oxides (red lines). The plot considers a $\log[SO_4^{2-}] = -3$ and a $\log[HCO_3^-] = -2.264$ (average measured value). The choice of an average value for $\log[HCO_3^-]$ is justified from its relative small variation in the measurements. The figure 11.3 shows that the two types of equilibrium lines (with or without siderite) differ slightly. This implies that it will be difficult to distinguish systems controlled by just equilibrium with FeS from a system controlled by both FeS and siderite. The siderite plot in figure 11.1, where the observations are not well aligned with the siderite equilibrium line, indicates that siderite plays a minor role in this system.

To strengthen the hypothesis that the simultaneous equilibrium of Fe-oxide and sulfate reduction and FeS and siderite precipitation could control the Fe^{2+} concentration, other processes that could control the relation between Fe^{2+} and pH were tested. These processes are siderite precipitation and vivianite precipitation each on their own. The former is described by the reaction 7 and by the following equilibrium line equation:

$$-\log[Fe^{2+}] = pH + \log[HCO_3^-] - \log K_7 \quad (11)$$

and the latter by the following reaction and equation:

$$Fe_3(PO_4)_2{:}8H_2O + 2H^+ \leftrightarrow 3Fe^{2+} + 2HPO_4^{2-} + 8H_2O \qquad \log K_{12} = -11.308 \quad (12)$$

$$-\log[Fe^{2+}] = 0.67pH + 0.67\log[HPO_4^{2-}] - 0.33\log K_{12} \quad (13)$$

These two equilibrium line are plotted in the figure 11.4 (blue lines), considering the average measured value of $\log[HCO_3^-] = -2.264$ and the average historical measured value of $\log[HPO_4^{2-}] = -5.328$. The field data are not aligned on these

lines which have a different slope compared to the previous considered equilibrium lines. Therefore precipitation of siderite and vivianite seems to not control the relation between Fe^{2+} and pH.

In summary, the Fe^{2+} concentration seems to be governed by the simultaneous equilibrium between Fe-oxide and sulfate reduction and FeS and siderite precipitation. Probably, the presence in the system of Fe-oxides with medium stability allows the sulfate reduction to be energetically feasible, so the two reduction processes can take place simultaneously. The processes of precipitation-dissolution of the minerals that are formed with the products of Fe-oxides and sulfate reduction (FeS) and with the product of Fe-oxides reduction and carbonates (siderite) seem also to be in a simultaneous equilibrium.

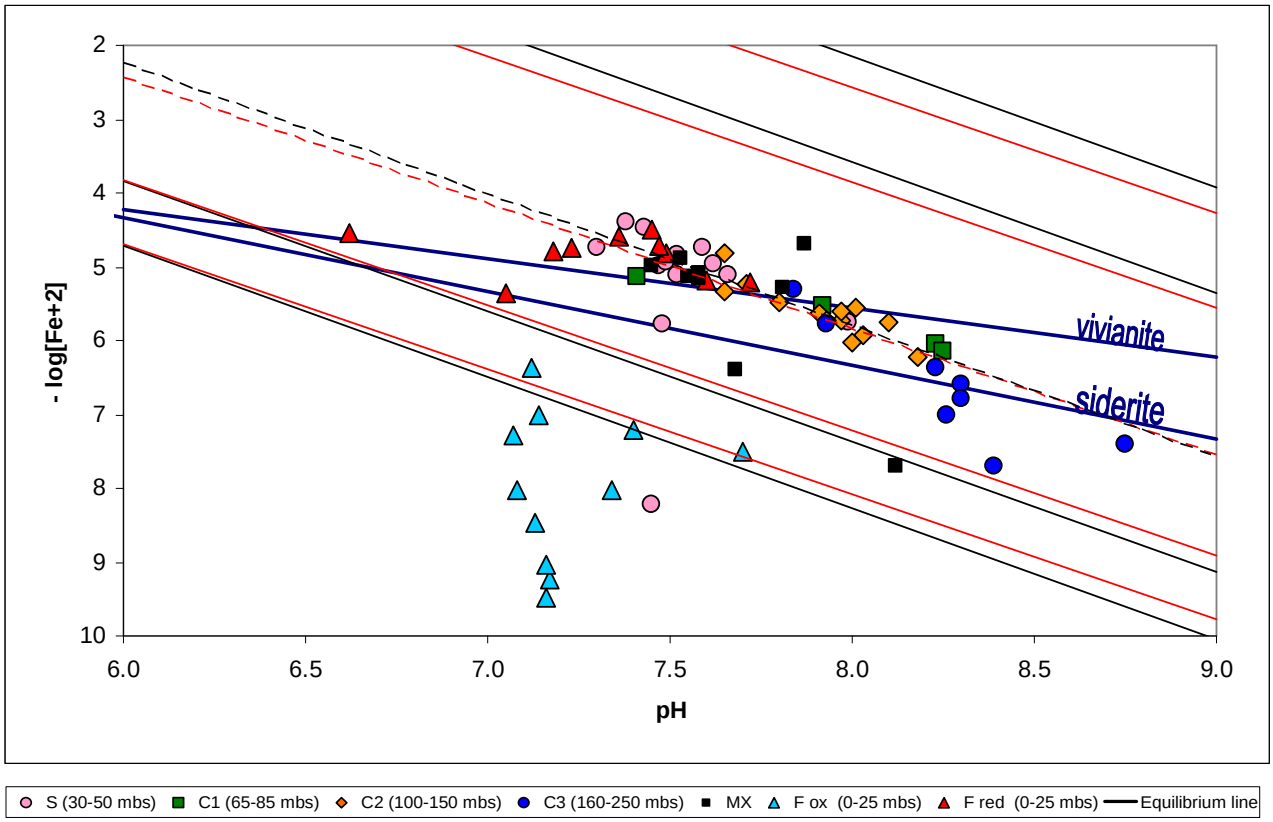

Figure 11.4. Plot of the equilibrium lines of single siderite and vivianite precipitation (blue lines; Eqn. 11 and 13 respectively) on the same graph of figure 11.3.

The process of Mn-oxides reduction was also examined. Two Mn(IV)-oxides were considered: birnessite and pyrolusite. The reaction of Mn(IV)-oxides reduction is:

$$MnO_2 + 4H^+ + 2e^- \leftrightarrow Mn^{2+} + 2H_2O \qquad logK_{14} \qquad (14)$$

from which the equilibrium line equation is:

$$- \log[Mn^{2+}] = 4pH + 2pe - logK_{14} \qquad (15)$$

Figure 11.5 shows the plot of the birnessite and pyrolusite equilibrium lines (black lines) in a -log[Mn^{2+}] *versus* pH graph, considering the value of $logK_{14}$ of *wateq4f* database equal to 43.601 (birnessite) and 41.38 (pyrolusite) and the average measured value of pe = -0.54. These equilibrium lines are far from the measured data.

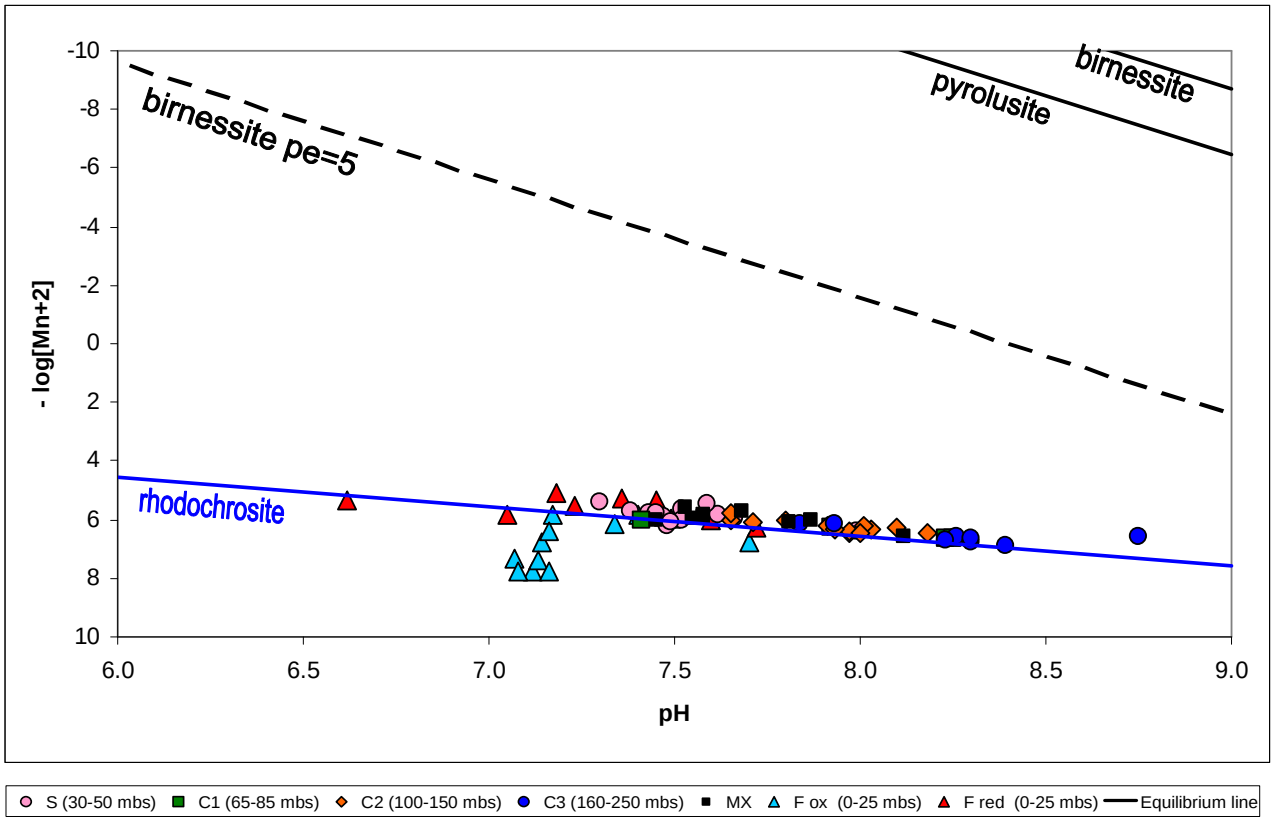

Figure 11.5. Plot of the field data, classed for each aquifer, and of the equilibrium lines for the birnessite and pyrolusite reduction considering a pe = -0.54 (black lines; Eqn. 15), for the birnessite reduction with a pe = 5 (black dotted lines; Eqn. 15) and for the rhodochrosite precipitation (blue line; Eqn. 17).

Considering a higher pe value, for example equal to 5 that is near to the maximum measured value of 4.81, the equilibrium lines are still far from the field

data (black dotted line in figure 11.5 for birnessite). Also the slope of the equilibrium lines is clearly different from the slope of the data alignment. This could means that the Mn-oxide reduction does not occur at equilibrium and so it does probably not control the Mn^{2+} concentration in water.

We also considered the rhodochrosite precipitation-dissolution described by the following reaction and equilibrium line equation:

$$MnCO_3 + H^+ \leftrightarrow Mn^{2+} + HCO_3^- \qquad \log K_{16} = -0.83 \qquad (16)$$

$$-\log[Mn^{2+}] = pH + \log[HCO_3^-] - \log K_{16} \qquad (17)$$

The plot of this equilibrium line (blue line in figure 11.5) shows a good fitting with the measured data. The equilibrium line was plotted considering the average value of $\log[HCO_3^-] = -2.264$. The points far from this line are from the F ox aquifer, similarly to figure 11.1.

In summary, the Mn^{2+} concentration seems to be controlled by the rhodochrosite precipitation-dissolution equilibrium. The reduction of Mn-oxides does not proceed under equilibrium control. An explanation of this could be that at the low pe of the system, equilibrium with the Mn-oxides would require enormously high Mn^{2+} values - values that can never be obtained because the Mn^{2+} concentration is limited by the solubility of rhodochrosite. For the case of Fe-oxides there are some rather stable Fe-oxides so equilibrium for both Fe-oxide reduction and siderite precipitation-dissolution could be present. Trying to explain again the Mn data, a hypothesis could be that nowadays the Mn^{2+} is coming mainly from dissolution of the rhodochrosite, while previously there were Mn-oxides being reduced forming the rhodocrosite. This process could be also be inferred moving from the youngest shallow to the older deep sediments: in the F ox aquifer the younger Mn-oxides are not reduced due to more oxidative condition and the rhodochrosite is subsaturated, in the F red aquifer the younger Mn-oxides are reduced due to more reducing conditions and the rhodochrosite is supersaturated, in the older deep aquifer the Mn-oxides have been reduced and the rhodochrosite is near the equilibrium controlling the Mn^{2+} concentration.

11.1.3. Conceptual model summary

On the basis of the previous analysis and the preliminary conceptual model (chap. 7), the main aspects that characterize the chemistry of the system and therefore form the conceptual model are:

- the whole water chemistry of the studied system is mainly governed by the degradation of organic matter (mainly peat), that is coupled with different terminal electron accepting processes;
- ammonium is probably released in water due to the degradation of organic nitrogen that forms the peat;
- the system is supersaturated with respect to carbonate minerals;
- the concentration of Fe^{2+} is probably governed by the simultaneous equilibrium of Fe-oxide and sulfate reduction and FeS and siderite precipitation;
- the concentration of Mn^{2+} is probably governed by the rhodochrosite precipitation-dissolution equilibrium, while the reduction of Mn-oxides does not proceed under equilibrium control;
- the concentration of dissolved As is mainly governed by different processes that operate as sources and sinks of As in water: the source of As in water is mainly represented by the release from the Fe-oxides and Mn-oxides subjected to reductive dissolution, the sinks of As could be the co-precipitation of As in iron sulfides, the precipitation of arsenic sulfides, the sorption of As on the remaining Fe-oxides, etc.

11.2. Model settings

We implemented a 1D reactive transport model using PHREEQC, that solves the following *ARD* equation (*Advection Reaction Dispersion* equation; Appelo and Postma, 2005):

$$\partial c/\partial t = -v(\partial c/\partial x) - \partial q/\partial t + D_L(\partial^2 c/\partial x^2)$$

where:
c is the solute concentration (mol/L),

v is the pore water flow velocity (m/s),
D_L is the hydrodynamic dispersion coefficient (m^2/s),
q is the concentration in the solid (mol/L of pore water).

PHREEQC solves this equation numerically using the approach for which transport (A and D parts of the equation) and chemistry (R) are solved separately in each time step.

The implemented modelling considers a 1D vertical column composed by 12 cells of 10 m that represent the first 120 m of depth corresponding to the aquifers F, S and C1 (Table 11.3). The hydrodynamic properties analysis (par. 5.2) shows that possible vertical water exchanges, caused by aquitards discontinuities and/or leakage through them, could be directed from aquifer F to C1.

Table 11.3. Geometries and hydrogeological correspondence of the 1D model.

Cell n.	Depth (m b.s.)	Correspondence
1	0-10	aquifer F
2	10-20	
3	20-30	aquitard F/S
4	30-40	aquifer S
5	40-50	
6	50-60	
7	60-70	aquitard S/C1
8	70-80	
9	80-90	aquifer C1
10	90-100	
11	100-110	
12	110-120	aquitard C1/C2

11.2.1. Transport settings

The transport was set in a steady-state condition and involves a constant vertical flow directed from the top to the bottom of the system. The vertical flow velocity, considered as leakage flow velocity through aquitards, was estimated using the following equation, based on Darcy law:

$$v_z = \Delta H/\Delta z \cdot K \cdot (1/n_e)$$

where:
v_z is the vertical flow velocity (m/s),
ΔH is the hydraulic head difference between top and bottom of the aquitard (m),
Δz is the thickness of the aquitard (m),
K is the hydraulic conductivity (m/s),
n_e is the effective porosity.

We calculated the v_z value using measured values of H in near located wells and modelled value of K and n_e. The considered values of H are: (a) 38.5 m a.s.l. for aquifer F, measured in CR84bis well; (b) 34.2 m a.s.l. for aquifer S, measured in CR21; (c) 32.3 m a.s.l. for aquifer C1, measured in CR9. The considered values of K and n_e are respectively 10^{-8} m/s and 0.05 that represent clay layers (chap. 4).

For the F/S aquitard, with a thickness of 5 m, the calculated flow velocity is $1.72 \cdot 10^{-7}$ m/s, while for the S/C1 aquitard, with a thickness of 15 m, it is $2.6 \cdot 10^{-8}$ m/s. The mean of the two values is equal to $9.9\ 10^{-8}$ m/s, corresponding to 3.12 m/y, and it was considered as the flow velocity value in the modelling. Anyways, this calculation does not affect the chemical modelling because, as shown in the following, no kinetics were imposed. Therefore, considering a flow velocity equal to 3.12 m/y and the cell length of 10 m, the resulting time step is 3.21 years - representing the residence time of water in every model cell.

Dispersion was not considered in the model because it seems to play a minor role in the vertical flow, similarly to what Postma et al. (2007) considered in the Red River (VN) model, while a diffusion coefficient of $0.3 \cdot 10^{-9}$ m^2/s (PHREEQC default value) was included. A total period of 160 years was modelled.

11.2.2. Chemistry settings

The chemistry was set on the basis of the conceptual model (par. 11.1.3) as follow:

- equilibrium reactions (*EQUILIBRIUM_PHASES* keyword in PHREEQC):
  - reductive dissolution of Fe-oxide with trace As(V);
  - precipitation of calcite, dolomite, siderite, rhodochrosite and vivianite;
  - precipitation of FeS with trace As(III);

- irreversible reactions (*REACTION* keyword in PHREEQC):
  - oxidation of organic matter ($(CH_2O)(NH_3)(H_3PO_4)$);
  - reductive dissolution of Mn-oxide.

The equilibrium reactions include all the processes of mineral precipitation-dissolution that occur near the equilibrium (par. 11.1.1) and the reduction of Fe-oxide and the precipitation-dissolution of FeS that seem to approach the equilibrium (par. 11.1.2), while the irreversible reactions include the processes that seem to occur at non-equilibrium that are the reduction of Mn-oxides (par. 11.1.2) and the oxidation of organic matter, that is governed by its quantity and reactivity.

Concerning the As, the model only considers an Fe-oxide with trace amount of As as the source of arsenic in water. Mn-oxide was not considered as source of As due to the probable consecutive sorption of the released As on to Fe-oxides, that are reduced after the Mn-oxides (McArthur et al., 2004). Within the different probable sink of dissolved As, the model considers the co-precipitation in iron sulfides (Thomas et al., 2008). On the basis on what Postma et al. (2007) considered in the in the Red River (VN) model, the adsorbed arsenic on the Fe-oxide is As(V), that is reduced, after its release in water, to As(III) due to the prevailing reductive condition. Therefore, the arsenic that co-precipitates in FeS is As(III).

The composition of initial solutions (solution in the cells at time zero) and solution 0 (solution that enters the column every time step) was based on a shallow sample (CR89) and it is listed in table 11.4.

Table 11.4. Composition of solution 0 and initial solutions.

Parameters	**value (mg/l)**	**Parameters**	**value (mg/l)**
pH (ad.)	7.17	Mg	46
pe (ad.)	4	K	5
Temp (℃)	15.2	Na	23
Ammonium	0.7	Fe(II)	0.177
Cl	44	As	0.0015
Sulfate	156	Mn(II)	0.219
Alkalinity	548.9	Phosphate	0.3
Ca	193		

Following the methodology applied by Jakobsen and Cold (2007) the SI of minerals that are near equilibrium was imposed as geochemical boundary

condition. The imposed SI values (Table 11.5) were calculated from the measured groundwater compositions. As shown in figure 11.1, different conditions can be observed for each aquifer unit. Therefore, different SI values were imposed for each aquifer and aquitard. In particular, for calcite and dolomite the supersaturation increases over depth probably due to an increasing precipitation inhibition, which could be related to a higher phosphate and/or DOC concentration, so generally increasing SI values were imposed from aquifer F to C1. Rhodochrosite could probably precipitate at supersaturation in the layers where Mn-oxide reduction could occur releasing extra Mn^{2+} in water, while in the other parts of the system precipitation could occur at equilibrium. Therefore positive SI values were imposed in aquitard F/S and aquifer S, where more reactive organic matter could be present, and a SI = 0 was considered in the remaining cells. Siderite could probably have a similar behaviour to rhodochrosite, but in this case the reduction of Fe-oxide probably continues in the underlying layers, so positive SI values were imposed from aquitard F/S decreasing over the underlying units. Vivianite probably plays a minor role in the system, so a constant SI value was imposed in the whole system.

Table 11.5. Saturation indexes imposed in the model as geochemical boundary condition.

Cell n.	Depth (m)	Correspondance	Calcite	Dolomite	Rhodochrosite	Siderite	Vivianite
1	0-10	Aquifer F	0.54	0.68	0.0	0.0	0.5
2	10-20	Aquifer F	0.54	0.68	0.0	0.0	0.5
3	20-30	Aquitard F/S	0.66	0.84	0.31	0.99	0.5
4	30-40	Aquifer S	0.54	0.6	0.22	0.86	0.5
5	40-50	Aquifer S	0.54	0.6	0.22	0.86	0.5
6	50-60	Aquifer S	0.54	0.6	0.22	0.86	0.5
7	60-70	Aquitard S/C1	1.03	1.48	0.0	0.23	0.5
8	70-80	Aquitard S/C1	1.03	1.48	0.0	0.23	0.5
9	80-90	Aquifer C1	2	1.45	0.0	0.36	0.5
10	90-100	Aquifer C1	2	1.45	0.0	0.36	0.5
11	100-110	Aquifer C1	2	1.45	0.0	0.36	0.5
12	110-120	Aquitard C1/C2	0.9	1.2	0.0	0.35	0.5

11.3. Model calibration and results

The model was calibrated by fitting the model results to the field data. This procedure was used in previous 1D and 2D reactive transport modelling (Jakobsen and Postma, 1999; Jakobsen and Cold, 2007; Postma et al., 2007).

The 68 measured wells in the survey of July 2010 was separated into 3 different groups on the basis of their locations. This operation was done due to create groups with more homogenous hydrogeological characteristics. The created 3 groups are (Figure 11.6): (a) western area, with 26 points, (b) central area, with 27 points and (c) eastern area, with 15 points. The 3 groups could be related to three different N/S hydrogeological transects.

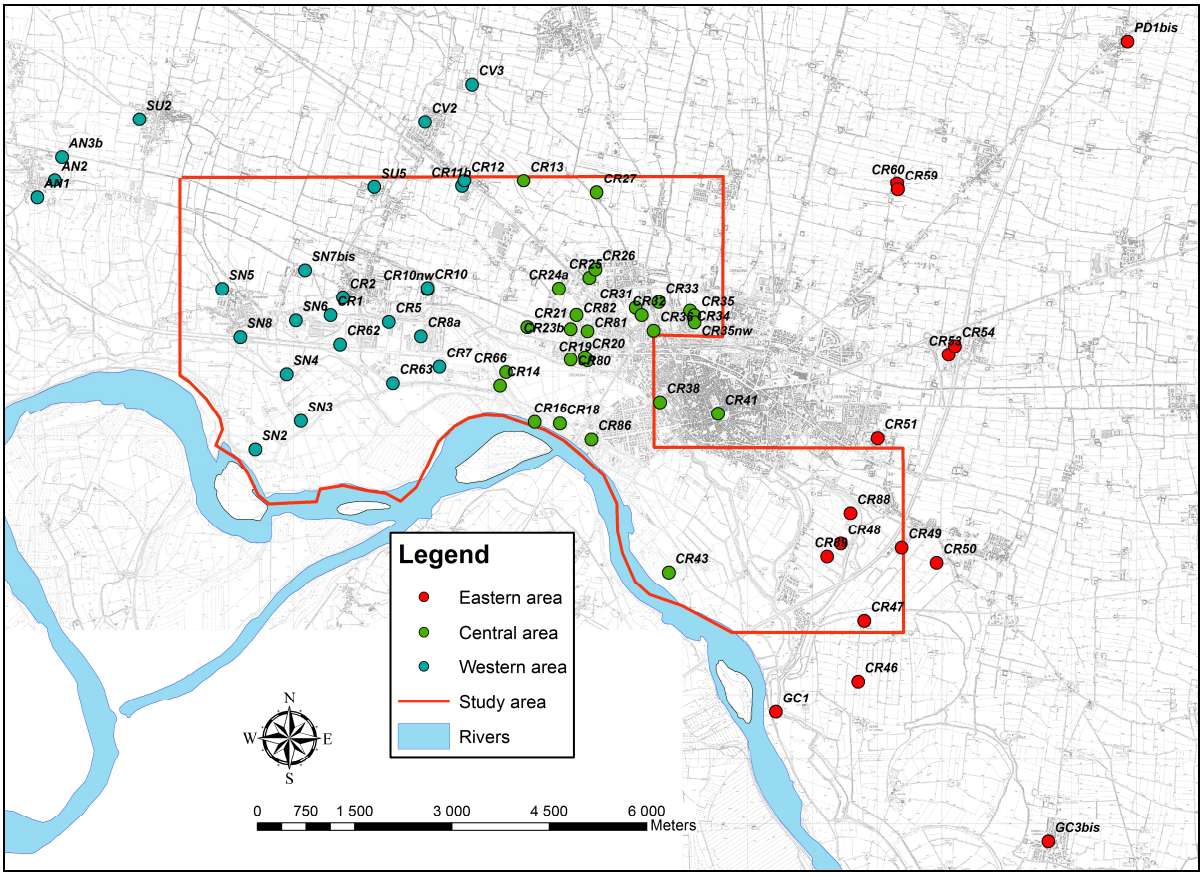

Figure 11.6. The 68 measured wells in the survey of July 2010 separated into 3 groups.

In the present thesis, the eastern area data were only considered. The other two data groups will be treated in future developments. From the 15 points of the eastern area, 2 points were eliminated due to a probable influence of the near landfill (CR88) and to the presence of a multiaquifer screen (CR59). Therefore the measured well dataset that was considered for the reactive transport modelling is composed of 13 points.

The most critical parameters for the model calibration resulted: (a) the rate of organic matter degradation, (b) the SI of the Fe-oxide, that control its stability, and (c) the SI of the FeS. The rate of organic matter degradation was calibrated

considering the fitting between simulated and measured ammonium data, which could be considered "conservative" due to the reductive conditions of the system. The optimal C/N molar ratio of the organic matter results equal to 23.6. This value is close to the soil C/N ratio of 25.73 of Aitkenhead and McDowell (2000) for the boreal/peat mix biome. This could support the hypothesis of the origin of organic matter from peat deposits. The SI of the Fe-oxide was used to control the concentration of Fe^{3+}, that is further reduced in the reaction with the organic matter, and therefore to calibrate the Fe^{2+} concentration indirectly. The SI of the FeS, which has trace As, was used to control its precipitation and therefore to calibrate the dissolved As concentration. The As concentration is also controlled by the content of As in the Fe-oxide and in the FeS. The As content of both Fe-oxide and FeS imposed in the model is given below.

The figure 11.7 represents the measured (as points) and modelled (as lines) concentrations of some major components and redox sensitive species over depth. The modelled rates of the main processes involving iron, manganese and arsenic are listed in tables 11.6, 11.7 and 11.8. Figure 11.7 shows a general good agreement between field data and model results.

Ammonium concentration increases after 20 m corresponding to the aquitard F/S layer, where peat deposits are located and thus degradation of organic matter probably starts to take place. The decreasing sulfate concentration and the increasing of Mn^{2+} and Fe^{2+} after 20 m also indicate that the organic matter degradation probably becomes relevant from this depth. This condition was simulated in the model imposing a higher rate of organic matter degradation from 20 to 50 m b.s., corresponding to cells 3, 4 and 5 (Table 11.6). The average rate for these 3 cells is equal to $5.2 \cdot 10^{-3}$ mM/y, that is comparable with Pleistocene sediments (Jakobsen and Postma, 1994). This is compatible with the geology of the study area, indeed the sediments of the studied system were deposited in the Pleistocene age.

The profile of the Fe^{2+} concentration is characterized by an increase after 20 m b.s. and a decrease after 40 m b.s.. The calibration indicates that the model results match the field data considering a stability of Fe-oxide of around logK = -0.11, that is in the stability range of goethite and it is very close to the Fe-oxide that is considered in figure 11.3 (microcrystalline goethite, logK = 0.78) and for which a lot of field data seem to be at equilibrium. This result could confirm the validity of the model results. The modelled evolution of the Fe^{2+} concentration over depth could be seen analysing the rates of the processes involving Fe (Table 11.6).

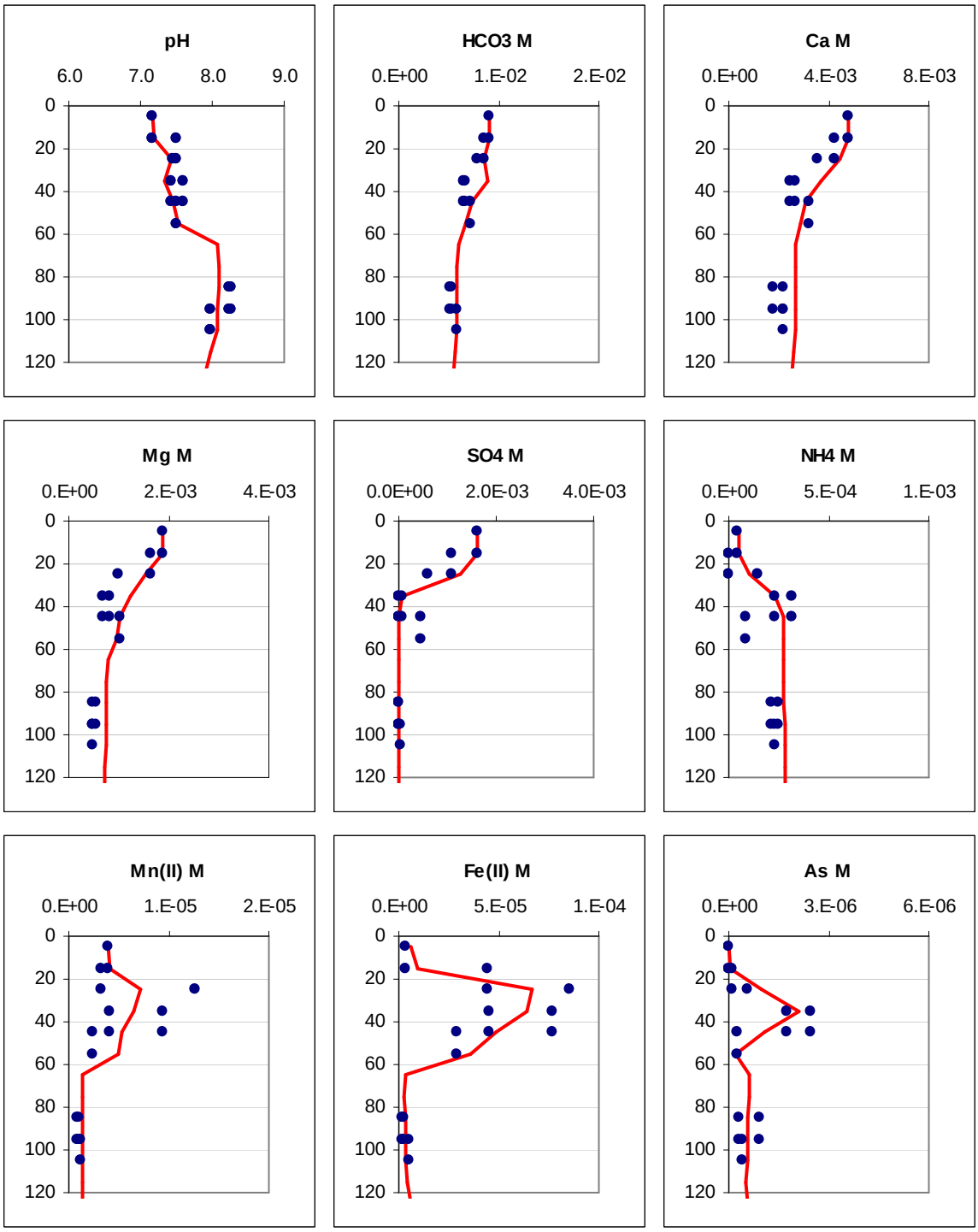

Figure. 11.7. Measured (as points) and modelled (as lines) concentrations of some major components and redox sensitive species over depth.

The net Fe^{2+} rate was calculated considering the reductive dissolution of Fe-oxide as source and the precipitation of siderite and FeS as sinks. The higher net dissolution of Fe^{2+} is in cell 3, corresponding to aquitard F/S layer, where organic

matter degradation becomes relevant. In the underlying two cells the rate of net dissolution of Fe^{2+} decreases until cell 6 is reached. Here the rate of organic matter decreases and the net rate indicates that precipitation of Fe^{2+} (in siderite and FeS) becomes prevalent. In cells 7 and 8 the precipitation remains prevalent, while from cell 9 to 8 the rates are generally lower and indicate a smaller dissolution of Fe^{2+}.

Table 11.6. Rates of organic matter (O.M.) degradation and main processes involving Fe; negative values indicate consumption, positive formation; in the net rate negative values indicate dissolution in water, positive precipitation in solid phase.

Cell n.	Depth (m)	Correspondance	O.M. (mM/y)	Fe-oxide (mM/y)	Siderite (mM/y)	FeS (mM/y)	Net Fe (mM/y)
1	0-10	Aquifer F	-2.94E-05	-9.29E-04	0.00E+00	0.00E+00	-9.29E-04
2	10-20	Aquifer F	-2.94E-05	-2.39E-02	2.29E-02	0.00E+00	-1.03E-03
3	20-30	Aquitard F/S	-3.82E-03	-6.68E-01	5.34E-01	9.99E-02	-3.47E-02
4	30-40	Aquifer S	-8.82E-03	-8.03E-01	4.27E-01	3.54E-01	-2.26E-02
5	40-50	Aquifer S	-2.94E-03	-6.11E-01	5.70E-01	3.18E-02	-9.34E-03
6	50-60	Aquifer S	-2.94E-05	-1.55E-01	1.39E-01	1.73E-02	1.51E-03
7	60-70	Aquitard S/C1	-2.94E-05	-2.87E-01	2.97E-01	0.00E+00	1.03E-02
8	70-80	Aquitard S/C1	-2.94E-05	-4.47E-02	4.39E-02	9.25E-04	6.25E-05
9	80-90	Aquifer C1	-2.94E-05	-6.61E-04	0.00E+00	5.60E-04	-1.02E-04
10	90-100	Aquifer C1	-2.94E-05	-3.70E-04	0.00E+00	2.99E-04	-7.06E-05
11	100-110	Aquifer C1	-2.94E-05	-2.54E-04	0.00E+00	1.84E-04	-7.09E-05
12	110-120	Aquitard C1/C2	-2.94E-05	-3.29E-04	0.00E+00	9.53E-05	-2.34E-04

Concerning manganese, the profile of Mn^{2+} concentration shows a peak between 20 and 50 m b.s. and a general decrease at lower depth. Considering the conceptual model, Mn-oxide reduction seems to occur at non-equilibrium so it was modelled as irreversible reaction, that is governed by the rate of Mn-oxide dissolution. The model matches the field Mn^{2+} concentration imposing a higher rate of Mn-oxide reductive dissolution in cells 3, 4 and 5 (Table 11.7), where the rate of organic matter degradation is also higher. This could mean that the organic matter degradation occurs using also Mn-oxide as electron acceptor, producing a peak in the Mn^{2+} concentration. Below 50 m b.s. the Mn^{2+} concentration decrease due to the prevailing rhodochrosite precipitation. The net Mn rate, that is calculated as the difference between Mn-oxide reductive dissolution and rhodochrosite precipitation (Table 11.7), shows the general evolution of Mn^{2+} concentration over depth: the prevailing dissolution in cells 3, 4 an 5 is followed by a lower dissolution in cell 6 and by a prevailing precipitation in cell 7; in the underlying cells the rate is smaller and indicate a general low dissolution of Mn^{2+}.

Table 11.7. Rates of organic matter degradation and processes involving Mn; negative values indicate consumption, positive formation; in the net rate negative values indicate dissolution in water, positive precipitation in solid phase

Cell n.	Depth (m)	Correspondance	O.M. (mM/y)	Mn-oxide (mM/y)	Rhodochrosite (mM/y)	Net Mn (mM/y)
1	0-10	Aquifer F	-2.94E-05	-1.32E-04	0.00E+00	-1.32E-04
2	10-20	Aquifer F	-2.94E-05	-1.32E-04	0.00E+00	-1.32E-04
3	20-30	Aquitard F/S	-3.82E-03	-1.72E-02	3.06E-03	-1.41E-02
4	30-40	Aquifer S	-8.82E-03	-3.97E-02	2.10E-03	-3.76E-02
5	40-50	Aquifer S	-2.94E-03	-1.32E-02	9.60E-04	-1.23E-02
6	50-60	Aquifer S	-2.94E-05	-1.32E-04	1.22E-04	-1.04E-05
7	60-70	Aquitard S/C1	-2.94E-05	-1.32E-04	1.14E-03	1.01E-03
8	70-80	Aquitard S/C1	-2.94E-05	-1.32E-04	1.75E-05	-1.15E-04
9	80-90	Aquifer C1	-2.94E-05	-1.32E-04	0.00E+00	-1.32E-04
10	90-100	Aquifer C1	-2.94E-05	-1.32E-04	8.61E-08	-1.32E-04
11	100-110	Aquifer C1	-2.94E-05	-1.32E-04	2.14E-06	-1.30E-04
12	110-120	Aquitard C1/C2	-2.94E-05	-1.32E-04	0.00E+00	-1.32E-04

The As profile is characterized by an increase in concentration until 30-40 m b.s. and a consecutive general decrease at lower depth. A good fitting between modelled and measured data was reached considering a As(V)/Fe molar ratio in the Fe-oxide, which has trace As, of 0.00045 and a variable As(III)/Fe molar ratio in the FeS, which has trace As, over depth with a maximal value of 0.02. The variable As(III)/Fe ratio in the FeS was obtained considering two different FeS phases: one is pure FeS and the other is FeS with trace As in a As(III)/Fe ratio of 0.02. These two FeS phases were defined to allow FeS precipitation even if the As concentration is low. The optimal As(III)/Fe molar ratio in the FeS (the sum of the two phases), that results in the model, is listed over depth in table 11.8 (last column). The As(III)/Fe ratio changing over depth probably reflects the following mechanism: at the beginning only pure FeS precipitates and then, with increasing concentration of As, As starts to co-precipitate with a kinetic control, then, when equilibrium is reached, As co-precipitates with constant As(III)/Fe ratio. The table 11.8 also shows the resulting rates of As(III) precipitation, together with the rates of As(V) dissolution. The highest rates of As precipitation are between 40 and 60 m b.s., at this depth the occurring Fe-oxide and sulfate reduction allows FeS to precipitate together with trace As. The general evolution of the modelled As concentration is described by the net As rate: the As is mainly dissolved at cells 3 and 4 due to the reductive dissolution of Fe-oxide and it mainly precipitates in cells

5 and 6 due to the co-precipitation in FeS; at cells 7 and 8 As dissolution is prevalent, while from cell 9 to 12 precipitation occurs with low rates.

Table 11.8. Rates of organic matter degradation, As(V) dissolution from Fe-oxide and As(III) co-precipitation in FeS; concerning the As, positive values indicate dissolution in water, negative precipitation in solid phase; the last column lists the As(III)/Fe molar ratio in FeS.

Cell n.	Depth (m)	Correspondance	O.M. (mM/y)	As(V) (mM/y)	As(III) (mM/y)	Net As (mM/y)	As(III)/Fe in FeS (M)
1	0-10	Aquifer F	-2.94E-05	4.18E-07	0.00E+00	4.18E-07	no FeS pr.
2	10-20	Aquifer F	-2.94E-05	1.08E-05	0.00E+00	1.08E-05	no FeS pr.
3	20-30	Aquitard F/S	-3.82E-03	3.01E-04	-2.07E-05	2.80E-04	0.0002
4	30-40	Aquifer S	-8.82E-03	3.61E-04	0.00E+00	3.61E-04	0.0000
5	40-50	Aquifer S	-2.94E-03	2.75E-04	-6.00E-04	-3.25E-04	0.0189
6	50-60	Aquifer S	-2.94E-05	6.96E-05	-3.45E-04	-2.76E-04	0.0200
7	60-70	Aquitard S/C1	-2.94E-05	1.29E-04	0.00E+00	1.29E-04	no FeS pr.
8	70-80	Aquitard S/C1	-2.94E-05	2.01E-05	-1.85E-05	1.62E-06	0.0200
9	80-90	Aquifer C1	-2.94E-05	2.98E-07	-1.12E-05	-1.09E-05	0.0200
10	90-100	Aquifer C1	-2.94E-05	1.66E-07	-5.98E-06	-5.82E-06	0.0200
11	100-110	Aquifer C1	-2.94E-05	1.15E-07	-3.67E-06	-3.56E-06	0.0200
12	110-120	Aquitard C1/C2	-2.94E-05	1.48E-07	-1.91E-06	-1.76E-06	0.0200

The role of the co-precipitation of As in FeS in the dynamic of dissolved As concentration over depth is better explained in figure 11.8. Considering in the model the precipitation of pure FeS, the resulting As concentration increases over depth and the fitting with the field data is not reached (Figure 11.8 a). While imposing in the model the precipitation of FeS with trace As, the modelled profile matches the field data with nice agreement (Figure 11.8 b). The figure 11.8 shows another relevant aspect: the model indicates that the dissolved arsenic is only As(III), while dissolved As(V) has very low concentrations.

11.4. Conclusions

The implemented 1D reactive transport modelling represents an approximation but it appears to give useful information on the chemical mechanisms occurring in the system. The main approximation concerns the hydrodynamic component in that a 1D model is made to simulate a 3D system. Future developments will consider the implementation of a 2D model to better simulate the studied system including variation of the hydrodynamic properties. The

chemical modelling does not pretend to be exhaustive but is aimed at reproducing the main processes occurring in the system.

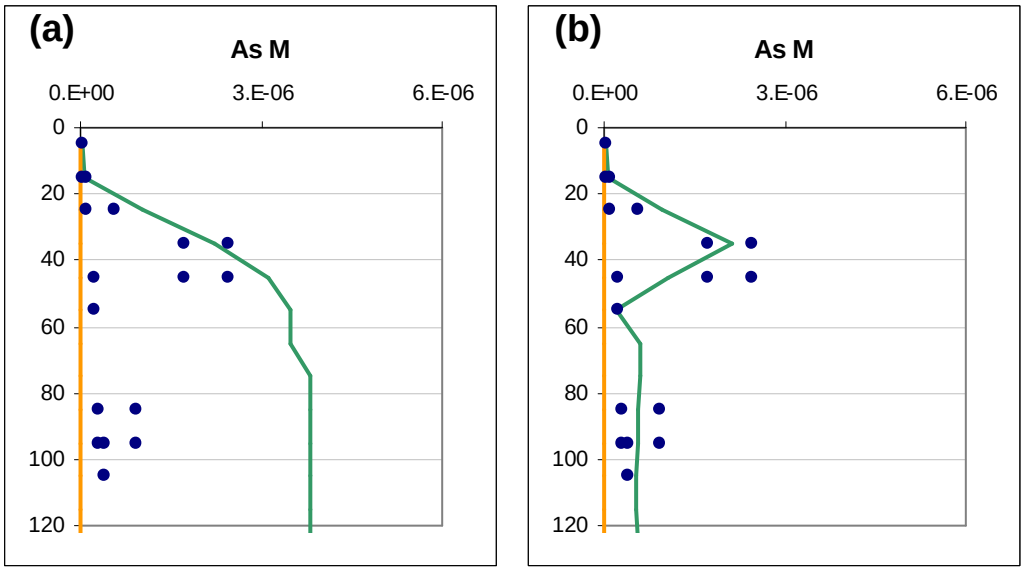

Figure 11.8. Total As measured (as points), As(III) modelled (as green line) and As(V) modelled (as orange line) concentrations over depth, considering the precipitation of pure FeS (a) and the precipitation of FeS with trace As (b).

The main aspects that could be derived from the modelling results are:

- the Fe^{2+} concentration is mainly governed by the reduction of Fe-oxides, in association with the oxidation of organic matter, and the precipitation-dissolution of siderite and iron sulfides;
- the Mn^{2+} concentration is mainly governed by the precipitation-dissolution of rhodochrosite; peaks of Mn^{2+} concentration could be explained by the occurring of Mn-oxides reduction, in association with the oxidation of organic matter;
- the dissolved As could be mainly As(III); even if different authors reported that As(III) is more toxic than As(V) (i.e. Voigt et al., 1996; Jain and Ali, 2000) up to 60 times (Ferguson and Gavis, 1972), recent studies pointed out that there is no difference in the toxicity of As(III) and As(V) once ingested, because the As(V) is reduced and methylized to the really toxic compound (MMA) in the digestive system anyway (Steinmaus et al., 2010);
- the main source of dissolved As is probably the release from Mn and Fe oxides, that are subjected to reductive dissolution; different processes could

represent a sink of dissolved As (the co-precipitation of As in iron sulfides, the precipitation of arsenic sulfides, the sorption of As on the remaining Fe-oxides and Mn-oxides, etc.), within these processes, one of the most relevant could be the co-precipitation in iron sulfides;

- the original source of dissolved Fe^{2+} and Mn^{2+} was probably the reductive dissolution of Fe and Mn oxides, the presence of reductive condition allows the formation of siderite, iron sulfide and rhodochrosite as authigenic mineral (Berner, 1981), these minerals also excerpt a control on the concentration of Fe^{2+} and Mn^{2+}.

In conclusion, the good agreements between modelled and measured concentrations could support the validity of the conceptual model. Therefore the elaborated conceptual model could be considered as a reasonable approximation of the real system.

References

Aitkenhead J. A. & McDowell W. H. (2000) – *Soil C:N ratio as a predictor of annual riverine DOC flux at local and global scales*. Global Biogeochemical Cycles 14(1), 127-138.

Appelo C. A. J. & Postma D. (2005) – *Geochemistry, groundwater and pollution (2nd edition)*. Balkema Publishers, Leiden, 649 pp.

Ball J. W. and Nordstrom D. K. (1991) – *WATEQ4F - User's manual with revised thermodynamic data base and test cases for calculating speciation of major, trace and redox elements in natural waters*. U.S. Geological Survey Open-File Report 90-129, 185 pp.

Berner R. A. (1981) – *A New Geochemical Classification of Sedimentary Environments*. Journal of Sedimentary Petrology 51(2), 359-365.

Bleam W. F. (2011) – *Soil and Environmental Chemistry*. Academic press, Burlington, 478 pp.

Cornell R. M. & Schwertmann U. (2003) – *The Iron Oxides (2nd edition).* Wiley-VCH, Weinheim, 664 pp.

Davis K. J., Dove P. M. & De Yoreo J. J. (2000) – *The role of Mg^{2+} as an inpurity in calcite growth*. Science 290, 1134-1137.

Degens E.T. (1965) – *Geochemistry of sediments: a brief survey*. Prentice-Hall, Englewood Cliffs, 342 pp.

Ferguson J. F. & Gavis J. (1972) – *A review of the arsenic cycle in natural water*. Water Research 6, 1259-1274.

Jain C. K. & Ali I. (2000) – *Arsenic: Occurrence, toxicity and speciation techniques*. Water Research 34(17), 4304-4312.

Jakobsen R. & Postma D. (1994) – *In situ rates of sulfate reduction in an aquifer (Rømø, Denmark) and implications for the reactivity of organic matter*. Geology 22, 1103-1106.

Jakobsen R. & Postma D. (1999) – *Redox zoning, rates of sulfate reduction and interactions with Fe-reduction and methanogenesis in a shallow sandy aquifer, Rømø, Denmark*. Geochimica et Cosmochimica Acta 63(1), 137-151.

Jakobsen R. & Cold L. (2007) – *Geochemistry at the sulfate reduction-methanogenesis transition zone in an anoxic aquifer - A partial equilibrium interpretation using 2D reactive transport modeling.* Geochimica et Cosmochimica Acta 71, 1949-1966.

Langmuir D. (1969) – *The gibbs free energies of substances in the system Fe-O_2-H_2O-CO_2 at 25 ℃.* U.S. Geological Survey Professional Paper 650-B, B180-B184.

Lindberg R. D. & Runnells D. D. (1984) – *Ground water redox reactions: an analysis of equilibrium state applied to Eh measurements and geochemical modeling*. Science 255, 925-927.

Martinelli M., Marcaccio M., Farina M., Canepa P., Cantagalli L. & Billi L. (2005) – *L'arsenico nei sedimenti profondi della pianura emiliano-romagnola: prime evidenze (Arsenic in the deep sediments of Emilia-Romagna plain: first evidence)*. In: Arpa Emilia-Romagna (Eds), Presenza e diffusione dell'arsenico nel sottosuolo e nelle risorse idriche italiane (Occurrence and distribution of arsenic in sediments and water resources of Italy), 215-224. I quaderni di Arpa.

McArthur J. M., Banerjee D. M., Hudson-Edwards K. A., Mishra R., Purohit R., Ravenscroft P., Cronin A., Howarth R. J., Chatterjee A., Talukder T., Lowry D., Houghton S. & Chadha

D. K. (2004) – *Natural organic matter in sedimentary basins and its relation to arsenic in anoxic ground water: the example of West Bengal and its worldwide implications.* Applied Geochemistry 19, 1255-1293.

Ori G. G. (1992) – *Continental depositional systems of the Quaternary of the Po Plain (northern Italy)*. Sedimentary Geology 83, 1-14.

Parkhurst D. L. & Appelo C. A. J. (1999) – *User's guide to PHREEQC: A computer program for speciation, reaction-path, 1D-transport, and inverse geochemical calculations.* U.S. Geological Survey Water-Resources Investigations Report 99-4259, 312 pp.

Postma D. & Jakobsen R. (1996) – *Redox zonation: Equilibrium constraints on the Fe(III)/SO_4-reducing interface*. Geochimica et Cosmochimica Acta 60(17), 3169-3175.

Postma D., Larsen F., Hue N. T. M., Duc M. T., Viet P. H., Nhan P. Q. & Jessen S. (2007) – *Arsenic in groundwater of the Red River floodplain, Vietnam: Controlling geochemical processes and reactive transport modeling*. Geochimica et Cosmochimica Acta 71, 5054-5071.

Steinmaus C., Yuan Y., Kalman D., Rey O. A., Skibola C. F., Dauphine D., Basu A., Porter K. E., Hubbard A., Bates M. N., Smith M. T. & Smith A. H. (2010) – *Individual differences in arsenic metabolism and lung cancer in a case-control study in Cordoba, Argentina*. Toxicology and Applied Pharmacology 247, 138-145.

Thomas M. A., Diehl S. F., Pletsch B. A., Schumann T. L., Pavey R. R. & Swinford E. M. (2008) – *Relation Between Solid-Phase and Dissolved Arsenic in the Griund-Water System Underlying Northern Oreble Country, Ohio*. U.S. Geological Survey Scientific Investigations Report 5205, 56 pp.

U.S. EPA (2013) – *Field measurement of oxidation-reduction potential (ORP)*. SESD Operating Procedure SESDPROC-113-R1, 21 pp.

Voigt D. E., Brantley S.L. & Hennet Remy J. C. (1996) – *Chemical fixation of arsenic in contaminated soils*. Applied Geochemistry 11, 633-643.

Walter L. M. & Hanor J. S. (1979) – *Effect of orthophosphate on the dissolution kinetics of biogenic magnesian calcites.* Geochimica et Cosmochimica Acta 43, 1377-1385.

12. Derivation of preliminary natural background levels for As, Fe, Mn and NH_4

The derivation of preliminary natural background levels (NBL) for As, Fe, Mn and NH_4 was done according to the BRIDGE methodology (Muller et al., 2006), which is also implemented by ISPRA (Bartolucci et al., 2009). The pre-selection approach (Wendland et al., 2006) was applied. This approach generally concerns: (1) collection of hydrochemical data; (2) separation of the data referring to the natural background from the data referring to anthropogenic influences, according to specific criteria; (3) derivation of the NBL from the 90° percentile of the data referring to the natural background.

The NBL were separately derived from two different datasets, July 2010 and historical data, due to their different quality: the July 2010 dataset is characterized by a homogeneous methodology of sampling and analysis but it is referred to a short time period, while the historical dataset is referred to a longer time period (1999-2010) but it is characterized by different methods of sampling and analysis.

In the derivation of the NBL from the July 2010 dataset the following criteria are applied:

a) exclusion of samples influenced by human activities - the criteria are NaCl content of more than 1000 mg/L; $[NO_3^-] > 50$ mg/L (modified from BRIGDE as Preziosi et al., 2010); $[SO_4^{2-}] > 500$ mg/L (as D. Lgs. 152/06);
b) exclusion of samples with incorrect ion balance (exceeding 10%);
c) subdivision of the dataset for each defined aquifer unit, the samples from multi-aquifer wells are excluded;
d) subdivision in reduced and oxidized groundwater within the dataset of each aquifer - the criterion is $[Fe^{2+}] < 0.2$ mg/L, $[Mn^{2+}] < 0.05$ mg/L for oxidized groundwater and $[Fe^{2+}] \geq 0.2$ mg/L & $[Mn^{2+}] \geq 0.05$ mg/L for reduced groundwater;
e) derivation of the NBL on the remaining dataset calculating the 97.7° percentile (BRIGDE allows the use of 97.7° instead of 90° percentile in the case of well defined aquifers are available and no human influence exists).

The derived NBL values from the July 2010 dataset are reported in Table 12.1. It should be noted that for the aquifer F a separation between reduced (F red) and

oxidized (F ox) groundwater results. Figure 12.1 shows the extent of F ox and F red zones with the respective sampled wells. The limits of the zones were defined following hydrogeological criteria. In the southern part of the study area the F red zone corresponds to the Po river valley, characterized by peat and superficial clay deposits that allow semi-confined and reductive condition. In the central-northern part of the study area the F red zone correspond to the superficial clay layer that allows semi-confined and reductive condition too. The remaining zone are considered as F ox. This is confirmed by the sampled wells in the area behind the terrace scarp but it must be verified with new sampling in the zone with no measurements.

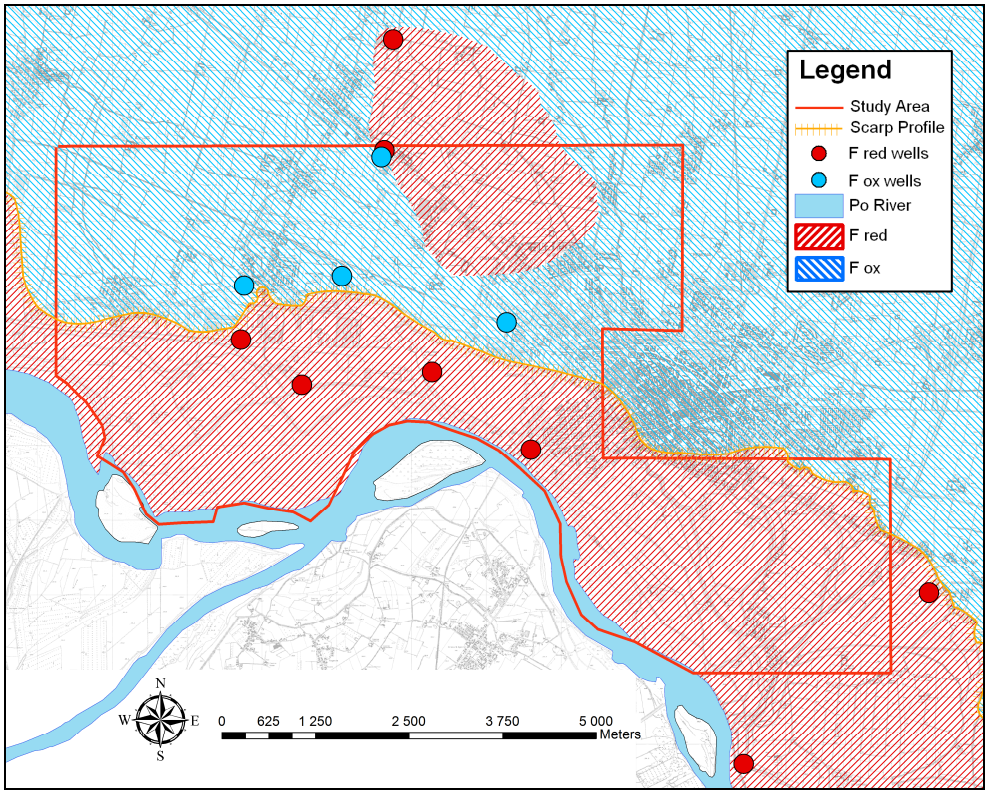

Figure 12.1. Extent of F red and F ox zones and location of the sampled wells used in the NBL derivation from July 2010 dataset.

The derivation of NBL from the historical dataset follows a simplified methodology due to missing information. The applied criteria are:

a) exclusion of wells where possible anthropogenic influences could be occurred - for As, Fe and Mn, the data referred to the oil refinery, the

municipal solid waste landfill and the group of sites with low hydrocarbons pollution (chap. 9) are excluded, concerning aquifer F; the data referred to the oil refinery are only excluded, concerning aquifer S; - for NH_4, the data referred to the municipal solid waste landfill are excluded, concerning aquifer F;

b) calculation of a single value representing the whole time series for each sampled well (90° percentile) in order to guarantee that all wells contribute equally to the NBL derivation;
c) subdivision of the aquifer F data in F red and F ox on the basis of the zonation showed in figure 12.1;
d) derivation of the NBL on the remaining dataset calculating the 90° percentile.

The derived NBL values from the historical dataset are reported in Table 12.2.

Table 12.1. Derived NBL values from the July 2010 dataset.

	REF	**F Ox**	**F Red**	**S**	**C1**	**C2**	**C3**
N. of samples		*4*	*8*	*11*	*3*	*10*	*8*
Ammonium (mg/L)	0.5	0.05	3.36	6.47	4.68	4.20	4.57
Iron (µg/L)	200	608	4665	3890	1015	698	718
Arsenic (µg/L)	10	5	42	171	149	54	37
Manganese (µg/L)	50	107	1197	537	136	140	125

Table 12.2. Derived NBL values from the historical dataset.

	REF	**F Ox**	**F Red**	**S**	**C1**	**C2**	**C3**
N. of sampled wells		*7*	*56*	*18*	*5*	*9*	*27*
Ammonium (mg/L)	0.5	0.10	2.30	2.45	2.01	1.72	2.01
N. of sampled wells		*15*	*23*	*19*	*19*	*10*	*27*
Iron (µg/L)	200	105	3924	3083	1050	548	149
N. of sampled wells		*12*	*27*	*19*	*13*	*7*	*22*
Arsenic (µg/L)	10	8	35	21	106	34	28
N. of sampled wells		*15*	*24*	*19*	*19*	*10*	*28*
Manganese (µg/L)	50	130	1350	425	376	147	71

The two types of derived NBL values (from July 2010 and historical data) result comparable for Mn and Fe. Also for As, the two type of values are comparable, with the exception of aquifer S. This difference reflects the discrepancy observed in the comparison between historical and July 2010 data (par. 9.5). Considering the ammonium, the two NBL values considerably differ, with the exception of aquifer F. The NBL values from the July 2010 dataset result

always higher. These differences could probably be related to specific conditions occurred in the survey of July 2010, as discussed in paragraph 9.5.

Considering the reference values (REF in tables 12.1 and table 12.2) for As, NH_4 (D. Lgs. 30/09) and Fe, Mn (D. Lgs. 152/06), the derived NBL are higher with respect to REF up to more than one order of magnitude, with the exception of F ox zone. Comparing these results with the NBL derived in Emilia-Romagna region (Marcaccio et al., 2012) for As and NH_4 in the aquifer with an average depth of 75 m, the NBL are similar for NH_4 (4.6 mg/L in Emilia-Romagna) but they differ for As (33 µg/L in Emilia-Romagna).

In conclusion, the NBL were derived on the basis on two different datasets, related to the July 2010 field survey and to historical data. In both cases this derivation could be considered as preliminary calculation due to the short time period of the measurements for the former and to the poor quality of the data (different methodologies of sampling and analysis) for the latter. The derivation of definitive NBL requires specific long-term monitoring. A monitoring along a time period of one year has been proposed to the Province of Cremona for the derivation of definitive NBL.

References

Bartolucci E., Bussettini M., Calace N., D'Aprile L., Fratini M., Guerra M., Marangio L., Pirani G. & Vecchio A. (2009) – *Protocollo per la Definizione dei Valori di Fondo per le Sostanze Inorganiche nelle Acque Sotterranee (Procedure for the definition of background levels for inorganic compounds in groundwater)*. Protocollo ISPRA, 17 pp. http://www.isprambiente.gov.it/site/it-IT/

Marcaccio M., Molinari A., Guadagnini L. & Guadagnini A. (2012) - *Valori di fondo naturale di metalli e sostanze inorganiche nelle acque sotterranee dell'Emilia-Romagna (Natural background levels for metals and inorganic compounds in groundwater (Emilia-Romagna region))*. Atti del convegno "Le acque sotterranee fra tutela ed utilizzo sostenibile della risorsa" GEOFLUID 2012, 3 ottobre 2012, Piacenza.

Muller D., Blum A., Hart A., Hookey J., Kunkel R., Scheidleder A., Tomlin C. & Wendland F. (2006) – *Final proposal for a methodology to set up groundwater threshold values in Europe.* In: Report to EU project BRIDGE, Deliverable D18, 63 pp. http://www.wfd-bridge.net

Preziosi E., Giuliano G. & Vivona R. (2010) – *Natural background levels and threshold values derivartion for naturally As, V and F rich groundwater bodies: a methodological case study in Central Italy*. Environmental Earth Sciences 61, 885-897.

Wendland F., Blum A. & Kunkel R. (2006) – *Approach to asses Natural Background Levels (NBLs)*. Annex I to the Report to EU project BRIDGE, Deliverable D18, 63 pp. http://www.wfd-bridge.net

13. Conclusions

The present work involved the analysis of the hydrogeology and the hydrogeochemistry of the As, Fe, Mn rich groundwater of the alluvial multi-layer aquifer in the lower Po Plain (northern Italy), referring specifically to the territory of Cremona. The main aim was to understand the origins and mechanisms of the high groundwater As, Fe and Mn concentrations. The present work was developed in three main steps: (1) *collection of data* - historical data were collected and new field data were measured in two surveys, executed in July 2010 and 2012; (2) *elaboration of data* - a 3D modelling of aquifer hydrogeological properties, the analysis of the hydrodynamic properties, the characterization of groundwater quality and a 1D reactive transport modelling were implemented; (3) *summary of elaborations* - a hydrogeochemical conceptual model for the high concentrations of As, Fe, Mn and NH_4 in groundwater, considering also possible anthropogenic influences, was developed and operational tools for groundwater resources management, as derivation of natural background levels of As, Fe, Mn and NH_4, were defined.

The present study leads to the following outcomes, which form the overall conceptual model of the studied aquifer system.

The 3D aquifer modelling underlines that:

- the territory of Cremona has a multi-layer aquifer system which is characterized by the alternation of silty-clayey layers with lower conductivity (10^{-7}-10^{-8} m/s) and sandy layers with higher conductivity (10^{-3}-10^{-5} m/s);
- five aquifer units, which are separated by low-permeable or semi-permeable aquitards, can be identified: aquifer F (0-25 m b.s.), aquifer S (30-50 m b.s.), aquifer C1 (65-85 m b.s.), aquifer C2 (100-150 m b.s.) and aquifer C3 (160-250 m b.s.);
- discontinuities of silty-clayey aquitards produce a different degree of separation between overlapping aquifers, which are isolated in some zones and connected, with possible water exchanges, in other zones;
- superficial silty-clayey deposits are located in the Po river valley and in the central-northern part of the study area;

- peat deposits frequently characterize the aquifer and aquitard sediments: in the aquifer F, peats are only located in the Po river valley, probably generated in the wetland formed by recent Po river activity; between aquifers F and S peats are related to the silty-clayey deposits that form the aquitard; in the other deeper units, peats have a diffuse presence in the study area, generally involving the fine-grained sediments that form the aquitards, this larger diffusion of peat in the deeper units could be probably related to the past meandering activities of the rivers.

The analysis of hydrodynamic properties points outs the following aspects:

- aquifer F generally has phreatic conditions even if it can be subjected to local confined conditions due to the presence of superficial silty-clayey lenses, located in the central-northern part of the study area and in some zones of the Po valley; the main groundwater flow direction is N/S, with a relevant drainage effect of Po river, that can vary according to the variation of the hydrometric level of the river over time; with high flow rate of the river, the hydrometric levels can be higher with respect to the groundwater heads, generating a perturbation of the groundwater flow that interferes with the normal discharge in the river;
- aquifer S can be defined as semi-confined due to the presence of confined conditions in the central part of the study area, where the silty-clayey aquitard is located, and phreatic conditions in the remaining zones; the supposed flow direction is from N/S; the hydraulic heads seem to be lower than aquifer F but higher than aquifer C1;
- aquifer C1 has confined conditions; a flow direction from NW to SE can be supposed, according to the other confined aquifers; the hydraulic heads seem to be lower than aquifers S and C2;
- aquifer C2 has confined conditions; the general flow direction is NW/ SE; the hydraulic heads seem to be higher than aquifer C1 but lower than aquifer C3;
- aquifer C3 has confined conditions; the supposed flow direction is NW/ SE; the hydraulic heads seem to be similar or higher than aquifer C2 but lower than aquifer S.

The hydrochemical characterization, in particular the characterization of groundwater As, Fe, Mn and NH_4 concentrations of July 2010, underlines the following aspects:

- each aquifer has a quite homogeneous hydrochemical behaviour, with the exception of aquifer F; in aquifer F, reduced *facies* can be identified in the Po valley and in the central-northern part of the study area, while oxidized *facies* can be indentified in the area behind the terrace scarp; in the underlying aquifers (S, C1, C2 and C3), reduced *facies* can be identified.
- Mn: in the aquifer F, concentrations are lower in the area behind the scarp (around the regulatory limit of 50 µg/L), while higher and more variable values are found in the Po valley (ranging from 8 to 1255 µg/L); the concentrations are generally lower in the aquifer S, ranging between 84 and 543 µg/L; in the aquifers C1, C2 and C3 the concentrations decrease (ranging from 34 to 208 µg/L);
- Fe: in the aquifer F, concentrations are lower in the area behind the scarp (around the regulatory limit of 200 µg/L), while higher and more variable values are found in the Po valley (ranging from 10 to 4756 µg/L); the concentrations are also high in aquifer S, ranging from 10 to 5975 µg/L; from aquifer C1 to C3 the concentrations decrease (ranging from 60 to 1836 µg/L);
- As: in the aquifer F, concentrations are generally below the regulatory limit of 10 µg/L in the area behind the scarp higher, while higher values are found in the Po valley (ranging from <3 to 53 µg/L); in the aquifer S, the concentrations are higher and more variable, ranging from <3 to 183 µg/L; the concentrations are also high in the aquifer C1 (22-154 µg/L) and they decrease in aquifers C2 and C3 (<3-95 µg/L);
- NH_4: in the aquifer F, concentrations are generally below 0.1 mg/L in the area behind the scarp higher, while higher values are found in the Po valley (generally ranging from 0.4 to 3.7 mg/L); in the aquifer S, the concentrations are higher and more variable, ranging from <0.1 to 6.7 mg/L; constant high concentrations are found in aquifers C1, C2 and C3 (1.6-4.7 mg/L);
- the analysis of historical chemical data referred to the natural background and the July 2012 data generally confirms the hydrochemical characterization emerged from the data of July 2010.

The conceptual model concerning origins and mechanisms of high groundwater As, Fe, Mn and NH_4 concentrations considers that:

- the primary process controlling groundwater As, Fe, Mn and NH_4 concentrations seems to be the degradation of organic matter, in the form of peats deposits. Therefore, a natural origin of As, Fe, Mn and NH_4 can be assumed;
- in addiction, anthropogenic influences on groundwater As, Fe, Mn and NH_4 concentrations could locally exist in the study area: (1) groundwater pollution by hydrocarbons can influence the As, Fe and Mn concentrations, as probably occurred in the oil refinery, on the basis of the hydrogeochemical mechanisms involving organic matter degradation; the hydrocarbons are not a direct source of As, Fe and Mn in groundwater, but they intensify the processes of mobilization of As, Fe and Mn, which naturally form the aquifer sediments; (2) groundwater pollution by organic matter with vegetable or animal origin can influence the As, Fe, Mn and NH_4 concentrations, as probably occurred in the municipal solid waste landfill characterized by probable organic leachate spills, on the basis of the same mechanisms involving organic matter degradation; in this case, the influence also involves NH_4 which derives from organic nitrogen degradation.

The 1D reactive transport modelling supports the validity of the conceptual model, underling the following aspects:

- the Fe concentration is mainly governed by the reduction of Fe-oxides, in association with the oxidation of organic matter, and the precipitation-dissolution of siderite and iron sulfides;
- the Mn concentration is mainly governed by the precipitation-dissolution of rhodochrosite; peaks of Mn^{2+} concentration could be explained by the occurring of Mn-oxides reduction, in association with the oxidation of organic matter;
- the As concentration is mainly governed by the release from Mn and Fe oxides, which are subjected to reductive dissolution and by different processes which represent a sink of dissolved As (co-precipitation of As in iron sulfides, precipitation of arsenic sulfides, sorption of As on the remaining Fe-oxides and Mn-oxides, etc.); within these processes, one of the most relevant could be the co-precipitation in iron sulfides;

- the original source of dissolved Fe and Mn is probably the reductive dissolution of Fe and Mn oxides (which form the aquifer sediments), coupled with the organic matter degradation; the presence of reductive condition allows the formation of siderite, iron sulfide and rhodochrosite as authigenic mineral, these minerals also excerpt a control on the concentration of dissolved Fe and Mn.
- the source of NH_4 is probably the degradation of organic nitrogen of peat; high NH_4 concentration can persist in groundwater due to reducing environments.

In addiction, the isotope and microbiological analysis, executed in the survey of July 2012, confirms:

- the natural origin of ammonium, which probably derives from the degradation of organic nitrogen of peat;
- the occurring of Fe-oxide and sulfate reduction processes, coupled with the organic matter (peat) degradation;

The derivation of natural background levels on the July 2010 dataset and the historical dataset represents a preliminary calculation, but it can give useful information to groundwater resources management and protection by public authorities. A specific long-term monitoring for the derivation of definitive natural background levels has been proposed to the Province of Cremona.

In conclusion, the present work can contribute to understand origins and mechanisms of high groundwater As, Fe, Mn and NH_4 concentrations in the lower Po Plain, supporting the management and protection of groundwater resources by public authorities.

Related publications

Articles in preparation:

1. Rotiroti M., Jakobsen R., Bonomi T. & Fumagalli L. – *Hydrogeochemistry of As, Fe, Mn rich groundwater: 1D reactive transport modelling of the multi-layer aquifer of Cremona (northern Italy).*
2. Rotiroti M., Fumagalli L. & Bonomi T. – *Anthropogenic influences on groundwater As, Fe, Mn and NH_4 concentrations, the case study of Cremona (northern Italy).*
3. Rotiroti M., Fumagalli L. & Bonomi T. – *Hydrochemical characterization of As, Fe, Mn and NH_4 rich groundwater of the multi-layer aquifer of Cremona (northern Italy).*
4. Rotiroti M., Bonomi T. & Fumagalli L. – *Analysis of the hydrodynamic properties of the alluvial multi-layer aquifer of Cremona (northern Italy).*
5. Rotiroti M., Bonomi T. & Fumagalli L. – *Parameterization of the alluvial multi-layer aquifer of Cremona (northern Italy) using kriging interpolation*.

Published articles:

1. Rotiroti M., Bonomi T., Fumagalli L., Azzoni A., Pisaroni B. & Demicheli G. (2012) – *Approccio metodologico nell'analisi di fenomeni di contaminazione da Arsenico, Ferro e Manganese nelle falde superficiali, il caso del territorio di Cremona (A method to analyse arsenic, iron and manganese groundwater contamination, the Cremona area case)*. EHE Geology 15, 117-128.

Communications to conferences (presented):

1. Rotiroti M., Bonomi T. & Fumagalli L. – *An integrated approach to asses origin and mobilization of As, Fe and Mn in groundwater: the case study of Cremona (northern Italy).* European Geosciences Union General Assembly 2013. 07-12 April 2013. Vienna, Austria. *(Submitted)*
2. Rotiroti M. & Fumagalli L. – *Derivation of preliminary natural background levels for naturally Mn, Fe, As and NH_4^+ rich groundwater: the case study of*

Cremona area (Northern Italy). IX AIGA Young Researchers Meeting. 14-15 February 2013. University of Napoli-Federico II, Napoli, Italy. (*Accepted*)

3. Rotiroti M., Bonomi T. & Fumagalli L. – *Presenza di ammonio e metalli nelle acque sotterranee in Provincia di Cremona (Occurrence of ammonium and metals in groundwater in the province of Cremona)*. Regione Lombardia & CNR workshop "Il contributo delle analisi isotopiche allo studio della contaminazione da nitrati in Pianura Padana". 6 December 2012. Palazzo Pirelli-Regione Lombardia, Milano, Italy. *(Oral)*
4. Rotiroti M., Bonomi T. & Fumagalli L. – *Preliminary conceptual model of groundwater contamination by Mn, Fe and As in a multi-layer alluvial aquifer, the case study of Cremona (Northern Italy)*. IAH Conference "Flowpath 2012". 20-22 June 2012. University of Bologna, Bologna, Italy. *(Poster & Abstract)*
5. Rotiroti M., Bonomi T., Fumagalli L., Azzoni A., Pisaroni B. & Demicheli G. – *Origine e dinamica della contaminazione da ferro, manganese, arsenico ed ammonio in acque sotterranee superficiali, il caso di Cremona (Origin and dynamic of shallow groundwater contamination by iron, manganese, arsenic and ammonium, the case of Cremona)*. IV AIGA National Meeting. 6-7 February 2012. University of Perugia, Perugia, Italy. *(Oral & Abstract)*
6. Rotiroti M., Bonomi T., Fumagalli L., Azzoni A., Pisaroni B. & Demicheli G. – *Groundwater quality characterization of Cremona area (Northern Italy) affected by As, Fe and Mn contamination, combining hydrochemical analysis and aquifer texture modeling*. “Geoitalia 2011” – VIII Italian Forum of Geosciences. 19-23 September 2011. Torino, Italy. *(Oral & Abstract)*
7. Bonomi T., Fumagalli L. & Rotiroti M. – *Approccio metodologico nell'analisi di fenomeni di contaminazione da Arsenico, Ferro e Manganese nelle falde superficiali: il caso del territorio di Cremona (A method to analyse arsenic, iron and manganese groundwater contamination: the Cremona area case)*. “Acqua 2011” – AIGA Water Resource Meeting. 24-25 February 2011, University of Udine, Udine, Italy. *(Poster & Abstract)*

Overall References

Aitkenhead J. A. & McDowell W. H. (2000) – *Soil C:N ratio as a predictor of annual riverine DOC flux at local and global scales*. Global Biogeochemical Cycles 14(1), 127-138.

Aiuppa A., D'Alessandro W., Federico C., Palumbo B. & Valenza M. (2003) – *The aquatic geochemistry of arsenic in volcanic groundwater from southern Italy*. Applied Geochemistry 18, 1283-1296.

Albrechtsen H. J. & Christensen T. H. (1994) – *Evidence for microbial iron reduction in a landfill leachate-polluted aquifer (Vejen, Denmark)*. Applied and Environmental Microbiology 60(11), 3920-3925.

Appelo C. A. J. & Postma D. (2005) – *Geochemistry, groundwater and pollution (2nd edition)*. Balkema Publishers, Leiden, 649 pp.

Armstrong M. (1998) – *Basic Linear Geostatistics*. Springer Verlag, Berlin, 153 pp.

Avanzini R., Beretta G. P., Francani V. & Nespoli R. (1994) – *Indagine preliminare sull'uso sostenibile delle falde profonde nella provincia di Milano (Preliminary investigation on the sustainable use of deep groundwater in the Milano province)*. Consorzio Acqua Potabile, Milano.

Baedecker M.J., Cozzarelli I. M., Eganhouse R. P., Siegel D. I. & Bennett P. C. (1993) – *Crude oil in a shallow sand and gravel aquifer—III. Biogeochemical reactions and mass balance modeling in anoxic groundwater*. Applied Geochemistry 8(6), 569-586.

Baiocchi A., Lotti F. & Piscopo V. (2011) – *Influence of hydrogeological setting on the arsenic occurrence in groundwater of the volcanic areas of central and southern Italy*. Aqua Mundi, DOI: 10.4409/Am-035-11-0035.

Ball J. W. and Nordstrom D. K. (1991) – *WATEQ4F - User's manual with revised thermodynamic data base and test cases for calculating speciation of major, trace and redox elements in natural waters*. U.S. Geological Survey Open-File Report 90-129, 185 pp.

Bartolucci E., Bussettini M., Calace N., D'Aprile L., Fratini M., Guerra M., Marangio L., Pirani G. & Vecchio A. (2009) – *Protocollo per la Definizione dei Valori di Fondo per le Sostanze Inorganiche nelle Acque Sotterranee (Procedure for the definition of background levels for inorganic compounds in groundwater)*. Protocollo ISPRA, 17 pp. http://www.isprambiente.gov.it/site/it-IT/

Bassi G. (2001a) – *Studio Geologico del Territorio Comunale (Geological study of the municipal territory)*. Relazione Tecnico-illustrativa, Comune di Cremona, 36 pp.

Bassi G. (2001b) – *Carta di Prima Caratterizzazione Geotecnica del Comune di Cremona (First Geotechnical map of the Municipality of Cremona).* Scala 1:12˙500. Allegato 3 allo Studio Geologico del Territorio Comunale, Comune di Cremona.

Berbenni P., Pollice A., Canziani R., Stabile L. & Nobili F. (2000) – *Removal of iron and manganese from hydrocarbon-contaminated groundwaters.* Bioresource Technology 74 (2), 109-114.

Beretta G. P. (1992) – Idrogeologia per il *disinquinamento* delle acque sotterranee (Hydrogeology for groundwater remediation). Pitagora Editrice, Bologna, 840 pp.

Beretta G. P., Francani V. & Fumagalli L., (1992) – *Studio Idrogeologico della Provincia di Cremona (Hydrogeological study of the Province of Cremona)*. Pitagora Editrice, Bologna, 141 pp.

Berner R. A. (1981) – *A New Geochemical Classification of Sedimentary Environments*. Journal of Sedimentary Petrology 51(2), 359-365.

Bianchi A. & Pezzera G. (1999) – *Il monitoraggio dell'arsenico nelle acque sotterranee della pianura mantovana e bergamasca: aspetti idrogeologici e idrochimici (Arsenic monitoring in groundwater in the Po Plain of Mantova and Bergamo: hydrogeological and hydrochemical aspects)*. Quaderni di geologia Applicata S2, 3.61-3.72.

Bjerg P. L., Ruegge K., Pedersen J. K. & Christensen T. H. (1995) – *Distribution of redox-sensitive groundwater quality parameters downgradient of a landfill (Grindsted, Denmark)*. Environmental Science and Technology 29(5), 1387-1394.

Bleam W. F. (2011) – *Soil and Environmental Chemistry*. Academic press, Burlington, 478 pp.

Bonomi T., Cavallin A. & De Amicis M. (1995) – *Un database per pozzi: Tangram (A wells database: Tangram)*. Quaderni di Geologia Applicata S3, 3.461-3.465.

Bonomi T., Cavallin A. & De Amicis M. (1999) – *Banca dati idrochimica applicata ai pozzi: protocollo informatico e prototipo di applicazione. (Hydeochemical database applied to wells: computer register and application prototype)*. Quaderni di Geologia Applicata S2, 3.73-3.77.

Bonomi T., Canepa P., Del Rosso F. & Rossetti A. (2008) – *Relazioni temporali pluridecennali di dati pluviometrici, idrologici e piezometrici nella pianura lombarda tra Ticino e Oglio (Temporal analysis of long-term pluviometric, hydrological and piezometric data in the Po Plain between Ticino and Oglio rivers).* Giornale di geologia applicata 9 (2), 227-248.

Bonomi T. (2009) – *Database development and 3D modeling of textural variations in heterogeneous, unconsolidated aquifer media: Application to the Milan Plain*. Computer and Geosciences 35, 134-145.

Bortolami G. C., Olivero G. F., Piovesana F., Ricci B. & Zuppi G. M. (1983) – *Idrogeologia isotopica della pianura vercellese-novarese (Piemonte) (Isotope hydrogeology of the Vercelli-Novara plain (Piemonte))*. Rendiconti Accademia Nazionale dei Lincei classe di scienze fisiche, matematiche e naturali LXXIV-3, 157-166.

Braunschweig J., Bosch J., Heister K., Kuebeck C. & Meckenstock R. U. (2012) – *Reevaluation of colorimetric iron determination methods commonly used in geomicrobiology*. Journal of Microbiological Methods 89, 41-48.

Burgess W. G. & Pinto L. (2005) – *Preliminary observations on the release of arsenic to groundwater in the presence of hydrocarbon contaminants in UK aquifers.* Mineralogical Magazine 69 (5), 887-896.

Burrato P., Ciucci F. & Valensise G. (2003) – *An inventory of river anomalies in the Po Plain, Northern Italy: evidence for active blind thrust faulting*. Annals of Geophysics 46 (5), 865-882.

Cambi C., Dragoni W., Passeri F. & Valigi D. (2005) – *Contribution to the hydrogeological knowledge of the Cremona aquifer system and the exploitation of new water resources*. Italian Journal of Engineering Geology and Environment 1, 71-89.

Canfield D. E., Thamdrup B. & Hansen J. W. (1993) – *The anaerobic degradation of organic matter in Danish coastal sediments: Iron reduction, manganese reduction and sulfate reduction*. Geochimica et Cosmochimica Acta 57, 3867-3883.

Castelli A., Chiesa S., Deriu G., Pezzera G., Vescovi E., Zanotti M. & Zonca B. (2005) –*Note sulla presenza di arsenico nel sottosuolo e nelle acque sotterranee della Lombardia (Occurrence of arsenic in aquifer sediments and groundwater in Lombardy region)*. In: Arpa Emilia-Romagna (Eds), Presenza e diffusione dell'arsenico nel sottosuolo e nelle risorse idriche italiane (Occurrence and distribution of arsenic in sediments and water resources of Italy), 39-50. I quaderni di Arpa.

Castiglioni G.B., Ajassa R., Baroni C., Biancotti A., Bondesan A., Bondesan M., Brancucci G., Castaldini D., Castellaccio E., Cavallin A., Cortemiglia F., Cortemiglia G.C., Cremaschi M., Da Rold O., Elmi C., Favero V., Ferri R., Gandini F., Gasperi G., Giorgi G., Marchetti G., Marchetti M., Marocco R., Meneghel M., Motta M., Nesci O., Orombelli G., Paronuzzi P., Pellegrini G.B., Pellegrini L., Rigoni A., Sommaruga M., Sorbini L., Tellini C., Turrini M.C., Vaia F., Vercesi P.L., Zecchi R. and Zorzin R. (1997) – *Carta Geomorfologica della Pianura Padana (Geomorphological map of the Po Plain)*. Scala 1:250˙000. SELCA, Firenze.

Cavallin A. & Maggi V. (2006) – *Regional Impact of Climatic Change in Lombardy Water Resources: Modelling and applications (RICLIC-WARM).* Technical Report of the first year activities. http://www.riclic.unimib.it/Report_tecnico-Ianno.pdf

Celico P. (1986) – *Prospezioni idrogeologiche (Hydrogeological prospection)*. Volume primo. Liguori Ed., Napoli, 735 pp.

Chapelle F. H., Bradley P. M., Thomas M. A. & McMahon P. (2009) – Distinguishing Iron-Reducing from Sulfate-Reducing Conditions. Ground Water 47 (2), 300-305.

Cheng H., Hu Y., Luo J. Xu B. & Zhao J. (2009) – *Geochemical processes controlling fate and transport of arsenic in acid mine drainage (AMD) and natural systems*. Journal of Hazardous Materials 165(1-3), 13-26.

Ciotoli G. & Finoia M. G. (2005) – *Dalla statistica alla Geostatistica: introduzione all'analisi dei dati geologici e ambientali (From statistics to Geostatistics: introduction to geological and environmental data analysis).* Aracne editrice S.r.l., Roma, 418 pp.

Clark I. & Fritz P. (1997) – *Environmental Isotopes in Hydrogeology*. Lewis Publishers, New York, 328 pp.

Conti A., Sacchi E., Chiarle M., Martinelli G. & Zuppi G.M. (2000) – *Geochemistry of the formation waters of the po plain (Northern Italy): an overview*. Applied Geochemistry 15, 51-65.

Cornell R. M. & Schwertmann U. (2003) – *The Iron Oxides (2nd edition).* Wiley-VCH, Weinheim, 664 pp.

Cremonini Bianchi M. (1989) – *Un antico percorso fluviale della pianura cremonese: la "Valle dei Navigli" (An ancient watercourse of the plain of Cremona: the "Navigli" valley)*. Pianura - Scienza e Storia dell'Ambiente Padano 3, 55-68.

Davis K. J., Dove P. M. & De Yoreo J. J. (2000) – *The role of Mg^{2+} as an inpurity in calcite growth*. Science 290, 1134-1137.

Degens E.T. (1965) – *Geochemistry of sediments: a brief survey*. Prentice-Hall, Englewood Cliffs, 342 pp.

Del Rosso F. (2011) – *Ricostruzione tridimensionale delle caratteristiche idrogeologiche della pianura lombarda, finalizzata all'applicazione di modelli di flusso e trasporto (3D reconstruction of the hydrogeological characteristics of the Po Plain (Lombardy Region) for flow and transport model implementation)*. Ph.D. thesis. http://boa.unimib.it/bitstream/10281/20033/1/phd_unimib_027168.pdf

Dowling C. B., Poreda R. J., Basu A. R., Peters S. L. & Aggarwal P. K. (2002) – *Geochemical study of arsenic release mechanisms in the Bengal Basin groundwater*. Water Resources Research, DOI:10.1029/2001WR000968.

Ferguson J. F. & Gavis J. (1972) – *A review of the arsenic cycle in natural water*. Water Research 6, 1259-1274.

Fetter C. W. (1994) – *Applied Hydrogeology*. Prentice Hall, Englewood Cliffs, 691 pp.

Francani V., Beretta G. P., Bareggi A., Nobile A., Cremonini Bianchi M. & Cattaneo F. (1994) – *Aspetti idrogeologici del problema della presenza di azoto ammoniacale nelle acque sotterranee della provincia di Cremona. (Hydrogeological aspects of the occurrence of ammonium in groundwater in the province of Cremona).* Pitagora Editrice, Bologna, 101 pp.

Francani V. & Trefiletti (2006) – *Relazioni fra sistema idrico superficiale e contaminazione delle acque sotterranee nella provincia di Cremona (Relations between surface water system and groundwater contamination in the province of Cremona).* Atti del convegno “Questioni ambientali nella gestione del territorio: strumenti e casi studio nel territorio cremonese”, Cremona, 9 giugno 2006.

Freeze R. A. & Cherry J. A. (1979) – *Groundwater*. Prentice Hall, Englewood Cliffs, 604 pp.

Gandolfi C, Ponzini G. & Giudici M. (2007) – *Realizzazione di un modello preliminare del flusso idrico nel sistema acquifero della Provincia di Cremona (Implementation of a preliminary flow model in the aquifer system of the Province of Cremona).* Relazione Tecnica, pp.222. *http://www.atlanteambientale.it/atlanteambientale/biblio/Intro.html*

Geologia Applicata & AEM Cremona (2002) – *Studio idrogeologico a supporto della realizzazione del campo pozzi Cremona est (Hydrogeological study supporting the realization of the water supply pumping station "Cremona est")*. Relazione Tecnica, pp. 49.

Ghosh R., Deutsch W., Geiger S., McCarthy K. & Beckmann D. (2003) – *Geochemistry, fate and transport of dissolved arsenic in petroleum hydrocarbon-impacted groundwater*. Petroleum hydrocarbons and organic chemicals in groundwater. American Petroleum Institute, National Ground Water Association. Costa Mesa, 266-280.

Guffanti S., Pilla G., Sacchi E. & Ughini S. (2010) –*Characterization of the quality and origin of groundwater of lodigiano (Northern Italy) with hydrochemical and isotopic instruments*. Italian Journal of Engineering Geology and Environment 1, 65-78.

Hounslow A. W. (1980) – *Ground-Water Geochemistry: Arsenic in Landfills*. Ground Water 18(4), 331-333.

Jain C. K. & Ali I. (2000) – *Arsenic: Occurrence, toxicity and speciation techniques*. Water Research 34(17), 4304-4312.

Jakobsen R. & Postma D. (1994) – *In situ rates of sulfate reduction in an aquifer (Rømø, Denmark) and implications for the reactivity of organic matter*. Geology 22, 1103-1106.

Jakobsen R. & Postma D. (1999) – *Redox zoning, rates of sulfate reduction and interactions with Fe-reduction and methanogenesis in a shallow sandy aquifer, Rømø, Denmark*. Geochimica et Cosmochimica Acta 63(1), 137-151.

Jakobsen R. & Cold L. (2007) – *Geochemistry at the sulfate reduction-methanogenesis transition zone in an anoxic aquifer - A partial equilibrium interpretation using 2D reactive transport modeling.* Geochimica et Cosmochimica Acta 71, 1949-1966.

Jessen S., Larsen F., Postma D., Viet P. H., Ha T. N., Nhan P. Q., Nhan D. C., Duc M. T., Hue N. T. M., Huy T. D., Luu T. T., Ha D. H. & Jakobsen R. (2008) – *Palaeo-hydrogeochemical control on groundwater As levels in Red River delta, Vietnam*. Applied Geochemistry 23, 3116-3126.

Jung H. B., Bostick C. B. & Zheng Y. (2011) – *Field, experimental and modeling study of arsenic partitioning across a redox transition in a Bangladesh aquifer*. Environmental Science & Technology 46, 1388-1395.

Kaiser H. F. (1958) – *The varimax criteria for analytical rotation in factor analysis*. Psychometrika 23, 187-200.

Kroopnick P. (1974) – *The dissolved O2-CO2-13C system in the eastern equatorial pacific*. Deep Sea Research and Oceanographic Abstracts 21(3), 211-227.

Langmuir D. (1969) – *The gibbs free energies of substances in the system Fe-O_2-H_2O-CO_2 at 25 ℃.* U.S. Geological Survey Professional Paper 650-B, B180-B184.

Lindberg R. D. & Runnells D. D. (1984) – *Ground water redox reactions: an analysis of equilibrium state applied to Eh measurements and geochemical modeling*. Science 255, 925-927.

Longinelli A. & Selmo E. (2003) – *Isotopic composition of precipitation in Italy: a first overall map*. Journal of Hydrology 270, 75-88.

Lovley D. R. & Phillips E.J.P. (1986) – *Organic matter mineralization with reduction of ferric iron in anaerobic sediments*. Applied and Environmental Microbiology 51(4), 683-689.

Malerba G., Galli C., Armanini B. & Ferrari V. (1995) – *La geomorfologia della provincia di Cremona (The geomorphology of the Province of Cremona)*. Quaderni del Centro di Documentazione Ambientale, Provincia di Cremona, 23 pp.

Marcaccio M., Molinari A., Guadagnini L. & Guadagnini A. (2012) - *Valori di fondo naturale di metalli e sostanze inorganiche nelle acque sotterranee dell'Emilia-Romagna (Natural background levels for metals and inorganic compounds in groundwater (Emilia-Romagna region))*. Atti del convegno "Le acque sotterranee fra tutela ed utilizzo sostenibile della risorsa" GEOFLUID 2012, 3 ottobre 2012, Piacenza.

Martin P. J. and Frind E. O. (1998) – *Modeling a Complex Multi-Aquifer System: The Waterloo Moraine*. Ground water 36 (4), 679-690.

Martinelli M., Marcaccio M., Farina M., Canepa P., Cantagalli L. & Billi L. (2005) – *L'arsenico nei sedimenti profondi della pianura emiliano-romagnola: prime evidenze (Arsenic in the deep sediments of Emilia-Romagna plain: first evidence)*. In: Arpa Emilia-Romagna (Eds), Presenza e diffusione dell'arsenico nel sottosuolo e nelle risorse idriche italiane (Occurrence and distribution of arsenic in sediments and water resources of Italy), 215-224. I quaderni di Arpa.

Martinis B. & Mazzarella S. (1971) – *Prima ricerca idrica profonda nella pianura lombarda (First deep water research in the plain of Lombardy region).* Memorie dell'Istituto di Geologia e Mineralogia dell'Università di Padova 28, 1-52.

McArthur J. M., Ravenscroft P., Safiulla S. & Thirlwall M. F. (2001) – *Arsenic in groundwater: Testing pollution mechanisms for sedimentary aquifers in Bangladesh.* Water Resources Research 37 (1), 109-117.

McArthur J. M., Banerjee D. M., Hudson-Edwards K. A., Mishra R., Purohit R., Ravenscroft P., Cronin A., Howarth R. J., Chatterjee A., Talukder T., Lowry D., Houghton S. & Chadha D. K. (2004) – *Natural organic matter in sedimentary basins and its relation to arsenic in anoxic ground water: the example of West Bengal and its worldwide implications.* Applied Geochemistry 19, 1255-1293.

McMahon P. B. & Chapelle F. H. (2008) – *Redox processes and water quality of selected principal aquifer systems*. Ground water 46 (2), 259-271.

MIPAAF (2002) – *Approvazione dei metodi ufficiali di analisi microbiologica del suolo (Endorsement of official methods for microbiological analysis)*. D.M. 8 luglio 2002.

Muller D., Blum A., Hart A., Hookey J., Kunkel R., Scheidleder A., Tomlin C. & Wendland F. (2006) – *Final proposal for a methodology to set up groundwater threshold values in Europe.* In: Report to EU project BRIDGE, Deliverable D18, 63 pp. http://www.wfd-bridge.net

Neumann R. B., Ashfaque K. N., Badruzzaman A. B. M., Ashraf Ali M., Shoemaker J. K. & Harvey C. F. (2009) – *Anthropogenic influences on groundwater arsenic concentrations in Bangladesh*. Nature Geoscience 3, 46-52.

Nicholson R. V., Cherry J. A. & Reardon E. J. (1983) *Migration of contaminants in groundwater at a landfill: A case study 6. Hydrogeochemistry*. Journal of Hydrology 63(1-2), 131-176.

Nriagu J. O., Bhattacharya P., Mukherjee A. B., Bundschuh J., Zevenhoven R. & Loeppert R. H. (2007) – *Arsenic in Soil and Groundwater: an overview.* In: Loeppert (Eds.), Arsenic in Soil and Groundwater Environment, Chapter 1, 3-60.

O'Day P. A., Vlassopoulos D., Root R. & Rivera N. (2004) – *The influence of sulphur and iron on dissolved arsenic concentrations in the shallow subsurface under changing redox conditions*. Proceedings of the National Academy of Sciences of the U.S.A. 101 (38), 13703-13708.

Ori G. G. (1992) – *Continental depositional systems of the Quaternary of the Po Plain (northern Italy)*. Sedimentary Geology 83, 1-14.

Paradigm (2008) – *Paradigm GOCAD 2008, User Guide*. Paradigm Geophisical Corp.

Parkhurst D. L. & Appelo C. A. J. (1999) – *User's guide to PHREEQC: A computer program for speciation, reaction-path, 1D-transport, and inverse geochemical calculations.* U.S. Geological Survey Water-Resources Investigations Report 99-4259, 312 pp.

Petrucci F. & Tagliavini S. (1969) – *Note illustrative della Carta Geologica d'Italia (Illustrative notes of the geological map of Italy)*. Foglio 61, Cremona, Servizio Geologico d'Italia, pp.43.

Petrunic B. M., MacQuarrie K. T. B. & T. A. Al (2005) – *Reductive dissolution of Mn oxides in river-recharged aquifers: a laboratory column study*. Journal of Hydrology 301, 163-181.

Pilla G. (1998) – *Caratterizzazione idrochimica e geochimica isotopica delle falde idriche nel sottosuolo della città di Pavia (Chemical and isotopic characterisation of groundwater from the city of Pavia)*. Atti Ticinensi di Scienze della Terra 40, 185-201.

Pilla G., Sacchi E., Zuppi G., Braga G. & Ciancetti G. (2006) – *Hydrochemistry and isotope geochemistry as tools for groundwater hydrodynamic investigation in multilayer aquifers: a case study from Lomellina, Po plain, south-western Lombardy, Italy*. Hydrogeology Journal 14, 795-808.

Pilla G. (2010) – *Gli acquiferi di pianura della provincia di Pavia: origine e qualità della risorsa (The alluvial aquifers in the province of Pavia: origin and quality of water resources).* Provincia di Pavia ed., Pavia, 112 pp.

Postma D. & Jakobsen R. (1996) – *Redox zonation: Equilibrium constraints on the Fe(III)/SO_4-reducing interface*. Geochimica et Cosmochimica Acta 60(17), 3169-3175.

Postma D., Larsen F., Hue N. T. M., Duc M. T., Viet P. H., Nhan P. Q. & Jessen S. (2007) – *Arsenic in groundwater of the Red River floodplain, Vietnam: Controlling geochemical processes and reactive transport modeling*. Geochimica et Cosmochimica Acta 71, 5054-5071.

Postma D., Larsen F., Thai N. T., Trang p. T. K., Jakobsen R., Nhan P. K., Long T. V., Viet P. H. & Murray A. S. (2012) – *Groundwater arsenic concentrations in Vietnam controlled by sediment age*. Nature Geoscience 5, 656-661.

Preziosi E., Giuliano G. & Vivona R. (2010) – *Natural background levels and threshold values derivartion for naturally As, V and F rich groundwater bodies: a methodological case study in Central Italy*. Environmental Earth Sciences 61, 885-897.

Rapti-Caputo D. & Martinelli G. (2009) – *The geochemical and isotopic composition of aquifer systems in the deltaic region of the Po River plain (northern Italy)*. Hydrogeology Journal 17, 467-480.

Regione Lombardia & Eni Divisione Agip (2002) – *Geologia degli acquiferi padani della Regione Lombardia (Geology of the aquifers of the Po Plain in Lombardy region).* A cura di Carcano C. & Piccin A. S.E.L.C.A, Firenze, 130 pp.

Regione Lombardia (2006) – *Monitoraggio qualitativo e classificazione delle acque superficiali e sotterranee (Qualitative monitoring and classification of surface water and groundwater).* Allegato 12 alla Relazione Generale, Programma di Tutela e Uso delle Acque.

Root R. A., Vlassopoulos D., Rivera N. A., Rafferty M. T., Andrews C. & O'Day P. A. (2009) – *Speciation and natural attenatuon of arsenic and iron in a tidally influenced shallow aquifer*. Geochimica et Cosmochimica Acta 73, 5528-5553.

Rozanski K., Araguás-Araguás L. & Gonfiantini R. (1993) – *Isotopic patterns in modern global precipitation*. In: Swart et al. (Eds), Climate Change in Continental Isotopic Records, 1-36. Geophysical Monograph 78.

Rowland H. A. L, Polya D. A., Lloyd J. R. & Pancost R. D. (2006) – *Characterisation of organic matter in a shallow, reducing, arsenic-rich aquifer, West Bengal*. Organic Geochemistry 37, 1101-1114.

Smedley P.L. & Kinniburgh D.G. (2002) – *A review of the source, behaviour and distribution af arsenic in natural waters*. Applied Geochemistry 17, 517-568.

Steinmaus C., Yuan Y., Kalman D., Rey O. A., Skibola C. F., Dauphine D., Basu A., Porter K. E., Hubbard A., Bates M. N., Smith M. T. & Smith A. H. (2010) – *Individual differences in arsenic metabolism and lung cancer in a case-control study in Cordoba, Argentina*. Toxicology and Applied Pharmacology 247, 138-145.

Thomas M. A., Diehl S. F., Pletsch B. A., Schumann T. L., Pavey R. R. & Swinford E. M. (2008) – *Relation Between Solid-Phase and Dissolved Arsenic in the Griund-Water System Underlying Northern Oreble Country, Ohio*. USGS Scientific Investigations Report 5205, 56 pp.

Towensend T., Dubey B., Tolaymat T. & Solo-Gabrile H. (2005) – *Preservative leaching from weathered CCA-treated wood*. Journal of Environmental Management 75(2), 105-113.

Tucillo M. E., Cozzarelli I. M. & Herman J. H. (1999) – *Iron reduction in the sediments of a hydrocarbon-contaminated aquifer.* Applied Geochemistry 14 (5), 655-667.

U.S. EPA (1999) – *Monitored natural attenuation of petroleum hydrocarbons.* Remedial Technology Fact Sheet, EPA/600/F-98/021, 3 pp.

U.S. EPA (2013) – *Field measurement of oxidation-reduction potential (ORP)*. SESD Operating Procedure SESDPROC-113-R1, 21 pp.

Voigt D. E., Brantley S.L. & Hennet Remy J. C. (1996) – *Chemical fixation of arsenic in contaminated soils*. Applied Geochemistry 11, 633-643.

Walter L. M. & Hanor J. S. (1979) – *Effect of orthophosphate on the dissolution kinetics of biogenic magnesian calcites.* Geochimica et Cosmochimica Acta 43, 1377-1385.

Weast R.C. (1968) – *Handbook of chemistry and physics*. The Chemical Rubber Co., Cleveland.

Webster R. & Oliver M. A. (2007) – *Geostatistics for Environmental Scientists*. Wiley & Sons Ltd, pp. 315.

Wendland F., Blum A. & Kunkel R. (2006) – *Approach to asses Natural Background Levels (NBLs)*. Annex I to the Report to EU project BRIDGE, Deliverable D18, 63 pp. http://www.wfd-bridge.net

Williams L.B., Wilcoxon B.R., Ferrell R.E. & Sassen R. (1992) – *Diagenesis of ammonium during hydrocarbon maturation and migration, Wilcox Group, Louisiana, U.S.A*. Applied Geochemistry 7(2), 123-134.

Zavatti A., Atramini D., Bonazzi A., Boraldi V., Malagò R., Martinelli G., Naldi S., Patrizi G., Pezzera G., Vandini W., Venturini L. & Zuppi G. M. (1995) – *La presenza di Arsenico nelle acque sotterranee della Pianura Padana: evidenze ambientali e ipotesi geochimiche (Occurrence of*

arsenic in the groundwater of Po Plain: environmental evidences and geochemical hypothesis). Quaderni di geologia Applicata S2, 301-325.

Acknowledgements

I would like to thank:

Prof. Tullia Bonomi and Dr. Letizia Fumagalli for competently guiding me through the Ph.D., for the professional support, help, advice and thesis review. A special thanks also for the opportunity of this Ph.D. project.

Prof. Angelo Cavallin for the interest in the project, providing useful articles, and also for the opportunity of this Ph.D. project.

Prof. Giovanni Pietro Beretta for reviewing the activities of the three years, providing useful advice and suggestion.

Prof. Rasmus Jakobsen for hosting me at DTU, the professional support in the hydrogeochemical modelling and the review of chapter 11 of the thesis.

Dr. Elisa Sacchi for the help and advice in the isotope data interpretation.

The Province of Cremona, in particular Dr. Mara Pesaro, Dr. Andrea Azzoni, Dr. Barbara Pesaroni and Dr. Giuseppina Demicheli, for funding the project and providing the historical data.

The microbiological laboratory of DISAT, in particular Dr. Andrea Franzetti and Dr. Matteo Daghio, for providing the microbiological analysis.

AEM Cremona, Padania Acque, Comune di Cremona and all the private owners of wells who have made possible the surveys of July 2010 and 2012.

The Master students Valeria Benastini, Luca Rossi and Matteo Lombardo for contributing to the project.

The Ph.D. students and assistant researchers of the Hydrogeology Research Group of DISAT, Dr. Andrea Merri, Dr. Paola Canepa, Dr. Francesca Del Rosso and Dr. Barbara Crestana, for the help and support.

Finally, a special thanks to my family and my partner Sara for being who they are.